Mucoadhesive Electrospun Patches for the Delivery of Therapeutic Peptides and Proteins to the Oral Mucosa

Jake Edmans

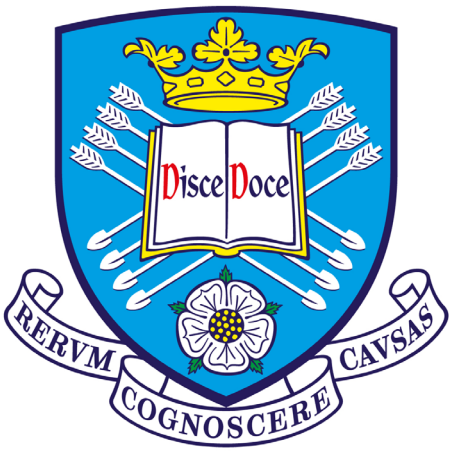

A thesis submitted in partial fulfilment of the requirements for the degree of

Doctor of Philosophy

School of Clinical Dentistry

University of Sheffield

Submitted December 2022

Abstract

Diseases of the oral mucosa are highly prevalent and can be debilitating. Treatment options are restricted by the limited range of therapeutic agents that can be delivered to the oral cavity using existing dosage forms, which offer little site-specificity and result in short exposure times. Fibrous mucoadhesive formulations prepared using electrospinning are promising for oral mucosal delivery because of their flexibility and high surface area, which allows them to adhere and efficiently deliver therapeutic agents to the affected tissue. This emerging technology has been investigated previously for a narrow range of conventional therapeutic agents. To expand the potential for novel therapies, this thesis has further developed the technology to allow the delivery of functional proteins, peptides, and antibody-based therapies. Lysozyme, bradykinin, and F(ab) antibody fragments were incorporated into polymeric mucoadhesive patch formulations that contained poly(vinyl pyrrolidone) and Eudragit® RS100 using electrospinning from ethanol/water solvent mixtures. These hydrophilic proteins were all eluted from the formulation over suitable timescales for oral mucosal delivery, within approximately 2 h. Proteins were stabilised by the polymer system during processing, resulting in highly conserved functionality. The formulation was investigated in greater detail for the delivery of cytokine-neutralising F(ab) antibody fragments to treat chronically inflamed autoimmune ulcers. Patches applied to tissue-engineered models of oral ulcers reduced detectable levels of key disease-causing molecules, providing the first experimental evidence that topical biologic therapies may be an effective treatment for oral diseases. Patches applied to tissue-engineered oral epithelia delivered a comparable dose of F(ab) to an equivalent dose in solution, providing preliminary evidence that patches may also be suitable for the systemic delivery of highly permeating peptides via the oral mucosa.

Acknowledgement of collaboration and prior publication

The candidate confirms that the work submitted is original and their own unless indicated below. This thesis contains previously published works for which the contribution of the candidate has been explicitly indicated below. The candidate confirms that appropriate credit has been given within the thesis where reference has been made to the work of others.

Chapter 1: The introductory chapter includes text and figures from a published review article by Edmans, Clitherow, *et al.* (2020).[1] Co-authors were involved in conceptualising the review, writing parts of the original draft, reviewing and editing the text and figures. The majority of the original draft was written by the candidate under supervision of the co-authors. The review article has since been extensively adapted and updated for use in this thesis under a CC BY 4.0 licence.

Chapter 2: This Chapter has been reproduced from Edmans, Murdoch *et al.* (2020) under a CC BY 4.0 license.[2] The candidate performed the experiments and wrote the original draft with guidance and supervision from the co-authors.

Chapter 4: This Chapter has been reproduced from Edmans *et al.* (2022) under a CC BY 4.0 license.[3] Dr Bethany Ollington performed the isolation and differentiation of monocyte-derived-macrophages and was jointly involved in generating the oral mucosal ulcer equivalents. Prof Craig Murdoch contributed towards writing the original draft. The candidate performed all other experiments and wrote the majority of the original draft with guidance and supervision from the co-authors.

Appendix 4: Klaudia Słowik contributed towards bupivacaine quantification and histological processing.

Acknowledgements

Thank you to my supervisors Dr Helen Colley, Prof Craig Murdoch, Prof Paul Hatton, Dr Seb Spain for making this PhD possible and for their continuous guidance and enthusiasm. The success of the project and my own development as a researcher have benefitted greatly from their input and breadth of expertise. My PhD was funded by the EPSRC CDT in Polymers, Soft Matter, and Colloids (EP/L016281/1) and AFYX Therapeutics. I am grateful to AFYX for sponsoring my PhD and industrial supervisors Dr Martin Santocildes-Romero and Dr Lars Madsen for their interest and advice.

Thank you to past and present members of the School of Clinical Dentistry and the Colley and Murdoch groups for being great colleagues. I am particularly grateful to Dr Katharina Clitherow for training and mentorship on the materials science aspects of my project and to Dr Amy Harding, Klaudia Słowik, Dr Inmaculada Barragan-Vasquez, Dr Bethany Ollington and Dr Asma El Howati for generously training me in a wide variety of cell culture and molecular biology techniques. Thank you to the Spain group for welcoming me into the Polymer labs. The project was supported by excellent technical staff including Jason Heath, Brenka McCabe, Dr Emilia Barker, Dr Robert Moorehead, Dr Magdalena Patel, Chris Hill, and Dr Nick Van Hateren.

The CDT programme, led by Prof Steve Armes, provided a useful series of business and polymer science workshops and the opportunity to undertake an industrial internship. I am grateful to The Electrospinning Company and Dr Mehri Behbehani for hosting me on an interesting and enjoyable internship that was funded by the EPSRC CDT and EIT INVENTHEI initiative.

Finally, thank you to my family and Cindy Ventura for love and support throughout my PhD.

List of outputs

Publications

- **Edmans, J. G**., Murdoch, C., Santocildes-Romero, M. E., Hatton, P. V., Colley, H.E., & Spain, S. G. (2020). Incorporation of lysozyme into a mucoadhesive electrospun patch for rapid protein delivery to the oral mucosa. *Mater. Sci. Eng. C*, **112**, 110917.
- **Edmans, J. G.**, Clitherow, K. H., Murdoch, C., Hatton, P. V., Spain, S. G., & Colley, H. E. (2020). Mucoadhesive electrospun fibre-based technologies for oral medicine. *Pharmaceutics*, **12**, 1–21.
- **Edmans, J. G.**, Ollington, B., Colley, H. E., Santocildes-Romero, M. E., Madsen, L. S., Hatton, P. V, & Murdoch, C. (2022). Electrospun patch delivery of anti-TNF α F(ab) for the treatment of inflammatory oral mucosal disease. *J. Control. Release*, **350**, 146–157.
- Submitted to Biomedical Materials Dec 2022: **Edmans, J. G.**, Murdoch, C., Hatton, P. V., Madsen, L. S., Santocildes-Romero, M. E., Spain, S. G., & Colley, H. E. Rapid bioactive peptide and protein release from a mucoadhesive electrospun membrane.
- In Preparation: **Edmans, J. G.**, Harrison, S., Murdoch, C., Hatton, P. V., Spain, S. G., & Colley, H. E.

Patents

- Santocildes-Romero, M. E., **Edmans, J. G.** (2021). Compositions for the delivery of proteins (WO/2021/072113)

Conference presentations

- Tissue and Cell Engineering Society (TCES) and United Kingdom Society of Biomaterials (UKSB) Joint Meeting, June 2019, Nottingham - Poster
- United Kingdom and Ireland Controlled Release Society (UKICRS) Annual Symposium, June 2019, Liverpool - Poster
- British Society for Oral and Dental Research (BSODR) Annual Meeting, September 2019, Leeds - Oral presentation
- White Rose Biomaterials and Tissue Engineering Group (BiTEG) conference, December 2019, York - Oral presentation
- BioMedEng21, September 2021, Sheffield - Oral presentation
- White Rose Biomaterials and Tissue Engineering Group (BiTEG) conference, December 2021, Sheffield - Online presentation, member of organising committee
- European Symposium on Controlled Drug Delivery (ESCDD), April 2022, Egmond aan Zee, Netherlands - Poster
- Tissue Engineering and Regenerative Medicine International Society (TERMIS) European Chapter Conference, July 2022, Kraków, Poland - Oral presentation
- Pan European Region of the International Association for Dental Research (IADR) Oral Health Research Congress, September 2022, Marseille, France - Oral presentation, runner up for Senior Colgate Prize

Contents

Abbreviations

3D	Three-dimensional
AA	Amino acid
ANOVA	Analysis of variance
API	Active pharmaceutical ingredient
BCA	Bicinchoninic acid assay
BHI	Brain heart infusion
BSA	Bovine serum albumin
CDR	Complementarity-determining region
DAPI	4′,6-diamidino-2-phenylindole
DCM	Dichloromethane
DMEM	Dulbecco’s modified Eagle’s medium
DMF	Dimethylformamide
EE	Encapsulation efficiency
ELISA	Enzyme-linked immunosorbent assay
F(ab)	Antigen-binding antibody fragment
FBS	Fetal bovine serum
Fc	Crystallisable antibody fragment
FDA	U.S. Food and Drug Administration
FITC	Fluorescein isothiocyanate

GLP-1	Glucagon-like peptide-1
HFIP	1,1,1,3,3,3-hexafluoro-2-propanol
HPLC	High performance liquid chromatography
IC_{50}	Half maximal inhibitory concentration
IgG	Immunoglobulin G
KGF	Keratinocyte growth factor
LPS	Lipopolysaccharide
Mab	Monoclonal antibody
MALDI-MS	Matrix-assisted laser desorption/ionization-mass spectroscopy
MDM	Monocyte-derived macrophage
MTT	3-(4,5-dimethylthiazol-2-yl)-2,5-diphenyltetrazolium bromide
NM	Nonmedicated
NOF	Normal oral fibroblast
NSAID	Non-steroidal anti-inflammatory drug
OC	Oral candidiasis
OD	Optical density
OECD	Organisation for Economic Co-operation and Development
OEE	Oral epithelium equivalent
OLP	Oral lichen planus
OMUE	Oral mucosal ulcer equivalent
PBS	Phosphate buffered saline

PCL	Poly(caprolactone)
PEG	Poly(ethylene glycol)
PEO	Poly(ethylene oxide)
PGA	Poly(glycolic acid)
PLA	Poly(lactic acid)
PLGA	Poly(lactic-*co*-glycolic acid)
PVA	Poly(vinyl alcohol)
PVP	Poly(vinylpyrrolidone)
qPCR	Real-time polymerase chain reaction
RAS	Recurrent aphthous stomatitis
RFU	Relative fluorescence units
RNA	Ribonucleic acid
RP-HPLC	Reverse phase high-performance liquid chromatography
rpm	Revolutions per minute
RS100	Eudragit® RS100
SD	Standard deviation
SDS	Sodium dodecyl sulfate
SDS-PAGE	Sodium dodecyl sulfate–polyacrylamide gel electrophoresis
SEM	Scanning electron microscopy
TEER	Transepithelial electrical resistance
TNFα	Tumor necrosis factor alpha

Chapter 1: Introduction

1.1. Motivation

Formulations for delivering medications to the inside of the mouth have, until recently, been greatly limited in the range of therapeutics that they can deliver effectively. This is the cause of many unmet clinical needs in oral medicine. Medicated polymer fibre-based oral patches prepared using electrospinning are a new technology offering numerous advantages including efficient drug release, site-specific delivery, increased exposure times, and flexibility. Further developing this technology for the delivery of peptide and protein drugs, classes of molecules which are particularly difficult to deliver with existing dosage forms, would introduce new treatment options for a wide range of debilitating mucosal conditions, including chronic oral ulcers caused by autoimmune disorders.

1.2. Oral mucosa

1.2.1 Anatomy

The oral mucosa is the mucous membrane lining the oral cavity and consists of a stratified squamous epithelium, basement membrane, lamina propria and submucosa (Figure 1.1).[4] The epithelium typically consists of five layers (stratum basale, stratum spinosum, stratum granulosum and stratum corneum) depending on level of keratinisation. The epithelium is made up of oral keratinocytes that originate in the stratum basale (basal layer), where they divide by uneven mitosis. In this process one daughter cell remains in the basal layer and is attached to the basement membrane where it can undergo further rounds of cell division. Daughter cells migrate apically into the stratum spinosum. Once in the spinous layer, the keratinocytes lose the ability to divide and begin a programme of terminal differentiation as they progress into the stratum granulosum. Here, the keratinocytes contain membrane coating granules that

extrude lipids and these, along with the low intracellular volume, act as a highly efficient permeability barrier against hydrophilic materials.[5] The keratinocytes finally enter the stratum corneum, where they can either shed their nuclei and increase keratin production to become keratinised or retain their nuclei and become non-keratinised, before eventually being lost to the oral cavity by desquamation.

The hard palate, dorsum of the tongue and the gingiva are covered in masticatory, keratinised stratified squamous epithelium whilst the inner lips (labial mucosa), cheek (buccal) mucosa, soft palate and floor of the mouth are covered in lining mucosa that consists of a non-keratinised stratified squamous epithelium. Although oral keratinocytes make up 95% of the total cell number in the oral epithelium, other important cells are present including dendritic cells that perform immuno-surveillance roles and sensory Merkel cells. The surface of the epithelium is bathed in mucins (highly glycosylated proteins) and inorganic salts are primarily secreted by sublingual salivary glands. These cause the gelation of the outer layer into a protective and lubricating layer of mucous 40–300 μm thick followed by an additional 70 μm coating of saliva.[4]

Basolateral to the oral epithelium is the lamina propria, a fibrous connective tissue layer where oral fibroblasts produce extracellular matrix, elastin, and type I and III collagen fibres. The lamina propria contains blood vessels and nerves. The submucosa beneath the lamina propria, which may or may not be present depending on the region of the oral cavity, consists of loose connective tissue that connects the oral mucosa to the underlying muscles. Healthy oral lining mucosa, such as that of the buccal mucosa, consists of approximately 40 to 50 epithelial cell layers,[6] with an average thickness of 294 ± 68 μm.[7] Epithelial thickness varies at different mucosal sites, with the floor of the mouth having the thinnest mucosa.

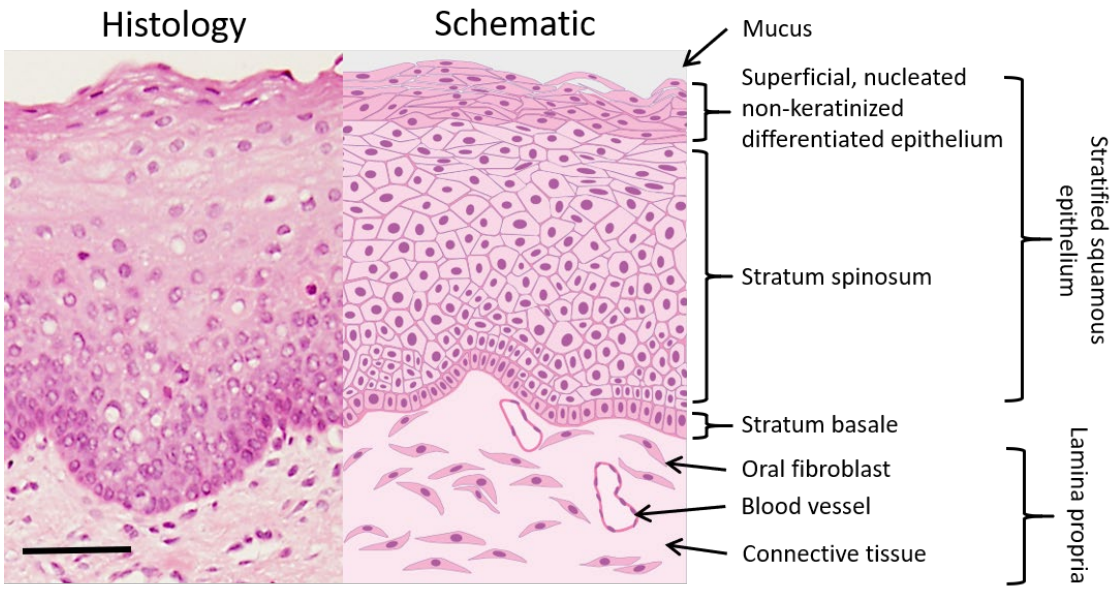

Figure 1.1. Histological (left) and schematic (right) image of the buccal oral mucosa (Histological image courtesy of Prof. Keith Hunter, Unit of Oral Pathology, University of Sheffield) Scale bar = 100 µm.

1.2.2 Drug permeation

The permeability of the oral epithelium is dependent on its thickness, lipid content in the granular layer and degree of keratinisation. In general, the higher lipid content in keratinised regions reduces the permeability.[6] Oral mucosal permeability is lower than in the intestine due to greater thickness and lower surface area of the epithelium. There are multiple routes for a drug to pass through the oral mucosa and the predominant route depends on the physicochemical properties of the drug.[8] Small lipophilic drugs such as fentanyl[9] often partition into cell membranes, and so diffuse predominantly through the epithelial cells (transcellular route) and often cross the oral mucosa efficiently without any permeation enhancers. In the case of ionisable small molecule drugs, such as lamotrigine, the pH of the delivery system may be adjusted to favour the non-ionised form to promote transcellular diffusion.[10]

Larger and more hydrophilic compounds, including peptides, tend to favour transport around keratinocytes (paracellular route) and are usually less well absorbed.[11] For certain drugs, transcellular transport across the oral mucosa may occur via carrier-mediated transport. For

example, there is evidence that monocarboxylate[12] and glucose[13] transporters are expressed on the keratinocyte cell surface; therefore, drugs that are substrates for transporters may have increased epithelial uptake.

Diseased oral tissue usually originates in the epithelium. For example, malignancy occurs due to genetic defects in the basal keratinocytes leading to uncontrolled cell division. Auto-inflammatory diseases such as oral lichen planus occur as a result of immune cell-mediated damage of the stratum basale, whilst fungi such as *Candida albicans* can infect the upper epithelial layers causing oral candidiasis or denture stomatitis. The epithelium is the main drug delivery target for most oromucosal indications;[14] therefore, the drug is required to permeate the epithelium to some extent to achieve therapeutic local concentrations. Many mucosal diseases produce lesions or ulcers in which the barrier properties of the epithelium are disrupted or absent, which may facilitate efficient topical delivery to the diseased tissue.

Transmucosal delivery through the oral mucosa is of interest for the minimally invasive delivery of drugs with low oral bioavailability. To achieve systemic transmucosal delivery, drugs must efficiently permeate the intact sublingual or buccal epithelium and reach the underlying tissue, which is well vascularised, enabling rapid absorption into the bloodstream and bypassing first-pass metabolism.[11] The oral mucosa has recently attracted attention as a site for vaccine delivery.[15] Theoretically, the delivered antigen could induce the desired immune response by activating resident immune cells within the epithelium or lamina propria. RNA-based vaccines would need to be delivered to the cytoplasm of epithelial cells using membrane-permeable carriers to translate the encoded antigen.

1.2.3 Current oromucosal drug delivery systems

A variety of commercially available formulation types target the oral cavity. These have been reviewed by Hearnden *et al.*[16] and some commercial examples are highlighted in Table 1.1. A

recent detailed market analysis on oromucosal formulations with a focus on systemic delivery has been published by Bastos *et al.*[17] Mouthwashes are commonly used for the local delivery of antimicrobials and fluoride.[18] Mucoadhesive gels, pastes, and hydrogel-forming films are also mostly used for topical delivery or to form protective layers over wounds, for example to treat ulcers and sores.[19] Gels have also been trialled for the systemic delivery of analgesics[20] and anti-hypertensives.[21] Buccal tablets and lozenges are used for both topical and systemic delivery and may include mucoadhesives. Here, drugs are released as the tablet dissolves, offering exposure times of up to 30 minutes.[22] The tablets are typically applied on the inside of the lip, sandwiched between the buccal and gingival mucosa, and are easily dislodged if applied to other surfaces within the oral cavity. Buccal tablets are primarily used for systemic delivery of drugs with low oral bioavailability and have been developed with several drugs including opioid painkillers,[22] nitroglycerin, and steroid hormones for hormone replacement therapy.[16] Buccal tablets have also been used for the local delivery of antifungals to treat oral candidiasis.[23]

Similarly, films are thin polymer strips that usually dissolve rapidly when applied.[16,24,25] They typically provide exposure times of less than thirty seconds. They are used for the systemic delivery of highly permeating drugs, are easy to self-administer, and enable rapid delivery due to the high blood flow in the oral mucosa. Films are in a late stage of development for the delivery of painkillers and antinausea drugs (IntelGenx corp.).

Patches are an emerging alternative dosage form for oromucosal drug delivery. They are flexible and can provide longer residence times than buccal films and tablets, lasting up to 15 h.[26] They can release drugs by dissolution or by diffusion, allowing a controlled release rate. Soluble patches are typically used to release drugs into the oral cavity for local delivery. Insoluble patches may also have an impermeable backing layer to promote unidirectional delivery into the oral mucosa. Besides drug delivery, buccal patches may also be useful on their

own as wound dressings for oral ulcers. Patches can consist of soluble or cross-linked polymer hydrogels[27] or more recently of electrospun fibres.[28]

Table 1.1 Commercial examples of oromucosal drug delivery systems

Type	Example	Reference
Mouthwashes	Chlorhexidine mouthrinses are antibacterial and are used to treat gingivitis and periodontal disease (Periogard®, Proctor and Gamble)	16
Creams/ointments/gels/pastes	Gelclair® mucoadhesive gel (EKR Therapeutics, Inc.) reduces the pain of mouth sores by providing a lubricating protective barrier	16
	Daktarin® oral gel (Johnson & Johnson) contains miconazole to treat fungal infections such as oral candidiasis	
Sprays	Mucosamin® spray (Professional Dietetics, S.p.A) contains amino acids and hyaluronic acid to promote regeneration of the oral epithelium thereby providing relief from oral mucositis	29
Tablets	Buccastem M® buccal tablets (Alliance Pharmaceuticals, Ltd.) allow transmucosal delivery of prochlorperazine maleate to relieve migraine nausea	30

1.3. Electrospun mucoadhesive materials

1.3.1 Electrospinning

Electrospinning uses a high voltage (5-30 kV) to produce polymer fibres with diameters ranging from 2 nm up to several μm from a polymer solution or melt.[31] At least 16 electrospun medical devices are in late stages of regulatory or market approval, with the majority being used as surgical grafts, coatings for medical devices, or for tissue regeneration.[1,32] The technique is particularly promising for drug delivery due to the high surface area of the resulting fibre mesh, which allows a drug to be incorporated and released at a controlled rate by either diffusion or the degradation of the fibres.[33]

A typical electrospinning setup consists of a spinneret loaded with polymer solution, a high voltage power supply, and a grounded or charged collector (Figure 1.2 A). The power supply injects charge into the solution causing a stream to accelerate away from the tip due to the electrical repulsion overcoming surface tension and viscosity. A syringe is pushed at a controlled flow rate by a syringe pump to refill the spinneret tip. Polymer entanglements increase viscosity, leading to the formation of continuous fibre rather than droplets. The polymer stream undergoes whipping motions caused by electrostatic repulsions between bends in the stream, which further elongates the fibres.[34] The solvent evaporates rapidly during the flight, leaving a mat of polymer fibres on the collector plate (Figure 1.3).

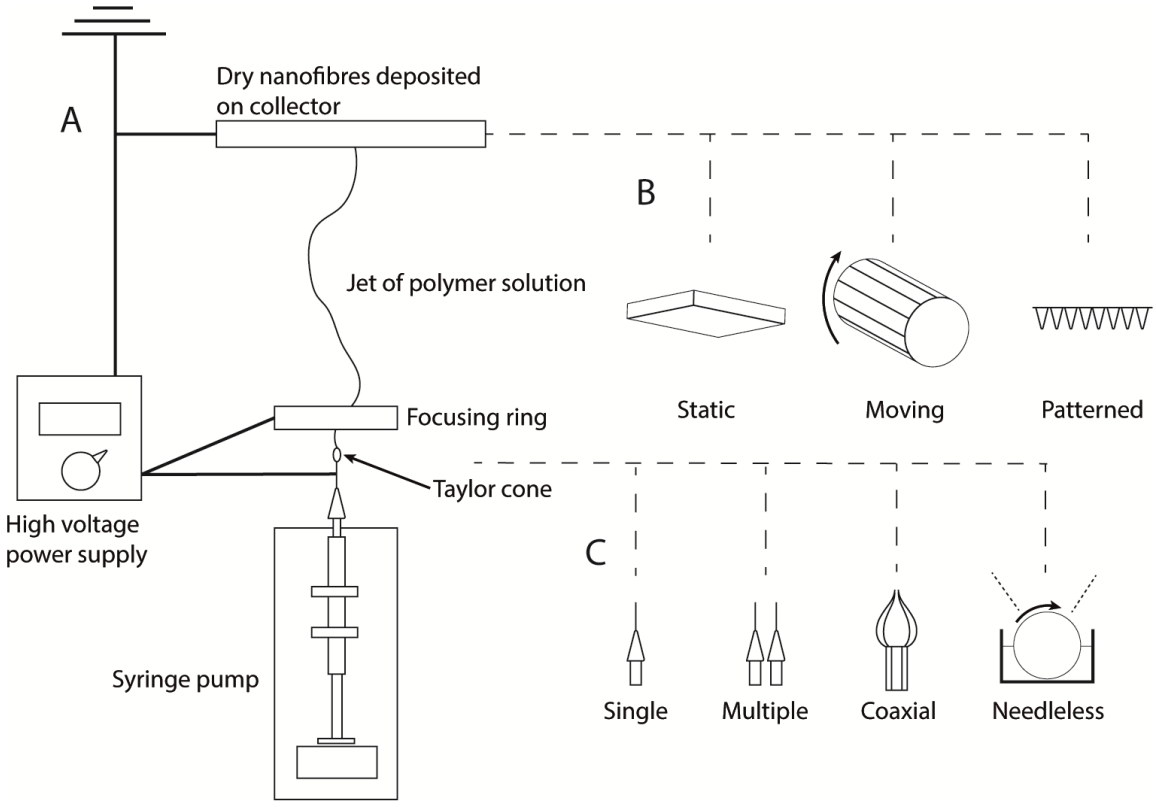

Figure 1.2 (**A**) Schematic diagram of typical electrospinning apparatus. A high voltage power supply injects charge into the metallic syringe tip causing a polymer jet to be ejected towards the grounded or oppositely charged collector plate. The jet dries during flight, depositing a micro- or nanofibre mesh. (**B)** Static collectors result in a randomly aligned mesh of fibres; moving collectors can be used to produce aligned fibres; patterned collectors result in textured membranes. (**C**) Multiple needles in combination with a moving collector allow increased output or the production of mixed fibre types; coaxial needles allow the production of core-sheath fibres with multiple polymer domains; needleless spinnerets allow many polymer jets to be produced simultaneous to give increased output.

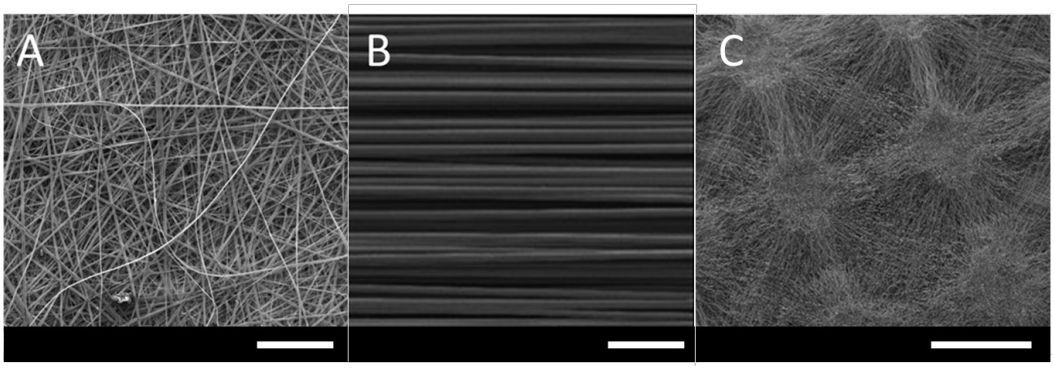

Figure 1.3. (**A**) Scanning electron microscopy image of fibres electrospun from a solution of Eudragit® RS100 and poly(vinylpyrrolidone) in ethanol/water using a static collector. Scale bar = 100 μm (**B**) Aligned polyhydroxyalkanoate blend fibres electrospun from chloroform using a rotating cylinder collector. Scale bar = 100 μm. Reproduced from *J. Tissue Eng. Regen. Med.* **2019**, *13*, 1581–1594 under CC BY 4.0.[35] (**C**) Poly(3-hydrroxybutyrate-co-3-hydroxyvalerate) fibrous membranes with rectangular micropatterns electrospun from dichloromethane/methanol using a micropatterned static collector. Image courtesy of Dr Ílida Ortega Asencio, University of Sheffield. Scale bar = 1mm.

Several different types of collectors can be used for electrospinning, most commonly a static plate or a rotating drum (Figure 1.2 B). Rotating drums allow a more uniform membrane thickness or the collection of aligned fibres, which are typically less porous and have different surface and mechanical properties.[31,36] Removable templates or device coating can also be used to produce a three-dimensional patterned surface.[37] Solution and processing parameters affect fibre morphology, including diameter and the incidence of defects. These effects have been reviewed in detail.[31] In general, higher solution conductivity and lower solution viscosity are associated with narrower fibres while viscosity must be suitable to counteract solution surface tension effects and allow a continuous stream to flow.

Other modifications to the electrospinning technique include the production of fibres with multiple polymer domains using coaxial, triaxial, emulsion, or side-by-side electrospinning (Table 1.2 C).[38–42] For drug delivery, these can be used to improve the processability of a drug-containing phase using a second polymer phase or to influence release rate or surface properties by encapsulating the drug within a sheath. There has recently been interest in high throughput micro- and nanofibre production to allow more economical mass production. Needleless electrospinning involves injecting charge into a trough or surface containing polymer solution, causing many polymer jets to be produced simultaneously.[43,44] Centrifugal spinning/electrospinning involves a heated rotating cylinder as the spinneret, which ejects molten polymer or solution through narrow outlets under centrifugal force or in combination with an applied electrical field. These techniques potentially enable high-throughput or solvent-free production but are challenging to optimise and validate for biomedical applications.[45] Currently, arrays of uniaxial needles are routinely used to increase scale in industrial settings.

Table 1.2. Variations and modifications to the electrospinning technique

Modification	Type	Application	Reference
Focusing ring	Attachment	Controlled jet shape	[46]
Solvent guard	Attachment	Prevents needle clogging	
Rotating mandrel collector	Collector	Aligned fibres, more uniform membrane thickness	[35]
Belt collector	Collector	Increased output	[47]
Patterned collector	Collector	Patterned membranes	[37]
Coaxial	Spinneret	Multiple domain fibres	[48]
Side-by-side/Janus	Spinneret	Multiple domain fibres	[42,49]
Simultaneous electrospinning	Spinneret and collector	Mixed-fibre membranes	[50]
Multi-needle	Spinneret	Increased output	[50]
Needleless	Spinneret	Increased output	[44]
Centrifugal	Spinneret	Increased output	[45]
Emulsion	Feedstock	Multiple domain fibres	[39]
Sequential electrospinning	Feedstock	Multiple-layered membranes	[50]
Melt	Feedstock	Solvent free manufacture	[51]
In Situ mixing	Feedstock	Porous fibres	[52]

1.3.2 Biocompatible polymers

It is important that the device and its components be non-irritant and non-toxic both in the oral cavity and in the gastrointestinal tract in case it is accidentally swallowed. The most commonly used polymers for electrospun drug delivery systems are biodegradable polyesters such as poly(lactic acid) (PLA), poly(glycolic acid) (PGA), poly(lactic-*co*-glycolic acid) (PLGA), and poly(caprolactone) (PCL).[53] These polymers, which have been extensively studied for use in orthopaedic devices where biodegradability is often desirable,[54] are typically soluble in organic and halogenated solvents such as chloroform, dichloromethane (DCM), dimethylformamide (DMF), and tetrahydrofuran[55] and have high tensile strengths.

Biodegradable polyesters are also suitable for oromucosal devices as they are often non-inflammatory over the relevant timescales, easily processed, easily sterilised, and have good shelf lives. These polymers are not typically adhesive but can be blended with a mucoadhesive or used as part of a composite system to improve residence time. Poly(ethylene glycol) (PEG),

poly(vinyl alcohol) (PVA) and poly(vinylpyrrolidone) (PVP) are commonly used water-soluble polymers. These have been included in a wide variety of pharmaceutical products and are generally considered biologically inert,[56,57] which makes them a good option for rapidly dissolving membranes or for increasing hydrophilicity in combination with an insoluble polymer.

1.3.3 Mucoadhesive polymers

The moistness of the oral mucosa makes it a challenging site for adhesion; therefore, mucoadhesives are often required to achieve acceptable residence times. Depending on the nature of the polymer, several different mechanisms may be involved in mucoadhesion. These include the effects of surface tension, dehydration, diffusion, electrostatic interactions, and chemical adsorption.[58] Water-soluble polymers such as PVP swell rapidly, causing the dehydration of the mucus layer.[58] The swelling results in intimate contact between the polymer and mucus glycoproteins and hydrates the polymers, further increasing the rate of diffusion into the substrate. Prolonged adhesion arises due to hydrogen bonding or ionic interactions between the interpenetrating polymers and glycoproteins.

In general, higher molecular weight water-soluble polymers result in improved residence times due to slower dissolution and increased chain length for interpenetration.[59] More flexible polymers with linear-chain configurations tend to diffuse more easily into the biological tissue, resulting in increased number of interactions and improved adhesion.[60] Non-linear polymers, such as dextrans, are more bulky and less able to interpenetrate with the tissue. Polymers with similar surface chemistry to the glycoproteins are likely to be miscible and able to diffuse into the mucus.[61]

Natural carbohydrate and protein polymers that have been widely reported to have mucoadhesive properties include chitosan,[62] gelatin,[63] hyaluronic acid,[64] and alginates.[65] These

polymers are charged at physiological pH; therefore, electrostatic interactions in combination with hydrogen bonding are likely involved in the adhesion mechanism. Synthetic polyionic polymers such as poly(acrylic acids), including Carbopol®,[66] and the Evonik Eudragit® series have also shown mucoadhesive properties.[67,68] Thiolated polymers such as thiolated chitosan[69] and thiolated hyaluronic acid,[70] adhere by forming disulfide bridges with cysteine domains in mucins, resulting in adhesion through chemical adsorption.

The mucoadhesive formulations investigated in this thesis are based on the work of Santocildes-Romero *et al.*, who developed an electrospun mucoadhesive patch for the oral mucosa containing adhesive fibres made from a blend of PVP, Eudragit® RS100 (RS100), and poly(ethylene oxide) (PEO).[67] PVP is a non-toxic water-soluble polymer that facilitates the hydration of the patch (Figure 1.4). The manufacturer states that RS100 is a statistical copolymer of ethyl acrylate, methyl methacrylate and trimethylammonioethyl methacrylate chloride (1:2:0.1 molar ratio, M_w = 32000 g/mol). It is insoluble in aqueous conditions, and so prevents the patch from dissolving but swells and becomes water permeable, allowing the patch to become rapidly hydrated. The high surface area associated with the microfibre morphology further increases the rate of hydration and brings the surfaces into contact through capillary action and osmotic pressure. Prolonged adhesion is most likely a result of electrostatic interactions involving the cationic RS100 segments as well as hydrogen bonding of both PVP and RS100 to the mucosa. PEO, a water-soluble polymer, is also included. PEO was found to reduce long-term mucoadhesion,[67] likely due to the overhydration of the interface and PEO interacting less strongly with the mucosa than the other polymers.

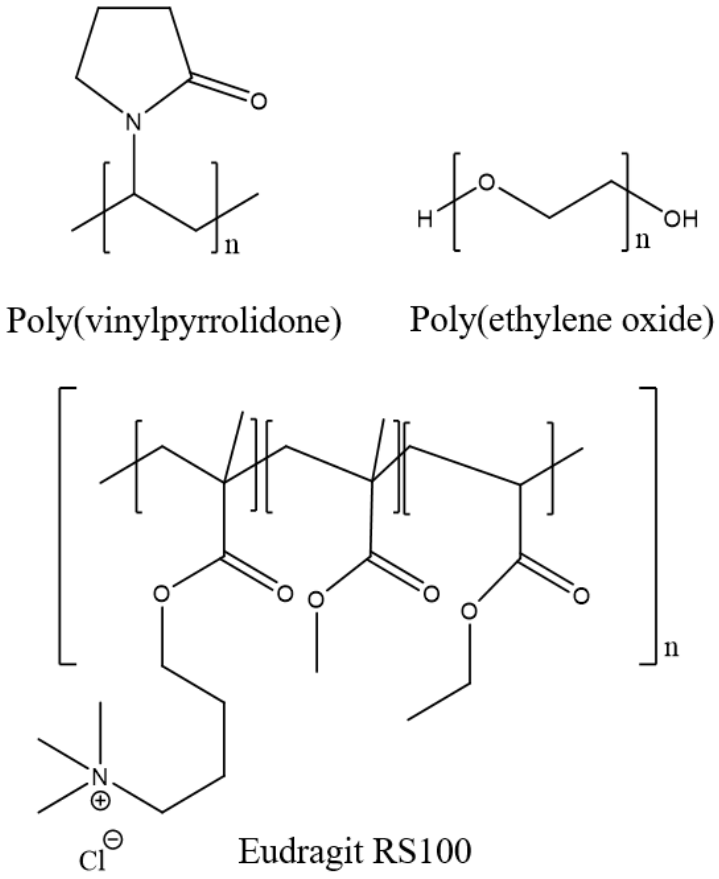

Figure 1.4. Polymer components of the mucoadhesive layer of the Rivelin® patch. PVP and PEO promote swelling and initial mucoadhesion. Prolonged adhesion is likely caused by interpenetration and hydrogen bonding of carbonyl groups with glycoproteins in the mucus layer as well as electrostatic interactions involving the quaternary amine groups of RS100.

1.3.4 Encapsulation and release of drugs and proteins

There has been extensive research into medicated electrospun fibres for various drug delivery applications.[53,71] These are typically prepared by adding drug to the polymer solution before electrospinning, which often results in highly efficient encapsulation. In general, drug compatibility with the solvent and the effect on solution properties, which affect electrospinning performance, are important considerations. Release of the drug is often rapid and efficient for hydrophilic fibres, which release the drug as they dissolve or swell.[72] Hydrophobic fibres are considered for controlled or sustained drug release. Drug release from

hydrophobic fibres is often bi- or trimodal, a phenomenon illustrated in an article by Wu *et al.*[73] An initial rapid burst of first-order release is frequently observed due to desorption of drug at the fibre surface or within pores. Burst release is often more prominent for drugs with a lower affinity for the solvent, which tend to partition to the fibre surface during electrospinning.[53] A period of sustained zero-order release is typical, often over a period of days or weeks, mediated by slow diffusion of the drug through the fused polymer structure.[73] For degradable fibres, a third stage may be observed in which the remaining drug is released as the fibres break down. Multiple-domain fibres are often considered for encapsulating drugs with incompatible solvent requirements or for tuning release kinetics. For example, coaxial and triaxial systems can be used to prevent burst release and achieve a sustained zero-order release.[41,74] Alternatively, bioactive molecules may be chemically or physically adsorbed onto pre-formed fibres.[75,76]

Protein encapsulation into synthetic polymer fibres by electrospinning has recently been reviewed by Moreira *et al.*[77] There has also been considerable investigation into entirely protein-based fibres for tissue engineering purposes, as reviewed by Khadka *et al.*[78] Encapsulation within monolithic uniaxial fibres is generally achievable using non-denaturing aqueous polymer solutions,[79] although this usually produces water-soluble materials with a limited range of uses. Chitosan is soluble in acidic solutions but insoluble at physiological pH. This has been exploited to allow encapsulation of proteins from an acidified aqueous solution within mucoadhesive gel-forming fibres.[80]

Multiple studies have attempted to encapsulate proteins within hydrophobic fibres by fully dissolving them in an organic solvent mixture before electrospinning, for example with DMF as a protein-solubilising cosolvent. Eriksen *et al.* incorporated a fluorescent labelled antimicrobial peptide into PCL fibres by electrospinning with 19:1 chloroform/methanol.[81] The peptides was found to aggregate into particles within the fibres and antimicrobial activity could

not be confirmed in inhibition zone assays, suggesting that the peptide may have been denatured. Gandhi *et al.* encapsulated an immunoglobulin G (IgG) antibody within PCL fibres using 60:40 w/w DMF/DCM with bovine serum albumin (BSA) as an excipient.[82] At least some activity was observed in the partially-released antibody using a non-quantitative cell staining assay.

To minimise exposure to denaturing solvents, emulsion or coaxial electrospinning have been investigated for protein encapsulation.[77] Emulsion electrospinning involves emulsifying the aqueous protein phase with the organic polymer solution before electrospinning. Coaxial electrospinning uses concentric needles to allow the processing of separate solutions (a protein-containing aqueous phase and an organic phase) such that the protein is encapsulated within the core of core-sheath fibres. Ji *et al.* compared coaxial and emulsion electrospinning for incorporating alkaline phosphatase into PCL fibres.[83] PCL in 2,2,2-trifluoroethanol was used as the organic phase and PEO used to improve electrospinning performance of the aqueous phase. An enzymatic assay showed that the protein maintained 49% and 76% activity for emulsion and coaxial electrospinning respectively. Both materials provided sustained protein release over a period of 2-3 weeks, although release was slower for the coaxial fibres. A solid-in-liquid emulsion strategy was used by Liu *et al.,* who added lysozyme nanoparticles to a solution of PLGA in 2,2,2-trifluoroethanol before electrospinning.[84] The lysozyme was dispersible but insoluble in the solvent, which facilitated electrospinning. The hydrophobic nature of the fibres resulted in incomplete release; however, the partially released lysozyme was functional. These studies, and others,[85] have reported that emulsion electrospinning is challenging to optimise to produce uniform fibres, although it is possible.[86] In most cases, these processes reduce, but may not fully eliminate, solvent-induced denaturation.

1.3.5 Excipients and other considerations

Where permeability is a limiting factor, permeation enhancers may be incorporated into the delivery system. There are a variety of classes of permeation enhancers with different modes of action that are outlined in reviews by Sudhakar *et al.* and Sohi *et al.*[11,87] In general, lipophilic uncharged drugs are more strongly affected by enhancers that increase membrane fluidity, such as fatty acids or laurocapram.[87] The mechanism of action of these classes is theorised to be a result of improved solubility of the drug in cell membranes, leading to faster uptake. Supporting evidence for this mechanism has recently been produced using permeation kinetic experiments and mass spectrometry imaging, showing co-localisation of the drug with the enhancer and increased capacity for the drug in the mucosa.[88]

Hydrophilic drugs are generally more affected by surfactants, including bile salts, which are believed to extract lipids from the epithelium and form aqueous reverse-micelle channels within the tissue.[87] This increases the intracellular space available for paracellular transportation and thus increases the rate of permeation. At this stage there has been little research involving electrospun systems containing permeation enhancers; however, many mucoadhesive polymers, in particular chitosan, are often theorised to enhance permeation by disrupting the structure of mucins, lipids, and tight junctions at the mucosal surface, although evidence for this in the oral mucosa is lacking.[89]

In some cases, excipients have been included in electrospun systems to further enhance drug solubility, for example emulsifiers or complexing agents.[90–92] Nanoparticle drug delivery vectors, such as liposomes have previously been incorporated into electrospun materials for a variety of non-oromucosal applications.[93–95] Research on oromucosal films containing nanoparticles has shown improvements to absorption and drug solubility and may protect certain drugs from enzymatic degradation.[96]

Other considerations for a topical dosage form that adheres to the oral mucosa include disturbances to taste, speech, eating, and drinking.[16] It is preferable to avoid foul tasting drugs and excipients or to deliver them unidirectionally into the mucosa. Thin and flexible dosage forms may reduce the likelihood of the device becoming dislodged by mechanical forces in the mouth; therefore, flexible polymeric films or patches may be preferable to more traditional tablets in this regard.

1.3.6 Material characterisation

No standardised method has been identified to measure mucoadhesion and there is no obvious correlation in results between methods. The most common tests involve use of a texture analyser to measure mucoadhesive strength, the perpendicular force required to break, pull, or peel away the sample from a model membrane.[97–99] Alternatively, *in vitro* residence time tests may be used to measure time until detachment, for example from *ex vivo* animal mucosa in a simulated saliva medium.[28]

Different experimental *in vitro* set-ups have been used to quantify drug release kinetics. One such set-up is the paddle-over-disc method for transdermal patches, which measures one-sided patch dissolution in a buffer at a paddle speed of 50–100 rpm. At the pre-determined time points, an aliquot is removed from the test solution and replaced with an equivalent volume of fresh buffer solution. The samples are then analysed by spectrophotometry techniques[72] or high performance liquid chromatography (HPLC)[100] to obtain a graph of the drug release over time. Simplified versions of this may also be performed by immersing the patch freely in the release medium[72] or adhered to a glass slide[101] and stirring the medium with a magnetic stirrer bar or laboratory shaker.

In vitro cell-based assays are important at the pre-clinical stage for evaluating irritation potential. Cell metabolic assays are often used to give an indirect measure of cytotoxicity, for

example the 3-(4,5-dimethylthiazol-2-yl)-2,5-diphenyltetrazolium bromide (MTT) assay which is recommended by the Organisation for Economic Co-operation and Development (OECD) to assess potential for skin irritation.[102] To obtain a more direct measure of irritancy, the concentrations of pro-inflammatory cytokines, such as interleukin-1 alpha, in the cell supernatant can be measured using an enzyme-linked immunosorbent assay or associated gene expression can be measured using quantitative polymerase chain reaction (qPCR).[103–105] Monolayers of cultured oral keratinocytes isolated from healthy tissue or keratinocyte cell lines can be used as *in vitro* models to test oromucosal materials.[106,107] Three-dimensional oral mucosal equivalents are increasingly preferred, being more physiologically representative and offering more accurate predictions of cell-toxicity while avoiding the use of animal models.[108,109]

Drug diffusion across *ex vivo* oral mucosa may be measured using drug permeation chambers, such as the Franz diffusion cell. In such chambers, the tissue is placed between donor and receptor chambers, where the donor chamber contains the dosage form and the receptor chamber holds a temperature-controlled physiologically relevant buffer solution. In some cases, synthetic membranes may be appropriate to eliminate variability in animal tissue.[110] For these methods the solution is removed from the receptor chamber at pre-determined time points to measure the drug permeation over time, for example using a spectrophotometer or HPLC.

More recently, the localisation of small molecule permeants within the oral mucosa itself has been visualised down to a micrometre scale resolution using matrix-assisted laser desorption ionisation-mass spectrometry imaging (MALDI-MS) on sectioned tissue.[111] Many biologics are detectable using antibodies; therefore, immunohistochemistry or immunofluorescence can be used to visualise their distribution within the targeted tissue.[112] Fluorescent labelling of the permeant is also possible; however, the effect on the physicochemical properties and specific interactions between the dye and the dosage form should be considered.

1.4. A review of mucoadhesive electrospun fibre-based dosage forms for oral medicine

1.4.1 Anti-inflammatory agents

Chronic inflammatory diseases in the oral cavity are often mediated by dysregulated immune responses initiated by pathogens, foreign bodies, ionising radiation, or autoimmune disorders. Diseases include oral lichen planus (OLP), which produces white lesions affecting 1–3% of the world's population, and recurrent aphthous stomatitis (RAS), also known as aphthous ulcers or canker sores.[113,114] The aetiology of many chronic oral inflammatory diseases is poorly understood and no prophylactic treatments are available. Instead, corticosteroids or other anti-inflammatory agents are commonly used off-label to manage the severity of ulcers and lesions. Systemic corticosteroid delivery often results in unacceptable side effects, whereas existing topical formulations, such as rinses, lozenges, and ointments, must be reapplied several times per day and result in inconsistent dosing. Topical corticosteroids are also associated with some serious adverse effects, including adrenal suppression and secondary candidiasis,[115] therefore formulations that allow the specific delivery of well-defined doses are desirable. Ulcers and lesions are often highly sensitive, therefore mucoadhesives, once carefully applied, may also prevent pain by providing a protective barrier against mechanical stimulation.

Colley *et al.* (2018) conducted a pre-clinical study on Rivelin® patches loaded with the corticosteroid clobetasol-17-propionate to treat chronic oral inflammatory diseases. The patches consisted of a drug-loaded (up to 20 μg per patch) layer of mucoadhesive fibres consisting of PVP and RS100 with PEO particles electrospun from 97% ethanol.[28] Drug-loaded patches released 80% of the drug over a 6 h period. *In vitro* cytotoxicity testing with tissue-engineered oral mucosal equivalents concluded that the patches were non-irritant.[109] This

formulation recently successfully met the primary end point in phase IIb clinical trials (ClinicalTrials.gov identifier: NCT03592342) for the treatment of OLP, showing a significant reduction in ulcer area, and is in the development pipeline to become the first such electrospun mucoadhesive on the market.

Wei *et al.* (2019) used needleless electrospinning with a double ring shaped spinneret for the rapid production of 3-layer composite meshes consisting of a layer of mucoadhesive PEO fibres containing 30% w/w diclofenac sodium electrospun from water, and a layer of hydrophobic PLA fibres electrospun from 1,1,1,3,3,3-hexafluoro-2-propanol (HFIP) containing curcumin at up to 4% w/w. Curcumin was used as a model anti-inflammatory agent that may be beneficial for the treatment of RAS and diclofenac sodium, an antimicrobial analgesic, to reduce the risk of infection and relieve pain. The fibres were then placed onto a hypromellose-based gel in a mould and allowed to dry to produce an adhesive backing layer. Diclofenac sodium was shown to inhibit the growth of *Staphylococcus aureus* by placing the patches onto a bacterial lawn grown on a blood agar plate. Curcumin was shown to maintain its anti-inflammatory properties by measuring reduced pro-inflammatory gene expression by activated human monocytes. The release of curcumin from the fibres was sustained over a period of two weeks.[43] A relatively slow release, which is typical of hydrophobic fibres loaded with a hydrophobic drug and would potentially be disadvantageous for more expensive drugs, given that shorter residence times are more appropriate for RAS ulcers. The multiple layers of fibres make the system suitable for the co-administration of water soluble and insoluble drugs, which is useful for inflammatory diseases, where a combination of different therapeutic agents may be beneficial (for example corticosteroids, antimicrobial agents, and analgesics).

Alipour *et al.* (2022) integrated triamcinolone, a corticosteroid, into fibres made from a blend of ethylcellulose and gliadin.[116] Gliadin is a plant-derived protein. It's inclusion in the fibres significantly increased the rate of drug release, likely due to increased hydrophilicity and

swelling. *In vitro* testing using human gingival fibroblasts cultured on the surface of the material indicated that the material was non-cytotoxic and the released steroid inhibited the release of inflammatory cytokines following stimulation with lipopolysaccharides, providing evidence for an anti-inflammatory effect.

Inflammatory oral diseases are highly prevalent and represent a great unmet clinical need. Electrospun patches offer improved residence times over topical ointments and rinses and, unlike buccal tablets, are flexible and therefore less likely to place mechanical stress on sensitive lesions and ulcers. There is potential for further biological research in this area to improve our understanding of the aetiology of these diseases and identify the most appropriate active pharmaceutical ingredients.

1.4.2 Local anaesthesia and analgesics

Chronic oral mucosal pain is a common complaint that can have a wide variety of causes including infections, inflammation, chemotherapy, or surgery.[117] Over the counter oral non-steroidal anti-inflammatory agents (NSAIDs) and paracetamol are effective for oral pain management, but with some side effects associated with long-term use. NSAIDs can cause or delay the healing of oral ulcers, and so may not be appropriate for all kinds of oral pain.[118] Topical anaesthetics, such as lidocaine, are also highly effective for local pain relief and are commonly applied as gels or lozenges. Over 50% of patients undergoing treatment for head and neck cancer suffer from oral mucositis,[119] a disruption in the oral epithelium, leading to painful inflammation and ulceration. Magic mouthwashes are a commonly used palliative treatment, typically containing combinations of local anaesthetics (lidocaine), antihistamines, antimicrobial agents, corticosteroids, and coating agents. These have unclear effectiveness and often result in side effects.[120] Some studies recommend morphine mouthwashes for superior pain relief with reduced side effects.[121,122]Anaesthetic injections are used for many dental

procedures; however, dental injections are the cause of dental anxiety for some patients.[123] Alcohol-based solutions may be applied topically using a cotton swab as an alternative. These have an unpleasant taste and can spread across the oral mucosa uncontrollably.[124] Electrospun mucoadhesive patches may offer another useful delivery method for dental anaesthesia or the treatment of chronic pain with improved site-specificity and prolonged delivery in comparison to rinses and ointments and with reduced thickness and improved flexibility over adhesive tablets.

Rapidly dissolving electrospun membranes were previously developed as a potential delivery method for dental anaesthetic. Illangkoon *et al.* (2014) successfully fabricated electrospun PVP fibres loaded with mebeverine (up to 30% w/w), a drug with several applications including as a local dental anaesthetic. As would be expected of high surface area fibres of a water-soluble polymer, dissolution studies showed very rapid release, with the fibres dissolving within 10 s, allowing for a convenient application method with improved dissolution over the neat drug.[72]

Reda *et al.* (2017) incorporated ketoprofen, a non-steroidal anti-inflammatory drug, into Eudragit EL or Eudragit ES polymer fibres by electrospinning from ethanol/water mixtures and investigated their use for treating oral mucositis.[125] The fibres were compared to solvent-cast films and found to release the drug much more efficiently due to their higher surface area. A simulated buccal ulcer was induced in rabbits by injuring with acetic acid and applying medicated Eudragit EL membranes daily for 5 days. Histological analysis seemed to show less serve ulceration in the treated rabbits in comparison to those left untreated. It is unclear to what extent this can be attributed to drug delivery or the effect of a wound dressing. The study does not provide evidence that the formulation would have a pain-relieving effect and a chemically induced ulcer may not be representative of oral mucositis.

Clitherow *et al.* (2019) investigated the Rivelin formulation, consisting of drug-loaded fibres of blended PVP and RS100 with a PCL backing film, for the delivery of lidocaine HCl to the oral mucosa for the management of prolonged pain and as a local anaesthetic. Lidocaine HCl was loaded into the fibres at 2.5% w/w. The patches released around 80% of the loaded lidocaine within 1 h and permeation experiments showed a permeability of 136 μg cm^{-2} min^{-1} in *ex vivo* porcine buccal tissue. Additionally, lidocaine released from the patches inhibited veratridine-mediated opening of voltage-gated sodium channels in SH-SY5Y neuroblastoma cells in a real-time functional assay, showing that therapeutic activity was maintained. The distribution of lidocaine in porcine buccal mucosa was imaged using MALDI-MS to show time-dependent permeation, providing for the first time strong evidence of the electrospun patches' efficacy as a local delivery method for dental anaesthetic to the oral mucosa.[113]

Oral pain represents a large market with multiple unmet clinical needs and is therefore a promising application for electrospun systems. Multiple studies have reported suitable release of lidocaine HCl from biocompatible mucoadhesive materials and some early results show effective targeted delivery. Further *in vitro* and *in vivo* investigation is expected in the near future. There is also scope to investigate the versatility of electrospun fibres for the delivery of alternative agents, which may be more effective for treating oral mucositis, such as benzydamine HCl, opiates, and amylmetacresol/dichlorobenzyl alcohol.[120,126]

1.4.3 Antimicrobials

Oral candidiasis is caused by the opportunistic overgrowth of Candida, most commonly *C. albicans* in the oral cavity. It is common in predisposed patients, such as people with dentures, diabetics, immunocompromised patients, and those on long-term antibiotic or steroidal therapy.[127] The infection can be present as superficial plaques, red lesions, or chronic plaques caused by fungal invasion of the epithelium. In some cases, oral candidiasis may cause burning

sensations, unpleasant tastes, or difficulty swallowing. Topical antifungal steroid rinses containing nystatin or miconazole are the first line treatment and are usually effective. Even the most well tolerated antifungal rinses are sometimes associated with side effects including vomiting and diarrhoea and their high sucrose content can exacerbate other conditions such as tooth decay and diabetes.[127] Although rinses are effective when applied 4 times per day, there is potential to minimise side effects using a specific delivery method. Sustained release through mucoadhesive patches may allow the minimum inhibitory concentration to be maintained without requiring such a high initial dose, thus reducing side effects. Recent increases in antifungal resistance show a need for alternative antifungal therapies.[128] Some alternative therapies that have been explored include surfactants,[129] synthetic peptides,[130] and fatty acids.[131] Fibre encapsulation can enhance drug solubility and may be useful for the delivery of alternative antifungal agents that are incompatible with rinses.

Tonglairoum *et al.* (2014) developed electrospun PVP fibres with hydroxypropyl-β-cyclodextrin to rapidly release and improve the solubility of clotrimazole, a poorly soluble antifungal drug, for the treatment of OC. PVP was used as a rapidly dissolving polymer and the cyclodextrin as an excipient to form inclusion complexes to enhance drug solubility. Clotrimazole was loaded at up to 20% w/w and the fibre mats electrospun from mixtures of ethanol, water, and benzyl alcohol. The fibres rapidly dissolved in artificial saliva and were effective at eliminating the viability of *C. albicans* and *C. dubliniensis* suspensions within 2 h.[90] To prolong the effect, the material was further developed into a sandwich patch by electrospinning a second mucoadhesive layer from water consisting of 5:1 w/w PVA/thiolated chitosan. The resulting sandwich patches released clotrimazole at a rate more suitable for prolonged antimicrobial effect, with around 70% released within 4 h.[106]

Similarly, Szabó *et al.* (2016) incorporated terbinafine HCl at around 7% w/w into 5:1 w/w PVA/chitosan fibres from an aqueous solution. The fibres dissolved rapidly in artificial saliva,

releasing all of the drug within four minutes. *In silico* modelling with GastroPlus™ software predicted that up to 66% of the dose would be absorbed in the oral cavity if oral transit is properly regulated.[91]

Aduba *et al.* (2013) also developed an electrospun material for the delivery of poorly soluble antifungal agents against oral candida. 1:1 w/w gelatin/nystatin fibres were electrospun from HFIP and subsequently immersed in PEG diacrylate and 2,2-dimethoxy-2-phenylacetophenone as a photoinitiator dissolved in ethanol. Removing and curing using UV exposure produced cross-linked fibres with improved structural stability in aqueous solutions. The release rate was dependent on the degree of cross-linking and relatively slow, with around 20–70% released within 24 h.[132]

Clitherow *et al.* (2020) incorporated various unsaturated fatty acids as alternative antifungal agents into both the PCL and PVP/RS100 layers of the Rivelin patch formulation at loadings of up to 22% and 12% w/w, respectively. Unlike in previous studies, disk diffusion inhibition and biofilm viability assays were used to demonstrate the potential of the patches at inhibiting both wild type and azole resistant *C. albicans* when applied directly to biofilms, thus clearly showing the effectiveness of mucoadhesive electrospun patches at treating OC. Dodecanoic acid was found to be the most effective of the fatty acids tested against pre-existing *C. albicans* biofilms.[115]

Research so far has shown that a wide variety of alternative antifungal agents that could otherwise not be delivered using rinses can be incorporated and released from electrospun mucoadhesives and one study has shown effectiveness against biofilms *in vitro*. It is expected that further *in vitro* and *in vivo* research could translate these materials for clinical use.

1.4.4 Chemotherapy applications

Head and neck cancer is the sixth most common cancer worldwide.[133] A significant proportion occurs as cancer of the mouth and lip, which has an annual incidence and mortality of approximately 378,000 and 178,000 respectively in 2020.[134] Malignancy most commonly affects the epithelium and presents as squamous cell carcinoma. Major risk factors include exposure to tobacco, alcohol, and human papillomavirus. Surgery and radiation therapy, separately or in combination, are the primary treatment modalities for malignant oral cancers.[133] Oral cancer requires the accumulation of multiple of genetic or epigenetic alterations to become malignant; hyperplastic or dysplastic lesions are frequently observed as a precancerous intermediate condition that may or may not eventually progress to invasive carcinoma. Preventative treatment of these lesions would have obvious benefits.

Preventative surgery is usually not recommended,[135] therefore lesions are repeatedly monitored for malignant transformation before starting treatment. There have been several trials investigating preventative chemotherapy with systemic agents (retinoids, cyclooxygenase-2 inhibitors, epithelial growth factor receptor inhibitors) to halt the progression to oral cancers.[136] In general these agents have shown some limited efficacy but with unacceptable systemic toxicity. The ability to deliver a chemopreventative agent topically to the affected epithelium could potentially produce improved efficacy with reduced systemic side effects. Potential therapeutics include cyclooxygenase-2 inhibitors (e.g. celecoxib) or histone deacetylase inhibitors (e.g. suberoylanilide hydroxamic acid, sodium valproate) which target enzymes overexpressed in many cancers.[136–138] Notably, sodium valproate is currently under assessment in a stage II trial as a chemopreventative agent that potentially treat high risk oral dysplasia through epigenetic modification.[139] Tyrosine kinases inhibitors (e.g. gefitinib) or monoclonal antibodies that block epidermal growth factor receptor (e.g. cetuximab) may reduce proliferation and promote apoptosis of overexpressing dysplastic cells.[140,141]

A case study reported that imiquimod, an immune response modifier available as a dermal cream, appeared to successfully treat oral dysplasia.[142] The case report highlighted the need for formulations suitable for the oral mucosa. Topical chemotherapy may also be beneficial for preventing recurrence of resected oral cancers.[133] Due to the great burden of these diseases, chemoprevention is perhaps the indication for which oral patches have the greatest potential benefit.

Zhang *et al.* (2022) incorporated astaxanthin into PCL/gelatin fibres by electrospinning from 2,2,2-trifluoroethanol and used PCL fibres as a hydrophobic backing layer.[143] Astaxanthin is a lipid-soluble antioxidant terpene that can block key molecules in oncogenic signalling pathways, causing apoptosis in oral cancer models.[144] It is highly hydrophobic and has low oral bioavailability, but is an interesting candidate as a topical chemopreventative treatment. The fibres eluted approximately 60% of the molecule within 4 h. Membranes applied to porcine mucosa adhered in the presence of flowing saliva and were non-cytotoxic to human gingival fibroblasts. Immunohistochemistry showed that membranes applied to rat oral mucosa supressed expression of ki67 and COX-2 slightly. These are biomarkers associated with oral cancers, suggesting early promise as a chemopreventative treatment.

There are few papers that have investigated mucoadhesive fibres specifically for chemoprevention in the oral cavity. Relatedly, Zong *et al.* (2015) prepared blended PEG/PLA fibres containing 10% cisplatin by electrospinning using dimethyl sulfoxide.[145] The material adhered to *ex vivo* tissue and released 60% of the loaded drug within 6 h, as shown using a media flow-based setup. Cervical cancer was induced in mice by injecting a cervical cancer cell line. Applying the medicated material caused a significant reduction in tumour mass. Such a treatment is more appropriate for unresectable malignant tumours rather than chemoprevention. Liu *et al.* (2022) prepared patches by 3D-printing that contained poly(acrylic acid) as an adhesive and a combination of oxaliplatin and mycophenolate.[146] Oral dysplasia

was induced in rats using 4-nitroquinoline-1-oxide and histological analysis appeared to show that the applied medicated patches caused ablation of superficial dysplastic keratinocytes, while the underlying healthy cells remained intact.

1.4.5 Summary and outlook

There are a great number of papers investigating the encapsulation of drugs by electrospinning and implantable electrospun materials for regenerative medicine. Therefore, the scope of this review is mostly limited to electrospun materials that are intrinsically mucoadhesive and illustrate an application for the topical treatment of oromucosal conditions (Table 1.3). These range from rapidly dissolving membranes to allow easy administration of poorly soluble drugs through to devices that adhere for hours, delivering sustained doses. It remains challenging to evaluate and compare mucoadhesive and mechanical performance due to the lack of standardised mucoadhesion tests.

Although several different electrospun devices for oral medicine are under development, the Rivelin patch is the only device so far that has been tested both *in vitro* and in humans to show a suitable residence time, of approximately 2 h, and good patient acceptability. Future drug delivery devices are likely to bring other advantages, such as longer residence times or the ability deliver drugs that are incompatible with non-aqueous electrospinning solvents. Therefore, it is expected that more electrospun drug delivery materials will be developed with an emphasis on clinical translation. So far, the technology has been applied to a narrow range of oral conditions as an improvement on exiting treatments; however, it is expected that, as the technology matures, it will enable more unmet clinical needs to be addressed.

Table 1.3. Electrospun mucoadhesives under development for use in oral medicine

Indication	Polymer	Drug	Solvent	Processing	Ref.
Oral lichen planus	Adhesive/drug release: PVP, RS100 Backing layer: PCL	Clobetasol-17-propionate	97:3 v/v ethanol/water 9:1 v/v DCM/DMF	Sequential electrospinning, heat treatment	[109,147]
Recurrent aphthous stomatitis	Lower layer: PEO Upper layer: PLA	Diclofenac sodium Curcumin	Water HFIP	Double-ring slit needleless spinneret	[43]
Oral ulcers	Gliadin, ethylcellulose	Triamcinolone	70% v/v ethanol with 10% w/w acetic acid	Conventional electrospinning	[116]
Pain relief	Adhesive/drug release: PVP, RS100 Backing layer: PCL	Lidocaine	97:3 v/v ethanol/water 9:1 v/v DCM/DMF	Multiple-layer electrospinning, heat treatment	[148]
	Eudragit L	Ketoprofen	10-25% w/v ethanol	Conventional electrospinning	[125]
Oral candidiasis	PVP	Clotrimazole Excipient: hydroxypropyl-β -cyclodextrin	7:2:1 ethanol/water/ benyl alcohol by volume	Conventional electrospinning	[90]
	PVP Backing layer: PVA/thiolated chitosan	Clotrimazole Excipient: hydroxypropyl-β -cyclodextrin	7:2:1 ethanol/water/ benyl alcohol by volume	Sequential electrospinning	[106]
	PVA/chitosan	Terbinafine hydrochloride	Water	Conventional electrospinning	[91]
	gelatin	Nystatin	HFIP	Electrospinning, UV crosslinking	[132]
	Adhesive/drug release: PVP, RS100 Backing layer: PCL	Dodecanoic acid	97:3 v/v ethanol/water 9:1 v/v DCM/DMF	Sequential electrospinning, heat treatment	[149]
Oral dysplasia	Adhesive layer: PCL/gelatin Backing layer: PCL	Astaxanthin	2,2,2-trifluoroethanol	Sequential electrospinning	[143]

Another potential use for electrospun mucoadhesive is to prevent and treat alveolar osteitis (dry socket), a painful condition caused by the lack of a blood clot at the site of tooth extraction.[150]

The device could act as protective cover to prevent loss of the blood clot or protect underlying bone and nerves and deliver pain relief. This would likely require a device with a residence time of a few days.

Electrospun mucoadhesives make use of a scalable and industrially proven manufacturing process and are highly versatile in the range of drugs they can incorporate. They are attractive for drug delivery to the oral mucosa in that they are flexible and have a high surface area for drug release and, unlike existing dose forms, allow targeted delivery and prolonged retention times. It is envisioned that electrospun drug delivery devices and wound dressings will expand the range of treatments that can be applied to the oral mucosa and will have wide-ranging implications for the treatment of oral diseases

1.5. Oromucosal delivery of therapeutic polypeptides

1.5.1 Systemic peptide delivery

Peptides are short polypeptide chains, usually under 20 amino acid residues in length. They represent a rapidly growing class of injectable therapeutics that are being applied to a wide range of diseases. An recent and detailed review of their applications has been published by Wang *et al.* (2022).[151] Oral delivery is the most convenient method of administration for small molecule drugs due to high levels of patient compliance and comfort, and a reduced risk of infection in comparison with intravenous administration. Peptides and proteins are degraded by proteases or denatured by the low pH inside the gastrointestinal tract. Furthermore, they are often hydrophilic and have high molecular weights, resulting in poor absorption. This typically gives rise to oral bioavailabilities of less than 1%.[152]

Despite substantial research,[153] oral peptide delivery remains challenging. Mucoadhesive dosage forms present an interesting alternative, as prolonged intimate contact with the oral mucosa may allow non-invasive transmucosal peptide delivery, which circumvents

gastrointestinal proteolytic degradation and hepatic first-pass metabolism. Sudhakar *et al.* (2006) list a variety of mucoadhesive systems that have been investigated for transmucosal peptide delivery in their review, including patches, tablets, and solutions.[11] An early study was carried out by Anders *et al.* (1983) on 10 human volunteers with protirelin as a 3 amino acid (AA) long model peptide drug.[154] A wet circle of filter paper was placed in the centre of a Teflon disk and 20 mg of the peptide spread over and dissolved. The device was placed on the buccal oral mucosa for 30 minutes and the blood plasma concentration of thyrotropin and prolactin, which are released in response to protirelin, monitored over time using radioimmunoassays. The results showed a response to the buccal-administered peptide with a peak plasma concentration at 30 – 60 minutes, whereas oral administration results in a peak after 2 – 3 h.

The earliest attempts at transmucosal peptide delivery involved insulin (51 AA), which has been studied in humans and several animal species since shortly after its first isolation in the 1920s.[155] Therapeutically relevant transmucosal bioavailability has only been achieved in humans by using permeation enhancers.[155,156] Generex Biotechnology developed an insulin buccal aerosol spray for the management of Type I and Type II diabetes called Oral-Lyn™. The proprietary formulation contains a mixture of surfactants which encapsulate and stabilise insulin in large aerosol particles and act as permeation enhancers.[157] The product reached a late stage of regulatory approval in a number of countries and has been on the market in India and Ecuador.[156] However, in its current formulation, the buccal absorption rate of 10% means that up to 10 puffs per dose are required and that a single canister can only provide 40 IU of insulin. There may also be concerns over the long-term tolerability of the surfactants.

Insulin is a challenging candidate for transmucosal delivery due to low permeability and the relatively high mass of the peptide that must be absorbed to provide the therapeutic effect. Other blood glucose-regulating peptides with higher potency and lower molecular weight may

be more feasible for transmucosal delivery.[151] Glucagon-like-peptide 1 (GLP-1) (30 AA) has been incorporated into 100 mg buccal tablets containing sodium taurocholate as a permeation enhancer.[158] The tablets were applied on 8 human volunteers for 4.5 h. The blood serum levels of the bioactive form of GLP-1 were monitored using a radioimmunoassay, showing that 7.1 ± 0.9% of the dose reached circulation in the active form. This corresponds to a bioavailability of 47% relative to subcutaneous administration. The desired therapeutic effect of GLP-1 was to reduce blood glucose levels as a potential treatment for noninsulin-dependent diabetes mellitus. Plasma glucose levels were monitored to show that hypoglycemia was induced for 90 minutes.

Calcitonin (32 AA) is secreted in thyroid C-cells.[159] It is responsible for regulating blood serum calcium concentration and has received attention for transmucosal delivery to treat osteoporosis.[160] Calcitonin is released in response to elevated calcium levels and has the effect of reducing calcium levels by activating membrane receptors on osteoclast cells in bone tissue, inhibiting bone resorption.[161]. Variants of calcitonin are commercially available from several different species, with salmon calcitonin being the most widely used in clinical practice due to its activity in mammals being 40-50 times higher than human calcitonin.[159]

Multiple mucoadhesive delivery systems for salmon calcitonin (32 AA) have been reported including buccal tablets containing Hakea Gibbosa gum as a mucoadhesive[162] and thin films of Eudragit S-100 and polycarbophil.[163] These methods result in relatively high bioavailabilities of 37 ± 6% and 43.8 ± 10.9% respectively without permeation enhancers when tested on rabbits. Reductions in serum calcium below baseline levels lasted longer compared to intravenous administration (400 minutes for the film; 240 minutes for solution) due to a steadier release rate (lower maximum serum concentration) and, possibly, the oral mucosa acting as a drug reservoir. A study with fluorescently labelled human calcitonin applied to bovine nasal mucosal tissue showed intracellular fluorescence.[164] This suggests that an

endocytotic pathway may contribute towards mucosal absorption, which would explain the relatively high bioavailability. Permeation of salmon calcitonin through porcine buccal tissue has been shown using Franz cells to be enhanced by applying ethanol, sodium deoxyglycocholate (a bile salt), or *N*-acetyl-L-cysteine (reducing agent).[165] Adding 1% *N*-acetyl-L-cysteine alone resulted in a 9.5 times higher permeability coefficient, and 1% sodium deoxyglycocholate gave 8.2 times higher. There seem to have been no investigations into oromucosal calcitonin delivery in humans.

In summary, only a narrow range of peptides have been investigated for transmucosal delivery in humans and absorption through the epithelium tends to be poor, although surfactant permeation enhancers can increase bioavailability. Animal studies have historically been the main option for studying transmucosal peptide delivery,[87] although there are large differences in oromucosal permeability between humans and small mammals.[166] Pigs are preferred for animal experiments, as their oral anatomy is similar to humans.[166] Increasingly, *ex vivo* porcine tissue is being used to study drug transport. This presents some limitations for studying peptide delivery. Hydrophilic drugs tend to accumulate within the lamina propria of *ex vivo* tissue, resulting long lag times, whereas rapid uptake from the lamina propria is expected *in vivo* due to high blood flow.[167] For therapeutically relevant doses of many peptides, saturation of the tissue may not be achievable *ex vivo*, as is required to produce steady state flux during Franz cell experiments.

Furthermore, the viability and effect of handling on the biological function of the tissue should be considered, as many peptide drugs are closely related to naturally occurring molecules and uptake cannot be presumed to occur through passive paracellular diffusion. For these reasons, tissue-engineered epithelial models are perhaps underutilised as a high throughput system for studying oromucosal transport while providing additional biological and viability readouts. Xue *et al.* grew monolayers of TR146 cells (a tumour-derived buccal cell line) on tissue culture

inserts.[168] These successfully acted as a permeability barrier to insulin and were used to screen potential buccal permeation enhancers in terms of permeation enhancement and toxicity. There is potential to develop on this strategy by using a model that more closely resembles the healthy oral epithelium.

1.5.2 Local peptide and protein delivery

Local delivery of polypeptides to the oral mucosa may be more easily achievable. Potential oral health applications of topical protein delivery to the oral mucosa include antimicrobial peptides and proteins to treat resistant infections or target specific strains of pathogen.[169,170] Lysozyme is an antimicrobial enzyme naturally present in human saliva that causes broad-spectrum inhibition of gram-positive bacteria.[171] It is included in oral rinses (e.g. bioXtra® dry mouth rinse) to treat patients with reduced saliva production (xerostomia).

Certain cytokines, such as keratinocyte growth factor (KGF), show potential for regenerating the oral mucosa,[172] for example following damage caused by oral mucositis, and could be effective if delivered directly to the affected site rather than systemically. Palifermin, a recombinant peptide closely related to KGF, can be administered intravenously to relieve mucositis in patients undergoing high dose chemotherapy.[172] Due to its high cost, targeted delivery may be useful. However, oral mucositis tends to affect the entire lining of the mouth; therefore, rinses containing delivery vectors may be more appropriate than patches.[173]

The pro-inflammatory cytokines interferon-alpha and interleukin-2 have been found to have minor benefit as an immunotherapy for certain cancers by increasing the anti-tumour immune response.[174] These may have potential as a topical chemotherapy or chemopreventative treatment in combination with other agents.

1.5.3 Monoclonal antibodies and derivatives

Antibodies, also known as immunoglobulins, are large glycoproteins that form an integral part of the adaptive immune system in all jawed vertebrates.[175] Antibodies comprise of a series of domains, including a highly variable complementary-determining region which is complementary to a particular antigen and binds with high specificity mediated through numerous non-covalent interactions. Other domains are present in a limited number of varieties known as isotypes. The isotype affects the functional properties of the antibody but has little or no effect on antigen specificity.

Immunoglobulin G (IgG) is the most common circulating antibody isotype, making up 75% of serum antibodies. IgGs have a 2-fold symmetrical structure and comprise two identical heavy chains and two identical light chains (Figure 1.5). In the centre of the molecule is the hinge, at which the heavy chains are attached together by 2 disulfide bonds. Light chains are attached at the second domain from the N-terminus of each heavy chain by a single disulfide bond (C_L to C_H1). Together, the variable domains at the N-termini of each heavy and light chain pair (V_L and V_H) form a CDR. The 2 lobes on one side of the hinge, each made up of a light chain and half of a heavy chain, are known as antigen binding fragments (F(ab)). The other side of the hinge, made up of the remainder of the heavy chains, is the fragment crystallisable (Fc) region. The Fc is glycosylated and is recognised by Fc receptors and complement proteins to perform various biological functions.[176]

Antibodies are secreted by B lymphocytes, each cell of which expresses a novel pair of polypeptide sequences. A functional gene encoding the antibody is assembled from a selection of gene segments by a process known as V(D)J recombination.[176] Antigen affinity is refined through the processes of somatic hypermutation and clonal selection. Antibodies have numerous effector mechanisms. Most simply, some antibodies can directly bind and neutralise

extracellular toxins or pathogens by blocking the surface or cross linking to induce agglutination. Various leukocytes recognise the Fc region of antigen-bound antibodies and perform effector functions, for example phagocytosis, apoptosis of an infected cell, or the release of inflammatory cytokines. Complement proteins can also interact with Fc receptors to form C1 complexes, which activate the classical pathway of the complement system, which further promotes phagocytosis and inflammation and eventually leads to the destruction of targeted cell membranes.[177]

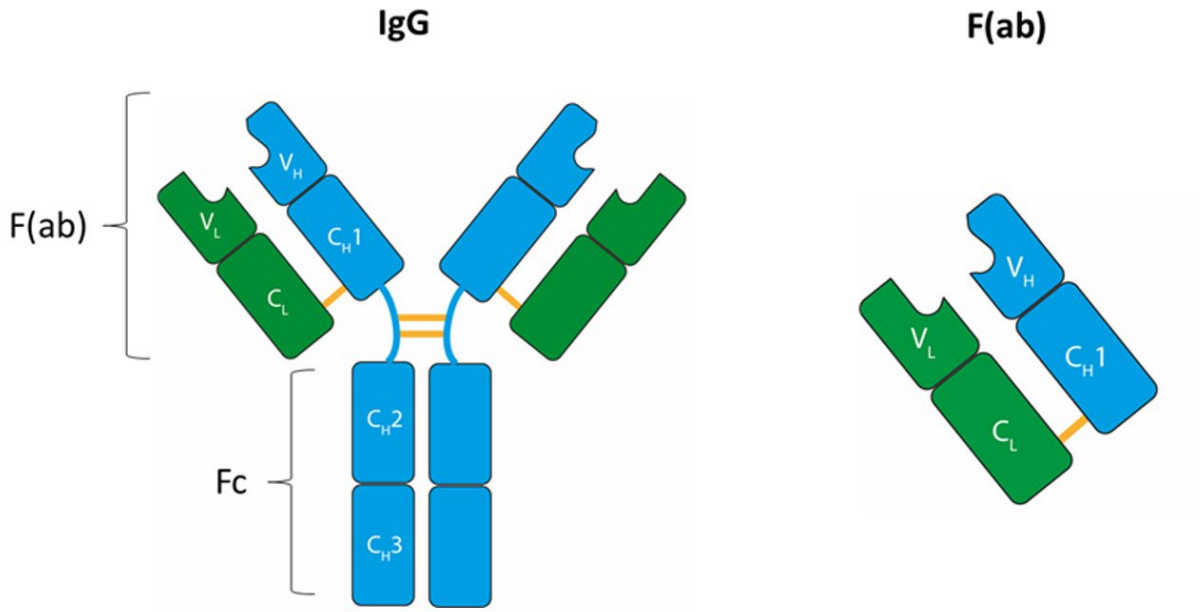

Figure 1.5. Schematic structure of an IgG antibody (150 kDa) and F(ab) IgG antibody fragment (50 kDa). Each IgG consists of 2 identical heavy polypeptide chains (azure) and 2 identical light chains (green) connected by disulfide bonds (yellow).

Therapeutic antibody-based drugs are traditionally derived by fusing a B cell with an immortalised cell.[178] The resulting cell line can be used to produce a population of identical antibodies, called monoclonal antibodies (Mab), which are specific to a single region (epitope) of the target antigen. The simplest Mab therapies involve whole IgG Mab that bind to and thereby directly block the activity of a molecule. For example, muromonab-CD3, the first

therapeutic Mab (approved in 1986), blocks the CD3 membrane protein on T cells, preventing their activation and thereby acting as an immunosuppressant.[179]

Therapeutic applications of Mabs include anti-cancer therapies (targeting cancer specific antigens) and treating autoimmune diseases (by blocking pro-inflammatory molecules). A detailed list of approved Mab drugs is included in a review by Carter *et al.*[180] Increasingly, recombinant technology and rational design approaches allow the development of new formats of antibody-based drugs. These include antibody fragments, antibody-drug conjugates, and bispecific antibodies.[180]

As with most biologic and peptide drugs, Mab drugs are almost exclusively administered systemically by injection. Multiple studies have investigated local delivery, primarily through local injections to the eye, skin, or tumours.[181] In general, this strategy tends to be effective and allows treatment with a lower dose and reduced side effects. Topical non-invasive delivery of vascular endothelial growth factor antagonist Mab is possible in the eye using eye drops, and lower molecular weight F(ab) antibody fragments (Figure 1.5) show moderately improved effectiveness due to greater epithelial permeation or the smaller protein.[182] Several studies show that topical delivery of anti-inflammatory Mab drugs to dermal ulcers can be effective, as the impaired barrier of the skin allows direct application to the affected tissue.[181] There has been little investigation into the topical delivery of antibody-based therapies to treat oral diseases. However, there seems to be considerable interest from the oral medicine community in topical Mab therapy to treat various lesions of the oral mucosa.[183,184]

1.6. Summary

Diseases of the oral mucosa are often unpleasant, painful, and interfere with day-to-day activities. Existing topical formulations offer little site specificity and dose control, which limits the selection of therapeutics that can be delivered. As a result, many oral diseases lack

effective clinical management. In particular, inflammatory ulcerative diseases, such as OLP, have no approved treatments, and medicines used off-label are poorly tolerated.

Among emerging oral patch technologies, electrospinning is of particular interest for fabricating flexible fibrous materials with a high surface area to facilitate mucoadhesion and efficient drug release. The technique is highly versatile in the range of materials and therapeutic agents that can be processed and allows the production of composite or multi-layered devices. Literature on electrospun mucoadhesive materials for use in oral medicine reports devices that address inflammatory diseases, infections, and provide pain relief. Previous research at the University of Sheffield led to the development of a mucoadhesive bilayer patch for site specific delivery that has since shown efficacy in phase II trials to deliver clobetasol to treat lichen planus ulcers.

Previous research has focused on mucoadhesive devices for enhancing the delivery of conventional therapeutics. Further research would be beneficial to consider novel therapies targeting the oral mucosa that would be impossible to deliver effectively using existing dosage forms. These include polypeptides, which represent a rapidly growing class of pharmaceuticals. Systemic delivery of therapeutic peptides (small polypeptides) via the oral mucosa is a challenging area of research that is limited, in part, by the lack of suitable dosage forms. Local delivery of peptides and proteins to the oral tissues may enable new antimicrobial therapies or allow the modulation of cell growth and immune response to restore healthy tissue function. Oral medics have identified neutralising antibody-based therapies as a particularly interesting candidate for topical delivery due to their potential to introduce new treatment options for inflammatory mucosal disorders.

1.7. Hypothesis

Biologically active peptides and proteins can be incorporated into mucoadhesive polymer patches using electrospinning and delivered to provide a potentially therapeutic effect in the oral mucosa.

1.8. Aims and objectives

1. Adapt an existing electrospun mucoadhesive patch formulation to allow the incorporation and release of biologically active proteins, peptides, and antibody-based therapies. The formulations will be characterised in terms of morphology, encapsulation efficiency, homogeneity, drug release kinetics, mucoadhesion, and preservation of protein function.
2. Investigate the effect of applying patches containing pro-inflammatory-cytokine-neutralising antibody derivatives (F(ab) fragments) to a tissue-engineered model of an inflammatory oral ulcer. The treatment will be assessed in terms of its ability to neutralise the target cytokine (tumour necrosis factor alpha) and the consequent effect on the concentrations of chemotactic cytokines that are implicated in disease progression.
3. Develop methods suitable for measuring protein delivery across an oral epithelium and assess the suitability of patches for transepithelial biologic delivery. Tissue-engineered *in vitro* models are preferred for their potential to mimic the biological functions of living tissue and provide additional biological and viability readouts.

Chapter 2: Incorporation of lysozyme into a mucoadhesive electrospun patch for rapid protein delivery to the oral mucosa

Supplementary information for the journal article is reproduced in Appendix 1.

Additional material characterisation that has not been published previously is available in Appendix 2.

Materials Science & Engineering C 112 (2020) 110917

Contents lists available at ScienceDirect

Materials Science & Engineering C

journal homepage: www.elsevier.com/locate/msec

Incorporation of lysozyme into a mucoadhesive electrospun patch for rapid protein delivery to the oral mucosa

Jake G. Edmans[a,b], Craig Murdoch[a], Martin E. Santocildes-Romero[c], Paul V. Hatton[a], Helen E. Colley[a,*], Sebastian G. Spain[b]

[a] School of Clinical Dentistry, 19 Claremont Crescent, University of Sheffield, Sheffield S10 2TA, UK
[b] Department of Chemistry, Brook Hill, University of Sheffield, Sheffield S3 7HF, UK
[c] AFYX Therapeutics, Lergravsej 57, 2. tv, 2300 Copenhagen, Denmark

ARTICLE INFO

Keywords:
Electrospinning
Drug delivery
Proteins
Mucoadhesion
Oral medicine

ABSTRACT

The delivery of biopharmaceuticals to the oral mucosa offers a range of potential applications including antimicrobial peptides to treat resistant infections, growth factors for tissue regeneration, or as an alternative to injections for systemic delivery. Existing formulations targeting this site are typically non-specific and provide little control over dose. To address this, an electrospun dual-layer mucoadhesive patch was investigated for protein delivery to the oral mucosa. Lysozyme was used as a model antimicrobial protein and incorporated into poly(vinylpyrrolidone)/Eudragit RS100 polymer nanofibers using electrospinning from an ethanol/water mixture. The resulting fibrous membranes released the protein at a clinically desirable rate, reaching 90 ± 13% cumulative release after 2 h. Dual fluorescent fibre labelling and confocal microscopy demonstrated the homogeneity of lysozyme and polymer distribution. High encapsulation efficiency and preservation of enzyme activity were achieved (93.4 ± 7.0% and 96.1 ± 3.3% respectively). The released lysozyme inhibited the growth of the oral bacterium *Streptococcus ratti*, providing further evidence of retention of biological activity and illustrating a potential application for treating and preventing oral infections. An additional protective poly (caprolactone) backing layer was introduced to promote unidirectional delivery, without loss of enzyme activity, and the resulting dual-layer patches displayed long residence times using an in vitro test, showing that the adhesive properties were maintained. This study demonstrates that the drug delivery system has great potential for the delivery of therapeutic proteins to the oral mucosa.

1. Introduction

Due to advances in protein synthesis in recent decades, proteins and peptides now represent one of the fastest growing classes of pharmaceuticals [1]. The ability to modify the chemical structure of native proteins allows the development of more stable analogues with high specificity, high potency, and low toxicity, resulting in higher success rates than traditional small molecule new chemical entities in clinical development stages [2]. A variety of potential applications for biopharmaceutical delivery to the oral mucosa have been identified. These include antimicrobial peptides as a treatment for bacterial [3] and fungal [4] infections, such as in periodontal disease or oral candidiasis, with resistance to traditional antimicrobials. Topical recombinant cytokines such as epidermal growth factor and basic fibroblast growth factor have shown potential in vivo for regenerating oral wounds or ulcers caused by oral mucositis [5,6]. Some therapeutic peptides, including salmon calcitonin and insulin, in combination with permeation enhancers, have been shown in animals or humans to permeate the oral mucosa sufficiently to achieve therapeutic doses [7,8]. Therefore, the oral mucosa is also of interest for systemic delivery, circumventing proteolytic degradation in the gastrointestinal tract and offering the potential for controlled release and needleless delivery.

A significant challenge for the delivery of proteins to the oral mucosa is the lack of suitable formulations that allow specific delivery. The most commonly used formulations targeting the oral mucosa include mouthwashes [9], gels [10], tablets [11], and dissolvable films [12]. These drug delivery systems work well for highly permeable drugs [13] but release of the active ingredient is often non-specific, across the entire oral cavity rather than localised into a specific region of the oral mucosa where the drug is required. Variations in salivary flow and mechanical forces mean that doses are poorly defined where prolonged contact is required. To address this, we have developed an electrospun

* Corresponding author.
E-mail address: h.colley@sheffield.ac.uk (H.E. Colley).

https://doi.org/10.1016/j.msec.2020.110917
Received 7 January 2020; Received in revised form 4 March 2020; Accepted 31 March 2020
Available online 01 April 2020

mucoadhesive patch with a backing layer film to promote unidirectional drug delivery [14]. The system is comprised of FDA-approved polymers and offers several advantages over existing alternatives including in vivo residence times of up to 2 h, high patient acceptability, high surface area, and fast release rates [15]. This system in currently undergoing phase 2 clinical trials for the delivery clobesasol-17-propionate to treat oral lichen planus. The patches also show early promise for the delivery of lidocaine as a topical dental anaesthetic or analgesic [16].

A range of proteins and peptides have previously been encapsulated into polymer nanofibers using electrospinning [17]. However, most examples of electrospun drug delivery systems focus on biodegradable polyesters, which tend to require chlorinated solvents to achieve solubility. This leads to concerns over protein denaturation and loss of activity [17]. Several different approaches for incorporating proteins into electrospun membranes have been identified, for example, surface functionalisation by chemically bonding proteins to pre-spun fibres [18]. However, this immobilises the protein and is therefore more relevant for slow release applications. Much current work focuses on electrospinning emulsions or suspensions to allow electrospinning of proteins and polymers with incompatible solvent requirements [19,20]. This can result in activity loss and poor encapsulation efficiency due to the solvent phases having different conductivities and separating during the spinning process. Two separate solutions may also be electrospun into core-shell fibres using coaxial electrospinning with two capillary feeding channels [21]. Proteins encapsulated in the fibre core from aqueous solutions have been shown to maintain some or all of their activity [22,23]. However, the outer sheath layer is likely to influence drug release profiles and the manufacturing process is considerably more complex. To date, there are no published studies describing the encapsulation and release of bioactive proteins from a single-phase organic solvent mixture using uniaxial electrospinning. Here, we report the incorporation of lysozyme as a model protein into an electrospun mucoadhesive patch and investigate its potential for therapeutic protein delivery. This protein delivery system is unique in that it uses a simple uniaxial electrospinning manufacturing process to encapsulate a biologically active protein into an insoluble drug delivery system. For the first time, we show that proteins encapsulated in these uniaxial fibres retain biological activity upon release and significantly advance the field of electrospun-mediated protein delivery.

2. Methods

2.1. Materials

Poly(vinylpyrrolidone) (PVP; M_W 2000 kDa) and Eudragit RS100 (RS100; M_W 38 kDa) were kindly donated by BASF, UK and Evonik Industries AG, Germany, respectively. Poly(caprolactone) (PCL; M_W 80 kDa), dichloromethane (DCM), lysozyme from chicken egg white, lyophilised *Micrococcus lysodeikticus* cells, phosphate-buffered saline tablets, fluorescein isothiocyanate isomer I (FITC), Texas red sulfonyl chloride, sodium bicarbonate, and sodium carbonate were purchased from Sigma-Aldrich (Poole, UK). Ethanol and dimethylformamide (DMF) were purchased from Fischer Scientific (Loughborough, UK). Pierce™ BCA protein assay kit was purchased from Thermo Scientific (Loughborough, UK). Brain heart infusion broth was purchased from Oxoid (Basingstoke, UK).

2.2. Electrospinning system

Electrospun membranes were fabricated using a system composed of a PHD2000 syringe pump (Havard Apparatus, Cambridge, UK) and an Alpha IV Brandenburg power source (Brandenburg, Worthing, UK). Plastic syringes (1 mL volume; Henke Sass Wolf, Tuttlingen, Germany) were used to drive the solutions into a 20-gauge blunt metallic needle (Fisnar Europe, Glasgow, UK). Electrospinning was performed at room temperature with a potential difference of 19 kV, a flow rate of 2 mL/h, and a flight path of 14 cm.

2.3. Preparation of polymer solutions and fabrication of bioadhesive membranes

All electrospinning solutions contained 0.1025 ± 0.00025 g/mL PVP and 0.1225 ± 0.0005 g/mL Eudragit RS100 (by total solvent volume before mixing). The required amounts of PVP and RS100 were added to ethanol or an ethanol/water mixture and mixed at room temperature using a magnetic stirrer until dissolved. Lysozyme was dissolved in ice cold PBS (75 mg/mL) and added to the polymer solution and stirred until uniformly distributed, contributing 3 v/v % to the final solvent composition. Electrospinning was started within 1 min of adding the lysozyme. Placebo solutions and membranes were prepared using 3 v/v % distilled water instead of lysozyme in PBS.

2.4. Conductivity of polymer solutions

Electrical conductivity of the polymeric solutions was measured using a Mettler Toledo FG3 conductivity meter (Mettler Toledo, Schwerzenbach, Switzerland), applying a conductivity standard of 1413 μS cm^{-1} (Mettler Toledo).

2.5. Rheology of polymer solutions

The viscosity of the polymeric solutions was measured using an MCR 301 rheometer (Anton Paar, Graz, Austria) with a cone-plate measuring system CP25-4/IMG1 (25 mm diameter, 4° cone angle, and 253 μm truncation) at a constant temperature (25 ± 0.1 °C) and a sample volume of approximately 0.4 mL. Logarithmic shear rate sweep tests were performed with 31 points in the range of 0.1 to 100 s^{-1} lasting 20 s per point.

2.6. Scanning electron microscopy

Electrospun membranes were imaged using a TESCAN Vega3 scanning electron microscope (SEM; Tescan, Cambridge, UK). Samples were sputter coated with gold and imaged using an emission current of 10 kV. All images were processed using ImageJ software tools [24]. Fibre diameters were measured by ImageJ, using randomly generated coordinates and a superimposed grid to select fibres to measure. Three images were analysed for each composition with at least 10 measurements per image.

2.7. Degree of swelling of electrospun membranes

Pre-weighed 15 mm discs (5–14 mg) were placed in sample tubes with 1 mL distilled water for 2 h. If intact, samples were removed, and each side pressed against a glass surface to remove excess water before reweighing. The percentage degree of swelling was calculated using the formula:

$$\frac{(M_s - M_d)}{M_d} \times 100$$

where M_s is the mass of the sample after swelling in distilled water and M_d is the dry mass of the sample before swelling.

2.8. Activity and encapsulation efficiency measurement

Electrospun membrane (9–12 mg) was prepared and immersed in 2 mL PBS for 24 h. to elute the protein. A bicinchoninic acid (BCA) protein assay was used as directed to determine encapsulation efficiencies. Absorbance was measured at 562 nm using a spectrophotometer (Tecan, Theale, UK). The apparent mass fraction determined from the protein concentrations in the samples was

normalised against the dry mass fraction of lysozyme in the electrospinning solution.

Lysozyme enzyme activity in samples was measured using a photometric enzyme kinetic assay as previously described [25]. Briefly, 10 μL of membrane supernatant diluted in PBS (1:10, v/v) was added to a clear plastic 96-well plate along with 200 μL of lyophilised *Micrococcus lysodeikticus* cells (0.4 mg/mL in PBS). The change in optical density at 450 nm (OD_{450}) was measured over time for 10 min. Active lysozyme concentrations of the samples were interpolated from a standard curve created using lysozyme standards (0, 20, 40, 60, 80, and 100 μg/mL) and normalised against the total protein concentration.

2.9. Homogeneity of lysozyme incorporation

Electrospun membranes were divided into three concentric regions: the central circle of the membrane with one third the diameter of the whole membrane, an intermediate ring with two thirds the diameter of the whole membrane, and the remaining outer ring. The activity and encapsulation efficiencies of the different regions where measured as previously described.

2.10. Fluorescent labelling of PVP and lysozyme

To label PVP, a complex with fluorescein isothiocyanate isomer I (FITC), as described by Aulton et al., was produced [26]. FITC in 0.1 M pH 9.2 carbonate-bicarbonate buffer (2 mg/mL, 1 mL) was added dropwise with vigorous stirring to PVP in the same buffer (25 mg/mL, 10 mL) in an opaque sample tube. The tube was sealed and incubated at room temperature for 3 h. The complex was purified by adding dropwise with stirring to acetone (500 mL) and the precipitate collected and washed with acetone (2 × 10 mL). Excess solvents were removed by freeze drying.

Lysozyme was labelled with Texas red sulfonyl chloride. Texas red sulfonyl chloride (1 mg) was added, with vigorous stirring until dissolved, to lysozyme in 0.1 M pH 9.2 carbonate-bicarbonate buffer (75 mg/mL, 1 mL) in an opaque sample tube. The tube was sealed and incubated at room temperature for 24 h and the product purified using gel permeation chromatography with Sephadex G-25 and PBS. The solvent was removed by freeze drying.

2.11. Fabrication and imaging of fluorescent electrospun fibres

Electrospun fibres were prepared as previously described with 97 v/v % ethanol but using Texas red labelled lysozyme and substituting 24 w/v % of the PVP with the FITC-PVP complex where appropriate. Samples were placed on glass slides and overlaid with glass cover slips. Imaging was performed in dual-channel mode using a Nikon A1 laser scanning confocal microscope with 457–514 nm argon and 561 nm sapphire lasers. All images were processed using ImageJ software tools [24].

2.12. Release profile

Samples of electrospun membranes (20 mg) were immersed in 4 mL PBS and 10 μL samples taken at time intervals (0, 10, 20, 30, 60, 120, 180 min.) following vortexing for 5 s. Active lysozyme concentration was measured as previously described. To calculate cumulative release, the active concentration was normalised against the theoretical maximum concentration, assuming 100% encapsulation efficiency, release, and activity.

2.13. Growth inhibition assay with Streptococcus ratti

Streptococcus ratti (NCTC 10920, Public Health England, Salisbury, UK) was grown overnight in 10 mL brain heart infusion broth (BHI) at 37 °C, 5% CO_2 before diluting to OD_{600} of 0.1 in BHI. Samples of electrospun membrane (50 ± 0.1 mg) were immersed in 1 mL sterile PBS for 24 h with vortexing for 30 s after immersing and before sampling the eluate. Sterile PBS was used as a negative control and 0.5 mg/mL lysozyme in PBS as a positive control. Additionally, placebo patch samples were eluted in a stock 0.5 mg/mL lysozyme solution. A 12-well plate was filled with BHI (0.5 mL per well) before adding eluate and controls in triplicate (0.5 mL). Each well was inoculated with 0.1 mL bacteria and the plate incubated at 37 °C with OD_{600} measured every 10 min for 15 h with shaking for 1 min before each reading.

2.14. Fabrication of hydrophobic backing layer

The hydrophobic backing layer (BL) was prepared by electrospinning a PCL solution on top of the bioadhesive PVP/RS100 layer. PCL was added to a blend of DCM and DMF (90:10 v/v %) and stirred at room temperature until dissolved to prepare a solution of concentration 10 w/v %. To enhance the attachment between the bioadhesive and backing layer a thermal treatment was applied by heating at 65 °C for 15 min in a dry oven.

2.15. In vitro adhesion study of dual-layer patches

The adhesive properties of electrospun membranes with backing layers were investigated in vitro. For each composition, two discs of 1 cm diameter were cut from three membranes (n = 6) and applied to 20 μL droplets of PBS on a plastic petri dish with gentle pressure from the index finger for 5 s. The petri dishes were filled with PBS (20 mL) and then incubated on an orbital shaker at 250 rpm at room temperature for a total of 2 weeks. The samples were inspected daily to observe any detachment of the backing layer.

2.16. Data analysis

All data and statistical analyses were performed using GraphPad Prism 8.0 software (GraphPad Software, La Jolla, CA). One-way ANOVA with post hoc Tukey tests or Welch's *t*-tests were used to compare differences between groups and results considered statistically significant if $p < 0.05$.

3. Results and discussion

3.1. Physical properties of solutions

The morphology of electrospun fibres is strongly influenced by processing parameters and solution properties. Conductivity and viscosity measurements were used to determine how the addition of a protein affects solution properties. A typical dose of a therapeutic peptide is in the order of micrograms [27–29], therefore a loading of 1% lysozyme by dry mass was used to simulate a loading that may be suitable for mucosal peptide or protein delivery. Including lysozyme in PBS caused an increase in solution conductivity from 118.4 ± 7.2 to 168.6 ± 8.6 μS/cm ($p = 0.0247$) and an increase in viscosity at 5 s^{-1} from 1.14 ± 0.18 to 1.477 ± 0.091 Pa·s ($p = 0.0369$) in comparison to the equivalent solution prepared with distilled water. The increase in conductivity on addition of lysozyme, a cationic protein, was expected due to increased electrolyte concentration. The increase in viscosity is typical of a protein solution [30]. An organic solvent such as ethanol is required for the dissolution of RS100, however ethanol can act as a protein denaturant [31]. It was therefore hypothesised that reducing the proportion of ethanol in the electrospinning solvent mixture would improve protein activity. Therefore, solvent mixtures with different proportions of ethanol were investigated. Decreasing the proportion of ethanol in the solution and replacing with water caused a linear increase in conductivity ($R^2 = 0.9878$) reaching 504 ± 33 μS/cm at 40 v/v % ethanol (Fig. 1A). This follows a similar trend to that previously reported for pure ethanol-water mixtures and is expected due to ethanol

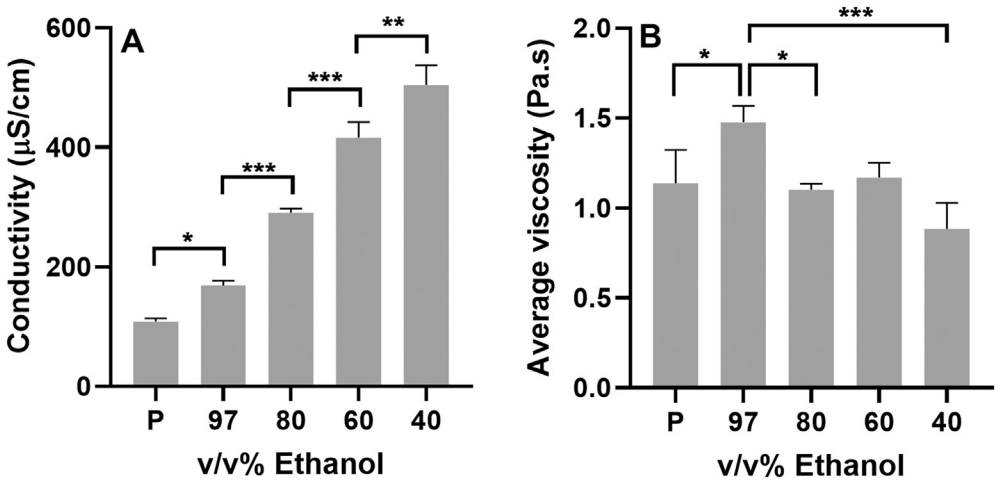

Fig. 1. Conductivity of electrospinning solutions containing lysozyme with different mixtures of ethanol and water as solvents and placebo (P) solutions in 97 v/v % ethanol without lysozyme (A). Viscosity of electrospinning solutions measured at a shear rate of 5 s^{-1} (B). Data are presented as mean ± SD, with 3 independent repeats and analysed using one-way ANOVA with post hoc Tukey tests. *, $p < 0.05$; **, $p < 0.01$; ***, $p < 0.001$.

having a much lower conductivity than water [32]. Reducing the proportion of ethanol from 97 to 80 v/v % reduced viscosity from 1.477 ± 0.091 to 1.103 ± 0.032 Pa·s ($p = 0.0214$, Fig. 1B). The decrease in viscosity at lower ethanol concentrations is consistent with polymers adopting a globule conformation with a smaller hydrodynamic volume due to poorer solvation. PVP in ethanol-water mixtures has previously been shown to have a reduced hydrodynamic radius at lower ethanol concentrations, suggesting a transition from chains to less solvated globules [33]. RS100 is a less hydrophilic, water-insoluble polymer, therefore it is also likely to be poorly solvated at lower ethanol concentrations. All polymer solutions behaved approximately as Newtonian fluids with no clear shear thickening or thinning trend (Fig. S1).

3.2. Fabrication and morphology of electrospun membranes

Electrospun fibres containing 1 w/v % lysozyme and made using 97, 80, 60, and 40 v/v % ethanol mixed with distilled water as solvent and a placebo membrane manufactured with 97 v/v % ethanol without lysozyme were analysed by scanning electron microscopy. All samples had some merged fibres and almost no bead defects (Fig. 2). No other defects were observed. Including lysozyme caused a decrease in diameter from 2.50 ± 0.71 to 2.04 ± 0.92 µm ($p = 0.0402$). The reduced fibre diameter is consistent with the observed increase in conductivity, which allows the polymer solution to hold more charge, resulting in more efficient elongation in the electric field. There was no significant difference in diameter between 97 and 80 v/v % ethanol, however there was a significant decrease in fibre diameter from 2.34 ± 0.63 µm to 1.28 ± 0.41 µm ($p < 0.0001$) and 0.58 ± 0.13 µm ($p < 0.0001$) when the ethanol content was reduced from 80 v/v % to 60 and 40 v/v % ethanol respectively. Higher solution conductivity and lower viscosity are well known to be associated with narrower fibres [34], therefore these measurements broadly follow the trend expected from the solutions properties. These results also similar to those reported by Nartetamrongsutt et al., who showed that including ionic salts in solutions of PVP in ethanol-water mixtures resulted in reduced fibre diameters and increased solution conductivity [35]. They also found that reducing the proportion of ethanol below 50 v/v % resulted in narrower fibres and a narrower distribution of fibre diameters along with reduced solution viscosity and increased solution conductivity.

3.3. Swelling and integrity of electrospun membranes

To be suitable as a mucoadhesive drug delivery system, the protein-loaded membranes must swell to promote adhesion but also remain intact in a wet environment. Samples were placed in distilled water for 2 h and visually inspected for loss of integrity and, where possible, the degree of swelling was measured. All samples electrospun using 40 v/v % ethanol and one of three membranes using 60 v/v % ethanol rapidly disintegrated into small insoluble particles when added to water. In contrast, fibres electrospun from 97 and 80 v/v % ethanol and placebo membranes remained intact after 2 h and did not differ significantly in degree of swelling (Fig. 3, $p = 0.4342$). These data suggest that 97 or 80 v/v % ethanol are suitable solvents for this polymer system and application. The disintegration of narrower fibres may be a result of PVP-rich domains rapidly dissolving and creating discontinuations in the fibres. This would be expected of narrower fibres, since the smaller diameter would make it easier for discontinuations to form and the higher surface area and smaller contacts between fibres facilitates the rapid dissolution of PVP.

3.4. Effect of solvent mixture on encapsulation and activity

Lysozyme was eluted from the fibres and the amount released measured using a protein assay and its activity assessed using an enzyme kinetic assay relative to freshly prepared lysozyme stock solutions. Encapsulation efficiency ranged from 75 ± 10 to 98 ± 8%, and no statistically significant difference between solvents was shown (Fig. 4, $p = 0.0750$). It was initially hypothesised that reducing the concentration of ethanol in the electrospinning solution would limit protein denaturation, leading to higher enzyme activity. However, it was found that enzyme activity was close to 100% (96 ± 3 to 108 ± 18%) with no difference between the solvent mixtures tested. Placebo membranes were used as negative controls and showed apparent protein loading, as measured by a BCA assay, close to zero, 0.017 ± 0.015 w/w % compared to 0.928 ± 0.070 w/w % for lysozyme loaded membranes ($p < 0.005$). The activity of the placebo patches was also close to zero, corresponding to an active lysozyme loading of 0.055 ± 0.042 w/w % compared to 0.892 ± 0.049 w/w % for lysozyme-loaded membranes ($p < 0.0005$). This shows that the observed protein release and enzyme activity was not a false positive caused by dissolved polymer. Changing the ratio of solvents did not provide a noticeable benefit in terms of activity, therefore further experiments focused on 97 v/v % ethanol as the solvent, which gave an encapsulation efficiency of 93 ± 7% and activity of 96 ± 3%. The high encapsulation efficiencies reported here are comparable to those previously reported for small molecule drugs encapsulated using uniaxial electrospinning. For example, Xie et al., reported the encapsulation of paclitaxel in PLGA nanofibers with loading of around 10 w/w % and an encapsulation efficiency over 90% [36]. There is very little published research reporting encapsulation of active proteins using uniaxial electrospinning of a single phase solution. Eriksen et al., incorporated a fluorescently-labelled antimicrobial peptide into PCL

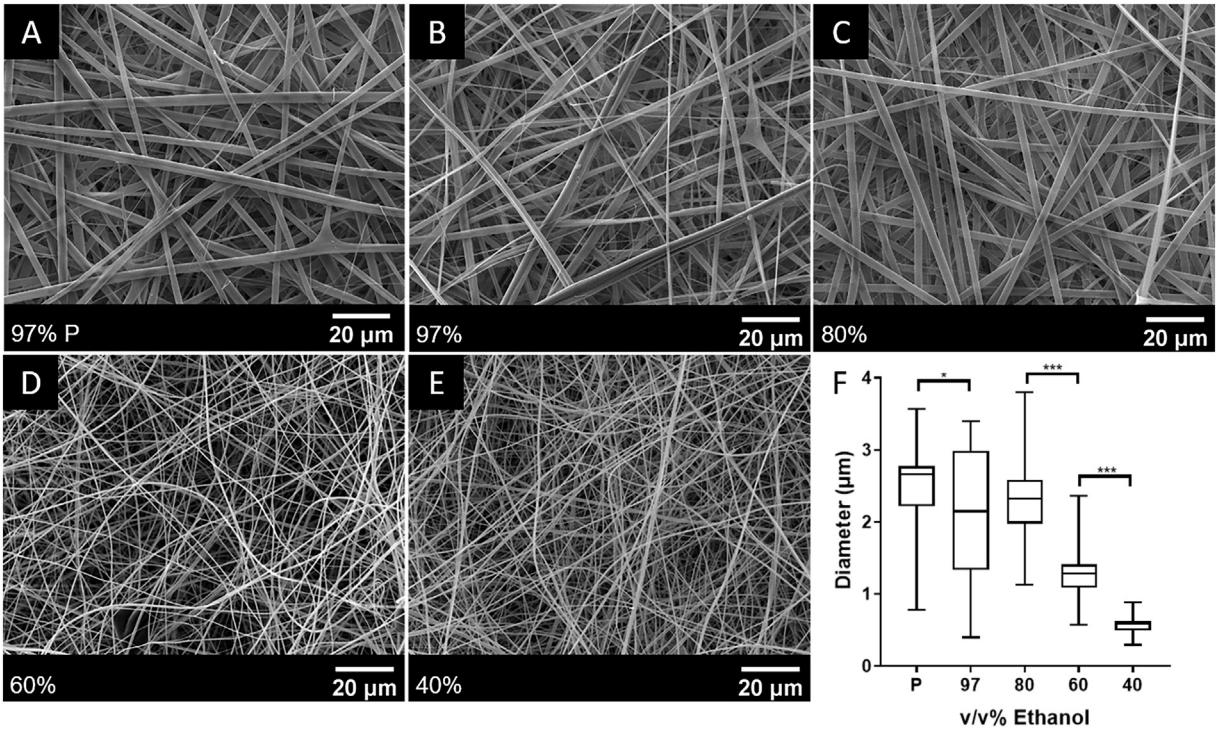

Fig. 2. Scanning electron micrographs of a placebo membrane (A) and electrospun fibres containing lysozyme manufactured using different concentrations of ethanol, shown in bottom left as v/v% (B–E). Fibre diameter distributions (F). Data are presented as median, interquartile range, and range with 3 independently prepared samples for each solvent mixture and 10 diameter measurements per sample and analysed using one-way ANOVA with post hoc Tukey tests. *, $p < 0.05$; ***, $p < 0.001$.

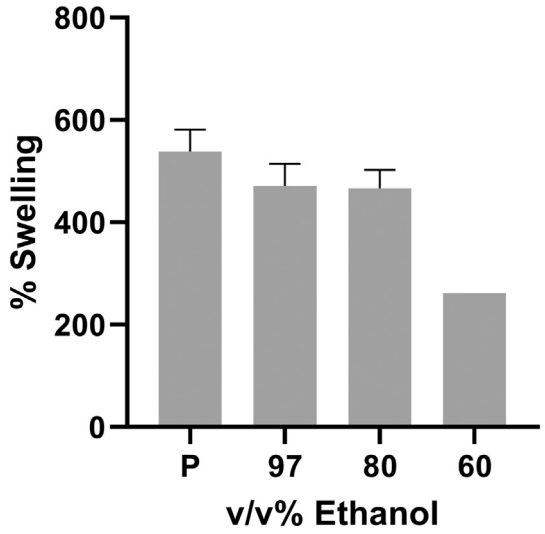

Fig. 3. Degree of swelling in water of lysozyme-containing electrospun fibres using different ethanol concentrations and placebo membranes (P). Data are presented as mean ± SD, with 3 independent samples and analysed using one-way ANOVA with post hoc Tukey tests. For 60 v/v % ethanol only 2 independent measurements could be made, therefore SD was not calculated.

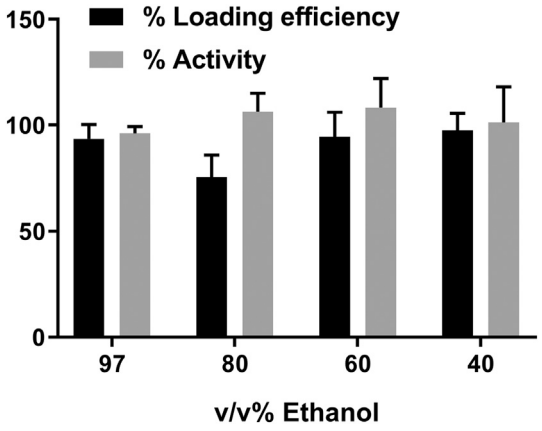

Fig. 4. Encapsulation efficiency and activity of lysozyme in fibres electrospun using different mixtures of ethanol and water as solvents. Data is presented as mean ± SD, with 3 independent samples per solvent mixture, and analysed using one-way ANOVA with post hoc Tukey tests.

fibres at a loading of approximately 0.1 w/w% using a miscible methanol/chloroform solvent mixture, but were unable to confirm biological activity [37]. Conversely, emulsion and coaxial electrospinning, with the protein in an aqueous phase, have been frequently studied for protein encapsulation. Due to separation of solvent phases in the Taylor cone, emulsion electrospinning often results in low encapsulation efficiencies of only a few percent for globular proteins [19], however a higher efficiency of 87.2 ± 1.8% has been achieved for collagen-like protein in poly(lactic-*co*-glycolic acid) (PLGA) fibres at a loading of 5 w/w% [20]. Ji et al., compared emulsion and coaxial electrospinning for the encapsulation of alkaline phosphatase into PCL fibres at a loading of 0.16 w/w% from water and 2,2,2-trifluoroethanol [23]. Coaxial electrospinning resulted in 76.2 ± 8.4% enzyme activity, while electrospinning from an emulsion resulted in 49.3 ± 4.5% activity. Lysozyme has also previously been encapsulated in PCL/poly (ethylene glycol) (PEG) fibres using coaxial electrospinning at loadings of 2–6 w/w% and shown to be active, however the activity was not quantified [22]. The polymer/solvent system described here enables encapsulation efficiencies and activity preservation superior to what has been achieved previously with uniaxial single phase and emulsion electrospinning and at least as high as that achieved with coaxial electrospinning.

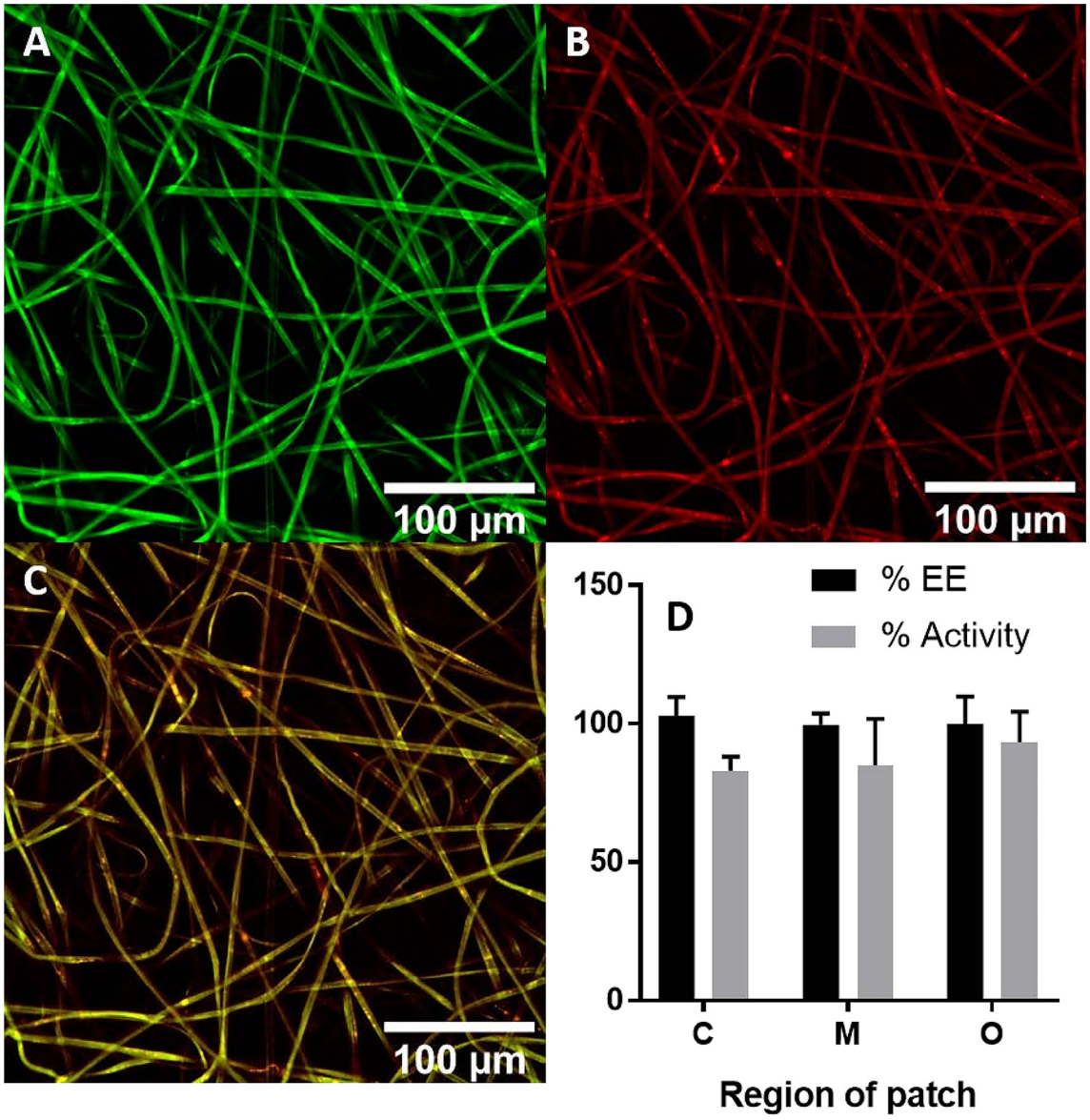

Fig. 5. Confocal micrographs of electrospun fibres containing FITC-PVP complex and Texas-red conjugated lysozyme to show the distribution of PVP (A, green) and lysozyme (B, red) within the fibres and an overlay of both distributions (C). Encapsulation efficiency (EE) and activity of central, intermediate, and outer regions of lysozyme-containing membranes electrospun from 97 v/v % ethanol (D). Data is presented as mean ± SD, with 3 independent samples for each region, and analysed using one-way ANOVA with post hoc Tukey tests. (For interpretation of the references to color in this figure legend, the reader is referred to the web version of this article.)

3.5. Homogeneity of electrospun membranes

To determine the distribution of PVP and lysozyme within the fibres a novel dual fluorescent labelling approach was used. A FITC-PVP complex and Texas red conjugated lysozyme were added before electrospinning and the resulting fibres imaged using confocal microscopy. Singly labelled control samples showed that signals were not caused by auto fluorescence or crosstalk between channels (Fig. S2). PVP appears to be homogenously distributed within the fibres, with any polymer phase separation occurring over a nanometre scale below the resolution of the microscope (Fig. 5A). Lysozyme is fully incorporated into the fibres and almost homogeneously distributed (Fig. 5B). Some aggregation is viably present over a microscopic scale as bright regions, however this does not appear to significantly affect its activity. To determine the homogeneity of the lysozyme distribution over a macroscopic scale, the loading and activity of different regions (centre, intermediate, outer edge) of the membrane were compared (Fig. 5D). The loading and activity were similar across all regions tested indicating that the protein is homogeneously distributed at the macroscopic level.

3.6. Characterisation of release kinetics using an enzymatic assay

We previously showed that a mucoadhesive drug delivery device with a similar polymer composition had a residence time of 96 ± 26 min when applied to the human buccal oral mucosa [15]. To be useful as a mucosal peptide delivery system, the membranes must release their payload over a similar timescale. To measure the release profile, lysozyme was eluted from the fibres and the active concentration measured using enzyme kinetics for up to 3 h (Fig. 6). Lysozyme was released rapidly with 76 ± 23% released within 30 min and 88 ± 16% within 1 h. The release then begins to plateau, reaching 90 ± 13% after 2 h. The release is likely to be facilitated by rapid water penetration due to the dissolution of PVP and the swelling of

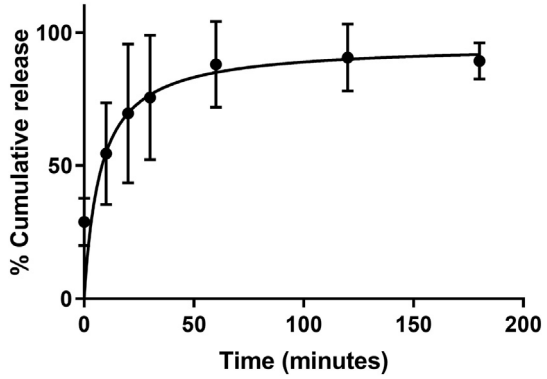

Fig. 6. Cumulative release of lysozyme from membranes electrospun using 97 v/v % ethanol as a solvent following immersion in PBS. Data is presented as mean ± SD, with 3 independent samples for each time point.

RS100. The lack of sheath layer associated with coaxial electrospinning also increases release rate by decreasing the diffusion path required for release [38]. Proteins previously encapsulated in water-insoluble polymer fibres have shown considerably slower release rates. Eriksen et al., reported that an antimicrobial peptide was released linearly from uniaxial PCL fibres, with < 50% released within 2 h [37]. Ji et al., reported that bovine serum albumin undergoes biphasic release from PCL fibres prepared both with emulsion and coaxial electrospinning, with an initial burst of around 15% released within 4 h, followed by prolonged release which begins to plateau at around 50–70% after 35 days [23]. Wei et al., showed that collagen-like protein was released from PLGA fibres prepared by emulsion electrospinning linearly for the first 1–2 weeks, reaching 50–70% depending on fibre diameter [20]. Although other polymer systems may be more suitable for sustained release over a period of days, the system reported here is unique in that it enables protein release over timescales relevant for delivery to the oral mucosa without rapidly dissolving.

3.7. Fabrication of backing layer and effect on activity

A film of hydrophobic PCL was introduced to act as a backing layer to promote unidirectional delivery and protect against mechanical forces in the mouth as previously described by Colley et al., in dual-layer patches for the unidirectional delivery of clobetasol to the oral mucosa [14]. PCL was electrospun on top of the protein-loaded mucoadhesive layer and the dual-layer patch heated at 65 °C to melt the PCL fibres into a continuous film. SEM micrographs show the fabrication of patches with a continuous backing film and that the fibrous structure of the lower layer was preserved (Fig. 7A–B). Activity measurements revealed that thermal treatment did not cause significant loss of enzyme activity ($p = 0.8326$). Applying dry heat at 100 °C for 1 week resulted in a decrease in activity from 84 ± 4% to 30 ± 16% ($p = 0.0017$), showing that lysozyme in the electrospun fibres is susceptible to heat denaturation in extreme conditions.

3.8. In vitro testing of residence time

A simple in vitro residence time test was applied to assess whether lysozyme had a detrimental effect on patch adhesion or structural integrity. Samples were applied to a petri dish, immersed in PBS and shaken for two weeks with daily inspection for detachment of the backing layer. Both the lysozyme-containing patches and the placebo patches remained attached until the end of the experiment, suggesting that lysozyme does not disrupt membrane integrity, adhesion, or attachment of the backing layer.

3.9. Lysozyme released from membranes inhibits the growth of *Streptococcus ratti*

Over 600 different species of microbes reside commensally within the oral cavity in healthy individuals [39]. Many of these organisms have the ability to become pathogenic if the oral mucosa is wounded or compromised, or if there is significant dysbiosis in the microbial flora. Lysozyme is a glycoside hydrolase and acts as an antimicrobial agent by catalysing the hydrolysis of linkages between *N*-acetylmuramic acid and *N*-acetyl-D-glucosamine residues in peptidoglycan, the major cell wall component of Gram-positive bacteria. We next tested if membrane-released lysozyme was able to cleave peptidoglycan and cause bacterial cell lysis in *Streptococcus ratti*, a Gram-positive oral bacterium found in the oral cavity that has been associated with dental biofilms [40] and is known to be affected by lysozyme activity [41]. Lysozyme was eluted from electrospun membranes and its effects on inhibiting bacteria growth assessed. Eluted lysozyme significantly inhibited the growth of *S. ratti* by 51% after 15 h compared to eluate from a placebo membrane control (51.1 ± 5.7 vs 0.6 ± 1.6, $p < 0.0001$, Fig. 8). These data clearly show that lysozyme released by electrospun membranes retains its biological activity and is able to inhibit bacterial growth and indicate that these membranes may be effective at treating oral bacterial infections or as covering for oral wounds or lesions that may be susceptible to bacterial infection.

Interestingly, the lysozyme membrane eluate contained 0.43 ± 0.07 mg/mL protein content and caused 51% bacterial inhibition, whereas purified lysozyme of a similar protein concentration (0.5 mg/mL) almost completely abolished *S. ratti* growth over the same time period ($p < 0.0001$, Fig. 8). To investigate the cause of this apparent reduction in activity, samples of placebo membranes were eluted in 0.5 mg/mL lysozyme solution. The resulting eluate inhibited growth

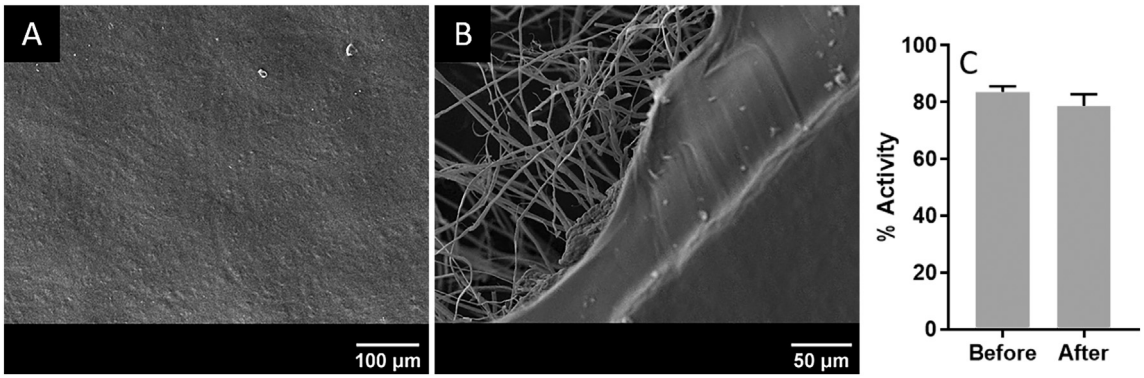

Fig. 7. SEM micrographs of the continuous PCL backing layer film formed after thermal treatment (A) and the edge of the patch showing the PCL film backing layer and lower layer of lysozyme-containing PVP and RS100 fibres (B). Activity of lysozyme released from patches with PCL backing layers before and after melting at 65 °C for 15 min (C). Data is presented as mean ± SD, with 3 independent samples, and analysed using Welch's *t*-test.

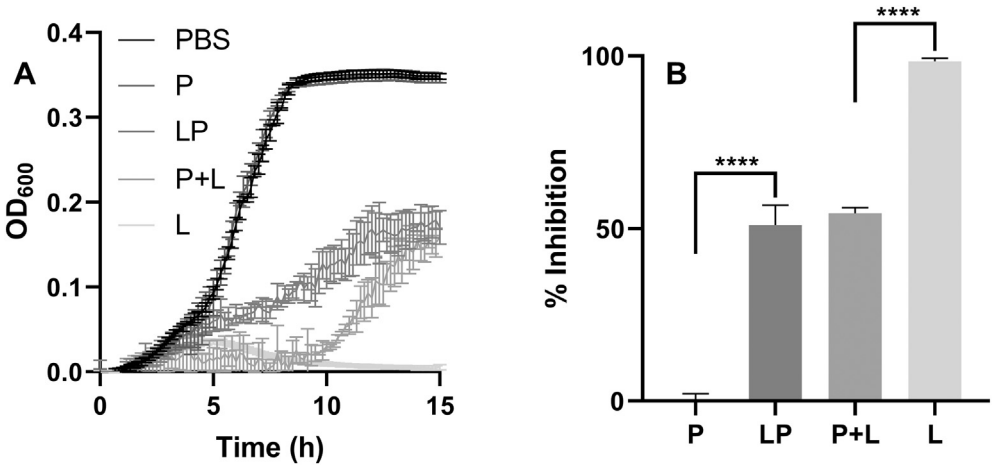

Fig. 8. Growth curve of *S. ratti* measured by optical density at 600 nm over time in the presence of PBS, eluent from placebo membranes (P), eluent from membranes containing lysozyme (LP), placebo membranes eluted in stock lysozyme solution (P + L), and a lysozyme stock solution (L) (A). % growth inhibition relative to PBS at 15 h (B). Data is presented as mean ± SD, with 3 independent samples, and the optical densities at 15 h analysed using one-way ANOVA with post hoc Tukey tests. ****, $p < 0.0001$.

to the same extent as the lysozyme membrane eluent, suggesting that this disparity related to polymer in the sample and not loss of activity during electrospinning. This may be a result of water soluble PVP leaching from the fibres and inhibiting lysozyme activity or encapsulating and protecting the bacteria. PVP has previously been shown to inhibit the enzyme phenolase [42], however its effect on lysozyme has not been studied. Further investigation would be required to elucidate the mechanism of this effect.

4. Conclusions

This mucoadhesive system enabled the encapsulation of an enzyme into polymer fibres with superior encapsulation efficiency and biological activity preservation compared to what has previously been accomplished with uniaxial electrospinning. The approach described here is considerably simpler to scale up to an industrial manufacturing setting than the frequently reported emulsion and coaxial electrospinning techniques, with fewer parameter to optimise and control. Unlike previous systems, the fibres released the majority of the protein in a single burst at a rate appropriate for drug delivery to the oral mucosa. Furthermore, the protein was homogenously distributed, and data suggest that the dual-layer patches maintained mucoadhesive properties similar to those previously reported [14]. The biological activity of the encapsulated protein was further demonstrated by the inhibition of growth of an oral bacterial strain. This illustrates that the patches could be useful for the local delivery of antimicrobial proteins. In practise, there are likely to be many more suitable candidate protein drugs, since lysozyme is only active against specific bacterial strains [41]. For example, patches loaded with the antifungal peptide histatin-5 may be effective against chlorhexidine resistant periodontal *Candida* biofilms [43]. The food-grade preservative nisin has broad spectrum activity against many Gram-positive bacteria, and could potentially be incorporated into the patches to treat multi-species bacterial biofilms [44]. The patch technology reported here holds great promise as a novel therapeutic protein delivery system for the oral mucosa.

CRediT authorship contribution statement

Jake G. Edmans: Conceptualization, Methodology, Investigation, Visualization, Writing - original draft. **Craig Murdoch:** Conceptualization, Methodology, Writing - review & editing, Supervision. **Martin E. Santocildes-Romero:** Conceptualization, Supervision. **Paul V. Hatton:** Conceptualization, Writing - review & editing, Supervision. **Helen E. Colley:** Conceptualization, Writing - review & editing, Supervision, Funding acquisition. **Sebastian G. Spain:** Conceptualization, Methodology, Writing - review & editing, Supervision, Funding acquisition.

Declaration of competing interest

The authors declare the following financial interests/personal relationships which may be considered as potential competing interests: The research presented was funding in part by AFYX Therapeutics. Dr H, Mr J Edmans, Dr S Spain and Professor C Murdoch declare that they have no other known competing financial interests or personal relationships that could have appeared to influence the work reported within this paper.

Dr M E. Santocildes-Romero is employed by AFYX Therapeutics. Professor P V. Hatton is on the AFYX Therapeutics APS Scientific Advisory Board, where AFYX have translated mucoadhesive electrospun patch technology for clinical use and have intellectual property (international patent application WO 2017/085262 A).

Acknowledgements

The authors would like to thank Jason Heath for training in microbiology, Katharina Clitherow for training and advice in electrospun materials. This work was funded by the UK EPSRC (EP/L016281/1) as a CASE PhD studentship with the Centre for Doctoral Training in Polymers & Soft Matter where AFYX Therapeutics was the industrial partner.

Appendix A. Supplementary data

Supplementary data to this article can be found online at https://doi.org/10.1016/j.msec.2020.110917.

References

[1] F. Albericio, H.G. Kruger, Therapeutic peptides, Future Med. Chem. 4 (2012) 1527–1531, https://doi.org/10.4155/fmc.12.94.
[2] J.L. Lau, M.K. Dunn, Therapeutic peptides: historical perspectives, current development trends, and future directions, Bioorg. Med. Chem. 26 (2018) 2700–2707, https://doi.org/10.1016/j.bmc.2017.06.052.
[3] H. Altman, D. Steinberg, Y. Porat, A. Mor, D. Fridman, M. Friedman, G. Bachrach, In vitro assessment of antimicrobial peptides as potential agents against several oral bacteria, J. Antimicrob. Chemother. 58 (2006) 198–201, https://doi.org/10.1093/jac/dkl181.
[4] K. Kavanagh, S. Dowd, Histatins: antimicrobial peptides with therapeutic potential, J. Pharm. Pharmacol. 56 (2004) 285–289, https://doi.org/10.1211/0022357022971.
[5] K. Fujisawa, Y. Miyamoto, M. Nagayama, Basic fibroblast growth factor and epidermal growth factor reverse impaired ulcer healing of the rabbit oral mucosa, J. Oral Pathol. Med. 32 (2003) 358–366, https://doi.org/10.1034/j.1600-0714.2003.t01-1-00111.x.
[6] J.P. Hong, S.W. Lee, S.Y. Song, S.D. Ahn, S.S. Shin, E.K. Choi, J.H. Kim, Recombinant human epidermal growth factor treatment of radiation-induced severe oral mucositis in patients with head and neck malignancies, Eur. J. Cancer Care (Engl.) 18 (2009) 636–641, https://doi.org/10.1111/j.1365-2354.2008.00971.x.
[7] A. Verma, N. Kumar, R. Malviya, P.K. Sharma, Emerging trends in noninvasive

insulin delivery, J. Pharm. 2014 (2014) 1–9, https://doi.org/10.1155/2014/378048.
[8] Z. C., R.J. M., Buccal transmucosal delivery of calcitonin in rabbits using thin-film composites, Pharm. Res. 19 (2002) 1901–1906, https://doi.org/10.1023/102146201.
[9] J. Autio-Gold, The role of chlorhexidine in caries prevention, Oper. Dent. 33 (2008) 710–716, https://doi.org/10.2341/08-3.
[10] M. Innocenti, G. Moscatelli, S. Lopez, Efficacy of Gelclair in reducing pain in palliative care patients with oral lesions, J. Pain Symptom Manag. 24 (2002) 456–457, https://doi.org/10.1016/S0885-3924(02)00524-9.
[11] R.J. Bensadoun, J. Daoud, B. El Gueddari, L. Bastit, R. Gourmet, A. Rosikon, C. Allavena, P. Céruse, G. Calais, P. Attali, Comparison of the efficacy and safety of miconazole 50-mg mucoadhesive buccal tablets with miconazole 500-mg gel in the treatment of oropharyngeal candidiasis: a prospective, randomized, single-blind, multicenter, comparative, phase III trial in patients, Cancer 112 (2008) 204–211, https://doi.org/10.1002/cncr.23152.
[12] V. Hearnden, V. Sankar, K. Hull, D. Vidovi, M. Greenberg, A.R. Kerr, P.B. Lockhart, L.L. Patton, S. Porter, M.H. Thornhill, New developments and opportunities in oral mucosal drug delivery for local and systemic disease, Adv. Drug Deliv. Rev. 64 (2012) 16–28, https://doi.org/10.1016/j.addr.2011.02.008.
[13] N.L. Schechter, S.J. Weisman, M. Rosenblum, B. Bernstein, P.L. Conard, The use of oral transmucosal fentanyl citrate for painful procedures in children, Pediatrics 95 (1995) 335 LP–339 http://pediatrics.aappublications.org/content/95/3/335.abstract.
[14] M.E. Santocildes-Romero, L. Hadley, K.H. Clitherow, J. Hansen, C. Murdoch, H.E. Colley, M.H. Thornhill, P.V. Hatton, Fabrication of electrospun mucoadhesive membranes for therapeutic applications in oral medicine, ACS Appl. Mater. Interfaces 9 (2017) 11557–11567, https://doi.org/10.1021/acsami.7b02337.
[15] H.E. Colley, Z. Said, M.E. Santocildes-Romero, S.R. Baker, K. D'Apice, J. Hansen, L.S. Madsen, M.H. Thornhill, P.V. Hatton, C. Murdoch, Pre-clinical evaluation of novel mucoadhesive bilayer patches for local delivery of clobetasol-17-propionate to the oral mucosa, Biomaterials. 178 (2018) 134–146, https://doi.org/10.1016/j.biomaterials.2018.06.009.
[16] K.H. Clitherow, C. Murdoch, S.G. Spain, A.M. Handler, H.E. Colley, M.B. Stie, H. Mørck Nielsen, C. Janfelt, P.V. Hatton, J. Jacobsen, Mucoadhesive electrospun patch delivery of lidocaine to the oral mucosa and investigation of spatial distribution in a tissue using MALDI-mass spectrometry imaging, Mol. Pharm. 16 (2019) 3948–3956, https://doi.org/10.1021/acs.molpharmaceut.9b00535.
[17] D.B. Khadka, D.T. Haynie, Protein- and peptide-based electrospun nanofibers in medical biomaterials, Nanomed. Nanotechnol. Biol. Med. 8 (2012) 1242–1262, https://doi.org/10.1016/j.nano.2012.02.013.
[18] V. Beachley, X. Wen, Polymer nanofibrous structures: fabrication, biofunctionalization, and cell interactions, Prog. Polym. Sci. 35 (2010) 868–892, https://doi.org/10.1016/j.progpolymsci.2010.03.003.
[19] S.Y. Chew, J. Wen, E.K.F. Yim, K.W. Leong, Sustained release of proteins from electrospun biodegradable fibers, Biomacromolecules 6 (2005) 2017–2024, https://doi.org/10.1021/bm0501149.
[20] K. Wei, Y. Li, X. Lei, H. Yang, A. Teramoto, J. Yao, K. Abe, F.K. Ko, Emulsion electrospinning of a collagen-like protein/PLGA fibrous scaffold: empirical modeling and preliminary release assessment of encapsulated protein, Macromol. Biosci. 11 (2011) 1526–1536, https://doi.org/10.1002/mabi.201100141.
[21] H. Qu, S. Wei, Z. Guo, Coaxial electrospun nanostructures and their applications, J. Mater. Chem. A 1 (2013) 11513–11528, https://doi.org/10.1039/c3ta12390a.
[22] H. Jiang, Y. Hu, Y. Li, P. Zhao, K. Zhu, W. Chen, A facile technique to prepare biodegradable coaxial electrospun nanofibers for controlled release of bioactive agents, J. Control. Release 108 (2005) 237–243, https://doi.org/10.1016/j.jconrel.2005.08.006.
[23] W. Ji, F. Yang, J.J.J.P. Van Den Beucken, Z. Bian, M. Fan, Z. Chen, J.A. Jansen, Fibrous scaffolds loaded with protein prepared by blend or coaxial electrospinning, Acta Biomater. 6 (2010) 4199–4207, https://doi.org/10.1016/j.actbio.2010.05.025.
[24] J. Schindelin, I. Arganda-carreras, E. Frise, V. Kaynig, T. Pietzsch, S. Preibisch, C. Rueden, S. Saalfeld, B. Schmid, J. Tinevez, D.J. White, V. Hartenstein, P. Tomancak, A. Cardona, PBMCs, Nat. Methods 9 (2012) 676–682, https://doi.org/10.1038/nmeth.2019.Fiji.
[25] D. Shugar, The measurement of lysozyme activity and the ultra-violet inactivation of lysozyme, Biomed. Biochim. Acta 8 (1952) 302–309, https://doi.org/10.1016/0006-3002(52)90045-0.
[26] M.E. Aulton, M. Banks, I.I. Davies, A fluorescent technique for the observation of polyvinylpyrrolidone binder distribution in granules, Drug Dev. Ind. Pharm. 4 (1978) 537–539, https://doi.org/10.3109/03639047809081825.
[27] P.B. Jeppesen, B. Hartmann, J. Thulesen, J. Graff, J. Lohmann, B.S. Hansen, F. Tofteng, S.S. Poulsen, J.L. Madsen, J.J. Holst, P.B. Mortensen, Glucagon-like peptide 2 improves nutrient absorption and nutritional status in short-bowel patients with no colon, Gastroenterology 120 (2001) 806–815, https://doi.org/10.1053/gast.2001.22555.
[28] C.H. Chesnut, M. Azria, S. Silverman, M. Engelhardt, M. Olson, L. Mindeholm, Salmon calcitonin: a review of current and future therapeutic indications, Osteoporos. Int. 19 (2008) 479–491, https://doi.org/10.1007/s00198-007-0490-1.
[29] R.M. Neer, C.D. Arnaud, J.R. Zanchetta, R. Prince, G.A. Gaich, J.-Y. Reginster, A.B. Hodsman, E.F. Eriksen, S. Ish-Shalom, H.K. Genant, O. Wang, D. Mellström, E.S. Oefjord, E. Marcinowska-Suchowierska, J. Salmi, H. Mulder, J. Halse, A.Z. Sawicki, B.H. Mitlak, Effect of parathyroid hormone (1-34) on fractures and bone mineral density in postmenopausal women with osteoporosis, N. Engl. J. Med. 344 (2001) 1434–1441, https://doi.org/10.1056/NEJM200105103441904.
[30] R. Giordano, A. Salleo, S. Salleo, F. Wanderlingh, Viscosity and density of lysozyme in water, Phys. Lett. A 70 (1979) 64–66, https://doi.org/10.1016/0375-9601(79)90329-3.
[31] T.T. Herskovits, H. Jaillet, Structural stability and solvent denaturation of myoglobin, Science (80-.) 163 (1969) 282–285, https://doi.org/10.1126/science.163.3864.282.
[32] Y.R. Personna, L. Slater, D. Ntarlagiannis, D. Werkema, Z. Szabo, Electrical signatures of ethanol-liquid mixtures: implications for monitoring biofuels migration in the subsurface, J. Contam. Hydrol. 144 (2013) 99–107, https://doi.org/10.1016/j.jconhyd.2012.10.011.
[33] M. Guettari, A. Belaidi, T. Tajouri, Polyvinylpyrrolidone behavior in water/ethanol mixed solvents: comparison of modeling predictions with experimental results, J. Solut. Chem. 46 (2017) 1404–1417, https://doi.org/10.1007/s10953-017-0649-0.
[34] N. Bhardwaj, S.C. Kundu, Electrospinning: a fascinating fiber fabrication technique, Biotechnol. Adv. 28 (2010) 325–347, https://doi.org/10.1016/j.biotechadv.2010.01.004.
[35] K. Nartetamrongsutt, G.G. Chase, The influence of salt and solvent concentrations on electrospun polyvinylpyrrolidone fiber diameters and bead formation, Polymer (Guildf) 54 (2013) 2166–2173, https://doi.org/10.1016/j.polymer.2013.02.028.
[36] J. Xie, C.H. Wang, Electrospun micro- and nanofibers for sustained delivery of paclitaxel to treat C6 glioma in vitro, Pharm. Res. 23 (2006) 1817–1826, https://doi.org/10.1007/s11095-006-9036-z.
[37] T.H.B. Eriksen, E. Skovsen, P. Fojan, Release of antimicrobial peptides from electrospun nanofibres as a drug delivery system, J. Biomed. Nanotechnol. 9 (2013) 492–498, https://doi.org/10.1166/jbn.2013.1553.
[38] S.-F. Chou, D. Carson, K.A. Woodrow, Current strategies for sustaining drug release from electrospun nanofibers, J. Control. Release 220 (2015) 584–591, https://doi.org/10.1016/j.jconrel.2015.09.008.
[39] F.E. Dewhirst, T. Chen, J. Izard, B.J. Paster, A.C.R. Tanner, W.H. Yu, A. Lakshmanan, W.G. Wade, The human oral microbiome, J. Bacteriol. 192 (2010) 5002–5017, https://doi.org/10.1128/JB.00542-10.
[40] K.Y. Lee, M.R. Jeong, S.M. Choi, S.S. Na, J.D. Cha, Synergistic effect of fucoidan with antibiotics against oral pathogenic bacteria, Arch. Oral Biol. 58 (2013) 482–492, https://doi.org/10.1016/j.archoralbio.2012.11.002.
[41] V.J. Iacono, B.J. MacKay, S. DiRienzo, J.J. Pollock, Selective antibacterial properties of lysozyme for oral microorganisms, Infect. Immun. 29 (1980) 623–632.
[42] J.R.L. Walker, A.C. Hulme, The inhibition of the phenolase from apple peel by polyvinylpyrrolidone, Phytochemistry 4 (1965) 677–685.
[43] C.R. Pusateri, E.A. Monaco, M. Edgerton, Sensitivity of Candida albicans biofilm cells grown on denture acrylic to antifungal proteins and chlorhexidine, Arch. Oral Biol. 54 (2009) 588–594, https://doi.org/10.1016/j.archoralbio.2009.01.016.
[44] J.M. Shin, I. Ateia, J.R. Paulus, H. Liu, J.C. Fenno, A.H. Rickard, Y.L. Kapila, Antimicrobial nisin acts against saliva derived multi-species biofilms without cytotoxicity to human oral cells, Front. Microbiol. 6 (2015) 1–14, https://doi.org/10.3389/fmicb.2015.00617.

Chapter 3: Rapid bioactive peptide and protein release from a mucoadhesive electrospun membrane

Rapid bioactive peptide and protein release from a mucoadhesive electrospun membrane

Jake G. Edmans[1, 2], Craig Murdoch[1*], Paul V. Hatton[1], Lars Siim Madsen,[3] Martin E. Santocildes-Romero,[3] Sebastian G. Spain[2] and Helen E. Colley.[1]

[1]School of Clinical Dentistry, University of Sheffield, 19 Claremont Crescent, Sheffield, S10 2TA, UK

[2]Department of Chemistry, University of Sheffield, Brook Hill, Sheffield, S3 7HF, UK

[3]AFYX Therapeutics, Lergravsvej 57, 2. tv, 2300 Copenhagen, Denmark

*Correspondence: Prof Craig Murdoch

School of Clinical Dentistry, University of Sheffield, 19 Claremont Crescent, Sheffield, S10 2TA, UK

c.murdoch@sheffield.ac.uk, Tel: +44 114 2159367

Keywords: Electrospinning; Drug delivery; Peptides; Oral mucosa; Mucoadhesion; Bradykinin; Insulin

Abstract

Protein-based biologics constitute a rapidly expanding category of therapeutic agents with high target specificity. Their clinical use has dramatically increased in recent years, but administration is largely via injection. Drug delivery across the oral mucosa is a promising alternative to injections for administration of local or systemic-bound proteins or peptides, so avoiding the gastrointestinal tract and first-pass metabolism. However, development is hindered by current drug delivery formulations such as liquid sprays, mucoadhesive tablets and films that lack precise dose control in the presence of salivary flow. To address this, electrospun membranes that adhere tightly to the oral mucosa surface and release drugs locally have been developed. Here we investigated the suitability of these membranes for peptide or protein release. Bradykinin or insulin were incorporated into mucoadhesive membranes by electrospinning from ethanol/water mixtures. Immersing the membranes in buffer resulted in rapid release of bradykinin, with a maximal release of 70 ± 12% reached after one hour for fibres with a loading of 0.1% w/w. Insulin was released more slowly with 88 ± 11% released after eight hours for fibres with a loading of 1% w/w. Membrane-eluted bradykinin retained pharmacological activity, inducing intracellular calcium release in oral fibroblasts at similar levels to bradykinin delivered in solution. These data show that electrospun membranes may be a highly effective vehicle for site-specific administration of therapeutic proteins or peptides directly to the oral mucosa to achieve either local or systemic drug delivery.

1. Introduction

Peptide and protein biologics are a rapidly growing class of pharmaceuticals with high clinical success rates, high specificity, high potency and low toxicity.[1] However, these types of therapeutics suffer from low oral bioavailability due to limited gastrointestinal absorption, enzymatic degradation and first-pass hepatic metabolism, and are therefore almost exclusively administered parenterally by injection. This has significant associated drawbacks including patient discomfort, non-compliance due to trypanophobia and, in many cases, the need for administration by healthcare professionals. For these reasons, there is much interest in drug delivery via mucosal surfaces.[2,3] Transmucosal drug delivery via the oral cavity enables easy self-administration and is painless, thus increasing compliance rates. Furthermore, the ability to deliver biologics topically to the oral mucosa may enable new treatments for oral diseases while mitigating off-target side effects. Although there is much interest in this mode of delivery, progress is limited by the lack of suitable dosage forms that allow site-specific delivery to mucosal surfaces.

The only formulation that has successfully reached market deployment for transmucosal peptide delivery to date is the Oral-Lyn™ insulin aerosol spray for the management of Type 1 Diabetes.[4] Unlike competing alternatives, this formulation is absorbed through the buccal oral mucosa rather than the respiratory tract and uses a mixture of surfactants to enhance epithelial permeation as well as to allow aerosol formation.[5] The relatively high doses of insulin required and its poor epithelial permeability make it a challenging candidate drug for transmucosal delivery. Indeed, significant disadvantages of buccal insulin sprays include modest bioavailability of approximately 10% and the large volume of spray required to achieve a therapeutic dose.[4] *In vivo* investigations into transmucosal biologic delivery suggest that several hydrophilic lower molecular weight therapeutic peptides including glucagon-like-peptide 1,[6] salmon calcitonin,[7] and desmopressin[8] delivered to the buccal or sublingual mucosa can permeate sufficiently to achieve therapeutically relevant systemic doses without the need for permeation enhancing excipients. Low molecular weight peptides with fewer rotatable bonds tend to permeate the oral epithelium more easily, facilitating uptake. Absorption of these molecules is often hypothesized to occur by passive diffusion through the epithelial paracellular spaces.[9] There is great potential to develop new dosage forms for the delivery of permeable proteins or peptides into or across the oral mucosa depending on epithelial or systemic targeting. However, previous studies have examined dosage forms with limited suitability for further translation, typically consisting of solutions or dissolving tablets/films that are readily removed from the mucosal surface by saliva, resulting in limited drug/tissue contact times.[10,11]

Electrospinning has recently attracted interest for the fabrication of oromucosal dosage forms with improved flexibility and high surfaces areas to facilitate drug release and mucoadhesive interactions.[12] Furthermore, dual-layer electrospun membranes with hydrophobic backing layers are highly effective at promoting the retention of drugs on the oral mucosa in the presence of saliva flow.[13,14] Previous studies investigating electrospinning for protein or peptide encapsulation have primarily focused on more complex emulsion and coaxial electrospinning techniques, due to the perception that organic electrospinning solvents would cause unacceptable denaturation during uniaxial electrospinning.[15] Emulsion and coaxial electrospinning tend to produce multi-domain fibres that are more applicable for sustained release applications.[16] Alternatively, protein-loaded fibres have been prepared from aqueous polymer solutions to avoid potential solvent-induced denaturation. This is possible using gel-forming polyelectrolyte carbohydrate polymers such as chitosan or alginate to prevent rapid dissolution and promote mucoadhesion.[17,18] A dual-layer mucoadhesive electrospun drug delivery patch consisting of a mucoadhesive inner membrane layer and a protective outer membrane layer has been developed to facilitate site-specific delivery to the buccal mucosa.[19] The patch is fabricated entirely from approved medical grade polymers using a simple uniaxial electrospinning technique with ethanol as a solvent. These membranes were highly effective in phase II clinical trials in the delivery of clobetasol-17-propionate for treatment of erosive oral lichen planus,[20] and have potential for several applications in oral medicine.[14,21,22]

Although several electrospun mucoadhesive materials have now been developed that might be suitable for oromucosal protein delivery, a limited range of proteins have been investigated and the pharmacological activity of a therapeutically relevant peptide following elution from the polymer fibres has not been investigated fully.[17] In this study, a peptide (bradykinin, 9 amino acids; 1060 Da) and protein (insulin, 51 amino acids; 5808 Da) of different molecular weights and physicochemical properties were incorporated into mucoadhesive electrospun fibres and their release kinetics examined to further investigate the versatility of the technology for mucosal delivery. Moreover, the biological activity of bradykinin following elution was assessed to determine if released molecules retain their biological activity upon release.

2. Material and Methods

2.1 Materials

Poly(vinylpyrrolidone) (PVP; MW 2000 kDa) and Eudragit® RS100 (RS100; MW 38 kDa) were kindly donated by BASF, Cheadle Hulme, UK and Evonik Industries AG, Essen, Germany, respectively. Bradykinin ELISA kit was purchased from Abcam, Cambridge, UK. Fluo-4 Direct™ calcium assay kit was

purchased from ThermoFisher Scientific, Loughborough, UK. Bradykinin and cell culture reagents were purchased from Sigma-Aldrich, Poole, UK.

2.2 Electrospinning system

Electrospun membranes were fabricated using a system composed of a PHD2000 syringe pump (Harvard Apparatus, Cambridge, UK) and an Alpha IV Brandenburg power source (Brandenburg, UK). Plastic syringes (1 mL volume; Henke Sass Wolf, Tuttlingen, Germany) were used to drive the solutions into a 20-gauge blunt metallic needle (Fisnar Europe, Glasgow, UK). Electrospinning was performed at room temperature with a potential difference of 19 kV, a flow rate of 2 mL/h, and a flight path of 14 cm.[19,23]

2.3 Fabrication of electrospun membranes containing bradykinin or Insulin

Electrospinning solutions contained 0.1025 g/mL PVP and 0.1225 g/mL Eudragit® RS100 (by total solvent volume before mixing). PVP and RS100 were added to ethanol and mixed at room temperature using a magnetic stirrer until dissolved. Bradykinin was dissolved in ice cold phosphate buffered saline (PBS), added to the polymer solution shortly before electrospinning and stirred until uniformly distributed, contributing 3% v/v to the final solvent composition. Placebo solutions and membranes were prepared using 3% v/v distilled water instead of bradykinin in PBS. For Insulin, all electrospinning solutions contained 0.0825 ± 0.00125 g/mL PVP and 0.1025 ± 0.00125 g/mL Eudragit® RS100 (by total solvent volume before mixing). The required amounts of PVP and RS100 were added to ethanol and mixed at room temperature using a magnetic stirrer until dissolved. The required concentration of insulin was prepared in 2 % acetic acid in PBS in a glass vial and vortexed for approximately 60 s with gentle heating until a clear solution was produced. Insulin solutions were combined with the polymer solutions at 20 % v/v and mixed until homogenous shortly before electrospinning. Placebo solutions and membranes without insulin were prepared under identical conditions.

2.4 Surface pH

Membrane samples (10 ± 0.5 mg) were placed in a 24-well plate, submerged in deionized water (1 mL), and shaken briefly until wetted. After 10 minutes, pH was measured using a pH meter (Hanna Instruments, Rhode Island, USA).

2.5 Scanning electron microscopy

Electrospun membranes were imaged using a TESCAN Vega3 scanning electron microscope (SEM; Tescan, Cambridge, UK). Samples were sputter coated with gold and imaged using an emission voltage of 10 kV. All images were processed and fibre diameters measured using ImageJ software tools,[24] using

randomly generated coordinates and a superimposed grid to select fibres. Three images were analysed for each membrane composition with at least 10 measurements per image.

2.6 Release profile of bradykinin from electrospun membranes

Samples of electrospun membranes (20 mg) containing bradykinin were immersed in 4 mL PBS and 10 µL samples taken at time intervals up to 4 h following vortexing for 5 s. Bradykinin concentration was quantified using a competitive ELISA kit (ab136936) and used according to the manufacturer's instructions (abcam, Cambridge, UK). To calculate percentage cumulative release, the active concentration was normalised against the theoretical maximum concentration, based on the dry mass fraction of bradykinin in the electrospinning solution.

2.7 Release profile of insulin from electrospun membranes

Membrane samples (3-6 mg) containing insulin were cut using a circular punch and placed in a 12-well plate. Pre-warmed PBS (2 mL) was added to the wells and the samples incubated at 37 °C with shaking. 50 µL aliquots were taken every 0.5 h for 8 h and the volume replaced with fresh media. Protein concentration was measured using a Pierce™ bicinchoninic acid (BCA) assay kit as directed (ThermoFisher Scientific). Percentage cumulative release was calculated and normalised against the theoretical maximum concentration, based on the dry mass fraction of insulin in the electrospinning solution.

2.8 Cell isolation and culture

Normal oral fibroblasts (NOF) were isolated from the connective tissue of biopsies obtained from the oral mucosa of patients during routine dental procedures with written informed consent (Ethical Approval No. 09/H1308/66) and cultured in Dulbecco's Modified Eagle's Medium supplemented with foetal bovine serum (FBS; 10% v/v), 2 mM L-glutamine, 100 IU/mL penicillin and 100 µg/mL streptomycin.[25]

2.9 Intracellular calcium mobilisation using flow cytometry

NOF were removed from cell culture flasks and resuspended as directed in buffered Fluo-4 cell-permeant acetoxymethyl ester (ThermoFisher Scientific) at a suspension of 10^6 cells/mL and incubated for 45 minutes at 37 °C followed by 30 minutes at room temperature. Bradykinin-loaded or placebo membranes (10 mg) were eluted in 2 mL PBS for 24 h and stored at -20 °C prior to the experiment. A stock solution of bradykinin in PBS matching the theoretical concentration of the membrane eluent (5 µg/mL) was prepared as a positive control and stored in identical conditions. Samples and standards were diluted by a factor of 10 in PBS before assaying by flow cytometry. To determine intracellular

calcium responses, fluorescence was measured at 488 nm excitation and 530 nm emission using a FACSCalibur flow cytometer (BD Biosciences, Wokingham, UK). For each sample, baseline fluorescence was measured for 40 s before sample addition (10 µL in 1 mL) after which fluorescence was measured for approximately 160 s. Change in relative fluorescent units (ΔRFU) was calculated by subtracting the median relative fluorescent unit value of the baseline from the maximum median fluorescence (over a 1 s interval) following sample addition. The experiment was performed in triplicate using three independently prepared sets of membranes and different batches of cells.

2.10 Intracellular calcium mobilisation using confocal microscopy

NOF (2.5×10^4 in 25 µL) were seeded in a half-area glass-bottomed 96-well plate and incubated overnight to give a confluent monolayer. Bradykinin samples and controls were prepared as previously described and diluted by a factor of 1000 prior to assaying. Before imaging, 25 µL buffered Fluo-4 cell-permeant acetoxymethyl ester was added and the cells incubated for 45 minutes at 37 °C, followed by 30 minutes at room temperature. Imaging was performed using a Nikon A1 laser scanning confocal microscope with 457-514 nm argon laser. Cells were imaged at room temperature with approximately 1200 cells per image to obtain a baseline. Samples (50 µL) were added, and images immediately acquired every 10 s for 60 s using identical capture settings. The fold-change in fluorescence was calculated from the mean intensity of each the micrograph relative to the baseline. All images were processed using ImageJ software tools using automatic brightness/contrast adjustment on each series of images. The experiment was performed in triplicate using three independently prepared sets of membranes and different batches of cells.

2.11 Data analysis

All data and statistical analyses were performed using GraphPad Prism 9.4.1 software (GraphPad Software, La Jolla, USA). Student's t-test was used for pairwise comparisons while One-way ANOVA with Tukey's post hoc test was used to compare differences between groups and results considered statistically significant if $p < 0.05$.

3. Results

3.1 Incorporation of bradykinin and insulin into electrospun membranes

Electrospun membranes containing 0.1% w/w bradykinin by dry mass were prepared by electrospinning from a solution of 97% v/v ethanol. SEM images revealed a randomly aligned fibre morphology similar to those previously observed,[19] with few defects, and an average diameter of 2.23 ± 0.81 µm that was similar to control membranes (Figure. 1).

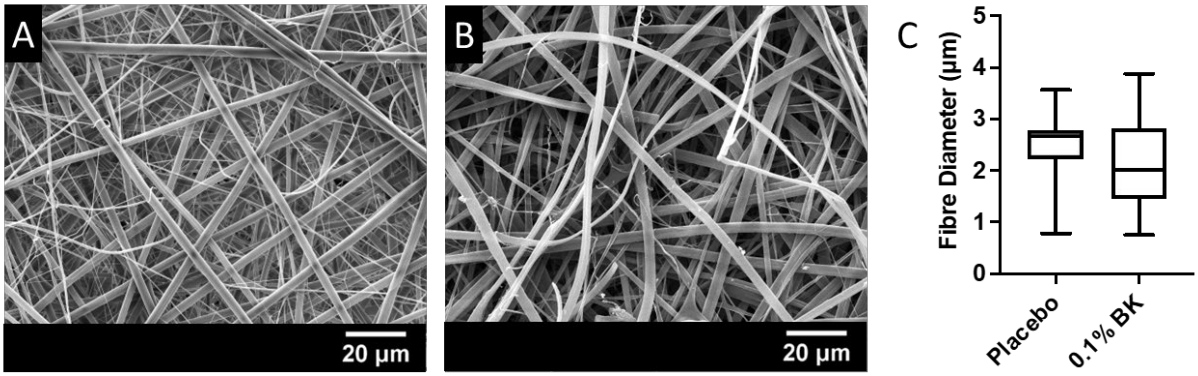

Figure 1. Characterisation of bradykinin-loaded mucoadhesive electrospun membranes. Bradykinin was incorporated into polymer fibres by mixing with ethanolic polymer solutions immediately before electrospinning. The resulting fibres were imaged by SEM. SEM micrographs of (A) control electrospun fibres (B) electrospun fibres containing 0.1% w/w bradykinin, scale bar = 20 µm. (C) Fibre diameter distribution presented as box and whisker plots displaying median, interquartile range and range (n = 30). Statistical analysis was performed by Student's t-test.

Due to the relatively low aqueous solubility of insulin, a solvent composition of 80 % v/v ethanol was used to allow the mixing of a larger volume of aqueous protein solution. The aqueous component of the electrospinning solution was acidified with acetic acid to dissolve the insulin. Membranes were fabricated to contain 0, 1, 3, and 5 % w/w insulin by dry mass. SEM analysis revealing a defect-free fibrous morphology in the absence of presence of insulin (Figure. 2 A). Membranes without insulin had a mean fibre diameter of 1.29 ± 0.36 µm (Figure. 2 B). Overall, inclusion of insulin produced fibres with increased diameters compared to controls. However, this reached statistical significance for fibres containing 3 % w/w (2.16 ± 0.78) compared to controls and fibres containing 1 % (1.56 ± 0.57) and 5 % (1.55 ± 0.39) w/w insulin (Figure. 2 B, $p < 0.001$). To investigate the effect of the use of acetic acid on surface pH, membranes were immersed in a small volume of distilled water before measuring pH with a digital probe. All samples prepared using this method had a surface pH of approximately 6 (Figure. 2 C), whereas the fibre formulation without acetic acid has a pH of 8.2.[14]

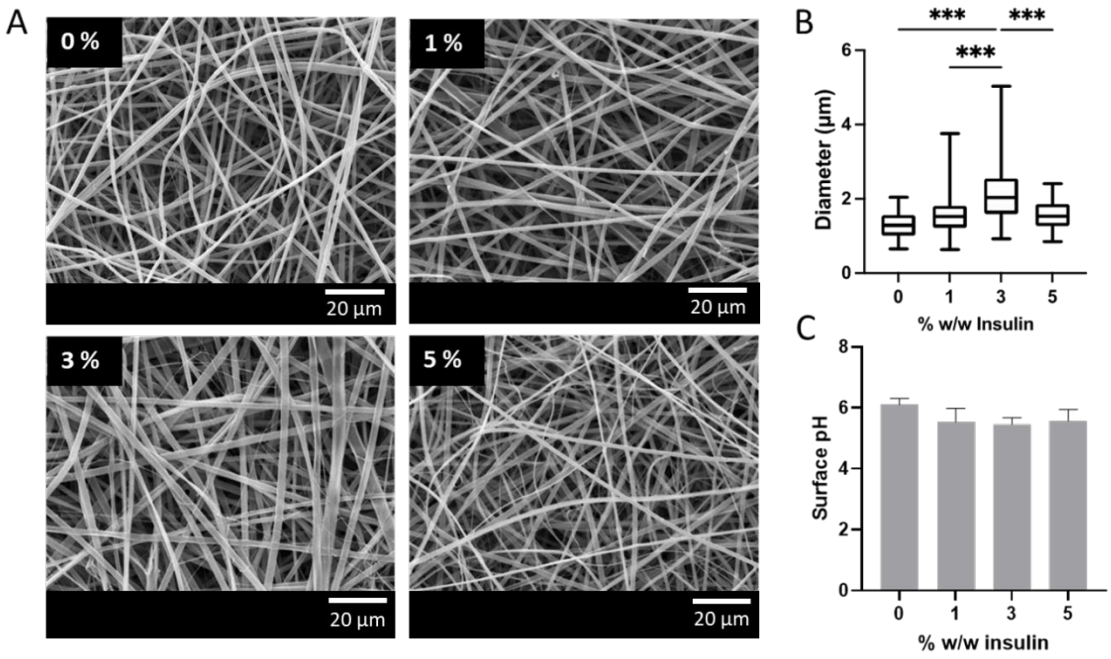

Figure 2. Preparation of mucoadhesive electrospun fibres containing 0, 1, 3, 5 % w/w insulin. Insulin was dissolved in 2 % v/v acetic acid in PBS and mixed 1:4 v/v with an ethanolic polymer solution shortly before electrospinning. (A) SEM micrographs of electrospun fibres containing 0, 1 3, and 5 % w/w insulin. Scale bar = 20 µm. (B) Fibre diameter distributions presented as median, interquartile range, and range. Data were analysed using one-way ANOVA with Tukey post hoc test. ***$p < 0.001$ (n = 30). (C) Surface pH of electrospun fibres presented as mean ± SD (n = 3) and analysed using one-way ANOVA.

3.2 Release of bradykinin and insulin from electrospun membranes

The release profile of bradykinin or insulin from membranes was measured by eluting in PBS and measuring bradykinin concentration by ELISA and insulin by BCA protein assay. Bradykinin release was rapid, with 55 ± 17% of the theoretical total dose released within 30 minutes. Maximum bradykinin release of 70 ± 12% was observed after 1 h (Figure. 3). Release of insulin was slower than that of bradykinin, with maximal but incomplete release after 8 h (Figure. 4 A). When evaluating liberation of insulin per mg membrane, release was dependent on insulin content, with the 5 and 3 % w/w patch releasing significantly more insulin than the 1 % w/w ($p < 0.001$ and $p < 0.05$, respectively) and placebo membrane. The percent cumulative insulin release after 8 h corresponded to 88 ± 11, 69.0 ± 5.4, and 63.9 ± 9.0 % of the total encapsulated dose for membranes containing 1, 3, and 5 % w/w insulin, respectively Figure. 4 B).

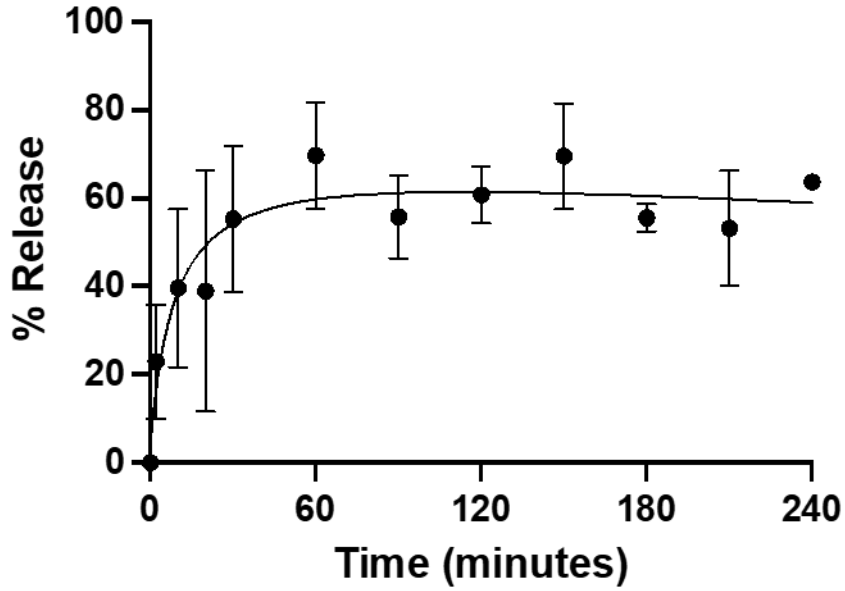

Figure 3. Release of bradykinin from mucoadhesive membranes following immersion in PBS. Membrane samples were eluted in PBS. Samples were periodically mixed using a vortex mixer and bradykinin concentrations in the media measured by ELISA. Data are presented as mean ± SD (n = 3).

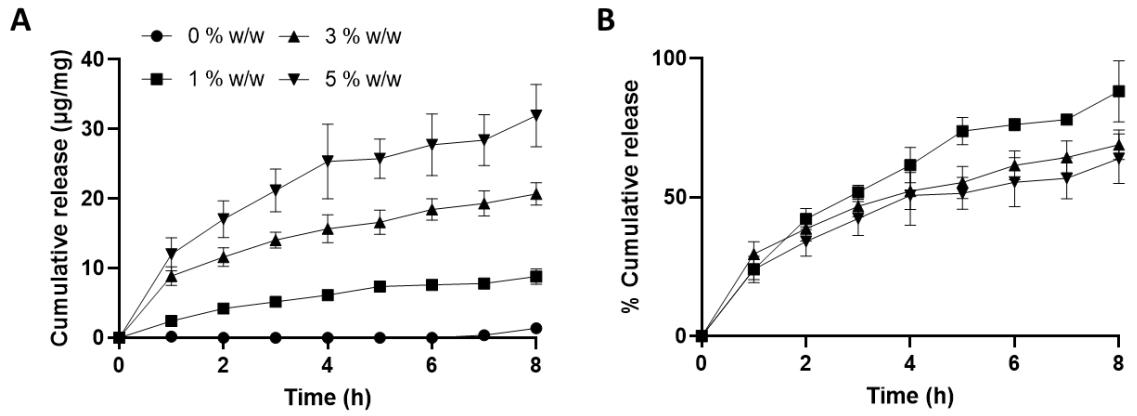

Figure 4. Cumulative release of insulin from electrospun membranes containing 1, 3, 5 % w/w insulin. (A) Release per mg of membrane. Statistical analysis was performed by ANOVA with Tukey's post hoc test *p<0.05, ***p<0.001. (B) Release as percentage of the total mass of insulin in the membrane samples. Membrane samples were eluted in PBS at 37 °C with shaking. Cumulative insulin release per mg of membrane. Data presented as mean ± SD (n = 3).

3.3 Membrane-eluted bradykinin stimulates intracellular calcium release in normal oral fibroblasts

The release of insulin from other polymer-based drug carriers for diabetic therapy has previously been reported in several studies.[4,17] We therefore decided to focus further experiments on bradykinin as an exemplar test molecule. Bradykinin is a hydrophilic nine amino acid (1060 Da) peptide that exerts its effects on cells such as fibroblasts, smooth muscle and endothelial cells that form blood vessels, causing vasodilation and increasing vascular permeability following engagement of G-protein coupled bradykinin receptors. To test whether the biological activity of bradykinin was preserved following release from membranes, its effect on intracellular calcium mobilisation following binding to its cell surface G-protein coupled receptor expressed by NOF was measured on a single-cell basis using flow cytometry. Bradykinin-containing membranes were eluted in PBS for 24 h and the supernatant added to cell suspensions at 5 ng/mL (assuming 100% loading efficiency and complete release from the membranes) to approximate physiological concentrations. The addition of placebo membrane eluent to NOF had negligible effect on fluorescence as a readout for intracellular calcium release, causing a 0.51 ± 0.46 maximum change in RFU relative to baseline (Figure. 5 A&D). Bradykinin solution caused a maximum 8.4 ± 1.3 ΔRFU (Figure. 5 B&D) while membrane eluted bradykinin caused a 13.2 ± 1.5 maximum ΔRFU (Figure. 5 C&D).

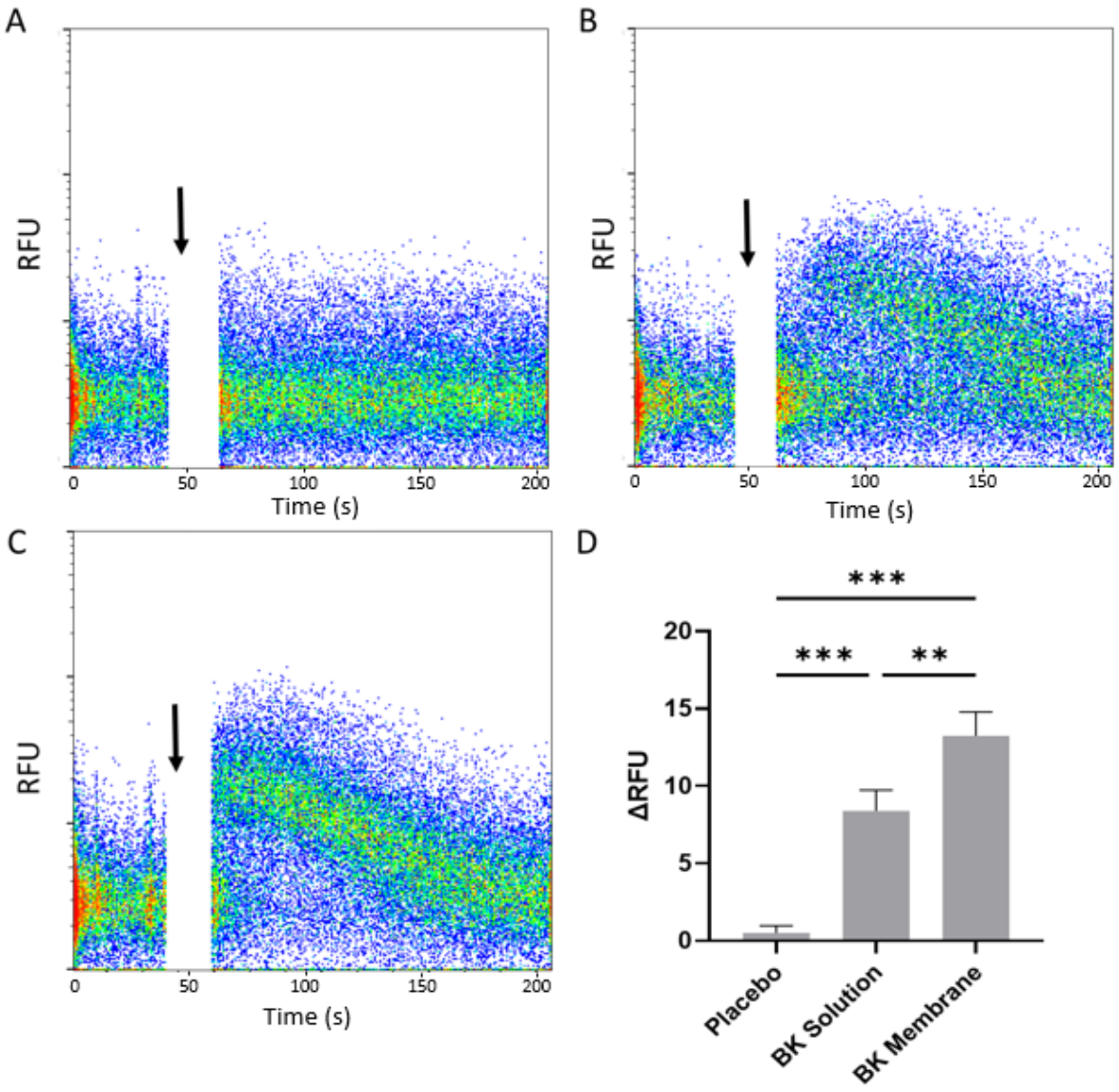

Figure 5. Bradykinin functionality was preserved following release from mucoadhesive membranes. Intracellular calcium mobilisation in fibroblasts was determined over time using flow cytometry. Each dot represents a fluorescence measurement for an individual cell. Baseline fluorescence was acquired for approximately 40 s before addition of samples (black arrow). (A) Placebo membrane eluent, (B) bradykinin (BK) solution, (C) BK membrane eluent. (D) Change in relative fluorescence units (RFU) were calculated by subtracting baseline median fluorescence from the maximal median fluorescence (over a 1 s interval) following sample addition. Data is presented as mean ± SD (n = 3) and analysed using one-way ANOVA with Tukey's post hoc test. $^{**}p < 0.01$, $^{***}p < 0.001$.

The effect on intracellular calcium mobilisation was also observed in fibroblast monolayers by confocal microscopy. Bradykinin samples were added at 2.5 ng/mL (assuming 100% loading efficiency and complete release), after which fluorescence micrographs were periodically captured for up to 60 s (Figure. 6). An eluted placebo membrane was used as a negative control and as expected, produced

negligible change in fluorescence (Figure. 6 A). Bradykinin in solution and as elute from the membrane cause a rapid (within 2 seconds) increase in intracellular calcium (Figure. 6 A). Bradykinin in solution caused a 2.13 ± 0.21 fold-change in fluorescence intensity peaking at 10 s ($p < 0.001$) relative to placebo, after which fluorescence intensity decreased linearly over time (Figure. 6 B&C). Membrane-eluted bradykinin produced similar behaviour, peaking at approximately 2 seconds, causing a 1.58 ± 0.16 fold-change after 10 s ($p < 0.001$) relative to placebo (Figure. 6B&C).

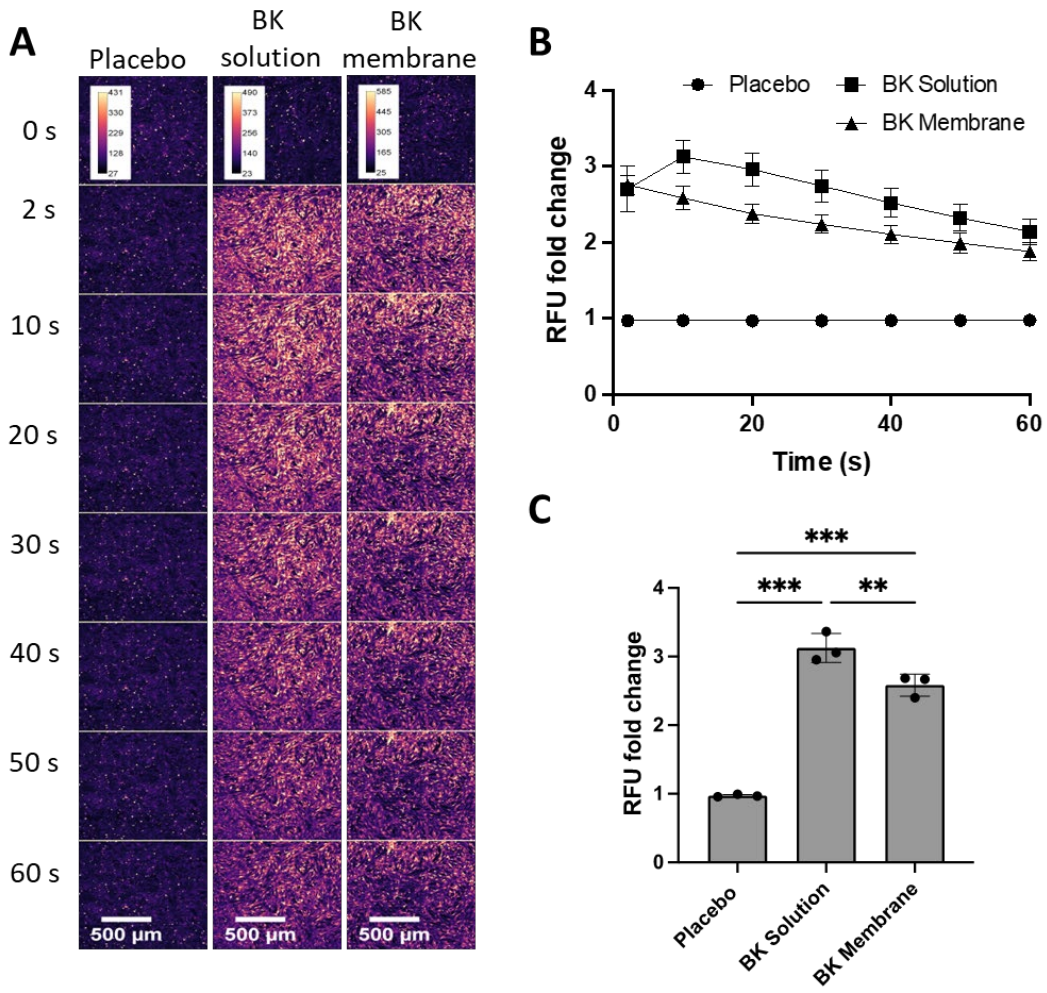

Figure 6. Membrane-eluted bradykinin increases intracellular calcium mobilisation in oral fibroblast monolayers. (A) Representative series of confocal micrographs showing the change in calcium mobilisation over time in NOF monolayers following treatment with PBS, placebo membrane eluent, bradykinin (BK) solution (2.5 ng/ml), or BK membrane eluent. (B) Fold-change in fluorescence relative units (RFU) over time following addition of solutions. (C) Fold-change in RFU after 10 s for each solution. Data is presented as mean ± SD (n = 3). Statistical analysis was performed using one-way ANOVA with Tukey's post hoc test. **$p < 0.01$, ***, $p < 0.001$.

4. Discussion

Electrospun mucoadhesive membranes have been developed to address the lack of formulations that enable site-specific drug delivery to the oral mucosa.[19] These membranes have been successfully developed for the delivery of several small molecule drugs[14,21,26] and lysozyme,[23] a robust antimicrobial enzyme, suggesting suitability for oromucosal protein delivery. In order to determine the potential of electrospun membranes for transmucosal peptide delivery it is necessary to demonstrate that a peptide can be incorporated and released at a suitable rate while maintaining pharmacological activity. Bradykinin is a small but highly potent vasoactive peptide. It was used in this study as an exemplar test molecule to provide proof-of-concept data that other such small peptides could be incorporated into electrospun membranes, released, and retain their biological activity.

Drug delivery from a membrane or patch applied to the oral mucosa is time-limited due to the requirement of patients to refrain from eating and drinking upon membrane application. A previous study observed a clinically measured membrane residence time of approximately 100 minutes for similar membranes applied to the human buccal mucosa.[14] Therefore, efficient peptide release over a maximum of 2 hours would be ideal for delivery within this timeframe. Indeed, maximal bradykinin release corresponding to around 70% of the total dose was detectable after 1 h. This rapid release is consistent with a release mechanism controlled by the swelling of highly hydrophilic fibres.[27] The release profile is similar to those previously reported for hydrophilic proteins encapsulated within swelling electrospun fibres. It was found previously that lysozyme was rapidly eluted from an identical polymer system, with approximately 90% of the dose released within 1 h.[23] In addition, Stie *et al*., showed that mucoadhesive fibres consisting of blended poly(ethylene oxide) and chitosan rapidly released the highly soluble peptide desmopressin through a similar mechanism.[13] Desmopressin release was even faster than observed in our system, reaching 80% release within 20 minutes. This can likely be attributed to narrower fibre diameter of approximately 200 nm, leading to a higher surface area and faster swelling.

Insulin was selected as a second model peptide to investigate the versatility of the patches for the delivery of larger, less soluble peptides, with the potential application of membrane that allows sustained insulin delivery for diabetics. Insulin has low aqueous solubility at neutral pH. However, it is moderately soluble at pH 3, and if necessary, the pH of the solution can be adjusted back to pH 7 without causing precipitation. The solubility is further increased by increasing the ionic strength of the solution, for example by using acidified PBS instead of acid in deionised water. Relatively high therapeutic doses in the order of hundreds of micrograms several times daily are required for managing diabetes. Therefore, to achieve suitably high loading in the mucoadhesive layer of the patch,

the aqueous portion of the electrospinning solvent was increased to 20 % v/v. Acidified PBS was used to solubilise insulin before mixing with the ethanolic polymer solution. This method allowed the fabrication of defect free fibres containing 0, 1, 3, 5 % w/w insulin.

The diameter of fibres containing 0 or 1 % w/w insulin was narrower than that those containing bradykinin. This is likely a result of the increased conductivity of the electrospinning solution, due to the higher water and salt content, which produces more rapid fibre elongation in an electric field. The fibres were also narrower than those previously observed for fibres containing 1 % w/w lysozyme, also prepared with 80 % v/v ethanol.[23] This is likely because PBS was used exclusively instead of deionised water, resulting in a more conductive solution, which is associated with narrower fibres.[28] Fibres containing 3 % w/w insulin were significantly wider than those with 1 or 5 % w/w. Insulin concentration affects both solution conductivity and viscosity. These properties are likely the cause of an unusual concentration-dependant effect on fibre diameter. The diameter of electrospun fibres can be modulated using high molecular weight polymers to increase viscosity or salts to increase conductivity.[28] Therefore, it would likely be possible to counteract this effect if desired. The use of acetic acid to solubilise insulin caused a decrease in surface pH to approximately 6, which is only slightly below the natural range for human saliva and so is likely to be tolerable.

Insulin was released more slowly from the fibres in comparison to the rapid release observed for highly water-soluble proteins.[13,23,29] A similar electrospun material containing insulin was investigated by Sharma et al. which also released insulin slowly, with complete release reached only after 10 h.[17] These fibres also comprised a blend of a water soluble polymer (poly(vinyl alcohol)) and a gel-forming polyionic polymer (sodium alginate). The authors hypothesised that the slow release was mediated by the biodegradation of sodium alginate. Considering the similar release profile observed for our system, it is possible that the slow release is caused by the intrinsically slow dissolution of insulin at physiological pH. A more rapid release profile may be desirable for oral mucosal insulin delivery, as eating and drinking could dislodge the membrane and overnight application may present a choking hazard.

There is potential to increase the release rate using off-the-shelf excipients, such as basic amino acids or ethylenediaminetetraacetic acid, which are known to increase the solubility of insulin.[30] Insulin release has been investigated from several polymer-based drug delivery systems. Moreover, it is a less promising candidate for transmucosal delivery using electrospun fibres, as the low density of fibrous materials means that only relatively small masses of drug can feasibly be delivered, whereas doses of several milligrams of insulin would likely be required for sufficient absorption to achieve the desired

therapeutic effect. Furthermore, proteins, such as insulin, tend to have low oromucosal permeability in comparison to low molecular weight peptides. For these reasons, further investigation into the pharmacological activity of insulin upon release was not performed as part of this study.

Bradykinin causes a rapid but transient increase in intracellular calcium levels in target cells upon binding to its cell surface receptor,[31] primarily through release from internal stores.[32] This effect can be measured using commercially available fluorescent calcium probes. Here we show that membrane-eluted bradykinin induced intercellular calcium mobilisation in oral fibroblasts both using flow cytometry and confocal microscopy. These results clearly indicate that bradykinin released from the membrane maintained pharmacological activity. We are aware of only one other study verifying the activity of a therapeutically relevant peptide following release from electrospun mucoadhesive membrane. Sharma et al., applied fibrous membranes containing insulin to rat sublingual mucosa. Upon application, these caused a gradual decrease in blood glucose concentration, indicating successful delivery of biologically active insulin.[17] In conclusion, this mucoadhesive membrane system is suitable for the delivery of biologically active small hydrophilic peptides over appropriate timescales to the oral mucosa. It is therefore a very attractive new technology for the targeted delivery of highly permeating peptides to the buccal or sublingual oral mucosa. Potential applications include the topical release of peptides to treat oromucosal diseases locally, or alternatively sub-lingual systemic delivery using an optimised dosing regimen.

Competing Interests:

The authors declare the following financial interests/personal relationships which may be considered as potential competing interests: The research presented was funded, in part, by AFYX Therapeutics APS. JE, HEC, SS and CM declare that they have no other known competing financial interests or personal relationships that could have appeared to influence the work reported within this paper. MES and LSM are employed by AFYX Therapeutics. PVH is on the AFYX Therapeutics APS scientific advisory board, where AFYX have translated mucoadhesive electrospun patch technology for clinical use and have intellectual property (international patent application WO 2017/085262 A, WO 2021/072113 A1).

Acknowledgements

This work was funded by the U.K. EPSRC (EP/L016281/1) as a CASE Ph.D. studentship within the Centre for Doctoral Training in Polymers & Soft Matter with sponsorship from AFYX Therapeutics as the industrial partner. The authors would like to acknowledge The Wolfson Light Microscopy Facility

(University of Sheffield) for help with imaging. This facility is supported by a Wellcome Trust grant (WT093134AIA). This work is associated with the Insigneo Institute at the University of Sheffield.

References

1 F. Albericio and H. G. Kruger, Therapeutic peptides, *Future Med. Chem.*, 2012, **4**, 1527–1531.

2 R. Kumar, T. Islam and M. Nurunnabi, Mucoadhesive carriers for oral drug delivery, *J. Control. Release*, 2022, **351**, 504–559.

3 M. Surendranath, M. R. Rekha and R. Parameswaran, Recent advances in functionally modified polymers for mucoadhesive drug delivery, *J. Mater. Chem. B*, 2022, **10**, 5913–5924.

4 L. Heinemann and Y. Jacques, Oral insulin and buccal insulin: A critical reappraisal, *J. Diabetes Sci. Technol.*, 2009, **3**, 568–584.

5 G. Bernstein, Delivery of insulin to the buccal mucosa utilizing the RapidMist ™ system, *Expert Opin. Drug Deliv.*, 2008, **5**, 1047–1055.

6 M. K. Gutniak, H. Larsson, S. J. Heiber, O. T. Juneskans, J. J. Holst and B. Ahrén, Potential therapeutic levels of glucagon-like peptide I achieved in humans by a buccal tablet, *Diabetes Care*, 1996, **19**, 843–848.

7 C. Z. and M. R.J., Buccal transmucosal delivery of calcitonin in rabbits using thin-film composites, *Pharm. Res.*, 2002, **19**, 1901–1906.

8 C. Pricop, D. D. Branisteanu, M. Orsolya, D. Puia, A. Matei and I. A. Checherita, Sublingual desmopressin is efficient and safe in the therapy of lithiasic renal colic, *Int. Urol. Nephrol.*, 2016, **48**, 183–189.

9 T. Caon, L. Jin, C. M. O. Simões, R. S. Norton and J. A. Nicolazzo, Enhancing the buccal mucosal delivery of peptide and protein therapeutics, *Pharm. Res.*, 2015, **32**, 1–21.

10 Y. Sudhakar, K. Kuotsu and A. K. Bandyopadhyay, Buccal bioadhesive drug delivery - A promising option for orally less efficient drugs, *J. Control. Release*, 2006, **114**, 15–40.

11 V. Hearnden, V. Sankar, K. Hull, D. Vidovi, M. Greenberg, A. R. Kerr, P. B. Lockhart, L. L. Patton, S. Porter and M. H. Thornhill, New developments and opportunities in oral mucosal drug delivery for local and systemic disease, *Adv. Drug Deliv. Rev.*, 2012, **64**, 16–28.

12 J. G. Edmans, K. H. Clitherow, C. Murdoch, P. V. Hatton, S. G. Spain and H. E. Colley,

Mucoadhesive electrospun fibre-based technologies for oral medicine, *Pharmaceutics*, 2020, **12**, 1–21.

13 M. B. Stie, J. R. Gätke, I. S. Chronakis, J. Jacobsen and H. M. Nielsen, Mucoadhesive Electrospun Nanofiber-Based Hybrid System with Controlled and Unidirectional Release of Desmopressin, *Int. J. Mol. Sci.*, 2022, **23**, 1458.

14 H. E. Colley, Z. Said, M. E. Santocildes-Romero, S. R. Baker, K. D'Apice, J. Hansen, L. S. Madsen, M. H. Thornhill, P. V. Hatton and C. Murdoch, Pre-clinical evaluation of novel mucoadhesive bilayer patches for local delivery of clobetasol-17-propionate to the oral mucosa, *Biomaterials*, 2018, **178**, 134–146.

15 A. Moreira, D. Lawson, L. Onyekuru, K. Dziemidowicz, U. Angkawinitwong, P. F. Costa, N. Radacsi and G. R. Williams, Protein encapsulation by electrospinning and electrospraying, *J. Control. Release*, 2021, **329**, 1172–1197.

16 U. Angkawinitwong, S. Awwad, P. T. Khaw, S. Brocchini and G. R. Williams, Electrospun formulations of bevacizumab for sustained release in the eye, *Acta Biomater.*, 2017, **64**, 126–136.

17 A. Sharma, A. Gupta, G. Rath, A. Goyal, R. B. Mathur and S. R. Dhakate, Electrospun composite nanofiber-based transmucosal patch for anti-diabetic drug delivery, *J. Mater. Chem. B*, 2013, **1**, 3410–3418.

18 M. B. Stie, J. R. Gätke, F. Wan, I. S. Chronakis, J. Jacobsen and H. M. Nielsen, Swelling of mucoadhesive electrospun chitosan/polyethylene oxide nanofibers facilitates adhesion to the sublingual mucosa, *Carbohydr. Polym.*, 2020, 116428.

19 M. E. Santocildes-Romero, L. Hadley, K. H. Clitherow, J. Hansen, C. Murdoch, H. E. Colley, M. H. Thornhill and P. V. Hatton, Fabrication of Electrospun Mucoadhesive Membranes for Therapeutic Applications in Oral Medicine, *ACS Appl. Mater. Interfaces*, 2017, **9**, 11557–11567.

20 M. T. Brennan, L. S. Madsen, D. P. Saunders, J. J. Napenas, C. McCreary, R. Ni Riordain, A. M. L. Pedersen, S. Fedele, R. J. Cook, R. Abdelsayed, M. T. Llopiz, V. Sankar, K. Ryan, D. A. Culton, Y. Akhlef, F. Castillo, I. Fernandez, S. Jurge, A. R. Kerr, C. McDuffie, T. McGaw, A. Mighell, T. P. Sollecito, T. Schlieve, M. Carrozzo, A. Papas, T. Bengtsson, I. Al-Hashimi, L. Burke, N. W. Burkhart, S. Culshaw, B. Desai, J. Hansen, P. Jensen, T. Menné, P. B. Patel, M. Thornhill, N. Treister and T. Ruzicka, Efficacy and Safety of a Novel Mucoadhesive Clobetasol Patch for Treatment of Erosive Oral Lichen Planus, *J. Oral Pathol. Med.*, 2021, 0–3.

21 K. H. Clitherow, T. M. Binaljadm, J. Hansen, S. G. Spain, P. V. Hatton and C. Murdoch, Medium-Chain Fatty Acids Released from Polymeric Electrospun Patches Inhibit Candida albicans Growth and Reduce the Biofilm Viability, *ACS Biomater. Sci. Eng.*, 2020, **6**, 4087–4095.

22 K. H. Clitherow, C. Murdoch, A. M. A. M. Handler, E. Helen, M. B. Stie, H. M. Nielsen, C. Janfelt, P. V Hatton, J. Jacobsen, S. G. Spain, A. M. A. M. Handler, H. E. Colley, M. B. Stie, H. Mørck Nielsen, C. Janfelt, P. V Hatton and J. Jacobsen, Mucoadhesive Electrospun Patch Delivery of Lidocaine to the Oral Mucosa and Investigation of Spatial Distribution in a Tissue Using MALDI-Mass Spectrometry Imaging, *Mol. Pharm.*, 2019, **16**, 3948–3956.

23 J. G. Edmans, C. Murdoch, M. E. Santocildes-Romero, P. V. Hatton, H. E. Colley and S. G. Spain, Incorporation of lysozyme into a mucoadhesive electrospun patch for rapid protein delivery to the oral mucosa, *Mater. Sci. Eng. C*, 2020, **112**, 110917.

24 J. Schindelin, I. Arganda-carreras, E. Frise, V. Kaynig, T. Pietzsch, S. Preibisch, C. Rueden, S. Saalfeld, B. Schmid, J. Tinevez, D. J. White, V. Hartenstein, P. Tomancak and A. Cardona, PBMCs, *Nat. Methods*, 2012, **9**, 676–682.

25 H. E. Colley, V. Hearnden, A. V. Jones, P. H. Weinreb, S. M. Violette, S. MacNeil, M. H. Thornhill and C. Murdoch, Development of tissue-engineered models of oral dysplasia and early invasive oral squamous cell carcinoma, *Br. J. Cancer*, 2011, **105**, 1582–1592.

26 K. H. Clitherow, C. Murdoch, S. G. Spain, A. M. Handler, H. E. Colley, M. B. Stie, H. Mørck Nielsen, C. Janfelt, P. V Hatton and J. Jacobsen, Mucoadhesive Electrospun Patch Delivery of Lidocaine to the Oral Mucosa and Investigation of Spatial Distribution in a Tissue Using MALDI-Mass Spectrometry Imaging, *Mol. Pharm.*, 2019, **16**, 3948–3956.

27 J. Wu, Z. Zhang, J. Gu, W. Zhou, X. Liang, G. Zhou, C. C. Han, S. Xu and Y. Liu, Mechanism of a long-term controlled drug release system based on simple blended electrospun fibers, *J. Control. Release*, 2020, **320**, 337–346.

28 N. Bhardwaj and S. C. Kundu, Electrospinning: A fascinating fiber fabrication technique, *Biotechnol. Adv.*, 2010, **28**, 325–347.

29 J. G. Edmans, B. Ollington, H. E. Colley, M. E. Santocildes-Romero, L. S. Madsen, P. V Hatton and C. Murdoch, Electrospun patch delivery of anti-TNF α F(ab) for the treatment of inflammatory oral mucosal disease, *J. Control. Release*, 2022, **350**, 146–157.

30 R. Quinn and J. D. Andrade, Minimizing the aggregation of neutral insulin solutions, *J. Pharm.*

Sci., 1983, **72**, 1472–1473.

31 K. W. Buchan and W. Martin, Bradykinin induces elevations of cytosolic calcium through mobilisation of intracellular and extracellular pools in bovine aortic endothelial cells, *Br. J. Pharmacol.*, 1991, **102**, 35–40.

32 B. F. X. Reber, R. Neuhaus and H. Reuter, Activation of different pathways for calcium elevation by bradykinin and ATP in rat pheochromocytoma (PC 12) cells, *Pflügers Arch. Eur. J. Physiol.*, 1992, **420**, 213–218.

Chapter 4: Electrospun patch delivery of anti-TNFα F(ab) for the treatment of inflammatory oral mucosal disease

Supplementary information for the journal article is reproduced in Appendix 3.

Journal of Controlled Release 350 (2022) 146–157

Contents lists available at ScienceDirect

Journal of Controlled Release

journal homepage: www.elsevier.com/locate/jconrel

Electrospun patch delivery of anti-TNFα F(ab) for the treatment of inflammatory oral mucosal disease

Jake G. Edmans [a,b], Bethany Ollington [a], Helen E. Colley [a,*], Martin E. Santocildes-Romero [c], Lars Siim Madsen [c], Paul V. Hatton [a], Sebastian G. Spain [b], Craig Murdoch [a]

[a] School of Clinical Dentistry, 19 Claremont Crescent, University of Sheffield, Sheffield S10 2TA, UK
[b] Department of Chemistry, Brook Hill, University of Sheffield, Sheffield S3 7HF, UK
[c] AFYX Therapeutics, Lergravsej 57, 2. tv, 2300 Copenhagen, Denmark

ARTICLE INFO

Keywords:
Electrospinning
Drug delivery
Antibodies
Oral medicine
Oral patches
TNFα

ABSTRACT

Chronic ulcerative oral mucosal inflammatory diseases, including oral lichen planus and recurrent aphthous stomatitis, are painful and highly prevalent, yet lack effective clinical management. In recent years, systemic biologic therapies, including monoclonal antibodies that block the activity of cytokines, have been increasingly used to treat a range of immune-mediated inflammatory conditions such as rheumatoid arthritis and psoriasis. The ability to deliver similar therapeutic agents locally to the oral epithelium could radically alter treatment options for oral mucosal inflammatory diseases, where pro-inflammatory cytokines, in particular tumour-necrosis factor-α (TNFα), are major drivers of pathogenesis.

To address this, an electrospun dual-layer mucoadhesive patch comprising medical-grade polymers was investigated for the delivery of F(ab) biologics to the oral mucosa. A fluorescent-labelled F(ab) was incorporated into mucoadhesive membranes using electrospinning with 97% *v*/v ethanol as a solvent. The F(ab) was detected within the fibres in aggregates when visualised by confocal microscopy. Biotinylated F(ab) was rapidly eluted from the patch (97 ± 5% released within 3 h) without loss of antigen-binding activity. Patches applied to oral epithelium models successfully delivered the F(ab), with fluorescent F(ab) observed within the tissue and 5.1 ± 1.5% cumulative transepithelial permeation reached after 9 h. Neutralising anti-TNFα F(ab) fragments were generated from whole IgG by papain cleavage, as confirmed by SDS-PAGE, then incorporated into patches. F(ab)-containing patches had TNFα neutralising activity, as shown by the suppression of TNFα-mediated CXCL8 release from oral keratinocytes cultured as monolayers. Patches were applied to lipopolysaccharide-stimulated immune-competent oral mucosal ulcer equivalents that contained primary macrophages. Anti-TNFα patch treatment led to reduced levels of active TNFα along with a reduction in the levels of disease-implicated T-cell chemokines (CCL3, CCL5, and CXCL10) to baseline concentrations. This is the first report of an effective device for the delivery of antibody-based biologics to the oral mucosa, enabling the future development of new therapeutic strategies to treat painful conditions.

1. Introduction

Chronic ulcerative oral mucosal inflammatory diseases greatly affect quality of life. Oral lichen planus (OLP) and recurrent aphthous stomatitis (RAS) are the most prevalent causes of oral ulcers, affecting up to 25% of the population worldwide to some degree [1,2]. Although the early pathogenesis of these diseases is not fully understood, progression towards tissue ulceration is known to be mediated by tumour necrosis factor alpha (TNFα), a potent pro-inflammatory cytokine secreted by activated T-cells, macrophages and mast cells at lesional sites [3,4]. TNFα induces neighbouring oral keratinocytes and fibroblasts to release chemokines that recruit further lymphocytes and other immune cells. Ultimately, cytotoxic T-cells in the inflammatory infiltrate along with TNFα trigger apoptosis of the oral mucosal basal keratinocytes, leading to loss of the epithelium and ulcer formation.

OLP and RAS have no approved licenced treatments and symptoms are currently managed using topical corticosteroid ointments or oral rinses [1,5]. These are often unpleasant to use and their efficacy is in

* Corresponding author at: School of Clinical Dentistry, 19 Claremont Crescent, University of Sheffield, Sheffield S10 2TA, UK.
E-mail address: h.colley@sheffield.ac.uk (H.E. Colley).

https://doi.org/10.1016/j.jconrel.2022.08.016
Received 2 May 2022; Received in revised form 1 August 2022; Accepted 10 August 2022
Available online 18 August 2022

clinical practise impacted by low patient compliance [6]. In recent years, there has been considerable interest in neutralising monoclonal antibody therapy as an emerging treatment for oral mucosal inflammatory diseases, with particular attention being paid to anti-TNFα agents (for example infliximab, adalimumab, etanercept and certolizumab pegol), as these have been effective for other inflammatory conditions such as rheumatoid arthritis [7]. These biologics are considered to have a more targeted immunosuppressive effect in comparison to corticosteroids and have already shown efficacy when administered intravenously to patients with chronic oral ulcers [8,9]. However, systemic delivery requires high dosing and is associated with off-target toxicity [8]. Topical delivery of biologics directly to oral ulcers may circumvent these problems [10,11]. Indeed, topical dressings containing infliximab have been shown to be effective in treating chronic dermal ulcers [12]. Despite clinical interest, there has been no investigation to date into their efficacy when delivered topically to oral mucosal diseases.

Oromucosal delivery of biologics is hampered by the lack of suitable dosage forms that meet the requirement for their specific and efficient delivery to mucosal surfaces. Existing formulations such as oral rinses [13], gels [14] and tablets [15] deliver poorly defined doses of active ingredients uncontrollably throughout the oral cavity with short exposure times. To address this, we previously developed a mucoadhesive bilayer patch fabricated using electrospinning technology to promote unidirectional mucosal drug delivery [16,17]. We have previously shown that this oromucosal patch is highly effective at delivering small molecules such as the potent corticosteroid, clobetasol-17-propionate *in vitro* and in humans, where it has been successful at phase II clinical trials [18,19]. Moreover, the patch technology is particularly promising for the rapid release of biologically active proteins and peptides to oral mucosal surfaces [20], an application for which there are currently no alternative devices [17].

In this study we developed and evaluated a mucoadhesive electrospun patch for the delivery of anti-TNFα biologics directly to oral mucosal ulcers (Fig. S1). We show effective release of a biotinylated antibody fragment (F(ab)) from the patch with no loss of antigen binding functionality. Next, a patch was fabricated containing neutralising anti-TNFα F(ab) to act as a model therapeutic agent. Patch-eluted anti-TNFα F(ab) bound to TNFα and inhibited its pro-inflammatory actions by preventing TNFα-mediated release of CXCL8 from monolayer cultures of oral keratinocytes. Moreover, anti-TNFα patch treatment inhibited the actions of TNFα in a 3D tissue engineered immunocompetent *in vitro* model of an oral mucosal ulcer, leading to a reduction in immunogenic TNFα and TNFα-sensitive chemokine levels. This represents the first solid dosage form suitable for topical oromucosal biologic delivery and provides the first pre-clinical evidence in support of a novel treatment strategy that could radically affect the treatment of oral mucosal inflammatory diseases.

2. Material and methods

2.1. Materials

Unless otherwise indicated, all reagents used in enzyme-linked immunoassays (ELISA) were purchased from Bio-Techne (Abingdon, UK); all other reagents purchased from Sigma-Aldrich (Poole, UK). Poly (vinylpyrrolidone) (PVP; MW 2000 kDa) and Eudragit RS100 (RS100; MW 38 kDa) were kindly donated by BASF (Cheadle Hulme, UK) and Evonik Industries AG (Essen, Germany), respectively.

2.2. ELISA for the measurement of biotinylated F(ab) concentration

Biotinylated polyclonal goat anti-mouse F(ab) was used as a model protein to assess the suitability of the electrospun polymer system for the delivery of a biologically active antibody fragment. A direct ELISA protocol was developed to quantify the antigen binding activity of biotinylated anti-mouse antibodies and derivatives. High-binding 96-well plates were coated with IgG from mouse serum (10 μg/mL, 100 μL per well; Abcam, Cambridge, UK) overnight at room temperature and then blocked with BSA (1% *w/v*) overnight at 4 °C. Standards (78–5000 pg/mL; Abcam, Cambridge, UK) and samples containing biotinylated goat anti-mouse IgG F(ab) were loaded in duplicate and incubated for 2 h at room temperature before aspirating. Streptavidin-conjugated horseradish peroxidase (50 μg/mL) was added for 20 minutes before aspirating. Stabilised 3,3′,5,5′-tetramethylbenzidine/hydrogen peroxide substrate solution was added and incubated at room temperature followed 20 minutes later by aqueous hydrochloric acid (50 μL per well, 2 M) to stop the reaction. Plates were washed (0.05% *w/v* Tween 20 in PBS) 3 times after each aspiration step. Absorbance at 450 nm with a correction filter reading of 570 nm was measured using a spectrophotometer (Tecan, Männedorf, Switzerland) and concentrations interpolated from a standard curve fitted using the 4-parameter logistic curve setting in Graphpad Prism 9.3 software (GraphPad Software, La Jolla, USA).

2.3. Activity of biotinylated F(ab) after exposure to ethanol-water mixtures

Biotinylated goat anti-mouse F(ab) (1 μg/mL, 30 μL) was added to ethanol or different ratios of ethanol/water mixtures (970 μL) in glass vials. The solutions were incubated at room temperature for 1 h with shaking. Samples were then immediately diluted (1:100) in 1% *w/v* BSA and antigen-binding concentrations measured by ELISA. The measured antigen binding concentration was normalised against the known concentration to calculate percentage antigen-binding activity.

2.4. Electrospinning system and fabrication of mucoadhesive dual-layer patches

Electrospun membranes were fabricated using a system comprising a PHD2000 syringe pump (Harvard Apparatus, Cambridge, UK) and an Alpha IV Brandenburg power source (Brandenburg UK Ltd., Worthing, UK) as previously described [16]. Plastic syringes (1 mL volume; Henke Sass Wolf, Tuttlingen, Germany) were used to drive the solutions into a 20-gauge blunt metallic needle (Fisnar Europe, Glasgow, UK). Electrospinning was performed at room temperature with a potential difference of 19 kV, a flow rate of 2 mL/h, and a flight path of 14 cm. Mucoadhesive protein-containing membranes were electrospun as previously described from solutions containing PVP (10% *w/w*) and Eudragit RS100 (12.5% *w/w*) in 97% *v/v* ethanol [20]. The required amounts of PVP and RS100 were added to ethanol and mixed at room temperature using a magnetic stirrer until dissolved. F(ab) solutions were added, contributing to 3% *v/v* to the final solvent composition, and mixed briefly until homogeneous. Non-medicated (NM) patches were prepared by substituting the F(ab) solution with 3% *v/v* PBS. Electrospinning was started within 1 minute of addition. Polycaprolactone (PCL; 10% *w/v*) was added to a blend of DCM and DMF (90:10 *v/v*) and stirred at room temperature until dissolved. Hydrophobic backing layers were introduced by subsequent electrospinning of PCL solutions on top of the mucoadhesive layer. The resulting materials were placed in a dry oven at 70 °C for 15 minute to melt the PCL layer into a continuous film [16]. Experimental samples were taken from the central region of the dual-layer patches and the thickness measured 6 times at 1 cm intervals using a digital micrometer (Mitutoyo, Kanagawa, Japan).

2.5. Scanning electron microscopy

Patches were imaged using a TESCAN Vega3 scanning electron microscope (SEM; Tescan, Cambridge, UK). Samples were sputter coated with gold and imaged using an emission voltage of 10 kV. All images were processed using ImageJ software tools [21]. Fibre diameters were measured by ImageJ using randomly generated coordinates and a

superimposed grid to select fibres to measure [22]. Three images were analysed for each composition with at least 10 measurements per image.

2.6. Fabrication and imaging of fluorescent electrospun fibres

Fluorescent electrospun mucoadhesive membranes were prepared as previously described using fluorescein-conjugated goat anti-mouse IgG F(ab) (FITC-F(ab); Abcam, Cambridge, UK). PVP is intrinsically fluorescent, allowing simultaneous imaging of the polymer fibres and FITC-conjugated F(ab) [23]. Samples were placed on glass slides and overlaid with glass cover slips. Imaging was performed in dual-channel mode using a Nikon A1 laser scanning confocal microscope using 403.55 nm and 488 nm sapphire lasers with 450/25 nm and 525/25 nm bandpass filters. All images were processed using ImageJ software tools.

2.7. Release profile of F(ab) from electrospun membranes

Three independently prepared biotinylated-F(ab)-containing or NM patches (as controls) were used to measure F(ab) release profiles in PBS. PCL backing layers were removed from patch samples using forceps and 5 mg samples of mucoadhesive membrane placed in a 12-well plate (pre-blocked with 1% *w/v* BSA overnight at 4 °C) and immersed in 2 mL PBS at 37 °C with shaking. Aliquots of 10 μL were taken at predetermined intervals and stored briefly at 4 °C. Samples were subsequently diluted (1:100) in 1% BSA and antigen-binding concentrations measured by ELISA. Measured antigen binding concentrations were normalised against the hypothetical maximum concentration, determined by the dry mass fraction of F(ab) in the electrospinning solution, to calculate percentage release.

2.8. Qualitative flexibility assessment

A 1 × 12 cm strip intersecting the centre of the electrospun dual-layer sheet was cut by scalpel. Flexibility and handleability testing were performed by firstly folding the strip in half and visually inspecting the mucoadhesive and backing layers for damage or permanent deformation. Secondly, the strip was wrapped around a metal tube (ø 10 mm) and inspected once more. These tests were performed using a dry strip and a wet strip after immersing in PBS for 30 s.

2.9. Patch residence time on ex vivo porcine buccal mucosa

Porcine buccal mucosa was excised from bisected porcine heads immediately after slaughter and buccal mucosal grafts (0.5 mm) taken using a Braithwaite grafting knife (Swann Morton, Sheffield, UK). Samples were sealed in plastic bags, preserved by flash freezing in liquid nitrogen and stored at −80 °C before use. Frozen samples were defrosted in a 37 °C water bath, attached to 100 mm petri dishes using cyanoacrylate glue and the surface of the mucosa moistened using PBS. Circular patch samples (ø 10 mm) were applied using gentle pressure with a gloved fingertip for 5 s. Pre-warmed PBS (30 mL) was added to submerge the samples and the petri dishes shaken on an orbital shaker at 37 °C, 250 rpm. The samples were inspected every 15 minutes for 3 h for detachment of the entire patch or backing layer.

2.10. Cell culture

FNB6-hTERT immortalized oral keratinocytes (FNB6; Ximbio, London, UK) were cultured in a flavin- and adenine-enriched medium consisting of high glucose Dulbecco's modified Eagle's medium (DMEM) and Ham's F12 medium in a 3:1 *v/v* ratio supplemented with 10% *v/v* fetal bovine serum (FBS), epidermal growth factor (10 ng/mL), adenine (0.18 mM), insulin (5 μg/mL), transferrin (5 μg/mL), L-glutamine (2 mM), triiodothyronine (0.2 nM), amphotericin B (0.625 μg/mL), penicillin (100 IU/mL), and streptomycin (100 μg/mL). Normal oral fibroblasts (NOF) were isolated from the connective tissue of biopsies obtained from the oral mucosa of patients during routine dental procedures with written informed consent (Ethical Approval No. 09/H1308/66) and cultured in DMEM supplemented with FBS (10% *v/v*), L-glutamine (2 mM), penicillin (100 IU/mL), and streptomycin (100 μg/mL). Monocyte-derived macrophages (MDM) were differentiated from peripheral blood primary human monocytes as previously described [24]. Briefly, buffy coats obtained from the National Blood Service, UK (Ethical Approval No. 012597) were diluted 1:1 in Hank's balanced salt solution (without Ca^{2+} and Mg^{2+}) and mononuclear cells separated by density-gradient centrifugation using Ficoll® Paque Plus (GE Healthcare, Chalfont Saint Giles, UK). Monocytes were purified by plastic adherence and differentiated to MDM by 7 days culture in Iscove's modified Dulbecco's medium supplemented with human AB serum (2% *v/v*), L-glutamine (2 mM), penicillin (100 IU/mL), and streptomycin (100 μg/mL).

2.11. Generation of oral epithelial equivalents

FNB6 cells (5×10^5 in 0.5 mL) were seeded onto the apical surface of fibronectin-coated (10 μg/mL) 12-well, 0.4 μm pore cell culture inserts (Greiner Bio One Ltd., Stonehouse, UK) and cultured submerged for 2 days, after which the models were raised to an air-liquid-interface and cultured for a further 10 days.

2.12. Transepithelial electrical resistance

Before measurement, FNB6 epithelial models were washed with PBS and placed in a 12-well plate, 0.5 mL PBS was added to basolateral chambers and 0.3 mL to apical chambers. Tissue integrity was assessed by measuring transepithelial electrical resistance (TEER) using an EVOM2 voltmeter (World Precision Instruments, Madison, USA) at three locations per model, and the average of these values calculated. The resistance across the epithelium was obtained by subtracting the resistance value derived from a blank cell culture insert. The following equation was used to calculate TEER: TEER ($\Omega.cm^2$) = Resistance (Ω) × Membrane area (cm^2).

2.13. F(ab) permeation in oral epithelium equivalents

TEER was measured to verify presence of barrier properties and oral epithelial equivalents (OEE) placed in a 12-well plate (pre-blocked with 10% *w/v* BSA overnight at 4 °C) containing 1 mL cell culture medium. Samples containing biotinylated-F(ab) were applied to the apical chamber and the models incubated with shaking. Sample dose forms included F(ab) solutions in PBS (1 μg/mL, 0.5 mL), F(ab) patch (5–7 mg), NM patch (5–7 mg). Patch samples were carefully placed on the apical surface using sterilised forceps without applying additional pressure. PBS (0.1 mL) was added before application of the patches to simulate the moisture of the oral cavity and hydrate the patches. Equivalent patch samples were weighed before and after removal of the backing layer, showing that the adhesive F(ab)-containing layer contributes 62 ± 2% *w/w* to the overall patch. Given a F(ab) content of 130 ng/mg in the adhesive layer, the patches contained doses of 496 ± 49 ng, which is equivalent to those applied as solution (500 ng). Media samples were taken from the basolateral chamber at predetermined intervals and the equivalent volume of media replaced (200 μL). Media samples were stored at −80 °C before measuring F(ab) concentration by ELISA and calculating cumulative amount permeated. Additionally, patches containing FITC-F(ab) were applied identically for 9 h before washing with PBS and fixing in neutral buffered formalin (10% *v/v*) for 24 h. The OEE were sectioned and mounted in antifade mounting medium with DAPI (Vector Laboratories, Upper Heyford, UK) or mounted without sectioning before imaging by laser scanning confocal microscopy.

2.14. Preparation of anti-TNFα F(ab)

Rabbit anti-TNFα IgG (5 mg/mL, 0.25 mL) was fragmented using a Pierce™ F(ab) preparation kit (Thermo Fisher Scientific, Loughborough, UK) as per the manufacturer's instructions. The concentration of the resulting F(ab) was estimated as recommended by the manufacturer from absorbance at 280 nm, assuming an extinction coefficient of 1.4 mL mg^{-1} cm^{-1}. The products were analysed without reduction or denaturation by SDS-PAGE using a NuPAGE™ 4–12% bis-tris gel as directed with NuPAGE™ MOPS running buffer (Thermo Fisher Scientific, Loughborough, UK) and visualised using Expedeon InstantBlue™ Coomassie-based stain (Abcam, Cambridge, UK). The F(ab) product was concentrated using Pierce™ 10 kDa molecular weight cut-off polyethersulfone membrane protein concentrators (Thermo Fisher Scientific, Loughborough, UK) as directed, and the final concentration calculated by mass balance.

2.15. TNFα neutralisation assay

The TNFα neutralising activity of anti-TNFα whole IgG and F(ab) were measured as a decrease in TNFα-mediated CXCL8 release by FNB6 monolayers. FNB6 cells (8×10^4 cells per well) were seeded in 24-well plates and incubated for 18 h until confluent. Samples in PBS were combined 1:1 with cell culture medium with or without recombinant human TNFα (10 ng/mL) and incubated at 37 °C for 1 h to allow any neutralisation to occur. Media were aspirated from the monolayers and the cells treated with either 10 ng/mL recombinant TNFα, F(ab)-neutralised TNFα or medium alone as control for 24 h. CXCL8 in the conditioned media was measured using an ELISA kit (Bio-Techne, Abingdon, UK) as directed. Patch-eluted F(ab) activity was measured in an identical manner. To elute, F(ab) patch and NM patch samples (30 mg) were immersed in 2 mL PBS for 3 h at 37 °C with shaking.

2.16. Effect of electrospun polymers on TNFα concentration

TNFα (1 ng/mL, 1 mL) was added to glass vials with or without samples of NM patch (10 mg). The vials were incubated at 37 °C for 24 h before measuring free TNFα concentration using an ELISA kit (Bio-Techne, Abingdon, UK) as directed.

2.17. Generation and treatment of immunocompetent oral mucosal ulcer equivalents

Immunocompetent oral mucosal ulcer equivalents (OMUE) were constructed as previously described [25]. NOF (2×10^5 cells/mL) and MDM (1×10^6 cells/mL) in cell culture media (1 mL) were added to a collagen gel-forming solution comprising rat tail collagen (3.48 mg/mL), 10 × DMEM (10% *v*/v), FBS (8.3% v/v), L-glutamine (2 mM), sodium bicarbonate (2.3 mg/mL), 4-(2-hydroxyethyl)-1-piperazineethanesulfonic acid (5 mg/mL), sodium hydroxide (0.25 mg/mL). The solution was adjusted to pH 7 by the addition of sodium hydroxide (1 mM) and 1 mL added to 12 mm cell culture inserts. The collagen used in all experiments contained <0.2 EU/mL endotoxin when quantified by limulus amebocyte lysate assay (Thermo Fisher Scientific, Loughborough, UK). The cell-populated collagen hydrogels were incubated in a humidified atmosphere at 37 °C for 2 h to solidify. Sterilised titanium cylinders (ø 5 mm, h 10 mm) were placed on the centre of the hydrogel before seeding FNB6 cells (0.5 mL, 5×10^5) and culturing submerged for 2 days. The models were raised to an air-to-liquid interface and cultured for a further 9 days, after which the titanium cylinders were removed.

OMUE were transferred to a 12-well plate containing cell culture media (1 mL). Models were pre-treated as required for 24 h by applying patch samples carefully to the apical surface using sterilised forceps without applying additional pressure. Lipopolysaccharide (LPS) from *Escherichia coli* 0111:B4 (500 ng/mL; Invitrogen, Waltham, USA) was added as required to the basolateral chambers to simulate an MDM inflammatory response. After 6 h incubation, samples of conditioned media were taken from basolateral chambers and replaced with the equivalent volume of cell media (300 μL). After a further 18 h, the entire conditioned media were collected. Samples were stored at −80 °C until analysis. To test for patch cytotoxicity, full thickness oral mucosal equivalents were treated with either NM or anti-TNFα-loaded patch for 18 h. Receptive medium samples from the lower transwell were tested immediately for lactate dehydrogenase release (CytoTox Non-radioactive Cytotoxicity Assay) as a marker of tissue damage according to the manufacturer's instructions (Promega, Chilworth, UK).

2.18. Cytokine release analysis

TNFα concentrations in conditioned media were measured by ELISA (Bio-Techne, Abingdon, UK) as directed. The C1 human chemokine antibody array (Antibodies-online GmbH, Aachen, Germany) was used to provide semi-quantitative measurements of the concentrations of 38 human chemokines in conditioned media collected after 24 h from immunocompetent OMUE. Membranes were visualised using a C-DiGit blot scanner (Li-cor, Cambridge, UK) and analysed using Quantity One software (Bio-Rad Laboratories, Hercules, USA). Selected chemokines (CCL3, CCL5, CXCL10) were further quantified using ELISA (Bio-Techne, Abingdon, UK). The experiment and ELISA quantification were performed 3 times using different batches of MDM. The presented data are from a single representative batch of MDM.

2.19. Histological analysis

OEE or OMUE were washed with PBS, fixed in neutral buffered formalin (10% *v/v*) for 24 h, and paraffin-wax embedded using standard histology procedures. Sections (5 μm) were cut using a Leica RM2235 microtome (Leica Microsystems, Wetzlar, Germany) and mounted on Superfrost Plus slides (Thermo Fisher Scientific, Loughborough, UK). Sections stained with haematoxylin and eosin were mounted in dibutylphthalate polystyrene xylene and imaged using an Olympus BX51 microscope with cellSens Imaging Software (Olympus GmbH, Hamburg, Germany).

2.20. Data analysis

All data and statistical analyses were performed using GraphPad Prism 9.3 software (GraphPad Software, La Jolla, USA). Unless stated data are presented as mean ± standard deviation of at least three independent experiments. Unpaired Student's *t*-test or one-way ANOVA with Tukey's post-hoc test was used for pairwise or groupwise comparisons and results considered statistically significant if $p < 0.05$. Half-maximal inhibitory concentrations (IC_{50}) were calculated using 4-parameter logistic regression and presented as mean ± SD.

3. Results and discussion

3.1. Stability of biotinylated-F(ab) in ethanol-water mixtures

Electrospinning involves applying a high voltage electric field to an extruded polymer solution, resulting in the production of a micron-scale, non-woven mesh of polymeric fibres [17]. We have utilised electrospinning technology to develop a dual-layer patch for drug delivery to the oral mucosa, which is comprised of a mucoadhesive drug-eluting layer that consists of a blend of poly(vinyl pyrrolidone) (PVP) and Eudragit® RS100 (RS100), and a water-impermeable backing layer made of heat-treated PCL [16]. The high surface area and hydrophilicity of the fibres promotes rapid swelling, efficient drug release while maximising mucoadhesive interactions.

The RS100 polymer is an integral component in the electrospun mucoadhesive layer of the patch, preventing dissolution in saliva and promoting adhesion through electrostatic interactions with mucins.

RS100 is not water soluble and therefore an organic processing solvent such as ethanol is required to dissolve RS100 for electrospinning. Ethanol is generally considered to be a protein denaturant; however, we previously observed that lysozyme could be electrospun into PVP/RS100 fibres from various ethanol-water mixtures without significant loss of enzyme activity [20]. F(ab) antigen binding activity following exposure to different ethanol-water mixtures was measured in order select a solvent composition suitable for F(ab) incorporation. Ethanol concentrations of 40% *v/v* and below did not cause significant F(ab) activity loss. Incubating F(ab) (1 μg/mL) in 97% *v*/v ethanol resulted in a decrease in antigen binding activity to 32 ± 11% of its initial activity ($p < 0.001$). In contrast, use of 80% *v*/v ethanol caused a complete loss of antigen binding ($p < 0.001$), whereas 60% v/v ethanol caused comparable activity loss to 97% *v*/v (Fig. 1). We previously overserved that fibres prepared with <60% v/v ethanol are prone to disintegration in aqueous media [20]. The relatively high F(ab) activity observed at 97% v/v ethanol may be a result of lower solvation of the unfolded protein at high ethanol concentrations, increasing the free energy barrier for ethanol-induced denaturation. Therefore, use of 97% v/v ethanol as the solvent was selected for patch fabrication.

3.2. Encapsulation and release from electrospun patches

Dual layer mucoadhesive electrospun patches were fabricated using a modification to our previously described protocol [20]. Briefly, biotinylated-F(ab) or FITC-F(ab) were incorporated within the adhesive layer by mixing the aqueous F(ab) solution with the ethanolic polymer solution directly before electrospinning, giving a theoretical maximum loading of 130 ng/mg by dry mass in the adhesive layer of the patch. No noticeable difference in fibre morphology between NM patches and biotinylated-F(ab)-loaded patches was observed by SEM (Fig. 2 A-B). Furthermore, the inclusion of F(ab) had little effect on fibre diameter, with NM fibres having an average diameter of 1.82 ± 0.88 μm and biotinylated-F(ab)-containing fibres of 2.31 ± 0.81 μm (Fig. 2C). Dual-layer sheets had a thickness of 307 ± 46 μm and 261 ± 22 μm for the useable area of NM and F(ab)-loaded sheets, respectively.

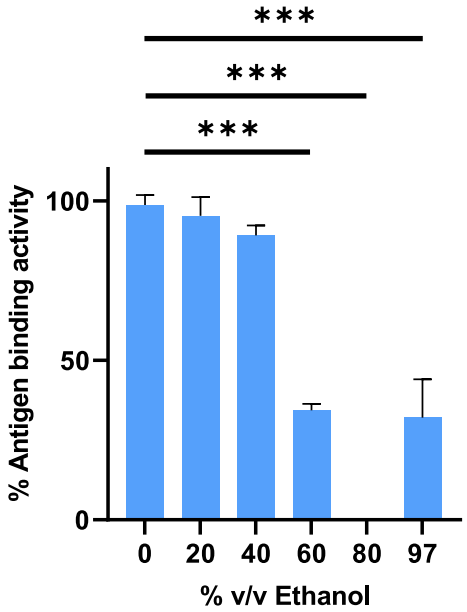

Fig. 1. Antigen binding activity of biotinylated-F(ab) following exposure to increasing ethanol concentrations. F(ab) was added to glass vials containing various ethanol/water mixtures and incubated for 1 h with shaking before measuring antigen binding F(ab) concentration by ELISA. Data are presented as mean ± SD ($n = 3$) and analysed by one-way ANOVA with Dunnett's post-hoc test comparing each group to 0% *v*/v ethanol. ***$p < 0.001$.

FTIC-conjugated F(ab) was also incorporated to visualise the distribution of F(ab) within the fibres by dual-channel confocal microscopy, where patch fibres were imaged making use of the intrinsic fluorescence of PVP (Fig. 2D). Interestingly, micrographs of FITC-conjugated F(ab)-containing fibres revealed that the F(ab) was dispersed throughout the fibres as micro- and nanometre-sized particles/aggregates (Fig. 2E), implying the formation of a colloidal precipitate following addition of the F(ab) to the polymer solution. Dissolved inert polymers, including PVP, are known to induce precipitation of antibodies and large proteins through a volume exclusion effect, whereby proteins are sterically excluded from interacting with the solvent [26,27]. This, along with the reduced solubility of proteins in ethanol, is likely involved in the precipitation mechanism.

Elution of the biotin-conjugated F(ab) from the mucoadhesive layer into PBS revealed complete preservation of antigen binding activity, with 97.1 ± 5.7% of the dose being detectable by ELISA after 3 h (Fig. 2F). This contrasts with the reduced activity observed for F(ab) after incubation in 97% *v/v* ethanol in the absence of polymers. It is likely that PVP stabilises F(ab) by limiting protein-solvent interactions through volume exclusion and by non-specific binding to F(ab) in its native conformation [28]. F(ab) was released rapidly, following first-order kinetics, with 64 ± 16% released within 0.5 h and 89 ± 28% after 1 h. Eluted NM patches produced negligible absorbance across all timepoints. This rapid release is similar to our previous observations for highly soluble proteins [20], and is likely facilitated by rapid swelling of the fibres. Complete release over a short timeframe is appropriate for oromucosal delivery, as patients can only be expected to refrain from eating and drinking for short periods. A mucoadhesive adhesion assay was performed using *ex vivo* porcine buccal mucosa. F(ab)-loaded patches displayed similar mucoadhesive residence times to NM patches (2.75 ± 0.32 h compared to 2.0 ± 1.2 h, respectively; Fig. S2). These residence times are similar to those previously observed in humans [18] and show that inclusion of F(ab) does not adversely affect patch adhesive properties. Flexibility is an important property for oral patches, which must adhere to curved surfaces within the mouth and withstand mechanical forces caused by movement of the tongue and jaw. Qualitative assessment of patch flexibility showed that strips of both F(ab)-loaded and NM patch in either a wet or dry condition could be folded in half or wrapped around a curved surface without breaking or permanently deforming.

Despite strong clinical interest in alternative formulations for antibodies and their derivatives, there have been few studies investigating the encapsulation of antibodies into polymer fibres by electrospinning and none that we are aware of involving F(ab). Gandhi et al. [29], examined the encapsulation of anti-$\alpha_v\beta_3$ integrin IgG within PCL fibres by uniaxial electrospinning from a 60:40 (*w/w*) mixture of dimethylformamide and dichloromethane. Burst release was observed by spectrophotometry followed by a period of sustained release, suggesting initial release driven by desorption from the polymer surface followed by slow release due to fibre degradation. Including bovine serum albumin (BSA) as a porogen facilitated anti-$\alpha_v\beta_3$ release, with 51% release being observed after 4 h at the highest BSA loading. Although the solvents used are generally considered to be denaturing, at least some antigen binding activity was maintained, as shown by the antigen-specific staining of integrin-expressing endothelial cell monolayers [29]. Notably, Angkawinitwong et al., encapsulated bevacizumab, a monoclonal antibody (mAb) that binds to and inhibits vascular endothelial growth factor A thereby reducing angiogenesis, within PCL core-shell fibres by coaxial electrospinning. The use of an aqueous core-forming solution enabled preservation of antigen binding activity, as confirmed by surface plasmon resonance. As is typical of coaxial fibres, slow zero-order release was observed over a 2-month period, suggesting a potential application as an implantable material for sustained antibody release [30].

Shelf-life is another important consideration in developing solid dosage forms for biologic delivery. In general, immobilisation of

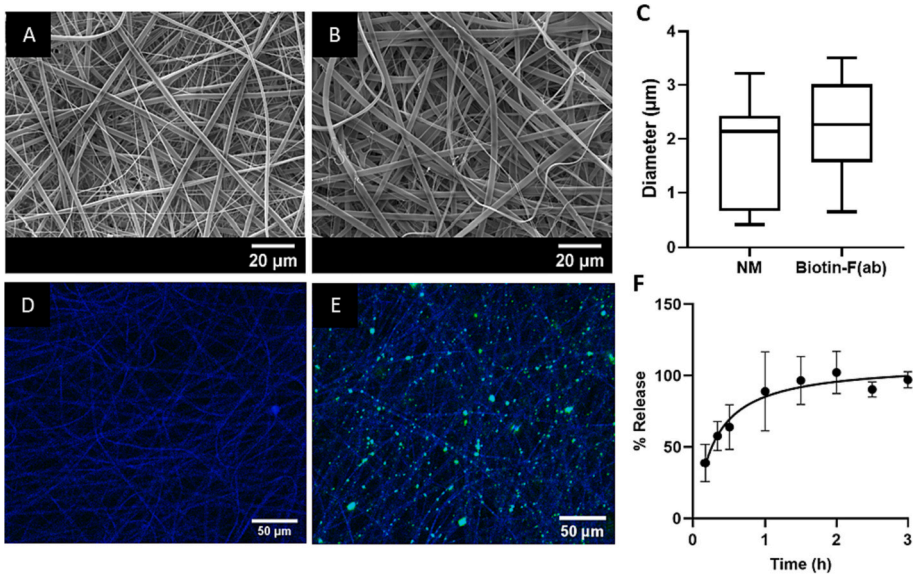

Fig. 2. Incorporation by electrospinning and release of F(ab) from mucoadhesive patches. Scanning electron micrographs of mucoadhesive electrospun (A) NM and (B) biotin-conjugated F(ab)-containing fibres. (C) Fibre diameter distributions presented as median, interquartile range, and range ($n = 30$). (E) Confocal micrographs of mucoadhesive electrospun (D) NM and (E) FITC-conjugated F(ab)-containing fibres. (F) Release of biotinylated F(ab) from mucoadhesive membranes following immersion in PBS. Presented as mean ± SD (n = 3).

proteins within a solid formulation can often improve shelf-life by preventing aggregation [31]. Indeed, lyophilisation in the presence of cryoprotectants can considerably increase the shelf-life of many antibodies [32]. Despite this, existing therapeutic antibodies are exclusively delivered as liquids [33] and there have been few detailed studies on the stability of antibodies within polymer-based solid formulations. Frizzell et al., observed that the shelf-lives of horseradish peroxidase and alkaline phosphatase are improved by encapsulating within electrospun

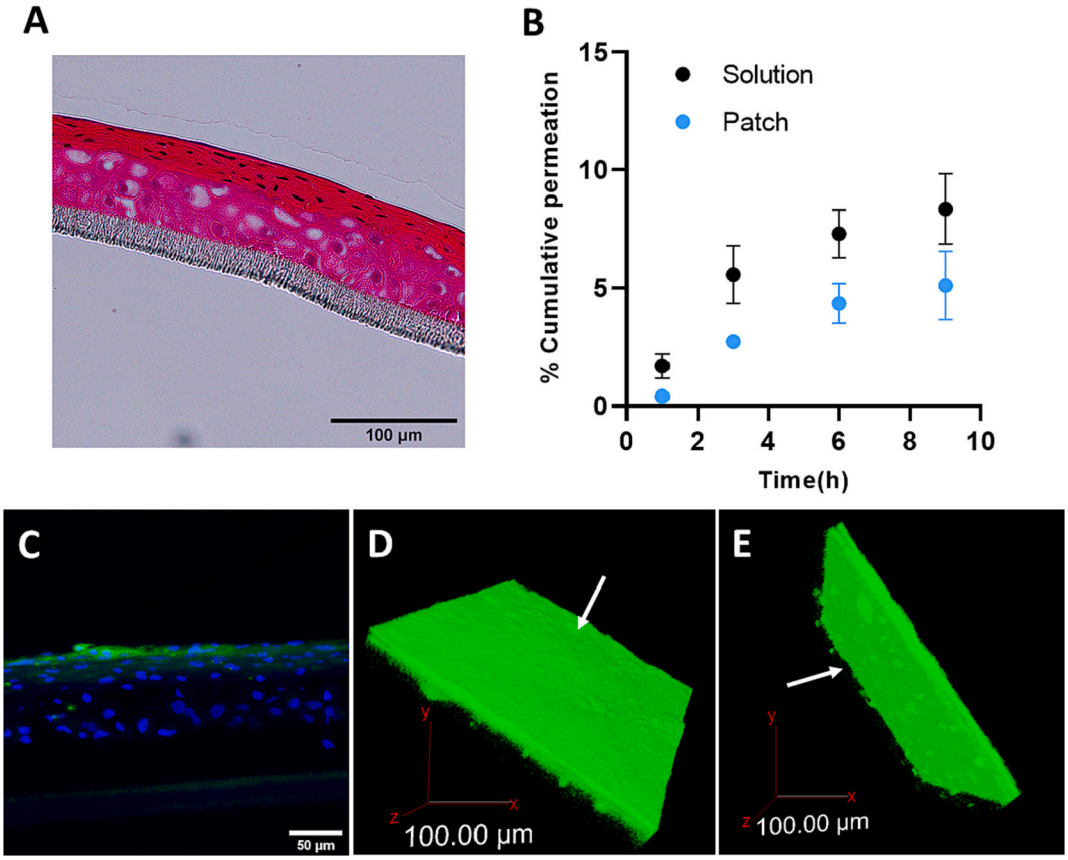

Fig. 3. F(ab) permeates the oral epithelium when applied as either a patch or solution. Patches and solutions containing biotinylated F(ab) were applied to the apical side of oral epithelial equivalents (OEE). (A) Representative haematoxylin and eosin stain of an OEE. Transepithelial permeation was measured by periodically measuring F(ab) concentration in the basolateral chamber. (B) Plot of cumulative percentage transepithelial biotinylated F(ab) permeation when applied to OEE as solution or patch. Data are presented as mean ± SD ($n = 3$). Patches containing FITC-F(ab) were applied to OEE for 9 h, formalin fixed, and the distribution of FITC-F(ab) visualised by confocal microscopy. (C) Cross section showing distribution of FITC-F(ab) (green) with DAPI nuclear counterstain (blue). Three-dimensional projections showing the distribution of FITC-F(ab) with white arrows indicating the (D) apical and (E) basolateral surface of the OEE.

polymer fibres and can be further extended by lyophilisation to remove residual water from the material [34]. Packaging with dry nitrogen and cold storage are routinely used in the pharmaceutical industry and might be considered to improve the shelf-life if required. Detailed studies on stability and storage conditions of antibody-based therapeutics within solid formulations would be beneficial and necessary for clinical translation.

The release rate and high antigen binding activity indicate that our formulation is promising for mucosal F(ab) delivery. The high preservation of protein function suggests that uniaxial electrospinning using organic solvents could be considered for the encapsulation of other complex biomacromolecules, as the denaturing effect of solvents that would otherwise be incompatible may be counteracted in the presence of stabilising polymers.

3.3. Delivery of F(ab) to oral epithelium equivalents

The intact oral epithelium is generally considered to be an efficient barrier against the permeation of hydrophilic molecules [35]. However, some small proteins, such as glucagon-like-peptide 1 and insulin, can permeate sufficiently to achieve therapeutically relevant blood serum concentrations [36,37]. The basal epithelium and lamina propria are the primary target for topical delivery to treat most oromucosal diseases. In severe RAS and OLP the epithelium is absent or eroded at the affected site, resulting in impaired barrier function. For successful delivery, an anti-TNFα agent would have to permeate the loose connective tissue of the lamina propria in order to neutralise cytokines in the inflammatory infiltrate. Ideally, it would also permeate the epithelium at least somewhat, to allow the continued treatment of partially regenerated epithelia during wound healing. To assess the ability of the patches to deliver F(ab) to a mucosal surface, tissue engineered OEE were used as a model barrier. The OEE consist of a stratified squamous layer of oral keratinocytes 60–80 μm in thickness (Fig. 3A). Although thinner than native healthy buccal mucosa, the OEE covered the entire insert and had an average TEER of 444 ± 74 Ω cm^2. This value is comparable to or higher than those typically observed for similar 3D oral epithelial models and suggests suitable barrier properties [38].

Patch samples and solutions containing an equivalent dose of biotinylated F(ab) were applied to OEE and the concentration of F(ab) in the basolateral chamber monitored over time (Fig. 3B). At earlier timepoints, permeation of F(ab) applied by patch was delayed compared to F(ab) applied by solution. This is likely caused by the additional time taken for F(ab) to be released from the patch fibres. After 9 h, similar levels of cumulative permeation were achieved corresponding to 5.1 ± 1.5% and 8.4 ± 1.5% of the total dose for F(ab) applied in a patch or solution, respectively. Patches containing FITC-F(ab) were applied to OEE for 9 h before fixing in formalin to immobilise any F(ab) present within the tissue. Confocal microscopy (Fig. 3C) followed by z-stack analysis (Fig. 3D-E) performed on sections, showed that F(ab) mainly accumulated within the upper 3–6 cell layers of the superficial epithelium but could also be detected in isolated regions throughout the lower layers of the OEE.

The data presented here provide the first evidence that biologics can be delivered efficiently to oral epithelia using mucoadhesive patches, with the patches performing comparably to an equivalent solution. In practise, oral rinses would be unsuitable for the delivery of biologics to the oral mucosa due to short exposure times and lack of site-specificity. Whereas, similar dual-layer patches with hydrophobic backing layers have recently been shown to be highly effective for promoting the retention of biologics on the oral mucosa in the presence of saliva flow [39]. To our knowledge, there are no previous studies investigating antibody delivery to the oral mucosa. Saltzman and *co*-workers observed that radiolabelled IgG applied *in vivo* to mouse vaginal mucosa using polymer discs permeated to a similar extent, reaching peak serum concentrations corresponding to approximately 1% of the total dose [40,41]. The higher permeating dose observed in this study may be due to the smaller size of F(ab), leading to increased permeability through the intracellular space, or the absence of additional biodistribution and elimination effects that would be present *in vivo*. Although the F(ab) permeated the top layers of the oral mucosal epithelium in our study, its presence in the lower layers and the levels of complete transepithelial delivery across intact epithelium were somewhat low, as might be expected due to the high permeability barrier this tissue has to high molecular weight proteins. However, as mentioned previously, in most oral mucosal inflammatory lesions the mucosal barrier is absent suggesting that topical F(ab) treatment may be feasible for these types of erosions and ulcers.

3.4. Preparation and activity of neutralising anti-TNFα F(ab)

TNFα neutralising agents are currently one of the most common classes of monoclonal antibody therapy [42]. They are available as whole IgG and other derivatives. Due to their smaller size, F(ab)s, such as certolizumab pegol, are expected to penetrate tissue more easily and therefore should be better suited for topical delivery [43]. A polyclonal neutralising rabbit anti-TNFα IgG was fragmented by enzymatic degradation with papain to generate a F(ab) to serve as a model biological therapeutic for this study. Fc and any unreacted whole IgG were separated from F(ab) by binding to immobilised protein A. Non-denaturing SDS-PAGE indicated the complete separation of the F(ab) and Fc fragments (Fig. 4A). The neutralising activities of the anti-TNFα F(ab) compared to whole IgG were measured by pre-incubating each with 5 ng/mL recombinant TNFα before adding to FNB6 oral keratinocyte monolayers, which are known to secrete CXCL8 in response to TNFα stimulation [44]. The neutralising activity of each antibody species was confirmed as a dose-dependent decrease in TNFα-mediated CXCL8 secretion, as detected by ELISA (Fig. 4B–C). Whole IgG exhibited an IC_{50} concentration of 1.08 ± 0.46 μg/mL, corresponding to a molar IgG to TNFα ratio of 74 ± 30 (assuming IgG and TNFα molecular weights of 150 kDa and 51 kDa respectively). F(ab) had an IC_{50} concentration of 1.45 ± 0.50 μg/mL, corresponding to a molar F(ab) to TNFα ratio of 295 ± 102 (assuming F(ab) molecular weight of 50 kDa). The higher stoichiometric ratio required for neutralisation with the F(ab) may be due to its univalency in comparison to the bivalency of whole IgG. It cannot be presumed that fragmentation of a neutralising antibody will yield a F(ab) with equivalent neutralising activity, as some neutralisation mechanisms rely on bivalency for crosslinking or increased avidity [45]. In this case, the resulting F(ab) maintained TNFα neutralising activity, suggesting utility as a model F(ab) biologic. The relatively high molar excess required for neutralisation is typical of affinity purified polyclonal antibodies, since not all binding will occur *via* epitopes that block activity. It is likely that approved monoclonal F(ab) drugs would have higher potencies because of their single-epitope specificity and optimised binding affinity, however, their availability to researchers is often limited.

3.5. Patch TNFα neutralising activity

Anti-TNFα F(ab) was electrospun into mucoadhesive patches at a theoretical maximum loading of 920 ng/mg by dry mass in the adhesive layer. Activity of the F(ab) following 3 h elution in PBS was measured by neutralisation of TNFα-mediated CXCL8 release by FNB6 monolayers (Fig. 5). Stimulating FNB6 oral keratinocytes with TNFα resulted in a significant increase in CXCL8 secretion from 0.093 ± 0.043 ng/mL to 1.68 ± 0.42 ng/mL ($p < 0.001$). Pre-incubation of TNFα with NM patch eluate reduced CXCL8 levels to 1.24 ± 0.31 ng/mL, although this was not statistically significant ($p = 0.22$). In contrast, preincubation with 10 μg/mL of an anti-TNFα F(ab) solution reduced CXCL8 secretion to baseline levels (0.078 ± 0.044 ng/mL, $p < 0.001$ relative to NM). Similarly, patch-eluted F(ab), with a theoretical maximum concentration of 8.3 μg/mL, also reduced CXCL8 secretion to baseline levels (0.115 ± 0.022 ng/mL, $p < 0.001$ relative to NM). Solutions containing

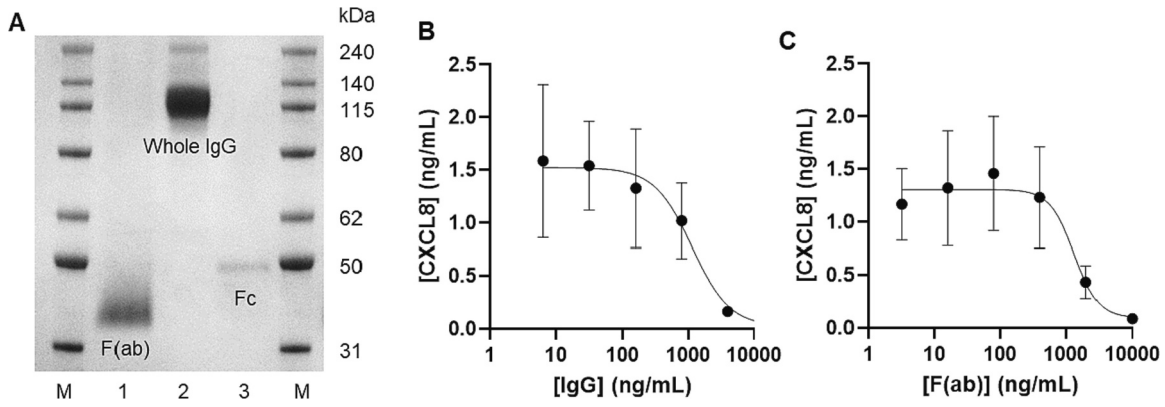

Fig. 4. Preparation and cytokine neutralising activity of anti-TNFα F(ab) as shown by the suppression of TNFα-mediated CXCL8 release. (A) Representative non-reducing SDS-PAGE analysis of papain-fragmented neutralising anti-TNFα IgG. (Lane 1) Purified F(ab) product, (Lane 2) whole IgG starting material, (Lane 3) Fc product, (M) molecular weight marker in kDa. Dose-response curve showing neutralisation of TNFα by (B) anti-TNFα whole IgG and (C) anti-TNFα F(ab) as a decrease in TNFα-mediated CXCL8 release by FNB6 keratinocyte monolayers. Data are presented as mean ± SD ($n = 3$).

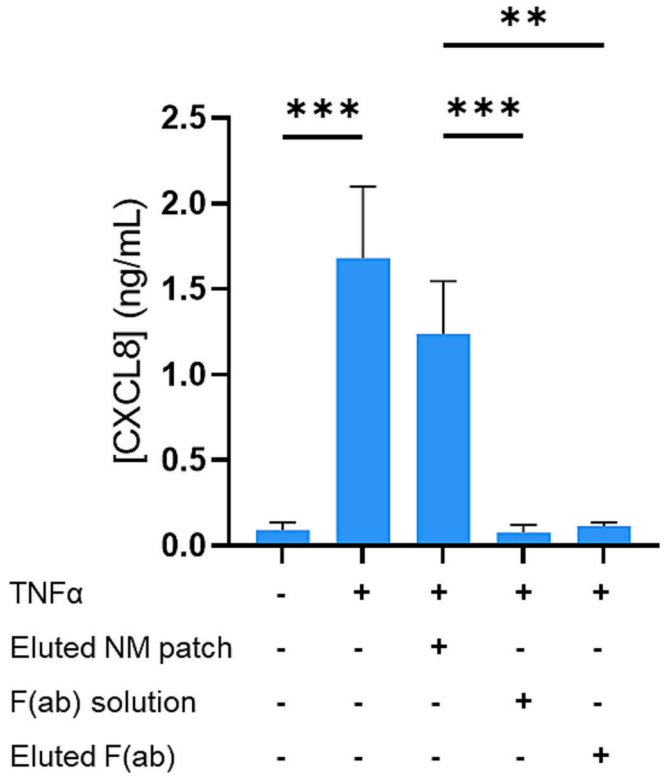

Fig. 5. Patch eluted F(ab) neutralises the activity of TNFα. Patch samples were eluted in PBS and the resulting eluates and controls were preincubated with TNFα before adding to FNB6 monolayers. TNFα neutralisation was detected as a decrease in TNFα-mediated CXCL8 release as measured by ELISA. Data are presented as mean ± SD ($n = 3$) and analysed by one-way ANOVA with Tukey's *post hoc* tests. **, $p < 0.01$; ***, $p < 0.001$.

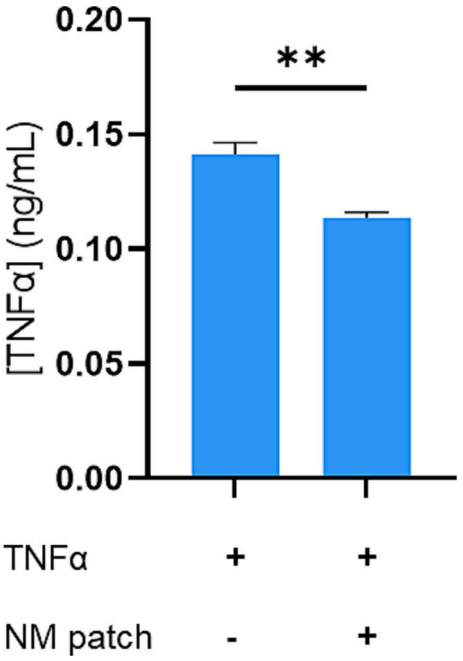

Fig. 6. Free TNFα concentration is reduced by contact with the patch. TNFα solutions were incubated 24 h in glass vials with or without samples of NM patch before measuring TNFα concentrations by ELISA. Data are presented as mean ± SD (n = 3) and analysed by unpaired *t*-test. **, $p < 0.01$.

TNFα (1 ng/mL) were also incubated with and without samples of NM patch at 37 °C for 24 h before measuring TNFα concentration in the media by ELISA (Fig. 6). Interestingly, the presence of the NM patch caused a small but significant decrease in TNFα concentration from 0.1413 ± 0.0051 ng/mL to 0.1135 ± 0.0026 ng/mL ($p < 0.01$), suggesting that the polymers in the patch itself affect active cytokine concentrations, likely through non-specific binding to proteins, which may explain the reduced levels of CXCL8 by FNB6 monolayers incubated with MN elute alone.

These results show that the mucoadhesive patch is suitable for releasing F(ab) with cytokine neutralising activity. CXCL8 is a neutrophil chemokine and although its secretion in 2D keratinocyte monolayers is highly sensitive to TNFα, its concentration is not typically elevated in OLP lesions, suggesting that it is unlikely to be a major driver of oral mucosal ulceration [46]. Furthermore, we have previously observed that CXCL8 secretion is significantly higher and affected to a lesser degree by immune challenge in 3D cultures in comparison to 2D cultures [25]. This emphasizes the importance of further investigation in a 3D disease-relevant model.

3.6. Oral mucosal ulcer equivalents

TNFα and several other chemokines are upregulated in the diseased tissue of patients suffering from oral mucosal inflammatory diseases, where they promote the recruitment and proliferation of cytotoxic T-cells, thus leading to the destruction of the basal epithelium and ulcer

formation [4,46]. We hypothesized that application of a topical anti-TNFα agent could have a potentially therapeutic effect by neutralising macrophage-released TNFα, causing a decrease in detectable TNFα concentrations and reverting secretion of TNFα-sensitive T-cell chemokines to baseline levels. The lack of clinically relevant oral disease models for the investigation of anti-inflammatory drugs is a major barrier to the investigation of anti-inflammatory drugs. There are currently no suitable *in vivo* animal models of OLP and RAS. In addition, small animal models may be inappropriate for studying targeted immunotherapies due to differences in innate immunity between rodents and humans [47]. Tissue-engineered oral mucosal equivalents, typically consisting of a fibroblast-populated collagen hydrogel seeded with keratinocytes and differentiated into a stratified squamous epithelium, are therefore increasingly being used to study disease processes in the oral mucosa [48–52]. To test for biocompatibility, levels of lactate dehydrogenase (as a measure of tissue damage) were measured in the transwell receptive medium following incubation of tissue engineered oral mucosal equivalents with topically applied NM and anti-TNFα F(ab)-containing patches and compared to control untreated models. We found no statistically significant difference between lactate dehydrogenase levels in any of the samples tested (OD_{492nm} untreated control 1.33 ± 0.13, non-medicated patch 1.48 ± 0.08 and F(ab) patch 1.66 ± 0.19), These data are similar to those previously published for similar patches containing clobetasol propionate [18], indicating that these patches are biocompatible.

We recently developed and characterised an immunocompetent oral mucosal equivalent containing primary monocyte-derived macrophages (MDM) [25]. These MDM specifically secreted TNFα in response to bacterial LPS, which then increased the gene expression and secretion of downstream chemokines, molecules known for the chemoattractant properties that are instrumental in driving leukocyte migration to inflammatory sites. Given the central role of TNFα-secreting immune cells, including macrophages [53], in the progression of RAS and OLP, this model is uniquely applicable for investigating novel therapies for these chronic inflammatory diseases.

RAS and ulcerative OLP produce areas of oral mucosa that are denuded of oral epithelium. In the case of RAS, the deleterious actions of both TNFα and cytotoxic T-cells result in round shallow ulcers, often covered by a thin layer of fibrin (Fig. 7Ai). Histologically, these lesions show exposed connective tissue populated by cytokine secreting leukocytes that perpetuate the disease, with epithelium only present at the edge of the ulcer (Fig. 7Aii). To replicate these lesions *in vitro* we cultured immunocompetent oral mucosal models in the presence of a 5 mm diameter titanium cylinder to occlude epithelial growth in a defined area (Fig. 7B). Removal of cylinders produced OMUE that resemble aphthous or OLP ulcers, with exposed simulated connective tissue, consisting of a fibroblast- and macrophage-populated collagen hydrogel. Above and at the edge of the ulcer is a stratified epithelium of oral keratinocytes (Fig. 7C) analogous to human ulcers. Aphthous ulcers typically have diameters ranging from 8 mm to 1 cm; severe OLP produces irregularly shaped ulcers with an area of approximately 60 mm^2 [19,54]. Therefore, the resulting area of exposed connective tissue in the OMUE is a conservative representation of that which would be present in patients and provides a useful model with impaired barrier function for investigating treatments for ulcerative oral mucosal diseases.

3.7. *Effect of patch application on cytokine release from immunocompetent oral mucosal ulcer equivalents*

To investigate their effect in a disease model, TNFα-neutralising

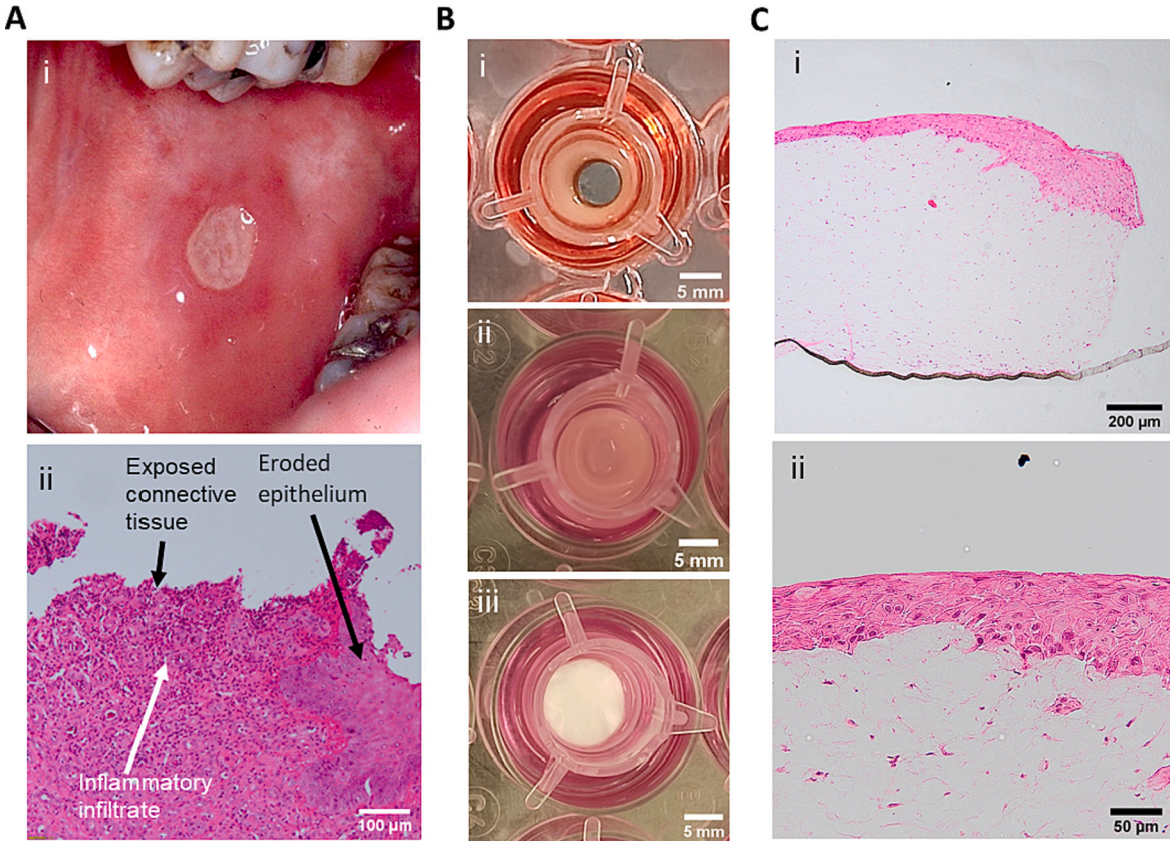

Fig. 7. Histological and photographic comparison of oral aphthous ulcers and tissue engineered immunocompetent ulcer equivalents. (Ai) Photograph of oral aphthous ulcer. (Aii) Haematoxylin and eosin stain of oral aphthous ulcer biopsy. Photographs of tissue engineered oral mucosal ulcer equivalents (Bi) before and (Bii) after removal of titanium cylinder and (Biii) after application of anti-TNFα F(ab) patch. (Ci, Cii) Haematoxylin and eosin stains of oral mucosal ulcer equivalent. (Image in Ai courtesy of Prof. Martin Thornhill, University of Sheffield, image in Aii courtesy of Dr. Ali Khurram University of Sheffield).

patches and NM patches were applied to OMUE for 24 h after which LPS was added to the media in the basolateral chamber to induce an immune response. MDM in 3D oral mucosal equivalents are known to secrete TNFα in response to LPS [25]. After 6 h, LPS stimulation in untreated OMUE caused a large increase in TNFα concentration to 1.67 ± 0.63 ng/mL compared to 0.116 ± 0.017 ng/mL for unstimulated OMUE (Fig. 8A; $p < 0.01$). Pre-treatment with TNFα-neutralising patches reduced TNFα concentrations to baseline levels of 0.30 ± 0.16 ng/mL ($p < 0.05$). Here, the anti-TNFα adheres to the TNFα released by MDM, preventing its binding to capture/detection antibodies in the ELISA, resulting in apparent decreased TNFα levels. TNFα concentrations at 24 h were mostly comparable to those at 6 h (Fig. 8B). OMUE treated with NM patches produced variable TNFα concentrations of 0.77 ± 0.45 ng/mL and 0.94 ± 0.56 ng/mL after 6 h and 24 h respectively. These data suggest successful delivery of potentially therapeutic doses anti-TNFα F(ab), sufficient to bind the secreted TNFα almost entirely.

The concentrations of chemokines in the media 24 h after LPS stimulation were profiled using a protein array (Fig. 9A-B). T-cell chemokines CCL3, CCL5 and CXCL10 were identified as having markedly increased levels in response to LPS stimulation and therefore these chemokines were further quantified by ELISA (Fig. 9 Ci-ii). CCL5 and CXCL10 have also been strongly implicated in the pathogenesis of OLP (Fig. 9Ciii) [55]. CCL3 concentrations were increased from 0.30 ± 0.11 to 5.9 ± 1.4 ng/mL in response to LPS stimulation ($p < 0.01$). Interestingly, treatment with either NM or anti-TNFα patches reduced CCL3 levels to approximately 2 ng/mL ($p < 0.05$). CCL3 belongs to the family of macrophage inflammatory proteins which promote cytotoxic T-cell recruitment and are secreted by several cell types including macrophages, monocytes, and fibroblasts [56]. Monocytes and macrophages express CCL3 in response to LPS stimulation [57], through a process at least partially mediated by TNFα [58]. Similarly, CCL5 concentrations were increased from 1.04 ± 0.22 to 2.28 ± 0.15 ng/mL by LPS stimulation ($p < 0.01$). Treatment with either NM patch or anti-TNFα patch reduced CCL5 to baseline concentrations ($p < 0.01$, $p < 0.001$). CCL5 is a potent T-cell chemokine abundantly expressed by oral keratinocytes in response to TNFα [59], as well as by fibroblasts, T-cells, and macrophages [60]. It has elevated levels in the oral epithelium and lamina propria of OLP biopsies [4]. CXCL10 concentrations were increased from 1.871 ± 0.098 to 2.30 ± 0.19 ng/mL by LPS stimulation ($p < 0.05$). Treatment with anti-TNFα patch reduced CXCL10 to baseline levels of 1.769 ± 0.059 ng/mL ($p < 0.05$).

These data show successful reduction in TNFα, CCL3, CCL5, and CXCL10 close to baseline levels in response to anti-TNFα patch treatment. Interestingly, NM patches also had some effect on cytokine and chemokine concentrations, with CCL3 and CCL5 both being significantly reduced by NM patch treatment, although levels in NM patch-treated OMUEs were variable. The patches likely reduce pro-inflammatory cytokine levels through a combination of selective neutralisation of TNFα by the released biologic and an anti-inflammatory effect caused by non-specific cytokine binding by the patch polymers. Interestingly, during a phase II clinical trial involving the same patches but containing clobetasol for delivery to OLP ulcers, both clinicians and patients reported that the non-medicated (NM) patches used as a placebo were beneficial for the management of OLP [19]. The PVP polymer used in these patches is also routinely used in cutaneous wound dressings and PVP-containing films were recently found to reduce inflammatory cytokine levels, including TNFα, and promote wound healing in a diabetic mouse model [61]. Similarly, PVP-coated nanoparticles have also been observed to reduce TNFα levels when added to bacteria-infected macrophages [62]. To our knowledge there are no other studies that have investigated topical delivery of cytokine neutralising antibodies for the treatment of oral mucosa diseases. Burgess et al. conducted a phase I clinical trial on an inhalable powder containing neutralising anti-IL-13 F(ab) for the treatment of asthma. The treatment was well tolerated and reduced exhaled nitric oxide levels, providing evidence of anti-inflammatory effect in the respiratory epithelium [63]. The suppression of these key disease-causing cytokines represents the first experimental evidence in support of topical anti-TNFα therapy to treat ulcerative oral diseases.

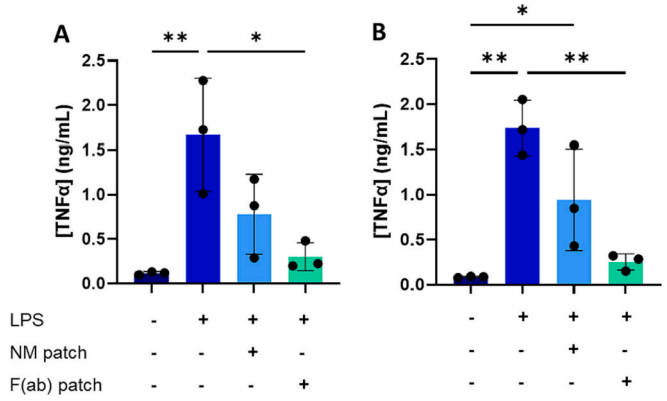

Fig. 8. Patches applied to immunocompetent oral ulcer models neutralise LPS-mediated TNFα release. NM and anti-TNFα F(ab)-containing patches were applied to OMUE for 24 h before stimulating with LPS. TNFα concentrations (A) 6 h and (B) 24 h following LPS stimulation. Data are presented as mean ± SD ($n = 3$) and analysed by one-way ANOVA with Tukey's *post hoc* tests. *, $p < 0.05$; **, $p < 0.01$.

4. Conclusions

F(ab) were successfully electrospun into mucoadhesive fibres using 97% *v*/v ethanol as a processing solvent. The antibody fragments were retained within the fibres as aggregates and were eluted at a clinically suitable rate with negligible activity loss. F(ab)-containing and non-medicated patches were tested using an *in vitro* oral epithelium model, resulting in transepithelial permeation and detectable levels of F(ab) present within the tissue. Patches containing anti-TNFα F(ab) neutralised the activity of TNFα, as shown by the suppression of TNFα-mediated CXCL8 release from oral keratinocytes grown as monolayer cultures. Patches applied to immune-stimulated oral mucosal ulcer models reduced detectable levels of inflammatory cytokines TNFα, CCL3, CCL5, and CXCL10 to baseline levels. These molecules are major drivers in the pathogenesis of oral ulceration; therefore, this study provides the first experimental evidence to support the efficacy of topical anti-TNFα therapy. This novel approach could improve interventions for debilitating oral diseases such as OLP and RAS, as well as representing a platform technology for the site-specific delivery of antibody fragments to tissue surfaces to treat a wide range of conditions.

CRediT authorship contribution statement

Jake G. Edmans: Conceptualization, Methodology, Investigation, Writing – original draft. **Bethany Ollington:** Methodology, Investigation, Writing – review & editing. **Helen E. Colley:** Conceptualization, Methodology, Supervision, Project administration, Writing – review & editing, Funding acquisition. **Martin E. Santocildes-Romero:** Supervision, Writing – review & editing. **Lars Siim Madsen:** Supervision, Writing – review & editing. **Paul V. Hatton:** Conceptualization, Methodology, Supervision, Writing – review & editing, Funding acquisition. **Sebastian G. Spain:** Conceptualization, Supervision, Writing – review & editing. **Craig Murdoch:** Supervision, Methodology, Writing – original draft, Writing – review & editing.

Declaration of Competing Interest

The authors declare the following financial interests/personal relationships which may be considered as potential competing interests: The research presented was funded, in part, by AFYX Therapeutics APS.

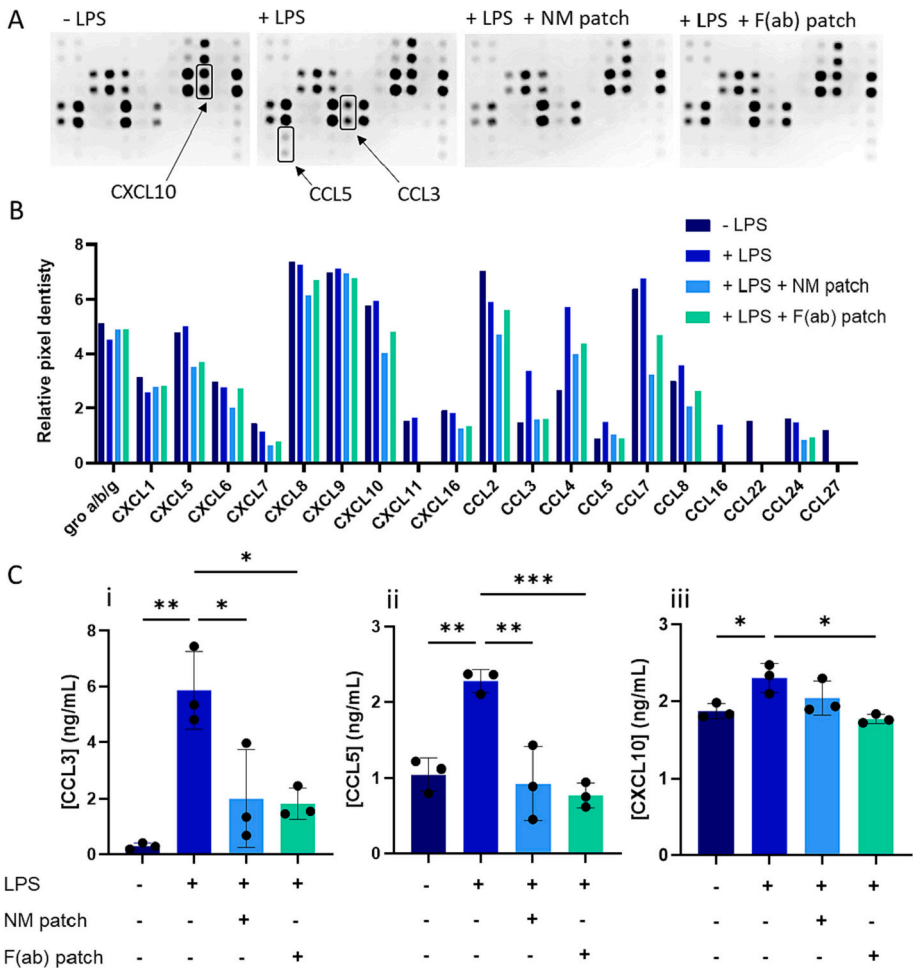

Fig. 9. Effect of patch treatment on chemokine release. NM patches and anti-TNFα F(ab)-containing patches were applied to OMUE for 24 h before stimulating with LPS. After 24 h, chemokine release into the media was profiled using a protein array and selected chemokines quantified by ELISA. (A) Scanned images of protein array membranes. (B) Semi-quantitative densitometric analysis of the array membranes, showing relative chemokine concentrations ($n = 1$). Concentrations of (Ci) CCL3, (Cii) CCL5, and (Ciii) CXCL10 were measured by ELISA. ELISA data are presented as mean ± SD ($n = 3$) and analysed by one-way ANOVA with Tukey's *post hoc* tests. *, $p < 0.05$; **, $p < 0.01$; ***, $p < 0.001$.

JE, BO, HEC, SS and CM declare that they have no other known competing financial interests or personal relationships that could have appeared to influence the work reported within this paper. MES and LSM are employed by AFYX Therapeutics. PVH is on the AFYX Therapeutics APS scientific advisory board, where AFYX have translated mucoadhesive electrospun patch technology for clinical use and have intellectual property (international patent applications WO 2017/085262 A, WO 2021/072113 A1).

Acknowledgements

The authors would like to thank Prof. Keith Hunter (University of Sheffield) for use of the FNB6 oral keratinocyte cell line. Confocal microscopy was performed at the Wolfson Light Microscope Facility where the microscope was purchased with funding from the Wellcome Trust [WT093134AIA, London, UK]. This work was funded by the Engineering and Physical Sciences Research Council [EP/L016281/1, London, UK] as a CASE PhD studentship with the Centre for Doctoral Training in Polymers, Soft Matter & Colloids where AFYX Therapeutics (Copenhagen, Denmark), was the industrial partner.

Appendix A. Supplementary data

Supplementary data to this article can be found online at https://doi.org/10.1016/j.jconrel.2022.08.016.

References

[1] C. Scully, S. Porter, Oral mucosal disease: recurrent aphthous stomatitis, Br. J. Oral Maxillofac. Surg. 46 (2008) 198–206.
[2] M.Á. González-Moles, S. Warnakulasuriya, I. González-Ruiz, L. González-Ruiz, Á. Ayén, D. Lenouvel, I. Ruiz-Ávila, P. Ramos-García, Worldwide prevalence of oral lichen planus: a systematic review and meta-analysis, Oral Dis. 27 (2021) 813–828.
[3] L.J. Taylor, J. Bagg, D.M. Walker, T.J. Peters, Increased production of tumour necrosis factor by peripheral blood leukocytes in patients with recurrent oral aphthous ulceration, J. Oral Pathol. Med. 21 (1992) 21–25.
[4] A. El-Howati, M.H. Thornhill, H.E. Colley, C. Murdoch, Immune mechanisms in oral lichen planus, Oral Dis. 0–3 (2022).
[5] C. Scully, M. Carrozzo, Oral mucosal disease: lichen planus, Br. J. Oral Maxillofac. Surg. 46 (2008) 15–21.
[6] D. Farhi, N. Dupin, Pathophysiology, etiologic factors, and clinical management of oral lichen planus, part I: facts and controversies, Clin. Dermatol. 28 (2010) 100–108.
[7] R. Fischer, R.E. Kontermann, K. Pfizenmaier, Selective targeting of TNF receptors as a novel therapeutic approach, Front. Cell Dev. Biol. 8 (2020) 1–21.
[8] E. Georgakopoulou, C. Scully, Biological agents: what they are, how they affect oral health and how they can modulate oral healthcare, Br. Dent. J. 218 (2015) 671–677.
[9] S. Gupta, S. Ghosh, S. Gupta, Interventions for the management of oral lichen planus: a review of the conventional and novel therapies, Oral Dis. 23 (2017) 1029–1042.
[10] V. Sankar, V. Hearnden, K. Hull, D.V. Juras, M. Greenberg, A. Kerr, P. Lockhart, L. Patton, S. Porter, M. Thornhill, Local drug delivery for oral mucosal diseases: challenges and opportunities, Oral Dis. 17 (2011) 73–84.
[11] I.D. O'Neill, C. Scully, Biologics in oral medicine: ulcerative disorders, Oral Dis. 19 (2013) 37–45.
[12] M. Streit, Z. Beleznay, L.R. Braathen, Topical application of the tumour necrosis factor-α antibody infliximab improves healing of chronic wounds, Int. Wound J. 3 (2006) 171–179.
[13] J. Autio-Gold, The role of chlorhexidine in caries prevention, Oper. Dent. 33 (2008) 710–716.

[14] M. Innocenti, G. Moscatelli, S. Lopez, Efficacy of gelclair in reducing pain in palliative care patients with oral lesions, J. Pain Symptom Manag. 24 (2002) 456–457.

[15] R.J. Bensadoun, J. Daoud, B. El Gueddari, L. Bastit, R. Gourmet, A. Rosikon, C. Allavena, P. Céruse, G. Calais, P. Attali, Comparison of the efficacy and safety of miconazole 50-mg mucoadhesive buccal tablets with miconazole 500-mg gel in the treatment of oropharyngeal candidiasis: a prospective, randomized, single-blind, multicenter, comparative, phase III trial in patients, Cancer 112 (2008) 204–211.

[16] M.E. Santocildes-Romero, L. Hadley, K.H. Clitherow, J. Hansen, C. Murdoch, H. E. Colley, M.H. Thornhill, P.V. Hatton, Fabrication of electrospun mucoadhesive membranes for therapeutic applications in oral medicine, ACS Appl. Mater. Interfaces 9 (2017) 11557–11567.

[17] J.G. Edmans, K.H. Clitherow, C. Murdoch, P.V. Hatton, S.G. Spain, H.E. Colley, Mucoadhesive electrospun fibre-based technologies for oral medicine, Pharmaceutics 12 (2020) 1–21.

[18] H.E. Colley, Z. Said, M.E. Santocildes-Romero, S.R. Baker, K. D'Apice, J. Hansen, L. S. Madsen, M.H. Thornhill, P.V. Hatton, C. Murdoch, Pre-clinical evaluation of novel mucoadhesive bilayer patches for local delivery of clobetasol-17-propionate to the oral mucosa, Biomaterials 178 (2018) 134–146.

[19] M.T. Brennan, L.S. Madsen, D.P. Saunders, J.J. Napenas, C. McCreary, R. Ni Riordain, A.M.L. Pedersen, S. Fedele, R.J. Cook, R. Abdelsayed, M.T. Llopiz, V. Sankar, K. Ryan, D.A. Culton, Y. Akhlef, F. Castillo, I. Fernandez, S. Jurge, A. R. Kerr, C. McDuffie, T. McGaw, A. Mighell, T.P. Sollecito, T. Schlieve, M. Carrozzo, A. Papas, T. Bengtsson, I. Al-Hashimi, L. Burke, N.W. Burkhart, S. Culshaw, B. Desai, J. Hansen, P. Jensen, T. Menné, P.B. Patel, M. Thornhill, N. Treister, T. Ruzicka, Efficacy and safety of a novel mucoadhesive clobetasol patch for treatment of erosive oral lichen planus, J. Oral Pathol. Med. (2021) 0–3.

[20] J.G. Edmans, C. Murdoch, M.E. Santocildes-Romero, P.V. Hatton, H.E. Colley, S. G. Spain, Incorporation of lysozyme into a mucoadhesive electrospun patch for rapid protein delivery to the oral mucosa, Mater. Sci. Eng. C 112 (2020), 110917.

[21] C.A. Schneider, W.S. Rasband, K.W. Eliceiri, NIH image to ImageJ: 25 years of image analysis, Nat. Methods 9 (2012) 671–675.

[22] J. Schindelin, I. Arganda-carreras, E. Frise, V. Kaynig, T. Pietzsch, S. Preibisch, C. Rueden, S. Saalfeld, B. Schmid, J. Tinevez, D.J. White, V. Hartenstein, P. Tomancak, A. Cardona, PBMCs, Nat. Methods 9 (2012) 676–682.

[23] G. Song, Y. Lin, Z. Zhu, H. Zheng, J. Qiao, C. He, H. Wang, Strong fluorescence of poly (N-vinylpyrrolidone) and its oxidized hydrolyzate, Macromol. Rapid Commun. 36 (2015) 278–285.

[24] C. Murdoch, S. Tazzyman, S. Webster, C.E. Lewis, Expression of Tie-2 by human monocytes and their responses to angiopoietin-2, J. Immunol. 178 (2007) 7405–7411.

[25] B. Ollington, H.E. Colley, C. Murdoch, Immunoresponsive tissue-engineered oral mucosal equivalents containing macrophages, Tissue Eng. - Part C Methods 27 (2021) 462–471.

[26] W.R. Gombotz, S.C. Pankey, D. Phan, R. Drager, K. Donaldson, K.P. Antonsen, A. S. Hoffman, H.V. Raff, The stabilization of a human IgM monoclonal antibody with poly(vinylpyrrolidone), Pharm. Res. 11 (1994) 624–632.

[27] D.H. Atha, K.C. Ingham, Mechanism of precipitation of proteins by polyethylene glycols. Analysis in terms of excluded volume, J. Biol. Chem. 256 (1981) 12108–12117.

[28] A.C. Miklos, C. Li, N.G. Sharaf, G.J. Pielak, Volume exclusion and soft interaction effects on protein stability under crowded conditions, Biochemistry 49 (2010) 6984–6991.

[29] M. Gandhi, R. Srikar, A.L. Yarin, C.M. Megaridis, R.A. Gemeinhart, Mechanistic examination of protein release from polymer nanofibers, Mol. Pharm. 6 (2009) 641–647.

[30] U. Angkawinitwong, S. Awwad, P.T. Khaw, S. Brocchini, G.R. Williams, Electrospun formulations of bevacizumab for sustained release in the eye, Acta Biomater. 64 (2017) 126–136.

[31] V. Truong-Le, P.M. Lovalenti, A.M. Abdul-Fattah, Stabilization challenges and formulation strategies associated with oral biologic drug delivery systems, Adv. Drug Deliv. Rev. 93 (2015) 95–108.

[32] N. Simon, C. Sperber, C. Voigtländer, J. Born, D. F. Gilbert, S. Seyferth, G. Lee, B. Kappes and O. Friedrich, Improved stability of polyclonal antibodies: a case study with lyophilization-conserved antibodies raised against epitopes from the malaria parasite plasmodium falciparum, Eur. J. Pharm. Sci., DOI:https://doi.org/10.1016/j.ejps.2019.105086.

[33] D.C. Geraldes, V.L. Beraldo-de-Araújo, B.O.P. Pardo, A. Pessoa Junior, M. A. Stephano, L. de Oliveira-Nascimento, Protein drug delivery: current dosage form profile and formulation strategies, J. Drug Target. 28 (2020) 339–355.

[34] H. Frizzell, T.J. Ohlsen, K.A. Woodrow, Protein-loaded emulsion electrospun fibers optimized for bioactivity retention and pH-controlled release for peroral delivery of biologic therapeutics, Int. J. Pharm. 533 (2017) 99–110.

[35] L.C. Junqueira, J. Carneiro, R.O. Kelly, Basic Histology, Prentice-Hall, London, 1995.

[36] L. Heinemann, Y. Jacques, Oral insulin and buccal insulin: a critical reappraisal, J. Diabetes Sci. Technol. 3 (2009) 568–584.

[37] M.K. Gutniak, H. Larsson, S.J. Heiber, O.T. Juneskans, J.J. Holst, B. Ahrén, Potential therapeutic levels of glucagon-like peptide I achieved in humans by a buccal tablet, Diabetes Care 19 (1996) 843–848.

[38] L. Bierbaumer, U.Y. Schwarze, R. Gruber, W. Neuhaus, Cell culture models of oral mucosal barriers: a review with a focus on applications, culture conditions and barrier properties, Tissue Barriers 6 (2018) 1–42.

[39] M. B. Stie, J. R. Gätke, I. S. Chronakis, J. Jacobsen and H. M. Nielsen, Mucoadhesive Electrospun Nanofiber-Based Hybrid System with Controlled and Unidirectional Release of Desmopressin.

[40] W.M. Saltzman, J.K. Sherwood, D.R. Adams, P. Haller, Long-term vaginal antibody delivery: delivery systems and biodistribution, Biotechnol. Bioeng. 67 (2000) 253–264.

[41] P.Y. Kuo, J.K. Sherwood, W.M. Saltzman, Topical antibody delivery systems produce sustained levels in mucosal tissue and blood, Nat. Biotechnol. 16 (1998) 163–167.

[42] C. Monaco, J. Nanchahal, P. Taylor, M. Feldmann, Anti-TNF therapy: past, present and future, Int. Immunol. 27 (2015) 55–62.

[43] R. K. Jain, Physiological barriers to delivery of monoclonal antibodies and other macromolecules in tumors, Cancer Res.

[44] L.R. Jennings, H.E. Colley, J. Ong, F. Panagakos, J.G. Masters, H.M. Trivedi, C. Murdoch, S. Whawell, Development and characterization of *in vitro* human oral mucosal equivalents derived from immortalized Oral keratinocytes, Tissue Eng. Part C Methods 22 (2016) 1108–1117.

[45] A. Henry, J. Kennedy, G. Fossati, A. Nesbitt, TNF binding by certolizumab pegol, adalimumab, and infliximab-stoichiometry, complex formation, and the biologic effects of complexes, Clin. Immunol. 123 (2007) S169–S170.

[46] R. Lu, J. Zhang, W. Sun, G. Du, G. Zhou, Inflammation-related cytokines in oral lichen planus: an overview, J. Oral Pathol. Med. 44 (2015) 1–14.

[47] J. Mestas, C.C.W. Hughes, Of mice and not men: differences between mouse and human immunology, J. Immunol. 172 (2004) 2731–2738.

[48] K. Moharamzadeh, H. Colley, C. Murdoch, V. Hearnden, W.L. Chai, I.M. Brook, M. H. Thornhill, S. MacNeil, Tissue-engineered oral mucosa, J. Dent. Res. 91 (2012) 642–650.

[49] N.P. Yadev, C. Murdoch, S.P. Saville, M.H. Thornhill, Evaluation of tissue engineered models of the oral mucosa to investigate oral candidiasis, Microb. Pathog. 50 (2011) 278–285.

[50] J.K. Buskermolen, C.M.A. Reijnders, S.W. Spiekstra, T. Steinberg, C.J. Kleverlaan, A.J. Feilzer, A.D. Bakker, S. Gibbs, Development of a full-thickness human gingiva equivalent constructed from immortalized keratinocytes and fibroblasts, Tissue Eng. - Part C Methods 22 (2016) 781–791.

[51] H.E. Colley, V. Hearnden, A.V. Jones, P.H. Weinreb, S.M. Violette, S. MacNeil, M. H. Thornhill, C. Murdoch, Development of tissue-engineered models of oral dysplasia and early invasive oral squamous cell carcinoma, Br. J. Cancer 105 (2011) 1582–1592.

[52] H.E. Colley, P.C. Eves, A. Pinnock, M.H. Thornhill, C. Murdoch, Tissue-engineered oral mucosa to study radiotherapy-induced oral mucositis, Int. J. Radiat. Biol. 89 (2013) 907–914.

[53] T. M. Ferrisse, A. B. de Oliveira, M. P. Palaçon, E. V. Silva, E. M. S. Massucato, L. Y. de Almeida, J. E. Léon and A. Bufalino, The role of CD68+ and CD163+ macrophages in immunopathogenesis of oral lichen planus and oral lichenoid lesions, Immunobiology, https://doi.org/10.1016/j.imbio.2021.152072.

[54] L. Preeti, K.T. Magesh, K. Rajkumar, R. Karthik, Recurrent aphthous stomatitis, J. Oral Maxillofac. Pathol. 15 (2011) 252–256.

[55] J. Fang, C. Wang, C. Shen, J. Shan, X. Wang, L. Liu, Y. Fan, The expression of CXCL10/CXCR3 and effect of the axis on the function of T lymphocyte involved in oral lichen planus, Inflammation 42 (2019) 799–810.

[56] F. Castellino, A.Y. Huang, G. Altan-Bonnet, S. Stoll, C. Scheinecker, R.N. Germain, Chemokines enhance immunity by guiding naive CD8+ T cells to sites of CD4+ T cell-dendritic cell interaction, Nature 440 (2006) 890–895.

[57] T. Suzuki, S.I. Hashimoto, N. Toyoda, S. Nagai, N. Yamazaki, H.Y. Dong, J. Sakai, T. Yamashita, T. Nukiwa, K. Matsushima, Comprehensive gene expression profile of LPS-stimulated human monocytes by SAGE, Blood 96 (2000) 2584–2591.

[58] H. Mühl, C.A. Dinarello, Macrophage inflammatory protein-1 alpha production in lipopolysaccharide-stimulated human adherent blood mononuclear cells is inhibited by the nitric oxide synthase inhibitor N(G)-monomethyl-L-arginine, J. Immunol. 159 (1997) 5063–5069.

[59] J. Li, G.W. Ireland, P.M. Farthing, M.H. Thornhill, Epidermal and oral keratinocytes are induced to produce RANTES and IL-8 by cytokine stimulation, J. Invest. Dermatol. 106 (1996) 661–666.

[60] V. Appay, S.L. Rowland-Jones, RANTES: a versatile and controversial chemokine, Trends Immunol. 22 (2001) 83–87.

[61] M. Contardi, M. Summa, P. Picone, O.R. Brancato, M. Di Carlo, R. Bertorelli, A. Athanassiou, Evaluation of a multifunctional polyvinylpyrrolidone/hyaluronic acid-based bilayer film patch with anti-inflammatory properties as an enhancer of the wound healing process, Pharmaceutics 14 (2022) 483.

[62] V. Dennis, S. Singh Yilma, S. Dixit, Anti-inflammatory effects of silver-polyvinyl pyrrolidone (Ag-PVP) nanoparticles in mouse macrophages infected with live chlamydia trachomatis, Int. J. Nanomedicine 2421 (2013).

[63] G. Burgess, M. Boyce, M. Jones, L. Larsson, M.J. Main, F. Morgan, P. Phillips, A. Scrimgeour, F. Strimenopoulou, P. Vajjah, M. Zamacona, R. Palframan, Randomized study of the safety and pharmacodynamics of inhaled interleukin-13 monoclonal antibody fragment VR942, EBioMedicine 35 (2018) 67–75.

Chapter 5: Discussion

5.1 An electrospun mucoadhesive patch formulation for the release of functional polypeptides

The first aim of this project was to adapt a mucoadhesive electrospun fibre formulation for the delivery of functional proteins, peptides, and antibody derivatives. Previous research in this group used 97% v/v ethanol as an electrospinning solvent to fabricate mucoadhesive polymer patches and to encapsulate various small molecule drugs (Chapter 1). This research led to the development of the Rivelin patch, which is currently in the process of clinical development. Ethanol is known to denature many proteins, yet it is an important processing solvent to allow the electrospinning of RS100, a polymer which prevents rapid dissolution in aqueous media and confers mucoadhesive properties to the patch fibres.

Lysozyme was used as a model protein to investigate the effect of protein incorporation and ethanol concentration on formulation performance (Chapter 2).[2] Lysozyme release and functionality were minimally affected, with similar loading efficiency and activity of the eluted protein for 97, 80, 60, and 40% v/v ethanol. However, solvent composition had a considerable effect on solution and material properties, with 60, and 40% v/v ethanol producing narrower fibres that do not maintain their integrity in aqueous media. Fibres prepared with 40% v/v ethanol also resulted in the weakest adhesion strength to smooth surfaces in a simple adhesion test, although the difference between 97 and 40% v/v was below the threshold of significance (Appendix 2). For these reasons, only 97% v/v or 80% v/v ethanol were investigated further in this thesis. However, if required, the fabrication of membranes with suitable properties would likely be possible at lower ethanol concentrations by increasing the concentration of high molecular weight polymers to increase solution viscosity, which would in theory counteract the higher conductivity and increase fibre diameter.[31] Indeed, Afyx therapeutics A/S, the legal

manufacturer of the Rivelin patch, have recently disclosed that the manufacturing process used to produce patches for clinical trials has been modified to use 50% v/v ethanol for electrospinning the mucoadhesive drug-eluting fibres.[185]

Proteins were primarily incorporated by dissolving in the aqueous component of the electrospinning solution and mixing with the ethanolic polymer component immediately before electrospinning. For highly soluble proteins such as lysozyme and antibodies, a maximum loading of 1-2% w/w is theoretically achievable using this method with 97% v/v ethanol (assuming a solubility of 75-150 mg/mL).[186] Although this is likely sufficient for high potency therapeutics, higher loading is possible by increasing the volume of the aqueous component. By using 80% v/v ethanol, up to 5% w/w loading was achieved for insulin, a less soluble protein that requires relatively high therapeutic doses (Chapter 3). Alternatively, very high lysozyme loadings of up to 50% w/w were also possible by mixing lysozyme powder directly into the 97% v/v ethanolic polymer solution (Appendix 2).

The mucoadhesive fibre formulation was found to be remarkably suitable for the release of a wide variety of proteins. Lysozyme (Chapter 2), bradykinin (Chapter 3), and F(ab) antibody fragments (Chapter 4)[3] were all eluted rapidly, with complete release reached within approximately 2 h. The release of these highly hydrophilic molecules followed first-order kinetics. This is consistent with a mechanism involving rapid swelling of the fibres, allowing free diffusion of the protein through the fibrous hydrogel.[73] Because of its intrinsically lower solubility, insulin release was slower than is ideal for oromucosal delivery and also followed first-order kinetics (Chapter 3).

Processing and release of lysozyme and F(ab) from the formulation produced a quantified negligible loss in protein function. Bradykinin maintained a high degree of biological activity, although it was not measured quantitatively. Incorporating proteins had little effect on the

mechanical and adhesive performance of the material (Chapter 2, Chapter 4, Appendix 2) and lysozyme was found to be distributed homogeneously throughout the material both on a macroscopic and microscopic scale. The high preservation of protein activity following electrospinning is somewhat surprising given the denaturing effects of ethanol and suggests that the polymer components may have a protective effect on protein function. Indeed, F(ab) were observed to lose most of their activity following exposure to 97% v/v ethanol for 1 h in the absence of polymers (Chapter 4).

Soluble polymers are theorised to stabilise proteins through a variety of mechanisms. Polymers with mild surfactant properties are known to act as blocking agents, preventing proteins from adhering or denaturing at surfaces.[187] Weakly interacting polymers can stabilise proteins through steric crowding, which limits interactions with denaturing solvents.[188] This can result in precipitation, which may further protect certain proteins. For some systems, polymers can protect against denaturing aggregation, possibly by restricting protein-protein interactions.[189] Protein-binding polymers, including PVP, which is a strong hydrogen bond acceptor, can protect proteins through a combination of steric crowding and binding to protein in its native state.[190] This transient protein binding is stabilising and increases the free energy barrier to solvent-induced denaturation.

The relative contributions of these effects in the preservation of protein function in the reported electrospinning fabrication process is unknown. Fluorescent F(ab) were observed in the fibres as micro- and nanoscale aggregates (Chapter 4). This suggests a likely stabilisation mechanism involving precipitation, induced by ethanol and volume-excluding polymers following addition to the electrospinning solution. However, phase separation could alternatively occur during the physical drying and shear processes involved in electrospinning. Lysozyme, a protein with high specific charge, did not display the same aggregation (Chapter 2). Literature on protein encapsulation by electrospinning is discussed in Chapter 1.3.5.

In summary, proteins can generally be electrospun without activity loss from aqueous solutions to produce rapidly dissolving monolithic fibres. Multiple-domain fibres prepared using emulsion or coaxial electrospinning with an aqueous component can be highly effective for slow sustained release of bioactive proteins. Chitosan has been electrospun from acidic solutions to encapsulate proteins within mucoadhesive gel-forming fibres for rapid release. The work in this thesis presents a useful alternative formulation that allows highly efficient protein encapsulation and release using fully synthetic pharmaceutical-grade polymers, with no specific pH requirements.

More generally, the results demonstrate that the denaturing effect of solvents can be negated at high concentrations of stabilising polymers to facilitate solvent-processing of biopharmaceutical formulations. This principle could be investigated further by considering other complex biomacromolecules (nucleic acids, viruses, delivery vectors) or alternative polymer/solvent systems. Although outside the scope of this thesis, it may also be possible to encapsulate bioactive proteins within hydrophobic polymer fibres by designing a biocompatible polymer system with high ethanol solubility and low water solubility. Such a material could incorporate proteins such as growth factors and have applications as an implantable material for sustained slow release or regenerative medicine.

5.2 Local delivery applications in oral medicine

The work in this thesis highlights several potential oral medicine applications for adhesive electrospun patches that can deliver biologics locally within the oral cavity. Patch-delivered lysozyme maintained its enzymatic activity and inhibited the growth of an oral bacterium (Chapter 2). Lysozyme is naturally produced in the saliva of healthy people and can be delivered safety using existing dosage forms, such as rinses. However, a patch formulation may be beneficial for improving residence time and acting as protective dressings for ulcers that are

infected or at risk of infection. Patches may potentially enable the topical application of other antimicrobial peptides with low solubility, poor stability in solution, or off-target toxicity. Antimicrobial peptides and proteins present several advantages over traditional antibiotics and antifungals, including the ability to selectively target specific pathogenic strains or treat antimicrobial-resistant strains.

Patch-released bradykinin induced calcium mobilisation in oral cells (Chapter 3). Although bradykinin has limited relevance as a therapeutic, the work illustrates the potential of topical biologic delivery to influence oral cells. For example, growth factors could be delivered to promote wound healing. Immune-modulating cytokines could treat autoinflammatory conditions or help clear abnormal cell growth.

The ability of the patches to deliver antibody derivatives to the oral mucosa was investigated in greater detail as a novel treatment for inflammatory oral ulcers (Chapter 4). There is strong interest from the oral medicine community in topical monoclonal antibody therapies to treat T-cell-mediated mucosal conditions, such as OLP, that are inadequately managed using existing medicines.[183,184] Tumour necrosis factor alpha (TNFα) is a key driver of pathogenesis in these diseases. It has been hypothesised that by neutralising TNFα using topical antibody-based drugs, the maladaptive recruitment of cytotoxic T cells can be prevented, thus allowing healthy tissue to regenerate.

The suitability of the patches for F(ab) release was first assessed using biotinylated F(ab) as model biologic and quantifying its antigen-binding activity using ELISA. F(ab) fragments with neutralising activity against TNFα were then prepared and electrospun into mucoadhesive patches. The effect of TNFα on oral keratinocytes was successfully blocked by the patch-released F(ab). A novel tissue-engineered model of an oral ulcer was developed, using macrophages to introduce immune-responsiveness and TNFα secretion. Patches applied

directly to immune-stimulated ulcer models successfully reduced detectable-levels of TNFα and key cytokines involved in T-cell recruitment. This provides the first experimental proof-of-concept evidence that topical patches containing anti-TNFα agents may be effective at treating inflammatory oral conditions.

Additional preclinical research would be beneficial to further investigate the potential of this technology. This research used polyclonal animal-derived F(ab)s. Monoclonal human or humanised antibodies are usually required in clinical practise to avoid immune-rejection and serum sickness. Further research would ideally involve approved monoclonal biologics that can be directly translated to human use. Shelf-life and storage of biologics in electrospun formulations requires further investigation. Additional drying, packaging in inert gases, and controlled storage conditions may be considered to prevent denaturation or oxidation of the biologic to improve shelf-life. Coaxial electrospinning may also be considered to encapsulate each individual fibre within a protective sheath.

Although the treatment reduced levels of T-cell chemoattractants, for further research it would be beneficial to investigate effectiveness using activated T cells, for example with standard chemotaxis assays on the conditioned media from oral mucosal models.[191] T-cell-mediated diseases are complex and not yet fully understood and a significant barrier to the development of new therapies is the lack of suitable disease models. Lesions resembling OLP can be induced in mice by injecting T helper cells that are reactive to self-antigens, causing the secretion of TNFα and interferon gamma to recruit an inflammatory infiltrate of neutrophils and mononuclear cells.[192,193] However, the involved immune mechanisms are likely somewhat different to naturally occurring OLP in humans, which involves basal cell apoptosis caused primarily by presentation of unknown antigens to cytotoxic T cells.[194] Tissue-engineered models of the mucosa and skin represent an active area of research,[195] and it is anticipated that new *in vitro* models incorporating T cells and other relevant leukocytes will introduce new

methods to evaluate treatments for T-cell-mediated diseases by directly measuring T-cell recruitment and T-cell-mediated basal cell apoptosis.

Interestingly, this work also showed that non-medicated patches significantly reduced detectable levels of some T-cell chemokines, although the effect was more variable in comparison to the medicated patches. Existing literature also reports that materials containing PVP can reduce detectable levels of pro-inflammatory cytokines, including TNFα.[185,196,197] This phenomenon is perhaps related to the observation that the polymer system protects proteins from ethanol-induced denaturation, and could be caused by non-specific binding of globular proteins to the patch polymers. Alternatively, macrophage phenotype may be affected by the material, as has been observed previously for certain wound dressings.[198] Analysis of RNA expression may provide an insightful readout in future experiments to detect changes in cytokines transcription in isolation from the effects of specific and non-specific binding following secretion. In addition to oral medicine, a platform technology for the delivery of antibody-based medicines to mucosal surfaces may also be applicable for a variety of other fields, including gynaecology and topical chemotherapy.

5.3 Transepithelial delivery

A third aim of this project was to develop methods suitable for investigating the transmucosal permeation of peptides or proteins and use them to assess the patch formulation. Insulin and biotinylated F(ab) were used as model compounds. Although there are more promising candidate peptides for systemic delivery through the oral mucosa (Chapter 1), the high cost of the peptides themselves and ELISA detection is prohibitive at this early stage of research. Flash-frozen *ex vivo* porcine oral mucosa was initially considered as a model permeability barrier due to its anatomical similarity to that of humans.[199] The tissue was fitted in Franz cells and validated using fluorescent dextran and bupivacaine as model permeants, showing that the

setup had suitable permeability barrier properties in agreement with previously reported literature values (Appendix 4).

Applying insulin solution produced negligible transmucosal permeation after 8 h for both buccal and sublingual tissue (Appendix 4). The insulin was observed using fluorescence labelling and immunofluorescence to be present only within the superficial layer of keratinocytes, where it accumulated within the cytoplasm and was most concentrated at the nuclei. Insulin is internalised by many cell types following binding to membrane-bound receptors.[200,201] Insulin can either be recycled back into the cell membrane, degraded by enzymes, or translocated to the nucleus, which, in many cells types, contains insulin receptors. This accumulation of insulin contrasts with observations that have been made *in vivo,* that showed that insulin can permeate the oral mucosa, albeit with modest bioavailability, to induce a systemic effect.[156,202,203]

This discrepancy is likely due to altered cell behaviour in non-living tissue. Treating the tissue with 5% sodium dodecyl sulfate (SDS) impaired the barrier properties, as confirmed by transepithelial electrical resistance (TEER). This treatment should be sufficient to lyse the epithelial keratinocytes, yet the amount of transmucosal insulin permeation remained negligible. The lamina propria of the oral mucosa is highly vascularised and the absence of blood flow in *ex vivo* tissue may cause accumulation of insulin in the connective tissue and greatly increased lag times that are not representative of living tissue. The epithelium can be separated from the lamina propria by a combination of heat and osmotic shock;[64] however, this is likely to further affect cell function.

These results suggest that porcine tissue is poorly suited for measuring the transmucosal permeation of bioactive peptides. Lancina *et al.* claimed that chitosan/PEO/insulin fibres applied to porcine buccal tissue could deliver high levels of insulin of corresponding to nearly

10% of the loaded dose within 3h.[204] This is misleading, as insulin was detected within the receptor medium within as little as 10 minutes, suggesting interference from porcine insulin released by the tissue itself. Their permeation experiment lacked suitable negative controls to account for this. Other articles, for example by Xu *et al.*, report low levels of insulin permeation through freshly excised porcine buccal tissue when applied as gelatin/insulin fibres or as a solution.[205]

In vitro models of the oral epithelium are interesting alternative for studying drug transport, as the barrier properties of a metabolically active epithelium can be studied in isolation from the lamina propria. Unfortunately, oral keratinocytes require an insulin-containing medium to form epithelia *in vitro*,[108] which means that human insulin cannot easily be used as a model permeant. Although it may be possible by using non-human insulin in the media and an ELISA without species cross reactivity for detection. For this reason, biotinylated F(ab) were used as a model biologic to investigate transmucosal delivery via patches *in vitro.* A protocol for the generation of tissue-engineered oral epithelium equivalents (OEE) was developed and barrier properties were verified using TEER (Chapter 4). OEE were also validated by measuring transepithelial permeation of bupivacaine, showing that permeation over time was similar between porcine buccal mucosa and OEE (Appendix 4, Appendix 5).

F(ab) permeated the OEE moderately, producing cumulative transepithelial permeation equivalent to approximately 5 and 8% of the total dose after 9 h for F(ab) applied by patch or by solution respectively (Chapter 4). This result is encouraging and suggests that patches could be used to efficiently deliver hydrophilic biologics through the oral epithelium, as the patch delivered a comparable dose to the applied solution. In practise, an exposure time of several hours is not possible for oral rinses but may be possible for mucoadhesive patches. F(ab) are relatively large proteins that are not expected to have high permeability in the oral mucosa.

Nevertheless, this moderate permeation suggests that patches may be suitable for delivering antibody-based therapies locally through either intact or impaired epithelia.

The low density of the formulation means that it would be difficult to deliver a high enough dose of antibody to be useful for systemic delivery. However, the patches may be promising for the systemic delivery of low molecular weight peptides with lower minimum effective doses, some of which have already been shown in humans or animals to be able to permeate the oral mucosa to induce a systemic effect (Chapter 1). The methods described in this thesis could be used to further develop the formulation for the systemic delivery of peptides and other drugs without relying on animal studies in the first instance.

It may be useful to improve the efficiency of drug transport through the oral mucosa by using permeation enhancers. Surfactants are considered the main option for hydrophilic drugs, including peptides and proteins (Chapter 1). However, tolerability is an important consideration, and it is difficult to assess irritancy potential using animal tissue. A useful feature of OEEs is the ability to assess irritancy potential and drug transport in the same model system. A preliminary investigation into the effect of a sodium deoxycholate as a bile salt permeation enhancer was performed (Appendix 5). MTT viability assay showed that the maximum tolerable dose was 0.4 mg/mL. The effect on permeability was assessed by applying solutions of model drugs with or without 0.4 mg/mL sodium deoxycholate and measuring transepithelial permeation over time or intratissue distribution.

Permeation of bupivacaine was unaffected by deoxycholate. Surprisingly, the permeation of F(ab) was significantly slower in the presence of deoxycholate. 3 kDa Fluorescent-labelled dextran was used as a model compound because it is a hydrophilic molecule with similar hydrodynamic radius to a large peptide. Fluorescent imaging showed that accumulation of dextran within the epithelium was increased in the presence of deoxycholate. At this

concentration, the epithelium appeared undamaged by the bile salt. Both the lysine-functionalised dextran and antibodies are cationic at neutral pH.[206] The anionic bile salt possibly causes increased accumulation within the epithelium through an ion-pairing effect.

These preliminary results show that sodium deoxycholate alone is not effective at enhancing the transepithelial permeation of hydrophilic molecules at non-irritant concentrations. Bashyal *et al.* also observed that sodium glycodeoxycholate, a similar bile salt, did not increase the transmucosal permeation of insulin through porcine tissue at a concentration of approximately 0.8 mg/mL, when applied as a solution of ion-paired complexes.[207] Although, it did increase accumulation within the epithelium. At approximately 4 mg/mL, insulin transmucosal permeation was significantly increased; however, tolerability was not confirmed at this concentration and permeation is likely facilitated by the lysis of epithelial cells. Although a suitable permeation enhancer was not identified during this project, chemically-enhanced oromucosal delivery of biologics has been achieved previously using mixtures of well-tolerated surfactants,[156] and the methods developed in this thesis could be useful for screening potential permeation enhancers and investigating their usefulness in a patch formulation.

Besides surfactants, several other classes of chemical permeation enhancers may be considered.[87] It has been stated in many articles that mucoadhesive polymers, in particular chitosan, can act as permeation enhancers in the oral mucosa by disrupting cell junctions.[11,204] It has been shown that chitosan can transiently open tight junctions in the intestinal epithelium by binding to junctional adhesion molecules.[208] However, to my knowledge, there is no evidence that chitosan can affect tight junctions in the oral mucosa and only weak evidence that it can act as a permeation enhancer at non-cytotoxic concentrations.[209] Misunderstandings may arise as researchers conflate chitosan's well-documented mucoadhesive properties,[89] that improve site retention, with a permeation enhancing effect.

Other options for increasing drug uptake include nanoparticle or vesicle drug delivery vectors.[96] In addition to potentially enhancing permeability, vectors may allow targeted delivery, for example for selective delivery to malignant cells within the epithelium.[210,211] Nanoparticles have been investigated extensively for encapsulation by electrospinning.[95] Electrospinning to encapsulate vesicles is more challenging but has been achieved previously.[212] In general, vesicles are often unstable in amphiphilic solvents; therefore, alternative formulations may be beneficial to allow versatile incorporation of vesicular vectors by electrospinning. However, some liposome formulations are stable in relatively high ethanol concentrations of up to at least 30% v/v ethanol,[213] which may allow electrospinning using a polymer/solvent system similar to that described in this thesis. Additionally, physical disruption of the epithelium using microneedles has been used to great effect for transdermal drug delivery and could also be considered for enhancing oromucosal delivery.[214,215]

Chapter 6: Conclusions and future work

6.1 Conclusions

The introduction identifies a variety of novel treatments in oral medicine that may be possible by using mucoadhesive fibre technologies to deliver therapeutic agents that are challenging to administer effectively using existing dosage forms. Of these, polypeptides, including antibody-based drugs, were identified as a particularly interesting class of therapeutics, and selected for further investigation. Lysozyme was used as model compound to develop a mucoadhesive patch formulation for release of functional proteins. This also illustrated a potential application of the formulation for the delivery of antimicrobial proteins to target oral bacteria. The versatility of the formulation was further demonstrated by confirming that bradykinin, a peptide hormone, could also be released from the formulation at a suitable rate and perform a biological function in oral cells. In contrast, Insulin was released slowly due to the intrinsically lower solubility of the protein. Finally, the patch formulation was found to be effective for the delivery of F(ab) antibody fragments with antigen-binding and TNFα-neutralising functionality.

The potential of the patches to treat inflammatory oral conditions was investigated by using a tissue-engineered model of an inflamed oral ulcer. The applied patches reduced detectable levels of TNFα and T-cell chemokines that are implicated in the pathogenesis of ulcerative oral diseases. This is the first experimental evidence that topical delivery of an anti-TNFα agent may be effective at treating inflammatory mucosal conditions and confirms the hypothesis that electrospun mucoadhesive patches can deliver biologically active polypeptides to provide a potentially therapeutic effect in the oral mucosa. Additionally, a tissue-engineered model of the oral epithelium was used to measure and compare transepithelial delivery of F(ab) applied as a solution or patch. The patches delivered a comparable dose to the solution, providing

preliminary evidence that that the formulation may be efficient for delivering highly permeating peptides systemically via the oral mucosa.

6.2 Future work

- The polymers in the electrospinning solution were observed to protect proteins from ethanol-induced denaturation to allow electrospinning without loss of function. Although existing literature provides possible explanations for this phenomenon, some additional investigation would be beneficial. For example, the effects of different polymers (PVP, RS100, or a weakly hydrogen binding polymer, such as PEO) could be studied in isolation and at different concentrations to identify any dependence on polymer chemistry or functional groups. For industrial scale manufacture, extended mixing and electrospinning times may be required. Therefore, it would be beneficial to measure protein activity following longer processing times. Alternatively *in situ* mixing during electrospinning could be considered to increase output.
- Chapter 2 suggested a potential application of the patches for the delivery of antimicrobial polypeptides for targeted inhibition of pathogenic strains or to treat resistant infections. Further microbiological research could be performed to identify the most promising antimicrobial agents and to investigate the patch technology using a biofilm or infected tissue model.[149]
- Further preclinical research would be beneficial to investigate the therapeutic potential of the patches for delivering anti-TNFα agents. Clinically approved monoclonal biologics would be preferred to allow direct translation to human use. Experiments involving T cells could be used to directly measure the effect of the treatment on recruitment and T-cell-mediated apoptosis of the epithelium. The shelf life and storage

could be investigated. The ability of deliver antibody-based therapies topically could also be investigated as a treatment for other mucosal or dermal conditions.

- Non-medicated patches may be useful for treating ulcers by acting as wound dressings. However, it is difficult to design a useful clinical trial for wound dressings as blinding is impossible. A possible anti-inflammatory effect of the patch polymers could be investigated using inflamed tissue-engineered ulcer models and a combination of transcriptome, secretome, and viability readouts.
- Alternative polymer systems could be investigated to improve adhesion or to enable sustained release. For example, more hydrophobic ethanol-soluble polymers may have a lower degree of swelling, resulting in restricted protein diffusion and promoting a sustained release profile.
- This formulation could be further adapted for the delivery of other complex biomolecules. For example, RNA-based therapies, viral vector vaccines, and liposomes. These classes of therapeutics tend to be unstable in ethanol. However, the polymers may have a stabilising effect, or lower ethanol concentrations could be used. Alternatively, simultaneous electrospinning could be used to encapsulate molecules that require aqueous processing within a mesh of water-soluble and water-insoluble fibres.[92]
- The formulation could be investigated in greater detail for the needleless systemic delivery of peptides. For example, to treat osteoporosis or manage diabetes. The tissue-engineered oral epithelium model used in this thesis provides a useful model barrier for studying the transport of bioactive substances through the epithelium. If necessary, chemical permeation enhancers could be screened with higher throughput than is possible using *ex vivo* tissue or animal studies while also allowing irritancy to be assessed.

Appendix 1: Supplementary information for Chapter 2

Incorporation of Lysozyme into a Mucoadhesive Electrospun Patch for Rapid Protein Delivery to the Oral Mucosa

Jake G. Edmans[1, 2], Craig Murdoch[1], Martin E. Santocildes-Romero[3], Paul V. Hatton[1], Helen E. Colley[1] and Sebastian G. Spain[2*]

[1] School of Clinical Dentistry, 19 Claremont Crescent, University of Sheffield, Sheffield, S10 2TA, UK

[2] Department of Chemistry, Brook Hill, University of Sheffield, Sheffield, S3 7HF, UK

[3] AFYX Therapeutics, Lergravsej 57, 2. tv, 2300 Copenhagen, Denmark

Corresponding author:

Dr Helen Colley, School of Clinical Dentistry, University of Sheffield, 19 Claremont Crescent, Sheffield, S10 2TA. Tel: ++44 1142 159352. E-mail: h.colley@sheffield.ac.uk

Supplementary information

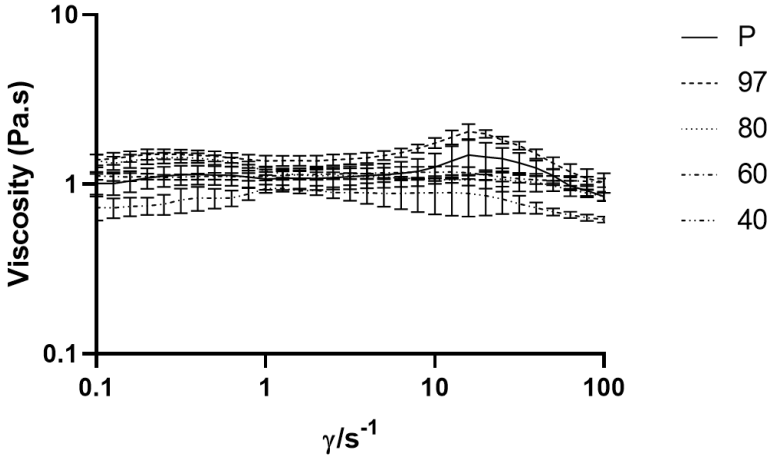

Supplementary Figure 1. Viscosity as a function of shear rate of electrospinning solutions containing lysozyme with different ethanol and water mixtures as solvents (shown as v/v%) and placebo solutions without lysozyme in 97 v/v% ethanol. Data are presented as mean ± SD, with 3 independent repeats.

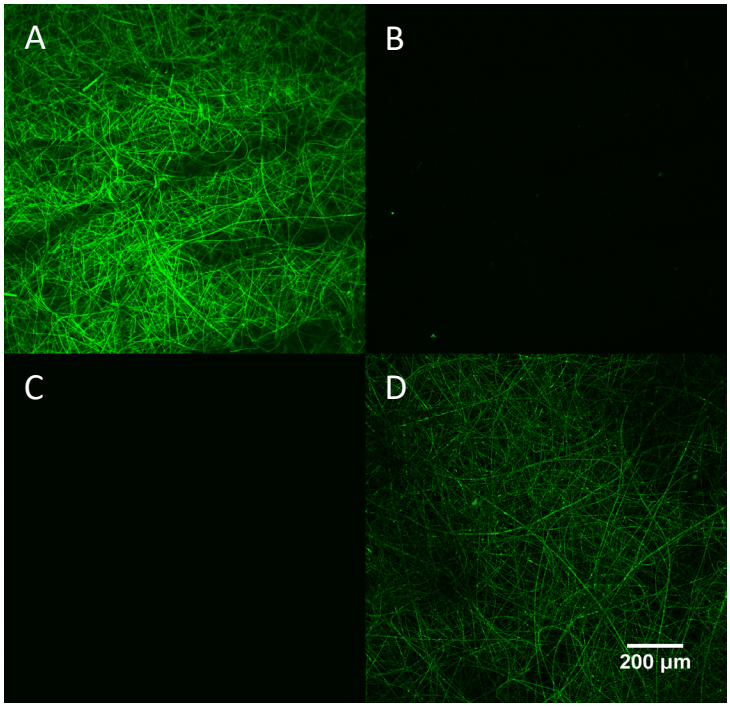

Supplementary Figure 2. Dual-channel confocal micrographs of electrospun fibres containing either FITC-PVP complex and unlabelled lysozyme (A-B) or unlabelled PVP and Texas red labelled lysozyme (C-D). Images were taken using identical capture settings and combined into a single image before processing using an automatic brightness/contrast adjustment, showing no crosstalk between the FITC (A, C) and Texas red (B, D) channels and very little auto-fluorescence.

Appendix 2: Additional characterisation of lysozyme-containing membranes

A2.1 Additional methods

Tensile testing

Dual layer sheets were cut into test specimens (7 cm × 1 cm) by scalpel and fitted within a Lloyd LRX mechanical tester with a 2.5 kN load cell (Lloyd Instruments, Bognor Regis, UK), such that the gauge length is 5 cm. Pull-to-break tests were performed at 10 mm/min.

In vitro membrane adhesion measurement using rheometer

Membrane adhesive properties were compared at 37 °C using an MCR 301 rheometer (Anton Paar, Graz, Austria) fitted with a glass lower plate and a 12 mm parallel plate attachment. 20 µL PBS was applied to the glass surface before placing 1 cm diameter membrane samples, followed by an additional 20 µL PBS on the top of the membrane. The probe was lowered to approximately 0.08 mm and a normal force of 5 N applied for 10 s to induce adhesion. The probe was raised at 1 mm/s while recording normal force. Data were processed using Graphpad Prism 8.0 software by plotting normal force against probe height and using area under curve analysis. The maximum normal force represents force of adhesion and the area under curve represents the work of adhesion. Testing was performed in triplicate using independently prepared membranes.

Differential scanning calorimetry

Measurements were performed using a Perkin Elmer Pyris 1 calorimeter (PerkinElmer). Polymer samples (2-5 mg) were sealed in aluminium pans and equilibrated at -50 °C before heating to 250 °C at 10 °C/min.

Preparation of membranes with high lysozyme content

Polymer solutions for adhesive membranes were prepared in 97% v/v ethanol as previously described (Chapter 2). To achieve high loading, the required mass of lysozyme powder was added directly to the polymer solution and stirred until homogeneous in appearance. Fabrication was performed once per composition and encapsulation efficiency and enzyme activity were measured in triplicate for each membrane as previously described (Chapter 2) with additional dilution of the eluted lysozyme as required.

A2.2 Additional results

Tensile testing of mucoadhesive patches

Tensile testing was performed to assess the effect of lysozyme incorporation on patch mechanical properties. Although all mucoadhesive membranes seemed resistant to bending and torsion during handling, the mucoadhesive layer of the patches is brittle under tension and fractures at a strain of less than 0.1 (Figure A2.1 A). The PCL film backing layer is ductile. The inclusion of 1% w/w lysozyme in the adhesive layer did not significantly affect ultimate tensile strength (Figure A2.1 B, $p = 0.35$).

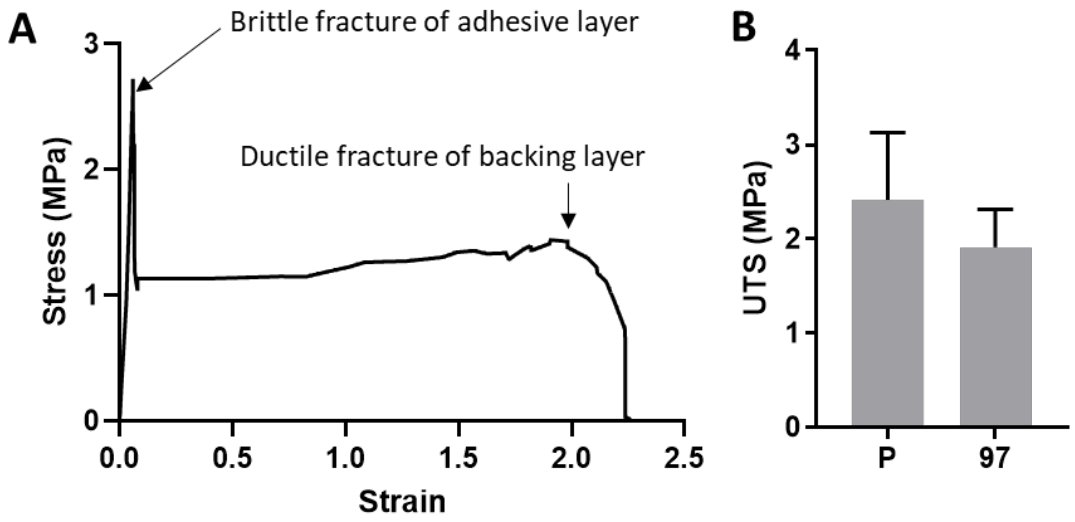

Figure A2.1. Pull-to-break tensile testing of mucoadhesive dual-layer patches. (**A**) Representative stress-strain graph of a placebo patch specimen. (**B**) Ultimate tensile strength (UTS) of placebo (P) and lysozyme-containing patches prepared using 97% v/v ethanol. UTS data are presented as mean ± SD (n = 3) and tested for significance using an unpaired t test ($p = 0.35$).

In vitro assessment of membrane adhesion strength using rheometer

Normal force rheometer measurements were used to compare the adhesive properties of membranes. Placebo membranes did not differ significantly in force of detachment to those containing 1% w/w lysozyme (Figure A2.2 A, $p = 0.38$). Lysozyme-containing membranes prepared using 40% v/v ethanol had a lower detachment force than placebo membranes ($p < 0.05$). This is likely because the 40% membranes disintegrate when wet, as observed in Chapter 2. Surprisingly, lysozyme-containing membranes had a significantly lower work of adhesion than placebo membranes (Figure A2.2 B). Given the similar maximum detachment force, this suggests that the lysozyme-containing membranes tear or deform to a lesser extent during removal. It is unclear how this would affect residence time *in vivo*.

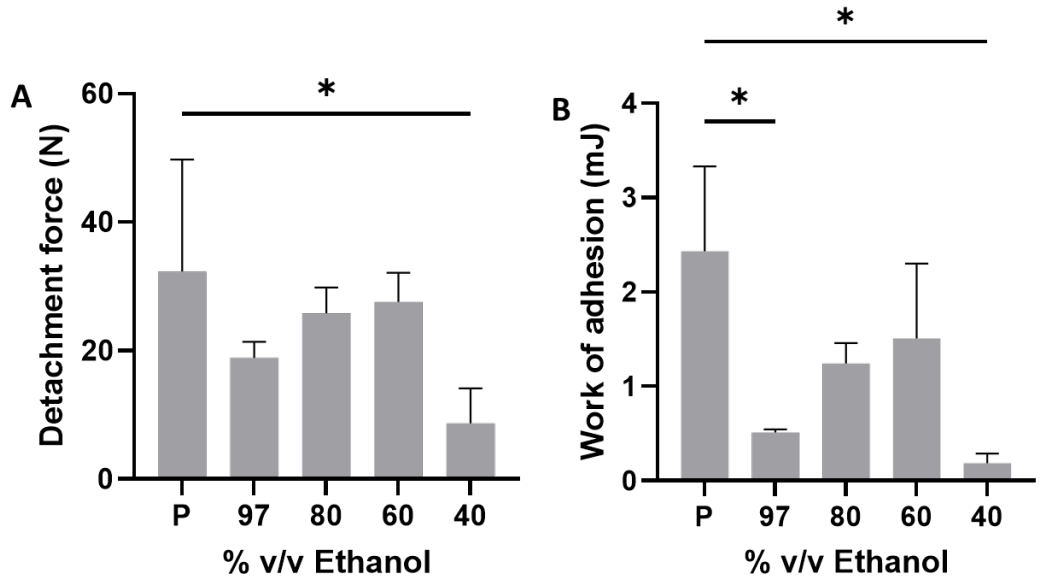

Figure A2.2. *In vitro* assessment of membrane adhesion strength using a rheometer. Moistened placebo (P) or 1% w/w lysozyme-containing membrane samples manufactured using different ethanol concentrations were sandwiched between a glass plate and flat probe before raising the probe while measuring normal force. (**A**) Maximum force of detachment. (**B**) Work of adhesion calculated by area under curve. Data are presented as mean ± SD (n = 3) and analysed using one-way ANOVA with Tukey's *post hoc* tests. *, $p < 0.05$.

PVP has a melting temperature of approximately 120 °C and RS100 undergoes a complex series of phase transitions upon heating, including an endothermic event at approximately 200 °C (Figure A2.3 A-B). In the electrospun placebo membranes, the melting point of PVP is depressed to 100 °C and an endothermic event associated with RS100 occurs at approximately 180 °C (Figure A2.3 C). Including lysozyme further reduces the PVP melting point to 80-90 °C for membranes prepared using 97, 80, 60% v/v ethanol and causes the peak associated with RS100 to broaden and change shape. Surprisingly, the thermogram for membrane prepared with 40% v/v ethanol appears similar to that of the placebo membrane (Figure A2.3 D-G).

Thermal analysis of electrospun membranes

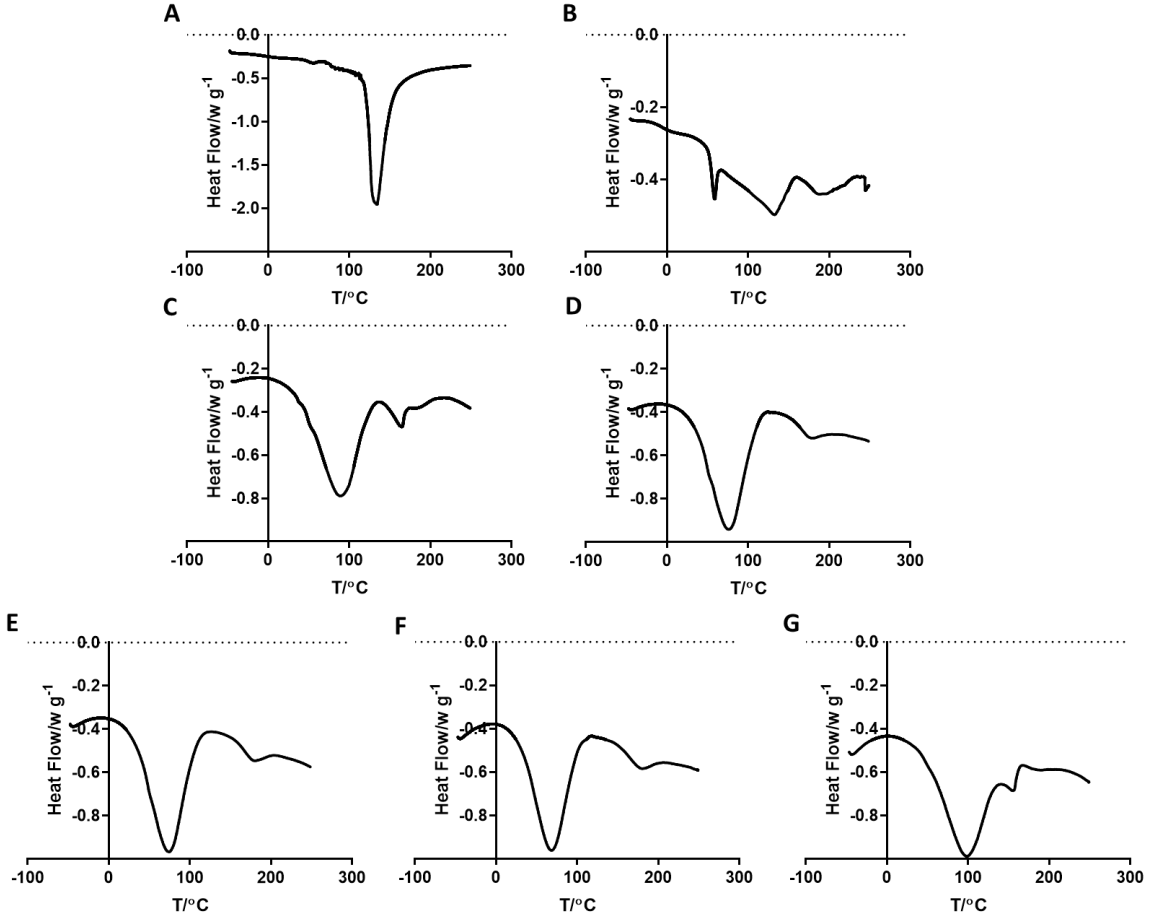

Figure A2.3. Endothermic differential scanning calorimetry traces of (**A**) PVP, (**B**) RS100, (**C**) Placebo membrane prepared using 97% v/v, (**D-G**) 1% w/w lysozyme-containing membranes prepared using 97, 80, 60, 40% v/v ethanol.

Membranes with high lysozyme content

To investigate the effect of high lysozyme loading, it was attempted to blend lysozyme powder directly into polymer solutions before electrospinning, such that loading is no longer limited by solubility of lysozyme in the aqueous component of the solution. Membranes containing 5-50% w/w lysozyme appeared mostly as continuous fibres, although some particles were present, particularly in the 10% w/w membrane, likely caused by incomplete mixing (Figure A2.4 A-E). Surprisingly, high lysozyme loading of up to 50% w/w had only a small effect on fibre morphology. Membranes did not disintegrate when immersed in PBS. Encapsulation

efficiency and enzyme activity ranged from 67-87% and 79-89% respectively, with no significant difference in pairwise comparisons between loading rates (Figure A2.4 F). Although not compared directly, these values are perhaps slightly lower than those observed by for lysozyme blended as an aqueous solution in Chapter 2, possibly due to greater susceptibility of lysozyme added as powder to solvent-induced denaturation.

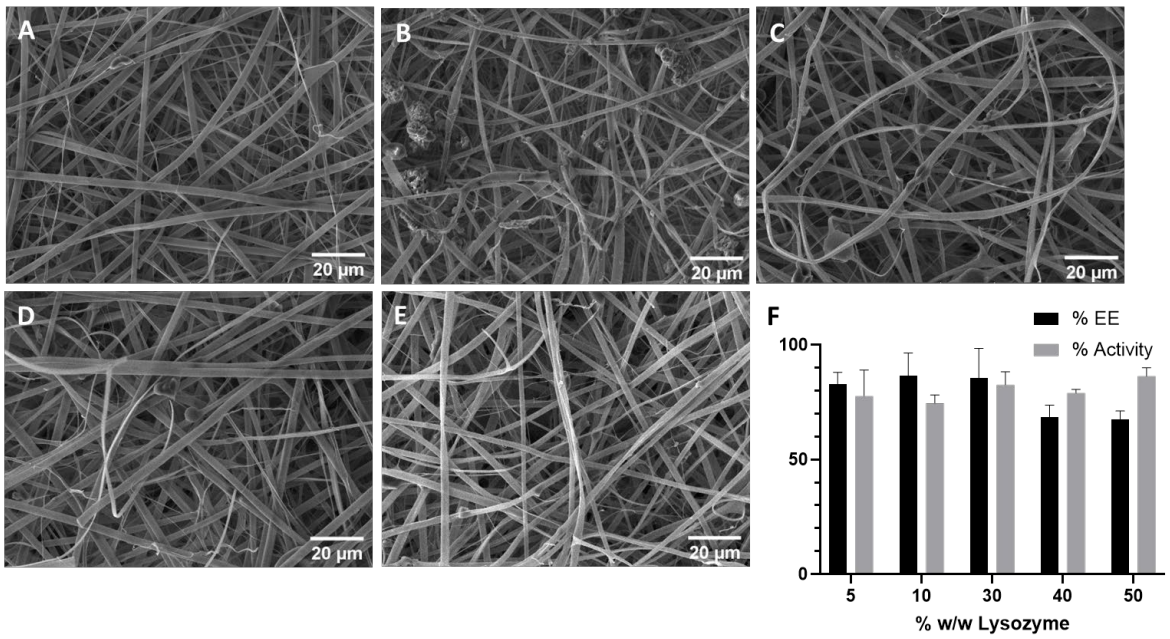

Figure A2.4. Analysis of membranes with high lysozyme content. To achieve high loading, lysozyme powder was added to electrospinning solutions and manually stirred until homogenous before electrospinning. (**A-E**) SEM images of membranes containing 5, 10, 30, 40, 50% w/w lysozyme. (**F**) Lysozyme encapsulation efficiency (EE) and enzymatic activity of released lysozyme. Data are presented as mean ± SD (n = 3) and analysed using one-way ANOVA (EE: $p < 0.05$, activity: $p = 0.24$) and Tukey's *post hoc* tests (ns).

Appendix 3: Supplementary information for Chapter 4

Electrospun patch delivery of anti-TNF*α* F(ab) for the treatment of inflammatory oral mucosal disease

Jake G. Edmans[1, 2], Bethany Ollington[1], Helen E. Colley[1*], Martin E. Santocildes-Romero[3], Lars Siim Madsen[3], Paul V. Hatton[1], Sebastian G. Spain[2] and Craig Murdoch[1].

[1] School of Clinical Dentistry, 19 Claremont Crescent, University of Sheffield, Sheffield, S10 2TA, UK

[2] Department of Chemistry, Brook Hill, University of Sheffield, Sheffield, S3 7HF, UK

[3] AFYX Therapeutics, Lergravsej 57, 2. tv, 2300 Copenhagen, Denmark

*Correspondence: Helen Colley, School of Clinical Dentistry, 19 Claremont Crescent, University of Sheffield, Sheffield, S10 2TA, UK. Email: h.colley@sheffield.ac.uk; Tel: +44 114 215 9352

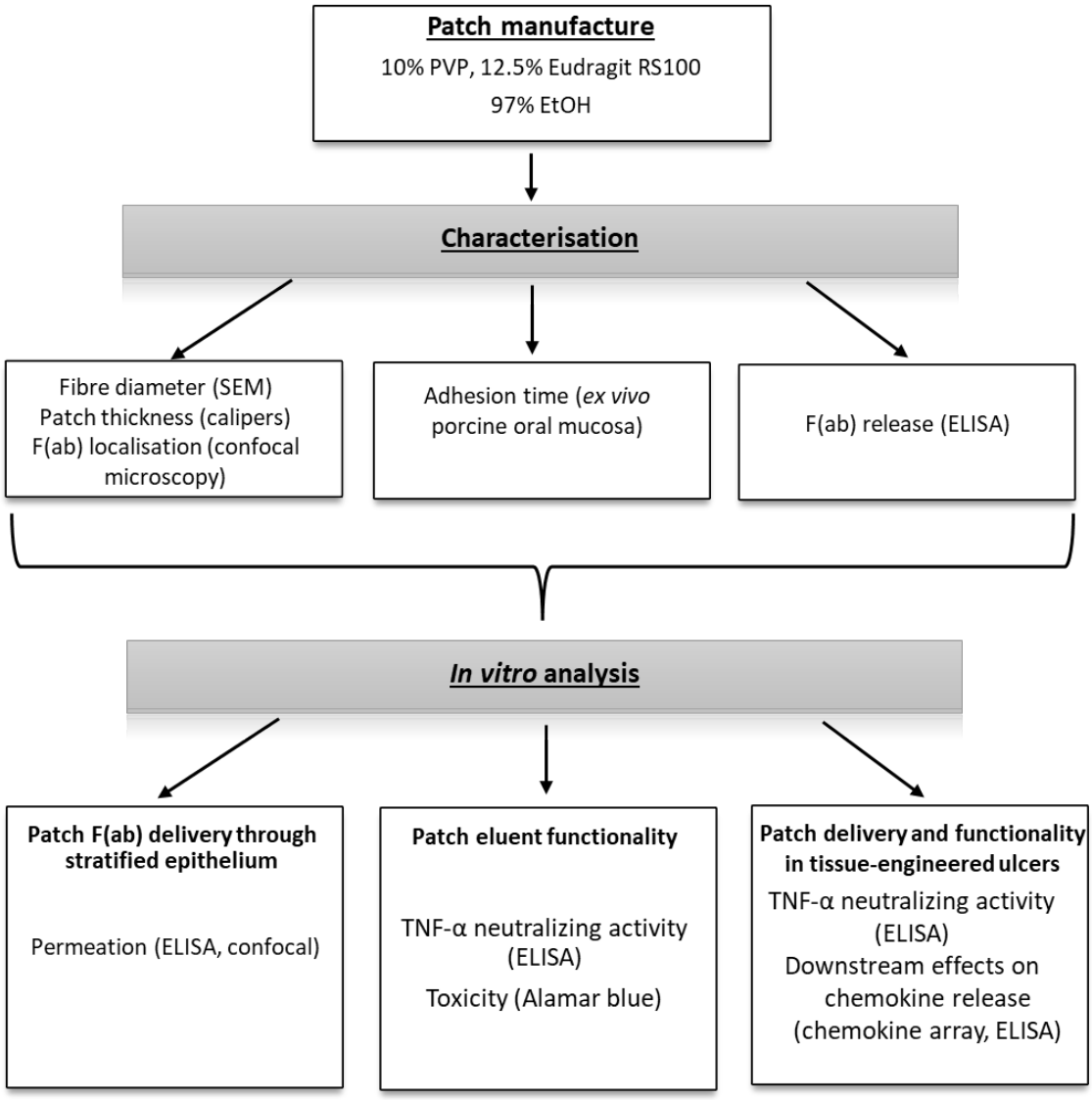

Supplementary figure 1. Flow diagram summarising patch manufacture, characterisation and investigation using *in vitro* cell models.

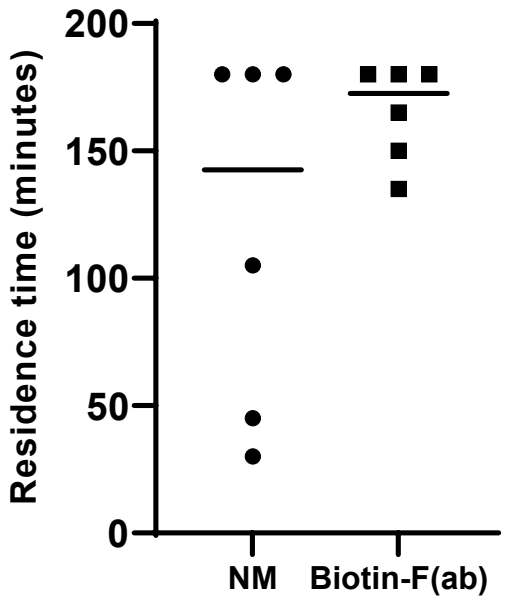

Supplementary figure 2. Residence time of mucoadhesive patches applied topically to *ex vivo* porcine buccal mucosa. Patch samples were applied to excised oral mucosa in a petri dish, immersed in PBS, shaken at 37 °C for 3 h and inspected every 15 minutes for detachment. Data are presented as median values with individual datapoints shown as closed circles (n = 6). Statistical analysis was performed using a Mann-Whitney U pairwise comparison test (p = 0.16).

Appendix 4. Insulin permeation in *ex vivo* porcine mucosa

A4.1 Additional methods

Preparation of FITC-insulin

Insulin was labelled with fluorescein isothiocyanate isomer I (FITC) using a modified version of a previously described method.[216] Insulin (50 mg) was dissolved in a few drops HCl (0.1 M) and 0.2 M ethylenediaminetetraacetic acid in phosphate buffer (0.1 M, 4 mL) added followed by NaOH (1 M) added dropwise until the white precipitate became clear. The total volume was made up to 5 mL in buffer. FITC in acetone (5 mg/mL, 2 mL) was added dropwise with stirring and the reaction mixture incubated for 1 h in the dark at room temperature. FITC-insulin was separated by size exclusion chromatography with Sephadex G-25 and eluted in PBS. The solution was concentrated by partial freeze drying. Protein concentration (6.3 mg/mL) and degree of labelling (2.0) were calculated using the following equations, where A is absorbance at a given wavelength, CF is a correction factor, ε is the molar extinction coefficient at 280 nm of insulin, ε′ is the molar extinction coefficient at 494 nm of fluorescein. The following values were used ε = 5734 M^{-1} cm^{-1}, CF = 0.3, ε′ = 68000 M^{-1} cm^{-1}.

$$[protein] = \frac{A_{280} - (A_{494} \times CF)}{\varepsilon} \qquad DOL = \frac{A_{494}}{\varepsilon' \times [protein]}$$

Excision and preservation of porcine oral mucosa

Fresh pig heads were obtained from a local abattoir and processed within 6 h. Intact tongues and cheeks were excised and the ventral tongue (sublingual) and buccal mucosa separated from the remaining muscle or connective tissue using a skin graft knife at a targeted thickness of 0.5

mm. Samples were preserved as previously described by immersing in 0.002% sodium azide for 20 minutes before flash freezing in liquid nitrogen.[199]

Franz cell permeation assay

Porcine mucosa was defrosted at 37 °C, cut into the required size using a scalpel, and thickness measured in triplicate using a micrometer. The tissue was fitted into Franz cells with circulating water jackets (Permegear, Hellertown, USA; flat ground joint, 5 mL receptor volume, 9 mm ø aperture). The receptor chamber was filled with simulated plasma (1% w/v BSA in PBS) and the Franz cells pre-incubated at 37 °C for at least 30 minutes to allow the receptor solution to degas and the bubbles removed by inverting. Donor solutions containing the permeant in pH 6.8 PBS were applied to the donor chamber (1 mg/mL bupivacaine, 200 µL; 10 mg/mL 20 kDa FITC-dextran, 400 µL; 1 mg/mL insulin, 400 µL; 1 mg/mL FITC-insulin, 400 µL) and the donor chamber and sampling arm covered with parafilm to prevent evaporation. 200 µL samples were taken from the receptor chambers using a glass Hamilton syringe and the equivalent volume of media replaced. Samples were stored in glass vials at 4 °C for up to 24 h before analysis. Treatment with SDS may be used to impair the epithelial barrier. As required, SDS (5% w/v, 0.5 mL) was added to the apical chamber for 18 h at 37 °C before removing and washing with PBS before adding the permeant. Permeant concentrations were measured using the relevant assay and cumulative release calculated. Apparent permeability coefficients were calculated, and significance testing performed using linear regression analysis with Graphpad Prism 8.0 software. Values are presented with 95% confidence intervals.

Transepithelial electrical resistance of *ex vivo* mucosa

Donor chambers were filled with simulated saliva (pH 6.8 PBS) and equilibrated at 37 °C with stirring for 30 minutes before measuring initial TEER values as previously decribed.[199] An LCR measurement device (Conrad Electronic SE, Hirschau, Germany) was connected to 20-

gauge blunt metallic needles (Fisnar Europe, Glasgow, UK) which were placed in the sample arm and donor chamber. Resistance was measured in series mode at 120 Hz and recorded as the average of 3 measurements.

Quantification of bupivacaine in receptor media

Reverse phase high performance liquid chromatography (RP-HPLC) with UV detection was performed to measure the concentration of bupivacaine in the receptor medium using a XBridge BEH-C18 column (4.6 mm × 250 mm; 130 Å pore size; Waters, Wilmslow, U.K.) and a mobile phase composed of acetonitrile/water (1:1, v/v), with a flow rate of 1 mL/min, wavelength 262 nm, 20 µL injection volume. Concentrations were interpolated using a standard curve ($R^2 = 0.996$) of bupivacaine (39 - 1250 µM) in PBS.

Quantification of 20 kDa FITC-dextran in receptor media

100 µL samples were loaded in a black 96-well plate and fluorescence measured at 495 nm excitation, 520 nm emission using a microplate reader with automatic gain optimisation (Tecan, Männedorf, Switzerland). Concentrations were interpolated from a standard curve prepared in PBS and measured simultaneously.

Quantification of insulin in receptor media

Insulin samples were stored for up to 24 h in glass vials at 4 °C before measuring concentrations using an ELISA kit as per the manufacturer's instructions (Biotechne, Abingdon, UK).

Intratissue distribution of insulin

Insulin or FITC-insulin were applied to porcine sublingual tissue in Franz cells as previously described. After 0.5 h or 4 h the samples were removed, washed with PBS, and fixed in neutral buffered formalin (10% v/v) for 24 h. Samples were perfused with 30% sucrose for a further 24 h before embedding in OCT compound (CellPath, Newtown, UK). Frozen sections (20 µm)

were collected at -14 °C using a Cryostar NX50 cryostat (ThermoFisher, Loughborough, UK). Samples containing FITC-insulin were mounted immediately in antifade mounting medium with 4′,6-diamidino-2-phenylindole (DAPI; Vector Laboratories, Upper Heyford, UK). Samples containing unmodified insulin were stained by immunofluorescence without antigen retrieval. Sections were permeabilised with 0.1% w/v triton X-100 in PBS, washed 3 times with PBS, and blocked with normal goat serum for 1 h. Samples were stained using mouse anti-insulin [D3E7] (20 µg/mL) in 10% v/v normal goat serum overnight at 4 °C followed by FITC-goat anti-mouse F(ab) for 1h. Samples were counterstained with DAPI (1 µg/mL) for 10 minutes and mounted in antifade mounting medium (Vector Laboratories, Upper Heyford, UK). Insulin distribution was visualised using a Nikon A1 laser scanning confocal microscope in dual channel mode with 403.55 nm and 488 nm sapphire lasers. Tissue containing unstained insulin was used as a negative control to adjust sensitivity.

A4.2 Additional results

Preparation and histology of *ex vivo* porcine oral mucosa

Oral mucosa was excised from recently slaughtered pig heads and the upper 0.5-1 mm of the mucosa isolated using a skin graft knife (Figure A4.1 A). Porcine oral mucosa is frequently used as a model barrier due to its similarity to humans. Indeed, haematoxylin and eosin-stained samples had a similar histological appearance to human oral mucosa. Buccal and labial mucosa are non-keratinised and have an epithelium approximately 300 µm thick (Figure A4.1 B-C). The ventral tongue and floor of the mouth are considered part of the sublingual mucosa have thinner epithelia than the buccal mucosa at approximately 100-200 µm (Figure A4.1 D-E). The hard palate and gingival mucosa have slightly thicker epithelia than the buccal mucosa and have a keratinised superficial layer (Figure A4.1 F-G). Although the labial mucosa is continuous with the buccal mucosa, and the ventral tongue with the floor of the mouth

(collectively referred to as the sublingual mucosa), the buccal mucosa and ventral tongue were used exclusively for *ex vivo* experiments for consistency and due to their higher yield of excision per animal. Buccal and sublingual mucosa were treated with sodium azide as a preservative and flash frozen with liquid nitrogen using an existing method described by Berka *et al.*[199] The flash frozen sections appeared to have undamaged epithelia, suggesting successful non-destructive preservation (Figure A4.1 I-J).

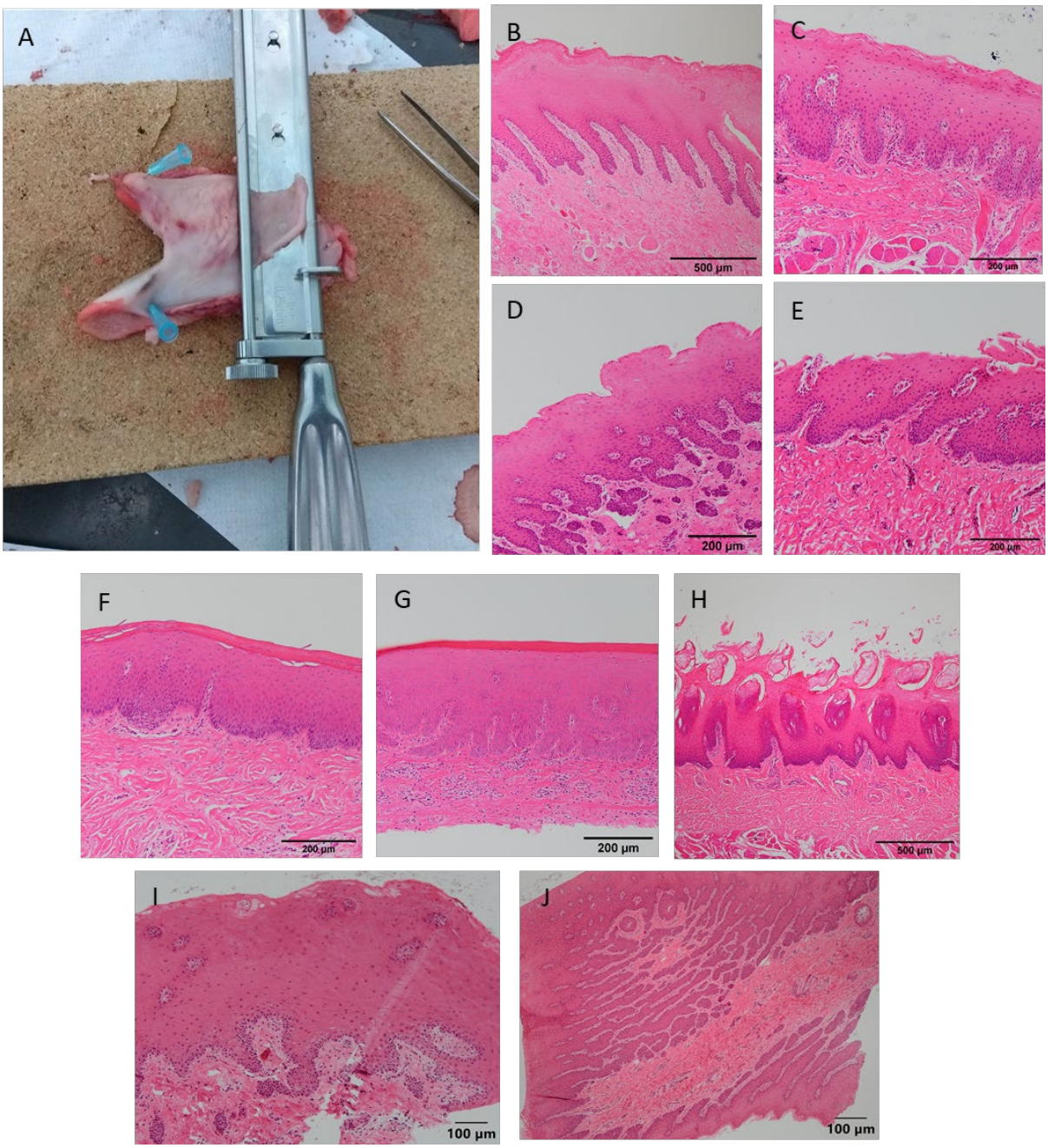

Figure A4.1. Preparation of porcine sublingual and buccal mucosa for *ex vivo* permeation experiments. Porcine oral mucosa with a targeted thickness of 500 µm was isolated using a skin graft knife. (**A**) Isolation of buccal oral mucosa. Hematoxylin and eosin staining of freshly isolated porcine oral mucosa: (**B**) buccal, (**C**) labial, (**D**) floor of mouth, (**E**) ventral tongue, (**F**) hard palate, (**G**) gingival, (**H**) dorsal tongue. Ventral tongue and buccal mucosa were preserved by flash freezing for future use. Flash freezing preserved (**I**) buccal, and (**J**) ventral tongue.

Validation of transmucosal permeation in Franz cells using bupivacaine and 20 kDa FITC-dextran

Defrosted flash-frozen porcine buccal and sublingual mucosa were fitted in Franz cells and the transmucosal permeation of different compounds measured (Figure A4.2 A). The oral mucosal permeability of bupivacaine and 20 kDa FITC-dextran (ThermoFisher, Loughborough, UK) are relatively well characterised and were therefore selected to validate the experimental setup. Bupivacaine (0.2 mL, 1 mg/mL) applied to buccal mucosa exhibited a lag time of 1.04 ± 0.81 h followed by steady state permeation between 2-5 h with an apparent permeability coefficient of 4.08 ± 0.24 $\times 10^{-6}$ cm/s (Figure A4.2 B). After 5 h, sink conditions were lost and the rate of permeation started to decrease. Cumulative permeation of 56.8 ± 6.2% of the total dose was observed after 24 h. 20 kDa FITC-dextran (10 mg/mL, 400 µL) applied to sublingual mucosa permeated slowly with negligible lag time (Figure A4.2 C). Permeation was linear over 5 h with an apparent permeability coefficient of 3.62 ± 0.25 $\times 10^{-9}$ cm/s. Buccal mucosa was significantly less permeable to 20 kDa FITC-dextran, with an apparent permeability coefficient of 5.03 ± 0.97 $\times 10^{-10}$ cm/s (Figure A4.2 D; $p < 0.001$).

We observed a somewhat lower apparent permeability coefficient for bupivacaine through porcine buccal mucosa of approximately 4×10^{-6} cm/s compared to Kulkarni *et al.*, who recorded 1.7×10^{-5} cm/s in unpreserved tissue.[167] This discrepancy may be attributed to differences in tissue preparation and better sink conditions due to the greater donor solution volume used in the previous study. Following this experiment, an increased donor volume of 400 µL was used. Our measurement for sublingual permeability to 20 kDa FITC-dextran was comparable to Berka *et al.*,[199] who recorded an apparent permeability coefficient of approximately 5×10^{-9} cm/s. Buccal tissue was significantly less permeable to 20 kDa FITC-dextran, which is as expected because of the increased thickness of the epithelium. These experiments suggest that the tissue handling was suitable, with minimal loss of tissue integrity

and no leakage between the Franz cell chambers. The permeability coefficients were in the expected range based on previous literature.

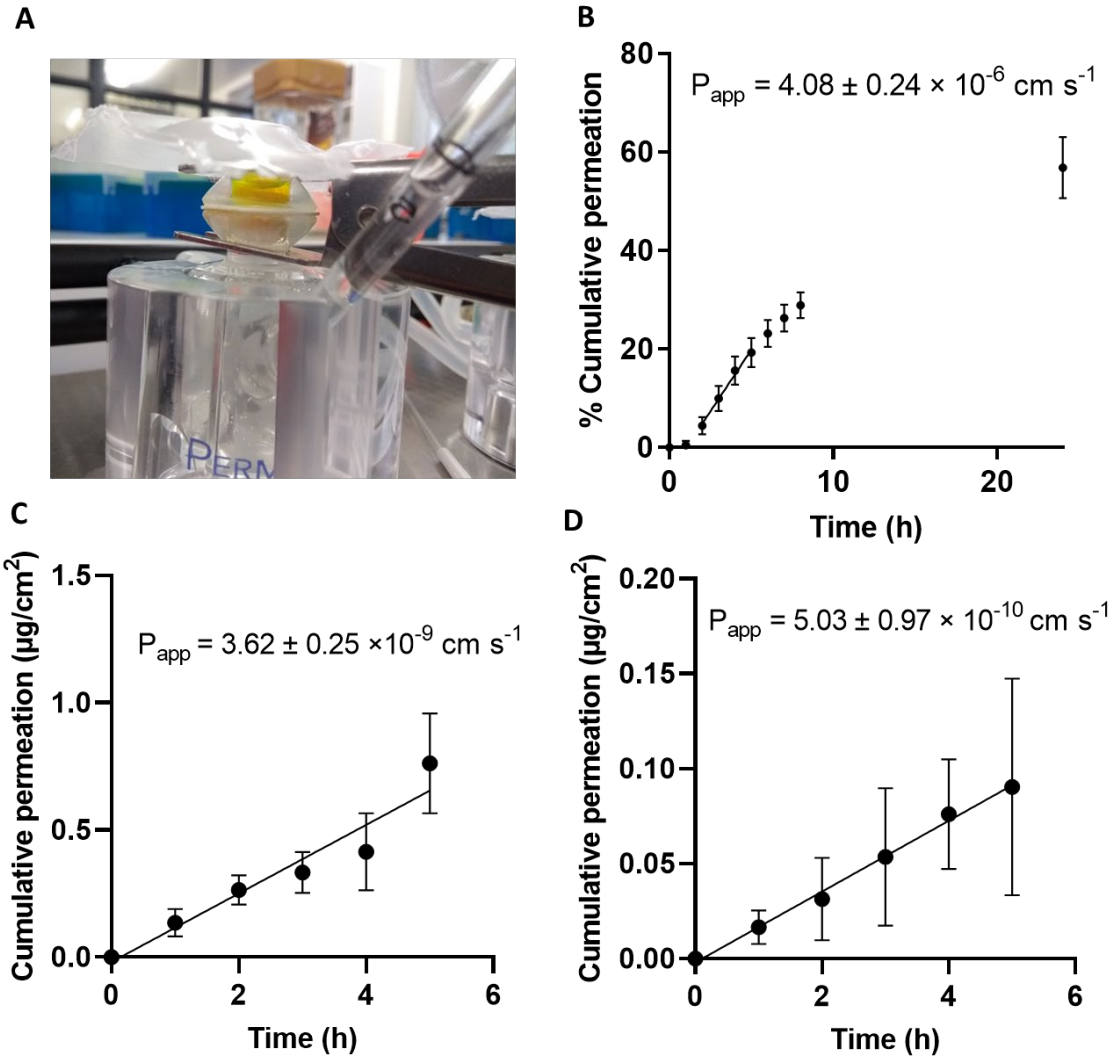

Figure A4.2. Validation of Franz cell permeation assay with flash freezing-preserved *ex vivo* porcine mucosa using bupivacaine and 20 kDa FITC-dextran as model permeants. (**A**) Photograph of Franz cell setup. Concentration of permeant in the basolateral chamber was measured over time and cumulative permeation calculated. By assuming sink conditions, the gradient of the linear portion of the permeation profile can be used to calculate apparent permeability. (**B**) Percentage cumulative permeation of bupivacaine over time through buccal mucosa. Cumulative permeation over time of 20 kDa FITC-dextran through (**C**) sublingual and (**D**) buccal mucosa. Data points presented as mean ± SD (n = 3).

Transmucosal permeation of insulin

Insulin applied as a solution in PBS permeated intact *ex vivo* buccal oral mucosa negligibly when applied as a solution for 8 h, with most samples having insulin concentrations below the ELISA detection limit (Figure A4.3 A). Buccal mucosa fitted in Franz cells were treated with 5% w/v SDS for 18 h to impair the barrier properties of the epithelium. Intact buccal mucosa had a TEER at 120 Hz of 2.38 ± 0.48 kΩ cm^2 and treatment with SDS decreased TEER to 1.49 ± 0.11 kΩ cm^2 (Figure A 4.3 C; $p < 0.01$). Insulin permeated SDS-impaired buccal mucosa very slowly, with less than 0.02% cumulative permeation after 8 h (Figure A4.3 B). Unlike for intact mucosa, insulin was detectable by ELISA at all timepoints. Insulin permeated intact sublingual mucosa slowly, with a long lag time of approximately 5 h (Figure. A4.4). A cumulative concentration corresponding to less than 0.04% of the applied 0.5 mg dose was measured after 8 h.

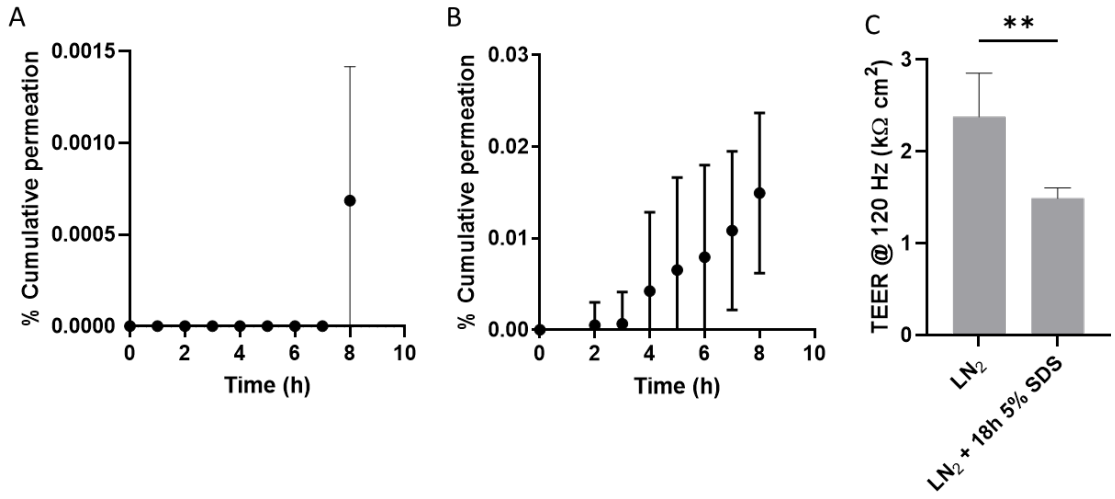

Figure A4.3. Transmucosal permeation of insulin through intact and impaired *ex vivo* porcine buccal mucosa. (**A**) Percentage cumulative permeation of insulin over time through flash frozen buccal mucosa (n = 3). (**B**) Buccal mucosa was pre-treated with 5% SDS for 18 h to impair barrier properties before measuring insulin permeation (n = 3). (**C**) Transepithelial electrical resistance at 120 Hz of intact and SDS impaired flash frozen buccal mucosa (n = 6). Presented as mean ± SD and analysed by unpaired t-test. **, $p < 0.01$.

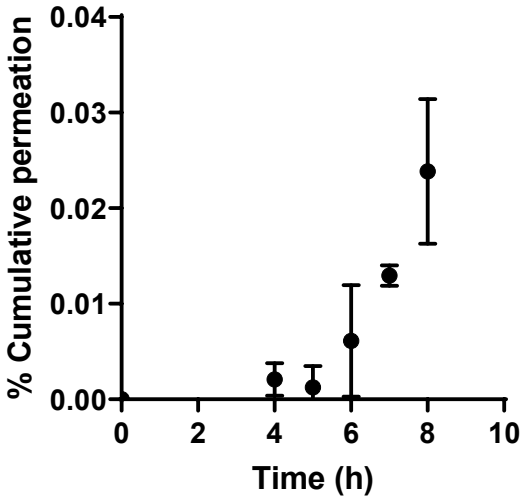

Figure A4.4. Transmucosal permeation of insulin through *ex vivo* porcine sublingual mucosa. Percentage cumulative permeation of insulin over time through flash freezing-preserved buccal mucosa. Presented as mean ± SD (n = 3).

Intratissue distribution of insulin

FITC-insulin was applied to sublingual tissue in Franz cells for 0.5 h or 4 h before fixing in formalin and visualising distribution using confocal microscopy. Cross sections of the tissue showed that FITC-insulin accumulates only within the surface layer of keratinocytes (Figure A4.5 A-B). A greater proportion of superficial keratinocytes were stained after 4 h compared to 0.5. Samples were also mounted without sectioning and the surface of the mucosa imaged using the z-stack function of the microscope. Once again, the FITC-insulin was visible only in a single cell layer. Average intensity projections showed that FITC-insulin accumulates within the cytoplasm and nuclei of the surface layer of keratinocytes (Figure A4.5 C-D). The images appeared similar after 0.5 h and 4 h. To verify if this cell uptake effect also occurs for unmodified insulin, sublingual samples treated with insulin for 4 h were stained for insulin using immunofluorescence techniques (Figure A4.6). Similarly, insulin accumulated exclusively in the superficial layer of keratinocytes. The fluorescence signal in the lamina propria was caused by non-specific staining or naturally occurring insulin and was also present in negative control samples.

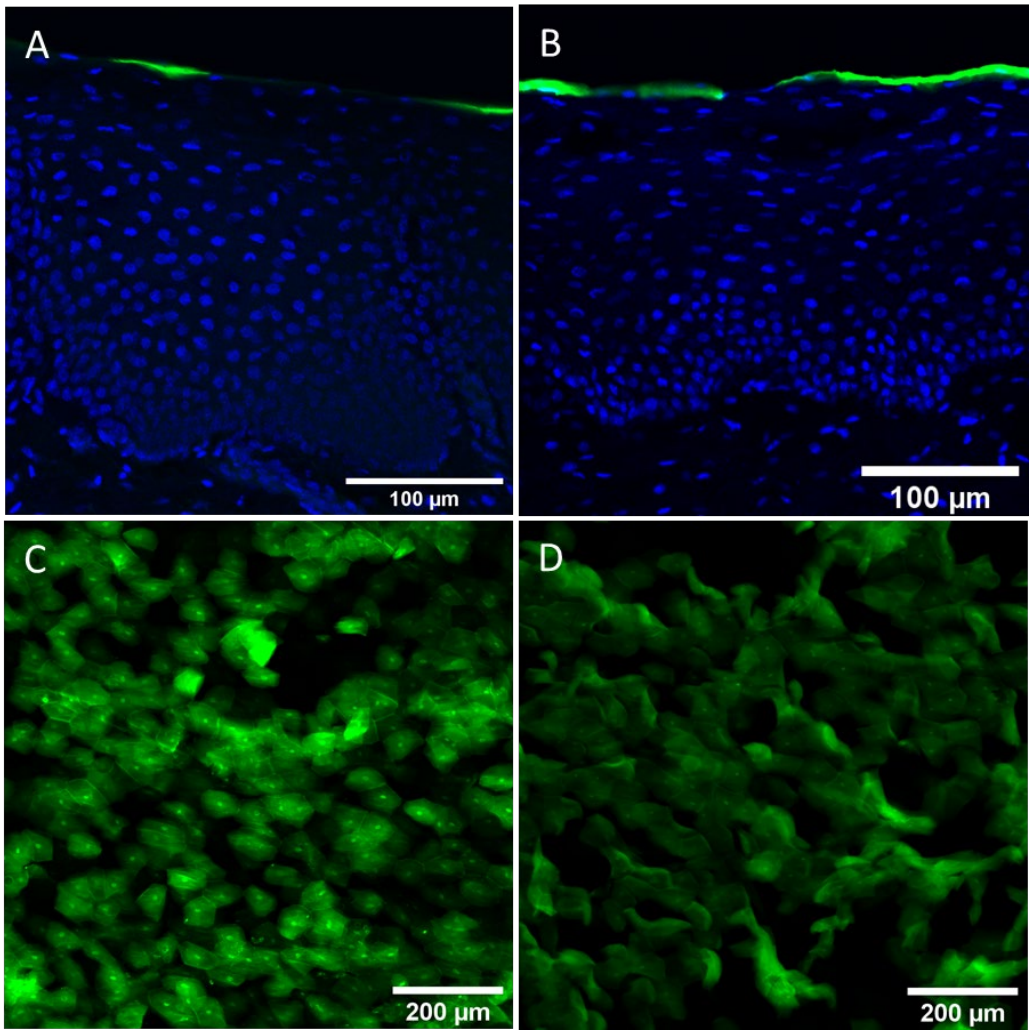

Figure A4.5. Intratissue permeation of FITC-insulin in *ex vivo* porcine sublingual mucosa. Porcine sublingual mucosa was fitted in Franz cells and FITC-insulin solution applied to the apical surface for 0.5 or 4 h before formalin fixing and imaging by confocal microscopy. Representative confocal micrographs of DAPI counterstained (blue) cross-sections showing distribution of FITC-insulin (green) after 0.5 h (A) and 4 h (B) of exposure. Top-down average-intensity projections showing distribution of FITC-insulin near the apical surface of the mucosa after 0.5 h (C) and 4 h (D) exposure to FITC-insulin.

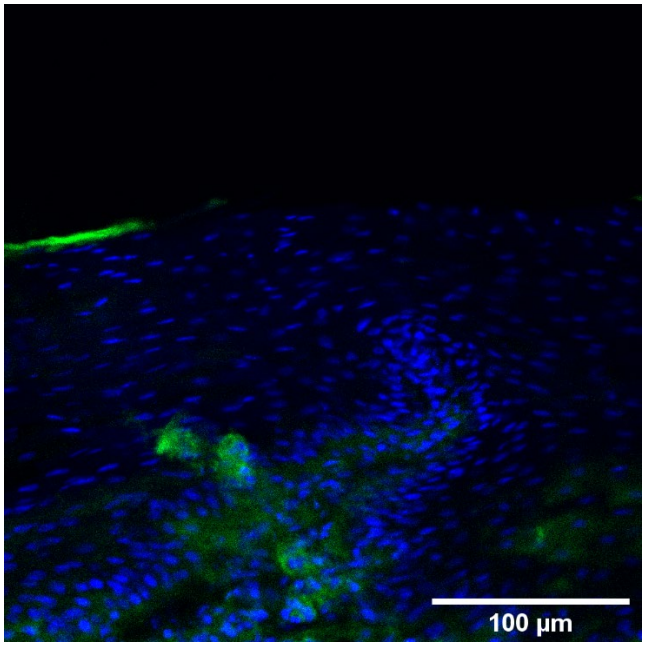

Figure A4.6. Immunofluorescence staining for insulin in *ex vivo* porcine sublingual mucosa. Porcine sublingual mucosa was fitted in Franz cells and insulin solution applied to the apical surface for 4 h before formalin fixing, sectioning, and performing immunofluorescence staining for insulin (green) with DAPI counterstain (blue). Scale bar = 100 µm.

Appendix 5. Investigation of sodium deoxycholate as a permeation enhancer for hydrophilic compounds using oral epithelium equivalents

A5.1 Additional Methods

Sodium deoxycholate toxicity in oral epithelium equivalents

OEE were constructed, and barrier properties validated by TEER as previously described in Chapter 4. OEE are considered suitable if TEER exceeds 250 Ω cm^2. Green's medium (1 mL) was added to the basolateral chamber and the required concentration of sodium deoxycholate in PBS (0.5 mL) added to the apical chamber. PBS was used as vehicle control and 5% SDS as a cytotoxic control. OEE were incubated for 24 h before washing with PBS and culturing for a further 24 h. The OEE were washed with PBS before adding 3-(4,5-dimethylthiazol-2-yl)-2,5-diphenyltetrazolium bromide (MTT) in media (0.5 mg/mL, 0.5 mL) to both the apical and basolateral chambers and incubating for 3 h. The solution was removed and 0.1 M HCl in propan-2-ol added (1 ml) to the apical and basolateral chambers of each model, with gentle agitation for 10 minutes to dissolve the formazan crystals. The solutions from the chambers were combined and absorbance at 570 nm measured using a spectrophotometer (Tecan, Männedorf, Switzerland). Percentage viability was calculated by subtracting the average absorbance of the cytotoxic control and normalising relative to the average value of the vehicle controls. The experiment was performed 3 times with at least 2 technical repeats per experiment. Half-maximal cytotoxic concentration was calculated using Graphpad Prism 8.0 software.

Permeation assays with bupivacaine, F(ab) and 3 kDa Texas Red-dextran

OEE were placed in a 12 well plate containing Green's medium (1mL). Solutions of biotinylated goat anti-mouse F(ab) (1 μg/mL), lysine fixable 3 kDa Texas Red-Dextran (50 μg/mL; ThermoFisher, Loughborough, UK), or bupivacaine (1 mg/mL; Sigma-Aldrich, Poole, UK) with or without sodium deoxycholate (0.4 mg/mL) in PBS (0.5 mL) were added to the apical chambers. Basolateral media samples (0.2 mL) were taken every 2 h and the equivalent volume replaced. F(ab) concentrations were measured by ELISA within 24 h as described in Chapter 4. Bupivacaine concentrations were measured as described in Appendix 2. Cumulative amount permeated was calculated and plotted as a percentage of the applied dose over time. Texas Red-dextran was not detectable in the basolateral media by fluorescence (596/615 nm). OEE containing Texas Red-dextran were cryogenically processed and mounted as described in Appendix 2 before visualising using a Nikon A1 laser scanning confocal microscope in dual channel mode with 403.55 nm and 562 nm sapphire lasers. Untreated OEEs were used as a negative control to adjust sensitivity and images captured and processed identically to allow comparison. The experiment was performed 3 times using different cell passages.

A5.2 Additional results

Cytotoxicity of sodium deoxycholate in oral epithelium equivalents

Most previous studies investigating permeation enhancers for the oral mucosa have involved live animal experiments or the use of animal tissue *ex vivo*.[87] These studies usually provide little insight into tolerability. Furthermore, *ex vivo* tissue may not accurately simulate biological processes that would affect uptake in living tissue. Tissue-engineered models of the oral epithelium may provide a useful high throughput option for simultaneously screening both the efficacy and cytotoxicity of potential permeation enhancers. Surfactants are generally considered to be the most appropriate class of permeation enhancer for proteins and hydrophilic

drugs for their ability to extract lipids from the epithelium.[87] Sodium deoxycholate is a frequently studied bile salt surfactant reported to act as a mucosal permeation enhancer.[217] To determine the maximum well-tolerated concentration, its cytotoxicity was assessed in OEE by MTT metabolic activity assay, similarly to methods recommended by OECD guidelines for assessing skin irritation potential.[102] The half maximal cytotoxic concentration was 0.426 ± 0.04 mg/mL; therefore, a concentration of 0.4 mg/mL was selected for investigating effect on the permeation of hydrophilic compounds (Figure A5.1).

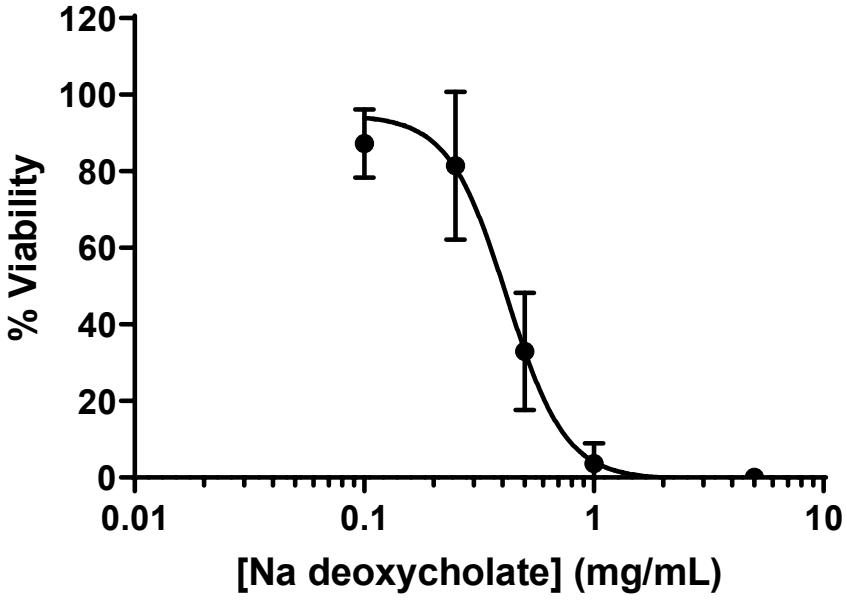

Figure A5.1 Dose-response curve to determine the tolerability the oral epithelium to sodium deoxycholate. Oral epithelium equivalents were treated for 24 h before culturing for a further 24 h and measuring metabolic activity by MTT assay. Data are presented as mean ± SD (n = 3).

Effect on the epithelial permeation of bupivacaine, F(ab), and 3 kDa dextran

Permeants were applied to OEE as solutions with or without 0.4 mg/mL sodium deoxycholate. Bupivacaine, a small molecule analgesic, was used to validate the experimental system. Sink conditions were not produced; therefore, apparent permeability coefficient cannot be accurately determined. However, the permeation profile closely resembles that of bupivacaine applied to

porcine buccal tissue (Appendix 4) and the total amount permeated after 8 h was comparable for both *ex vivo* and *in vitro* methods (Figure A5.2 A). This suggests that the OEE adequately simulates the barrier properties of the oral mucosa. Deoxycholate had a negligible effect on the transepithelial permeation of bupivacaine, perhaps because it favours transcellular uptake through cell membranes, a mechanism which is often less affected by surfactants.[87,88] Surprisingly, deoxycholate considerably reduced the transepithelial permeation of F(ab) antibody fragments (Figure A5.2 B). Texas-red dextran did not undergo transepithelial permeation sufficiently to allow detection in the basolateral chamber. In untreated OEE, dextran was detectable only within the superficial layer of keratinocytes (Figure A5.3 A). Deoxycholate increased dextran uptake, resulting in stronger fluorescence within the superficial layer of keratinocytes and detectable fluorescence within the upper 2-3 cell layers. (Figure A5.3 B).

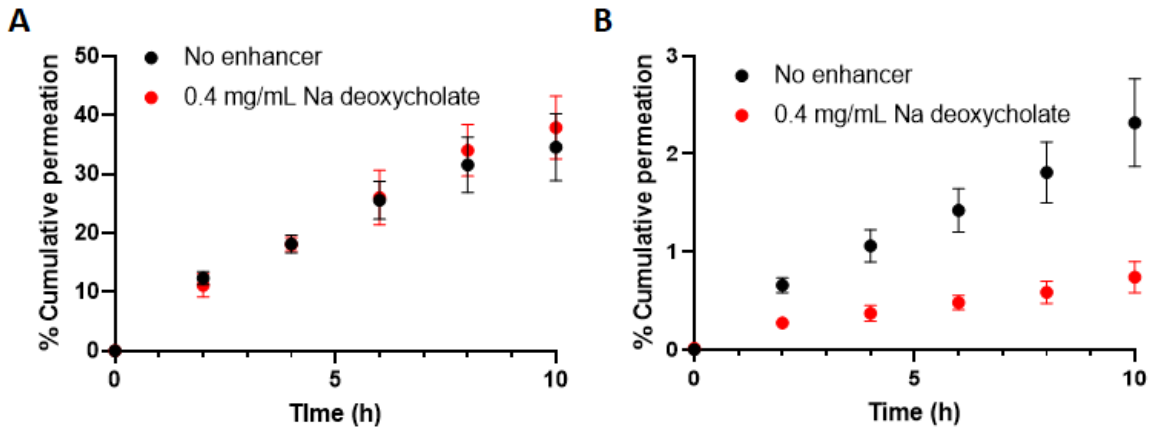

Figure A5.2 Sodium deoxycholate does not enhance the transepithelial permeation of (**A**) bupivacaine or (**B**) F(ab) through the oral epithelium at non-cytotoxic concentrations. Solutions containing the permeants with or without 0.4 mg/mL sodium deoxycholate were applied to the apical surface of oral epithelium equivalents and the concentration in the basolateral chamber monitored over time. Data are presented as mean ± SD (n = 3).

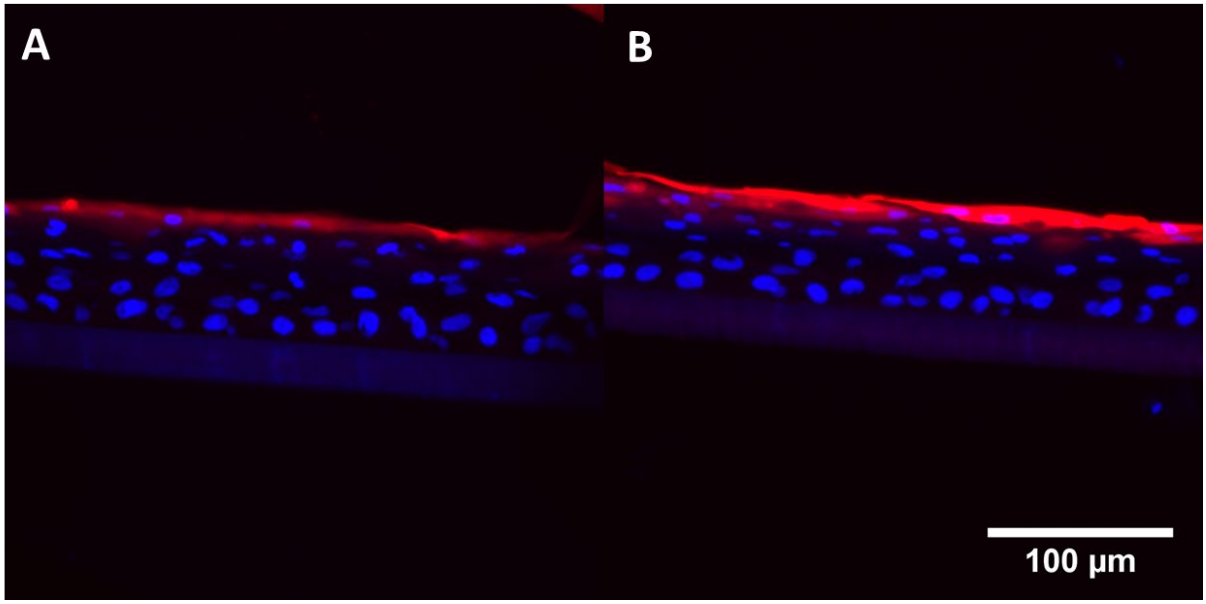

Figure A5.3 Sodium deoxycholate increases the uptake of 3 kDa Texas Red-dextran into the superficial layers of the oral epithelium. Representative images showing intratissue distribution of fluorescent dextran (red) in oral epithelium equivalents visualised by confocal microscopy following 10 h treatment (**A**) without or (**B**) with 0.4 mg/mL sodium deoxycholate as a permeation enhancer. DAPI (blue) is used as a nuclear counterstain. Scale bar = 100 µm.

References

1. Edmans, J. G. *et al.* Mucoadhesive electrospun fibre-based technologies for oral medicine. *Pharmaceutics* **12**, 1–21 (2020).
2. Edmans, J. G. *et al.* Incorporation of lysozyme into a mucoadhesive electrospun patch for rapid protein delivery to the oral mucosa. *Mater. Sci. Eng. C* **112**, 110917 (2020).
3. Edmans, J. G. *et al.* Electrospun patch delivery of anti-TNF α F(ab) for the treatment of inflammatory oral mucosal disease. *J. Control. Release* **350**, 146–157 (2022).
4. Squier, C. A. & Kremer, M. J. Biology of oral mucosa and esophagus. *J. Natl. Cancer Inst. Monogr.* **52242**, 7–15 (2001).
5. Junqueira, L. C., Carneiro, J. & Kelly, R. O. *Basic Histology*. (Prentice-Hall, 1995).
6. Harris, D. & Robinson, J. R. Drug delivery via the mucous membranes of the oral cavity. *J. Pharm. Sci.* **81**, 1–10 (1992).
7. Prestin, S., Rothschild, S. I., Betz, C. S. & Kraft, M. Measurement of epithelial thickness within the oral cavity using optical coherence tomography. *Head Neck* **34**, 1777–1781 (2012).
8. Hao, J. & Heng, P. W. S. Buccal delivery systems. *Drug Dev. Ind. Pharm.* **29**, 821–832 (2003).
9. Schechter, N. L., Weisman, S. J., Rosenblum, M., Bernstein, B. & Conard, P. L. The Use of Oral Transmucosal Fentanyl Citrate for Painful Procedures in Children. *Pediatrics* **95**, 335 LP – 339 (1995).
10. Mashru, R., Sutariya, V., Sankalia, M. & Sankalia, J. Transbuccal delivery of lamotrigine across porcine buccal mucosa: In vitro determination of routes of buccal transport. *J. Pharm. Pharm. Sci.* **8**, 54–62 (2005).
11. Sudhakar, Y., Kuotsu, K. & Bandyopadhyay, A. K. Buccal bioadhesive drug delivery -

A promising option for orally less efficient drugs. *J. Control. Release* **114**, 15–40 (2006).

12. Utoguchi, N. *et al.* Carrier-mediated transport of monocarboxylic acids in primary cultured epithelial cells from rabbit oral mucosa. *Pharm. Res.* **14**, 320–324 (1997).

13. Oyama, Y. *et al.* Carrier-mediated transport systems for glucose in mucosal cells of the human oral cavity. *J. Pharm. Sci.* **88**, 830–834 (1999).

14. Scully, C., Bagan, J., Flint, S., Moos, K. & Porter, S. R. *Oral and maxillofacial diseases: an illustrated guide to diagnosis and management of diseases of the oral mucosa, gingivae, teeth, salivary glands, bones and joints*. (Informa Healthcare, 2010).

15. Kraan, H. *et al.* Buccal and sublingual vaccine delivery. *J. Control. Release* **190**, 580–592 (2014).

16. Hearnden, V. *et al.* New developments and opportunities in oral mucosal drug delivery for local and systemic disease. *Adv. Drug Deliv. Rev.* **64**, 16–28 (2012).

17. Bastos, F., Pinto, A. C., Nunes, A. & Simões, S. Oromucosal products – Market landscape and innovative technologies: A review. *J. Control. Release* **348**, 305–320 (2022).

18. Autio-Gold, J. The Role of Chlorhexidine in Caries Prevention. *Oper. Dent.* **33**, 710–716 (2008).

19. Innocenti, M., Moscatelli, G. & Lopez, S. Efficacy of Gelclair in Reducing Pain in Palliative Care Patients with Oral Lesions. *J. Pain Symptom Manage.* **24**, 456–457 (2002).

20. Al-Hezaimi, K. *et al.* Evaluation of Novel Adhesive Film Containing Ketorolac for Post-Surgery Pain Control: A Safety and Efficacy Study. *J. Periodontol.* **82**, 963–968 (2010).

21. Save, T., Shah, M. U., Ghamande, A. R. & Venkitachalam, P. Comparative Study of Buccoadhesive Formulations and Sublingual Capsules of Nifedipine. *J. Pharm. Pharmacol.* **46**, 192–195 (1994).

22. Madhav, N. V. S., Shakya, A. K., Shakya, P. & Singh, K. Orotransmucosal drug delivery systems: A review. *J. Control. Release* **140**, 2–11 (2009).

23. Bensadoun, R. J. *et al.* Comparison of the efficacy and safety of miconazole 50-mg mucoadhesive buccal tablets with miconazole 500-mg gel in the treatment of oropharyngeal candidiasis: A prospective, randomized, single-blind, multicenter, comparative, phase III trial in patients . *Cancer* **112**, 204–211 (2008).

24. Shipp, L., Liu, F., Kerai-varsani, L. & Okwuosa, T. C. Buccal films : A review of therapeutic opportunities , formulations & relevant evaluation approaches. *J. Control. Release* **352**, 1071–1092 (2022).

25. Illangakoon, U. E. *et al.* Fast dissolving paracetamol/caffeine nanofibers prepared by electrospinning. *Int. J. Pharm.* **477**, 369–379 (2014).

26. Madhav, N. V. S., Shakya, A. K., Shakya, P. & Singh, K. Orotransmucosal drug delivery systems: A review. *Journal of Controlled Release* vol. 140 2–11 at https://doi.org/10.1016/j.jconrel.2009.07.016 (2009).

27. Gibson, J., Halliday, J. A., Ewert, K. & Robertson, S. A controlled release pilocarpine buccal insert in the treatment of Sjögren's syndrome. *Br. Dent. J.* **202**, 1–6 (2007).

28. Santocildes-Romero, M. E. *et al.* Fabrication of Electrospun Mucoadhesive Membranes for Therapeutic Applications in Oral Medicine. *ACS Appl. Mater. Interfaces* **9**, 11557–11567 (2017).

29. Shahrabi, M. *et al.* The effects of a combination oral spray (Mucosamin®) for the prevention of oral mucositis in pediatric patients undergoing hematopoietic stem cell

transplantation: a double blind randomized clinical trial. *Support. Care Cancer* 7963–7972 (2022) doi:10.1007/s00520-022-07231-y.

30. Hessell, P. G., Lloyd-Jones, J. G., Muir, N. C., Parr, G. D. & Sugden, K. A comparison of the availability of prochlorperazine following i.m. buccal and oral administration. *Int. J. Pharm.* **52**, 159–164 (1989).

31. Bhardwaj, N. & Kundu, S. C. Electrospinning: A fascinating fiber fabrication technique. *Biotechnol. Adv.* **28**, 325–347 (2010).

32. The Electrospinning Company Ltd. *Back to the Future - The Use of Biomaterials in Cell Therapy [White Paper]*. (2022).

33. Sill, T. J. & von Recum, H. A. Electrospinning: Applications in drug delivery and tissue engineering. *Biomaterials* **29**, 1989–2006 (2008).

34. Yarin, A. L., Koombhongse, S. & Reneker, D. H. Bending instability in electrospinning of nanofibers. *J. Appl. Phys.* **89**, 3018–3026 (2001).

35. Lizarraga-Valderrama, L. R. *et al.* Unidirectional neuronal cell growth and differentiation on aligned polyhydroxyalkanoate blend microfibres with varying diameters. *J. Tissue Eng. Regen. Med.* **13**, 1581–1594 (2019).

36. Thomas, V. *et al.* Mechano-morphological studies of aligned nanofibrous scaffolds of polycaprolactone fabricated by electrospinning. *J. Biomater. Sci. Polym. Ed.* **17**, 969–984 (2006).

37. Asencio, I. O. *et al.* A methodology for the production of microfabricated electrospun membranes for the creation of new skin regeneration models. *J. Tissue Eng.* **9**, 3–10 (2018).

38. Jiang, H. *et al.* A facile technique to prepare biodegradable coaxial electrospun nanofibers for controlled release of bioactive agents. *J. Control. Release* **108**, 237–243

(2005).

39. Wei, K. *et al.* Emulsion Electrospinning of a Collagen-Like Protein/PLGA Fibrous Scaffold: Empirical Modeling and Preliminary Release Assessment of Encapsulated Protein. *Macromol. Biosci.* **11**, 1526–1536 (2011).

40. Gupta, P. & Wilkes, G. L. Some investigations on the fiber formation by utilizing a side-by-side bicomponent electrospinning approach. *Polymer (Guildf).* **44**, 6353–6359 (2003).

41. Liu, X. *et al.* Tunable zero-order drug delivery systems created by modified triaxial electrospinning. *Chem. Eng. J.* **356**, 886–894 (2019).

42. Yu, D. G., Li, J. J., Zhang, M. & Williams, G. R. High-quality Janus nanofibers prepared using three-fluid electrospinning. *Chem. Commun.* **53**, 4542–4545 (2017).

43. Wei, L. *et al.* Large-Scale and Rapid Preparation of Nanofibrous Meshes and Their Application for Drug-Loaded Multilayer Mucoadhesive Patch Fabrication for Mouth Ulcer Treatment. *ACS Appl. Mater. Interfaces* **11**, 28740–28751 (2019).

44. Niu, H. & Lin, T. Fiber generators in needleless electrospinning. *J. Nanomater.* **2012**, (2012).

45. Peng, H., Liu, Y. & Ramakrishna, S. Recent development of centrifugal electrospinning. *J. Appl. Polym. Sci.* **134**, 1–10 (2017).

46. Bellan, L. M. & Craighead, H. G. Control of an electrospinning jet using electric focusing and jet-steering fields. *J. Vac. Sci. Technol. B Microelectron. Nanom. Struct.* **24**, 3179–3183 (2006).

47. Bjorge, D. *et al.* Performance assessment of electrospun nanofibers for filter applications. *Desalination* **249**, 942–948 (2009).

48. Loscertales, I. G. *et al.* Micro/nano encapsulation via electrified coaxial liquid jets.

Science (80-.). **295**, 1695–1698 (2002).

49. Wang, K. *et al.* Electrospun Hydrophilic Janus Nanocomposites for the Rapid Onset of Therapeutic Action of Helicid. *ACS Appl. Mater. Interfaces* **10**, 2859–2867 (2018).

50. Kidoaki, S., Kwon, I. K. & Matsuda, T. Mesoscopic spatial designs of nano- and microfiber meshes for tissue-engineering matrix and scaffold based on newly devised multilayering and mixing electrospinning techniques. *Biomaterials* **26**, 37–46 (2005).

51. Bing, N. *et al.* Annealing-induced oriented crystallization and its influence on the mechanical responses in the melt-spun monofilament of poly(L-lactide). *Macromolecules* **43**, 1156–1158 (2010).

52. Liu, W., Zhu, L., Huang, C. & Jin, X. Direct Electrospinning of Ultrafine Fibers with Interconnected Macropores Enabled by in Situ Mixing Microfluidics. *ACS Appl. Mater. Interfaces* **8**, 34870–34878 (2016).

53. Chou, S.-F., Carson, D. & Woodrow, K. A. Current strategies for sustaining drug release from electrospun nanofibers. *J. Control. Release* **220**, 584–591 (2015).

54. Middleton, J. C. & Tipton, A. J. Synthetic biodegradable polymers as orthopedic devices. *Biomaterials* **21**, 2335–2346 (2000).

55. Garlotta, D. A Literature Review of Poly(Lactic Acid). *J. Polym. Environ.* **9**, 63–84 (2001).

56. Haaf, F., Sanner, A. & Straub, F. Polymers of N-Vinylpyrrolidone: Synthesis, Characterization and Uses. *Polym. J.* **17**, 143–152 (1985).

57. Ulery, B. D., Nair, L. S. & Laurencin, C. T. Biomedical applications of biodegradable polymers. *J. Polym. Sci. Part B Polym. Phys.* **49**, 832–864 (2011).

58. Smart, J. D. The basics and underlying mechanisms of mucoadhesion. *Adv. Drug Deliv. Rev.* **57**, 1556–1568 (2005).

59. Tiwari, D., Sause, R., Madan, P. L. & Goldman, D. Evaluation of polyoxyethylene homopolymers for buccal bioadhesive drug delivery device formulations. *AAPS PharmSci* **1**, 1–8 (1999).

60. Rathbone, M. J., Drummond, B. K. & Tucker, I. G. The oral cavity as a site for systemic drug delivery. *Adv. Drug Deliv. Rev.* **13**, 1–22 (1994).

61. Brown, H. R. The adhesion between polymers. *Annu. Rev. Mater. Sci.* **21**, 463–489 (1991).

62. Mati-Baouche, N. *et al.* Chitosan as an adhesive. *Eur. Polym. J.* **60**, 198–212 (2014).

63. Liu, C. W. *et al.* Preparation and characterization of gelatin-based mucoadhesive nanocomposites as intravesical gene delivery scaffolds. *Biomed Res. Int.* **2014**, (2014).

64. Sandri, G. *et al.* Mucoadhesive and penetration enhancement properties of three grades of hyaluronic acid using porcine buccal and vaginal tissue, Caco-2 cell lines, and rat jejunum. *J. Pharm. Pharmacol.* **56**, 1083–1090 (2004).

65. Kesavan, K., Nath, G. & Pandit, J. K. Sodium alginate based mucoadhesive system for gatifloxacin and its in vitro antibacterial activity. *Sci. Pharm.* **78**, 941–957 (2010).

66. Dortunc̈, B., Özer, L. & Uyanik, N. Development and in vitro evaluation of a buccoadhesive pindolol tablet formulation. *Drug Dev. Ind. Pharm.* **24**, 281–288 (1998).

67. Santocildes-Romero, M. E. *et al.* Fabrication of Electrospun Mucoadhesive Membranes for Therapeutic Applications in Oral Medicine. *ACS Appl. Mater. Interfaces* **9**, 11557–11567 (2017).

68. Hosseinzadeh, S. *et al.* Mucoadhesive nanofibrous membrane with anti-inflammatory activity. *Polym. Bull.* **76**, 4827–4840 (2018).

69. Langoth, N. *et al.* Thiolated chitosans: Design and In Vivo evaluation of a

mucoadhesive buccal peptide drug delivery system. *Pharm. Res.* **23**, 573–579 (2006).

70. Kafedjiiski, K. *et al.* Synthesis and in vitro evaluation of thiolated hyaluronic acid for mucoadhesive drug delivery. *Int. J. Pharm.* **343**, 48–58 (2007).

71. Luraghi, A., Peri, F. & Moroni, L. Electrospinning for drug delivery applications : A review. *J. Control. Release* **334**, 463–484 (2021).

72. Illangakoon, U. E., Nazir, T., Williams, G. R. & Chatterton, N. P. Mebeverine-loaded electrospun nanofibers: Physicochemical characterization and dissolution studies. *J. Pharm. Sci.* **103**, 283–292 (2014).

73. Wu, J. *et al.* Mechanism of a long-term controlled drug release system based on simple blended electrospun fibers. *J. Control. Release* **320**, 337–346 (2020).

74. He, C. L. *et al.* Coaxial electrospun poly(L-lactic acid) ultrafine fibers for sustained drug delivery. *J. Macromol. Sci. Part B Phys.* **45 B**, 515–524 (2006).

75. Beachley, V. & Wen, X. Polymer nanofibrous structures: Fabrication, biofunctionalization, and cell interactions. *Prog. Polym. Sci.* **35**, 868–892 (2010).

76. Dziemidowicz, K., Brocchini, S. & Williams, G. R. A simple route to functionalising electrospun polymer scaffolds with surface biomolecules. *Int. J. Pharm.* **597**, 120231 (2021).

77. Moreira, A. *et al.* Protein encapsulation by electrospinning and electrospraying. *J. Control. Release* **329**, 1172–1197 (2021).

78. Khadka, D. B. & Haynie, D. T. Protein- and peptide-based electrospun nanofibers in medical biomaterials. *Nanomedicine Nanotechnology, Biol. Med.* **8**, 1242–1262 (2012).

79. Wang, X., Yue, T. & Lee, T. ching. Development of Pleurocidin-poly(vinyl alcohol) electrospun antimicrobial nanofibers to retain antimicrobial activity in food system

application. *Food Control* **54**, 150–157 (2015).

80. Stie, M. B., Gätke, J. R., Chronakis, I. S., Jacobsen, J. & Nielsen, H. M. Mucoadhesive Electrospun Nanofiber-Based Hybrid System with Controlled and Unidirectional Release of Desmopressin. *Int. J. Mol. Sci.* **23**, 1458 (2022).

81. Eriksen, T. H. B., Skovsen, E. & Fojan, P. Release of antimicrobial peptides from electrospun nanofibres as a drug delivery system. *J. Biomed. Nanotechnol.* **9**, 492–498 (2013).

82. Gandhi, M., Srikar, R., Yarin, A. L., Megaridis, C. M. & Gemeinhart, R. A. Mechanistic examination of protein release from polymer nanofibers. *Mol. Pharm.* **6**, 641–647 (2009).

83. Ji, W. *et al.* Fibrous scaffolds loaded with protein prepared by blend or coaxial electrospinning. *Acta Biomater.* **6**, 4199–4207 (2010).

84. Liu, X. *et al.* Stability of lysozyme incorporated into electrospun fibrous mats for wound healing. *Eur. J. Pharm. Biopharm.* **136**, 240–249 (2019).

85. Chew, S. Y., Wen, J., Yim, E. K. F. & Leong, K. W. Sustained release of proteins from electrospun biodegradable fibers. *Biomacromolecules* **6**, 2017–2024 (2005).

86. Yang, Y. *et al.* Promotion of skin regeneration in diabetic rats by electrospun core-sheath fibers loaded with basic fibroblast growth factor. *Biomaterials* **32**, 4243–4254 (2011).

87. Sohi, H., Ahuja, A., Ahmad, F. J. & Khar, R. K. Critical evaluation of permeation enhancers for oral mucosal drug delivery. *Drug Dev. Ind. Pharm.* **36**, 254–282 (2010).

88. Handler, A. M., Marxen, E., Jacobsen, J. & Janfelt, C. Visualization of the penetration modifying mechanism of laurocapram by Mass Spectrometry Imaging in buccal drug delivery. *Eur. J. Pharm. Sci.* **127**, 276–281 (2019).

89. Şenel, S. *et al.* Enhancing effect of chitosan on peptide drug delivery across buccal mucosa. *Biomaterials* **21**, 2067–2071 (2000).

90. Tonglairoum, P., Ngawhirunpat, T., Rojanarata, T., Kaomongkolgit, R. & Opanasopit, P. Fast-acting clotrimazole composited PVP/HPβCD nanofibers for oral candidiasis application. *Pharm. Res.* **31**, 1893–1906 (2014).

91. Szabó, P., Daróczi, T. B., Tóth, G. & Zelkó, R. In vitro and in silico investigation of electrospun terbinafine hydrochloride-loaded buccal nanofibrous sheets. *J. Pharm. Biomed. Anal.* **131**, 156–159 (2016).

92. Friedl, J. D. *et al.* SEDDS-loaded mucoadhesive fiber patches for advanced oromucosal delivery of poorly soluble drugs. *J. Control. Release* **348**, 692–705 (2022).

93. Li, Z. *et al.* Controlled release of liposome-encapsulated Naproxen from core-sheath electrospun nanofibers. *Carbohydr. Polym.* **111**, 18–24 (2014).

94. Zhang, C.-L. & Yu, S.-H. Nanoparticles meet electrospinning: recent advances and future prospects. *Chem. Soc. Rev.* **43**, 4423 (2014).

95. Wang, Y. *et al.* Electrospun composite nanofibers containing nanoparticles for the programmable release of dual drugs. *Polym. J.* **43**, 478–483 (2011).

96. Hua, S. Advances in nanoparticulate drug delivery approaches for sublingual and buccal administration. *Front. Pharmacol.* **10**, 1–9 (2019).

97. Donnelly, R. F., Shaikh, R., Raj Singh, T. R., Garland, M. J. & Woolfson, A. D. Mucoadhesive drug delivery systems. *J. Pharm. Bioallied Sci.* **3**, 89 (2011).

98. McCarron, P. A. *et al.* Evaluation of a water-soluble bioadhesive patch for photodynamic therapy of vulval lesions. *Int. J. Pharm.* **293**, 11–23 (2005).

99. McCarron, P. A., Donnelly, R. F., Zawislak, A. & Woolfson, A. D. Design and evaluation of a water-soluble bioadhesive patch formulation for cutaneous delivery of

5-aminolevulinic acid to superficial neoplastic lesions. *Eur. J. Pharm. Sci.* **27**, 268–279 (2006).

100. Yu, D. G. *et al.* Oral fast-dissolving drug delivery membranes prepared from electrospun polyvinylpyrrolidone ultrafine fibers. *Nanotechnology* **20**, (2009).

101. Potrč, T. *et al.* Electrospun polycaprolactone nanofibers as a potential oromucosal delivery system for poorly water-soluble drugs. *Eur. J. Pharm. Sci.* **75**, 101–113 (2015).

102. *Test No. 439: In Vitro Skin Irritation: Reconstructed Human Epidermis Test Method*. (OECD, 2019). doi:10.1787/9789264242845-en.

103. Kandarova, H. *et al.* Pre-validation of an in vitro skin irritation test for medical devices using the reconstructed human tissue model EpiDerm^{TM}. *Toxicol. Vitr.* **50**, 407–417 (2018).

104. Harding, A. L. *et al.* Determination of Chemical Irritation Potential Using a Defined Gene Signature Set on Tissue-Engineered Human Skin Equivalents. *JID Innov.* **1**, 100011 (2021).

105. Cottrez, F. *et al.* SENS-IS, a 3D reconstituted epidermis based model for quantifying chemical sensitization potency: Reproducibility and predictivity results from an inter-laboratory study. *Toxicol. Vitr.* **32**, 248–260 (2016).

106. Tonglairoum, P. *et al.* Fabrication of mucoadhesive chitosan coated polyvinylpyrrolidone/cyclodextrin/clotrimazole sandwich patches for oral candidiasis. *Carbohydr. Polym.* **132**, 173–179 (2015).

107. Reise, M. *et al.* Release of metronidazole from electrospun poly(l-lactide-co-d/l-lactide) fibers for local periodontitis treatment. *Dent. Mater.* **28**, 179–188 (2012).

108. Jennings, L. R. *et al.* Development and Characterization of *In Vitro* Human Oral

Mucosal Equivalents Derived from Immortalized Oral Keratinocytes. *Tissue Eng. Part C Methods* **22**, 1108–1117 (2016).

109. Colley, H. E. *et al.* Pre-clinical evaluation of novel mucoadhesive bilayer patches for local delivery of clobetasol-17-propionate to the oral mucosa. *Biomaterials* **178**, 134–146 (2018).

110. Morales, J. O. & McConville, J. T. Manufacture and characterization of mucoadhesive buccal films. *Eur. J. Pharm. Biopharm.* **77**, 187–199 (2011).

111. Marxen, E., Jacobsen, J., Hyrup, B. & Janfelt, C. Permeability Barriers for Nicotine and Mannitol in Porcine Buccal Mucosa Studied by High-Resolution MALDI Mass Spectrometry Imaging. *Mol. Pharm.* **15**, 519–526 (2018).

112. Vonarburg, C. *et al.* Topical application of nebulized human IgG, IgA and IgAM in the lungs of rats and non-human primates. *Respir. Res.* **20**, 1–16 (2019).

113. Scully, C. & Carrozzo, M. Oral mucosal disease: Lichen planus. *Br. J. Oral Maxillofac. Surg.* **46**, 15–21 (2008).

114. Scully, C. & Porter, S. Oral mucosal disease: Recurrent aphthous stomatitis. *Br. J. Oral Maxillofac. Surg.* **46**, 198–206 (2008).

115. González-Moles, M. A. & Scully, C. Vesiculo-erosive Oral Mucosal Disease—Management with Topical Corticosteroids: (2) Protocols, Monitoring of Effects and Adverse Reactions, and the Future. *J. Dent. Res.* **84**, 302–308 (2005).

116. Alipour, M. *et al.* Fabrication of a Novel Fibrous Mat Based on Gliadin/Ethylcellulose Incorporated with Triamcinolone for Treatment of Oral Ulcers. *J. Polym. Environ.* **30**, 2579–2588 (2022).

117. Robertson, J. J. Managing Pharyngeal and Oral Mucosal Pain. *Curr. Emerg. Hosp. Med. Rep.* **4**, 57–65 (2016).

118. Jinbu, Y. & Demitsu, T. Oral ulcerations due to drug medications. *Jpn. Dent. Sci. Rev.* **50**, 40–46 (2014).

119. Berger, K. *et al.* Burden of Oral Mucositis: A Systematic Review and Implications for Future Research. *Oncol. Res. Treat.* **41**, 399–405 (2018).

120. Rubenstein, E. B. *et al.* Clinical Practice Guidelines for the Prevention and Treatment of Cancer Therapy-Induced Oral and Gastrointestinal Mucositis. *Cancer* **100**, 2026–2046 (2004).

121. Hemati, S. *et al.* Morphine mouthwash for the management of oral mucositis in patients with head and neck cancer. *Adv. Biomed. Res.* **4**, 44 (2015).

122. Vayne-Bossert, P. *et al.* Effect of Topical Morphine (Mouthwash) on Oral Pain Due to Chemotherapy- and/or Radiotherapy-Induced Mucositis: A Randomized Double-Blinded Study. *J. Palliat. Med.* **13**, 125–128 (2010).

123. van Wijk, A. J. & Hoogstraten, J. Anxiety and pain during dental injections. *J. Dent.* **37**, 700–704 (2009).

124. Baart, J. A. & Brand, H. S. *Local Anesthesia in Dentistry*. (Blackwell, 2009).

125. Reda, R. I., Wen, M. M. & El-Kamel, A. H. Ketoprofen-loaded Eudragit electrospun nanofibers for the treatment of oral mucositis. *Int. J. Nanomedicine* **12**, 2335–2351 (2017).

126. Saunders, D. P. *et al.* Systematic review of antimicrobials, mucosal coating agents, anesthetics, and analgesics for the management of oral mucositis in cancer patients. *Support. Care Cancer* **21**, 3191–3207 (2013).

127. Akpan, A. Oral candidiasis. *Postgrad. Med. J.* **78**, 455–459 (2002).

128. Sanglard, D. Emerging threats in antifungal-resistant fungal pathogens. *Front. Med.* **3**, 1–10 (2016).

129. Yu, Q. *et al.* Novel mechanisms of surfactants against Candida albicans growth and morphogenesis. *Chem. Biol. Interact.* **227**, 1–6 (2015).

130. Lum, K. Y. *et al.* Activity of novel synthetic peptides against Candida albicans. *Sci. Rep.* **5**, (2015).

131. Hayama, K., Takahashi, M., Yui, S. & Abe, S. Inhibitory effects of several saturated fatty acids and their related fatty alcohols on the growth of Candida albicans. *Drug Discov. Ther.* **9**, 386–390 (2015).

132. Aduba, D. C. *et al.* Semi-interpenetrating network (sIPN) gelatin nanofiber scaffolds for oral mucosal drug delivery. *Acta Biomater.* **9**, 6576–6584 (2013).

133. Argiris, A., Karamouzis, M. V, Raben, D. & Ferris, R. L. Head and neck cancer. *Lancet* **371**, 1695–1709 (2008).

134. Ferlay, J. *et al.* Cancer statistics for the year 2020: An overview. *Int. J. Cancer* **149**, 778–789 (2021).

135. Mehanna, H. M., Rattay, T., Smith, J. & Mcconkey, C. C. TREATMENT AND FOLLOW-UP OF ORAL DYSPLASIA — A SYSTEMATIC REVIEW AND META-ANALYSIS. *Head Neck J. Sci. Spec. Head Neck* 1600–1609 (2009) doi:10.1002/hed.21131.

136. Saba, N. F. *et al.* Prevention of head and neck squamous cell carcinoma: Removing the 'chemo' from 'chemoprevention'. *Oral Oncol.* **51**, 112–118 (2015).

137. Lane, A. A. & Chabner, B. A. Histone deacetylase inhibitors in cancer therapy. *J. Clin. Oncol.* **27**, 5459–5468 (2009).

138. Shen, J. *et al.* Enhancement of cisplatin induced apoptosis by suberoylanilide hydroxamic acid in human oral squamous cell carcinoma cell lines. *Biochem. Pharmacol.* **73**, 1901–1909 (2007).

139. McCarthy, C. *et al.* SAVER: sodium valproate for the epigenetic reprogramming of high-risk oral epithelial dysplasia—a phase II randomised control trial study protocol. *Trials* **22**, 1–12 (2021).

140. Hamakawa, H. *et al.* Basic evidence of molecular targeted therapy for oral cancer and salivary gland cancer. *Head Neck* **30**, 800–809 (2008).

141. Huang, S. M., Bock, J. M. & Harari, P. M. Epidermal growth factor receptor blockade with C225 modulates proliferation, apoptosis, and radiosensitivity in squamous cell carcinomas of the head and neck. *Cancer Res.* **59**, 1935–1940 (1999).

142. Mullins, R., Ansell, M. & Laverick, S. Treatment of oral dysplasia with 5% imiquimod cream: short communication. *Br. J. Oral Maxillofac. Surg.* **54**, 1028–1029 (2016).

143. Zhang, H. *et al.* Fabrication of Astaxanthin-loaded Electrospun Nanofiber- based Mucoadhesive Patches with Water - Insoluble Backing for the Treatment of Oral Premalignant Lesions. *Mater. Des.* 111131 (2022) doi:10.1016/j.matdes.2022.111131.

144. Kavitha, K., Kowshik, J., Kishore, T. K. K., Baba, A. B. & Nagini, S. Astaxanthin inhibits NF-κB and Wnt/β-catenin signaling pathways via inactivation of Erk/MAPK and PI3K/Akt to induce intrinsic apoptosis in a hamster model of oral cancer. *Biochim. Biophys. Acta - Gen. Subj.* **1830**, 4433–4444 (2013).

145. Zong, S. *et al.* The use of cisplatin-loaded mucoadhesive nanofibers for local chemotherapy of cervical cancers in mice. *Eur. J. Pharm. Biopharm.* **93**, 127–135 (2015).

146. Liu, X. *et al.* Designing a Mucoadhesive ChemoPatch to Ablate Oral Dysplasia for Cancer Prevention. *Small* **18**, 1–13 (2022).

147. Said, Z., Murdoch, C., Hansen, J., Siim Madsen, L. & Colley, H. E. Corticosteroid delivery using oral mucosa equivalents for the treatment of inflammatory mucosal

diseases. *Eur. J. Oral Sci.* **129**, 1–12 (2021).

148. Clitherow, K. H. *et al.* Mucoadhesive Electrospun Patch Delivery of Lidocaine to the Oral Mucosa and Investigation of Spatial Distribution in a Tissue Using MALDI-Mass Spectrometry Imaging. *Mol. Pharm.* **16**, 3948–3956 (2019).

149. Clitherow, K. H. *et al.* Medium-Chain Fatty Acids Released from Polymeric Electrospun Patches Inhibit Candida albicans Growth and Reduce the Biofilm Viability. *ACS Biomater. Sci. Eng.* **6**, 4087–4095 (2020).

150. Cardoso, C. L., Rodrigues, M. T. V., Ferreira, O., Garlet, G. P. & De Carvalho, P. S. P. Clinical concepts of dry socket. *J. Oral Maxillofac. Surg.* **68**, 1922–1932 (2010).

151. Wang, L. *et al.* Therapeutic peptides: current applications and future directions. *Signal Transduct. Target. Ther.* **7**, (2022).

152. Shaji, J. & Patole, V. Protein and peptide drug delivery: Oral approaches. *Indian J. Pharm. Sci.* **70**, 269 (2008).

153. Hamman, J. H., Enslin, G. M. & Kotzé, A. F. Oral delivery of peptide drugs: Barriers and developments. *BioDrugs* **19**, 165–177 (2005).

154. Anders, R., Merkle, H. P., Schurr, W. & Ziegler, R. Buccal Absorption of Protirelin: An Effective Way to Stimulate Thyrotropin and Prolactin. *J. Pharm. Sci.* **72**, 1481–1483 (1983).

155. McCullagh, E. P. & Lewis, L. A. Comparison of effectiveness of various methods of administration of insulin. *J. Clin. Endocrinol. Metab.* **2**, 435–437 (1942).

156. Heinemann, L. & Jacques, Y. Oral insulin and buccal insulin: A critical reappraisal. *J. Diabetes Sci. Technol.* **3**, 568–584 (2009).

157. Park, K., Kwon, I. C. & Park, K. Oral protein delivery: Current status and future prospect. *React. Funct. Polym.* **71**, 280–287 (2011).

158. Gutniak, M. K. *et al.* Potential therapeutic levels of glucagon-like peptide I achieved in humans by a buccal tablet. *Diabetes Care* **19**, 843–848 (1996).

159. Chesnut, C. H. *et al.* Salmon calcitonin: A review of current and future therapeutic indications. *Osteoporos. Int.* **19**, 479–491 (2008).

160. Copp, D. H., Cameron, E. C., Cheney, B. A., Davidson, A. G. F. & Henze, K. G. Evidence for calcitonin-a new hormone from The parathyroid that lowers blood calcium. *Endocrinology* **70**, 638–649 (1962).

161. Nicholson, G. C., Moseley, J. M., Sexton, P. M., Mendelsohn, F. A. & Martin, T. J. Abundant calcitonin receptors in isolated rat osteoclasts. Biochemical and autoradiographic characterization. *J. Clin. Invest.* **78**, 355–360 (1986).

162. Alur, H. H., Beal, J. D., Pather, S. I., Mitra, A. K. & Johnston, T. P. Evaluation of a novel, natural oligosaccharide gum as a sustained- release and mucoadhesive component of calcitonin buccal tablets. *J. Pharm. Sci.* **88**, 1313–1319 (1999).

163. Z., C. & R.J., M. Buccal transmucosal delivery of calcitonin in rabbits using thin-film composites. *Pharm. Res.* **19**, 1901–1906 (2002).

164. Lang, S., Rothen-rutishauser, B., Perriard, J., Schmidt, M. C. & Merkle, H. P. Permeation and Pathways of Human Calcitonin (hCT) Across Excised Bovine Nasal Mucosa. **19**, 599–607 (1998).

165. Oh, D., Chun, K., Jeon, S., Kang, J. & Lee, S. Enhanced transbuccal salmon calcitonin (sCT) delivery : Effect of chemical enhancers and electrical assistance on in vitro sCT buccal permeation. *Eur. J. Pharm. Biopharm.* **79**, 357–363 (2011).

166. Patel, V. F., Liu, F. & Brown, M. B. Modeling the oral cavity: In vitro and in vivo evaluations of buccal drug delivery systems. *J. Control. Release* **161**, 746–756 (2012).

167. Kulkarni, U., Mahalingam, R., Pather, I., Li, X. & Jasti, B. Porcine buccal mucosa as

in vitro model: Effect of biological and experimental variables. *J. Pharm. Sci.* **99**, 1265–1277 (2010).

168. Xue, X. Y. *et al.* Promoting effects of chemical permeation enhancers on insulin permeation across TR146 cell model of buccal epithelium in vitro. *Drug Chem. Toxicol.* **35**, 199–207 (2012).

169. Pusateri, C. R., Monaco, E. A. & Edgerton, M. Sensitivity of Candida albicans biofilm cells grown on denture acrylic to antifungal proteins and chlorhexidine. *Arch. Oral Biol.* **54**, 588–594 (2009).

170. Shin, J. M. *et al.* Antimicrobial nisin acts against saliva derived multi-species biofilms without cytotoxicity to human oral cells. *Front. Microbiol.* **6**, 1–14 (2015).

171. Tenovuo, J. Antimicrobial function of human saliva - How important is it for oral health? *Acta Odontol. Scand.* **56**, 250–256 (1998).

172. Sonis, S. T. Efficacy of palifermin (keratinocyte growth factor-1) in the amelioration of oral mucositis. *Core Evid.* **4**, 199–205 (2009).

173. Campos, J. C., Cunha, J. D., Ferreira, D. C., Reis, S. & Costa, P. J. Challenges in the local delivery of peptides and proteins for oral mucositis management. *Eur. J. Pharm. Biopharm.* **128**, 131–146 (2018).

174. Berraondo, P. *et al.* Cytokines in clinical cancer immunotherapy. *Br. J. Cancer* **120**, 6–15 (2019).

175. Klein, J. & Nikolaidis, N. The descent of the antibody-based immune system by gradual evolution. *Proc. Natl. Acad. Sci. U. S. A.* **102**, 169–174 (2005).

176. Lodish, H. *et al. Molecular Cell Biology: 6th Edition*. (W.H. Freeman and Company, 2007).

177. Punt, J., Stranford, S., Owen, J. & Jones, P. *Kuby Immunology*. (Macmillan, 2009).

178. Zhang, C. Hybridoma Technology for the Generation of Monoclonal Antibodies. in *Antibody Methods and Protocols* (eds. Proetzel, G. & Ebersbach, H.) (Humana Press, 2012). doi:10.1007/978-1-61779-931-0_7.

179. Mahmud, N., Klipa, D. & Ahsan, N. Antibody immunosuppressive therapy in solid-organ transplant Antibody immunosuppressive therapy in solid-organ transplant. **0862**, (2010).

180. Carter, P. J. & Lazar, G. A. Next generation antibody drugs: Pursuit of the 'high-hanging fruit'. *Nat. Rev. Drug Discov.* **17**, 197–223 (2018).

181. Jones, R. G. A., Martino, A., Jones, R. G. A. & Martino, A. Targeted localized use of therapeutic antibodies : a review of non-systemic , topical and oral applications Targeted localized use of therapeutic antibodies : a review of non-systemic , topical and oral applications. *Crit. Rev. Biotechnol.* **8551**, 506–520 (2016).

182. Tevenson, W. I. S. *et al.* Corneal Neovascularization and the Utility of Topical VEGF Inhibition : Ranibizumab (Lucentis) Vs Bevacizumab (Avastin). **10**, (2012).

183. Sankar, V. *et al.* Local drug delivery for oral mucosal diseases: Challenges and opportunities. *Oral Dis.* **17**, 73–84 (2011).

184. O'Neill, I. D. & Scully, C. Biologics in oral medicine: Ulcerative disorders. *Oral Dis.* **19**, 37–45 (2013).

185. Brennan, M. T. *et al.* Efficacy and Safety of a Novel Mucoadhesive Clobetasol Patch for Treatment of Erosive Oral Lichen Planus. *J. Oral Pathol. Med.* 0–3 (2021) doi:10.1111/jop.13270.

186. Garidel, P., Kuhn, A. B., Schäfer, L. V., Karow-Zwick, A. R. & Blech, M. High-concentration protein formulations: How high is high? *Eur. J. Pharm. Biopharm.* **119**, 353–360 (2017).

187. Thurow, H. & Geisen, K. Stabilisation of dissolved proteins against denaturation at hydrophobie interfaces. *Diabetologia* **27**, 212–218 (1984).

188. Atha, D. H. & Ingham, K. C. Mechanism of precipitation of proteins by polyethylene glycols. Analysis in terms of excluded volume. *J. Biol. Chem.* **256**, 12108–12117 (1981).

189. Messina, M. S. *et al.* Effect of trehalose polymer regioisomers on protein stabilization. *Polym. Chem.* **8**, 4781–4788 (2017).

190. Miklos, A. C., Li, C., Sharaf, N. G. & Pielak, G. J. Volume exclusion and soft interaction effects on protein stability under crowded conditions. *Biochemistry* **49**, 6984–6991 (2010).

191. Murooka, T. T., Rahbar, R., Platanias, L. C. & Fish, E. N. CCL5-mediated T-cell chemotaxis involves the initiation of mRNA translation through mTOR/4E-BPl. *Blood* **111**, 4892–4901 (2008).

192. Boch, K. *et al.* Lichen Planus. *Front. Med.* **8**, 1–17 (2021).

193. Shiohara, T., Moriya, N., Tsuchiya, K., Nagashima, M. & Narimatsu, H. Lichenoid tissue reaction induced by local transfer of Ia-reactive T-cell clones. *J. Invest. Dermatol.* **87**, 33–38 (1986).

194. El-Howati, A., Thornhill, M. H., Colley, H. E. & Murdoch, C. Immune mechanisms in oral lichen planus. *Oral Dis.* 0–3 (2022) doi:10.1111/odi.14142.

195. Moharamzadeh, K. *et al.* Tissue-engineered oral mucosa. *J. Dent. Res.* **91**, 642–650 (2012).

196. Contardi, M. *et al.* Evaluation of a Multifunctional Polyvinylpyrrolidone/Hyaluronic Acid-Based Bilayer Film Patch with Anti-Inflammatory Properties as an Enhancer of the Wound Healing Process. *Pharmaceutics* **14**, 483 (2022).

197. Dennis, V., Yilma, Singh, S. & Dixit, S. Anti-inflammatory effects of silver-polyvinyl pyrrolidone (Ag-PVP) nanoparticles in mouse macrophages infected with live Chlamydia trachomatis. *Int. J. Nanomedicine* 2421 (2013) doi:10.2147/ijn.s44090.

198. Varela, P. *et al.* Response of Human Macrophages to Clinically Applied Wound Dressings Loaded With Silver. *Front. Bioeng. Biotechnol.* **8**, 1–13 (2020).

199. Berka, P., Stránská, D., Semecký, V., Berka, K. & Doležal, P. In vitro testing of flash-frozen sublingual membranes for storage and reproducible permeability studies of macromolecular drugs from solution or nanofiber mats. *Int. J. Pharm.* **572**, (2019).

200. Harada, S., Smith, R. M. & Jarett, L. Mechanisms of nuclear translocation of insulin. *Cell Biochem. Biophys.* **31**, 307–319 (1999).

201. Kesten, D., Horovitz-Fried, M., Brutman-Barazani, T. & Sampson, S. R. Insulin-induced translocation of IR to the nucleus in insulin responsive cells requires a nuclear translocation sequence. *Biochim. Biophys. Acta - Mol. Cell Res.* **1865**, 551–559 (2018).

202. Sharma, A. *et al.* Electrospun composite nanofiber-based transmucosal patch for anti-diabetic drug delivery. *J. Mater. Chem. B* **1**, 3410–3418 (2013).

203. Cui, F. *et al.* Preparation and evaluation of chitosan-ethylenediaminetetraacetic acid hydrogel films for the mucoadhesive transbuccal delivery of insulin. *J. Biomed. Mater. Res. - Part A* **89**, 1063–1071 (2009).

204. Lancina, M. G., Shankar, R. K. & Yang, H. Chitosan nanofibers for transbuccal insulin delivery. *J. Biomed. Mater. Res. - Part A* **105**, 1252–1259 (2017).

205. Xu, L. *et al.* Semi-interpenetrating network (Sipn) co-electrospun gelatin/insulin fiber formulation for transbuccal insulin delivery. *Pharm. Res.* **32**, 275–285 (2015).

206. Boswell, C. A. *et al.* Effects of charge on antibody tissue distribution and pharmacokinetics. *Bioconjug. Chem.* **21**, 2153–2163 (2010).

207. Bashyal, S. *et al.* Facilitated buccal insulin delivery via hydrophobic ion-pairing approach: In vitro and ex vivo evaluation. *Int. J. Nanomedicine* **16**, 4677–4691 (2021).

208. Sonaje, K. *et al.* Opening of epithelial tight junctions and enhancement of paracellular permeation by chitosan: Microscopic, ultrastructural, and computed-tomographic observations. *Mol. Pharm.* **9**, 1271–1279 (2012).

209. Portero, A., Remuñán-López, C. & Nielsen, H. M. The potential of chitosan in enhancing peptide and protein absorption across the TR146 cell culture model - An in vitro model of the buccal epithelium. *Pharm. Res.* **19**, 169–174 (2002).

210. Holpuch, A. S. *et al.* Nanoparticles for local drug delivery to the oral mucosa: Proof of principle studies. *Pharm. Res.* **27**, 1224–1236 (2010).

211. Colley, H. E. *et al.* Polymersome-mediated delivery of combination anticancer therapy to head and neck cancer cells: 2D and 3D in vitro evaluation. *Mol. Pharm.* **11**, 1176–1188 (2014).

212. Trindade, R. P., Renault, N., El Harane, N., Menasché, P. & Williams, G. R. Extracellular vesicles can be processed by electrospinning without loss of structure or function. *Mater. Lett.* **282**, 128671 (2021).

213. Touitou, E., Dayan, N., Bergelson, L., Godin, B. & Eliaz, M. Ethosomes - Novel vesicular carriers for enhanced delivery: Characterization and skin penetration properties. *J. Control. Release* **65**, 403–418 (2000).

214. Alkilani, A. Z., McCrudden, M. T. C. & Donnelly, R. F. Transdermal drug delivery: Innovative pharmaceutical developments based on disruption of the barrier properties of the stratum corneum. *Pharmaceutics* **7**, 438–470 (2015).

215. Larrañeta, E., McCrudden, M. T. C., Courtenay, A. J. & Donnelly, R. F. Microneedles: A New Frontier in Nanomedicine Delivery. *Pharm. Res.* **33**, 1055–1073 (2016).

216. Hentz, N. G. Synthesis and characterization of insulin-fluorescein derivatives for bioanalytical applications. *Anal. Chem.* **69**, 4994–5000 (1997).

217. Aungst, B. J. & Rogers, N. J. Comparison of the effects of various transmucosal absorption promoters on buccal insulin delivery. *Int. J. Pharm.* **53**, 227–235 (1989).